

# Design of an Aerial-Aquatic Inspection Drone

Final Report

AE3200

DSE07 SEAMOS

Delft University of Technology

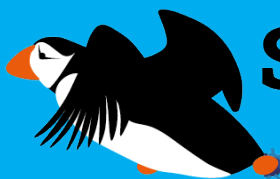


# Design of an Aerial-Aquatic Inspection Drone Final Report

by

DSE07 SEAMOS

Student Name	Student Number
Louis Ronsse	5240379
Mathis De Vusser	5222591
Billie Seffer	5274397
Soham Kumar	4818385
Elisabeth Oosthoek	5056470
Kosma Krzyżanowski	5063671
Jan Grobusch	5086205
Emma van Zutphen	5040507
Mikołaj Heliński	5300142
Reinier Zwikker	4994388



**SEAMOS** SUSTAINABLE ECOLOGY AND  
MONITORING OF SEAWEED  
DSE 07 2023 AQUACULTURE OFFSHORE

Tutors:	Salua Hamaza & Clemens Dransfeld
Coaches:	Simon van Oosterom & Kherlen Jigjid
Institution:	Delft University of Technology
Date of Submission:	21th June 2023
Report version :	V1

Think about the environment, only print this document if it is necessary.



# Executive Overview

## Project Objective

To meet net-zero goals, there is a strong drive towards sustainable, alternative products in the food industry, pharmaceuticals, and agriculture. Seaweed farming is the fastest-growing aquaculture industry, because of its promising qualities and efficiency, using space on Earth that is under-utilised, the coastal seas and ocean zones. For the growth of seaweed, only sunlight and naturally occurring marine nutrients are required. Producing seaweed has a positive impact on the marine environment, contributing to the restoration of these areas. Biomass removes excess nutrients from eutrophic areas and mitigates ocean acidification. A seaweed farm increases marine biodiversity by forming a habitat for various species of marine life.<sup>1</sup>



**Figure 1:** This project aims to further goals 9, 13, 14, and 15 of the United Nations Sustainable Development Goals



**Figure 2:** The Seaweed Company operates various seaweed farms and wants to expand into the offshore environment [TSC]

Current seaweed farms are typically located in a nearshore environment, providing easy access for maintenance and harvesting. The Seaweed Company operates various nearshore seaweed farms around the world and wants to expand its ventures into the offshore environment. The prime location for such an offshore seaweed farm is inside the Borselle Wind Turbine park. Ships are prohibited from sailing through this area and it thus has a plenty of unused space that can freely be used for aquaculture. To make the offshore production of seaweed feasible, a novel solution needs to be designed that can monitor the structure of the deployed farms and provide insight in the growth of the seaweed. The current method is a manual inspection with a large ship, that can lift the seaweed farm out of the water with a crane. This method is prohibitively expensive for the required scale of seaweed production. For this reason, The Seaweed Company has commissioned a design for an autonomous system that can monitor a proposed seaweed farm off the coast of the Netherlands, located in the Borssele Wind Turbine Park.

The system has to operate in the offshore conditions of the Southern North Sea. Wave height, wind velocity, and current velocity will be taken into account to determine the design of the system, providing limits on the amount of operating days that the vehicle can perform a mission each month. Another environmental factor is the presence of wind turbines and their turbulence in the air and in the water.

From the design exploration phase, many requirements for the design have been generated. Ten of these are highlighted in Table 1, to show the most important, driving requirements for the design.

<sup>1</sup>[The impact of The Seaweed Company](#)

**Table 1:** Top-Level Requirements Table

ID	Description
OPR-ENV-04	The system shall monitor an area of at least 1600000 m2 in size
OPR-NAV-01	The system shall monitor an area that is at least 30 km distant from the shore
PLD-STRC-04	The system shall perform unit structural integrity monitoring at least once every 30 days
PLD-SWG-04	The system shall perform unit seaweed growth monitoring at least once every 30 days
PLD-WTR-01	The system shall perform repeated water quality monitoring at the seaweed farm
SUS-01	The minimum complete system life cycle duration shall be 10 years
SUS-ECO-01	The system shall have a life cycle cost below 320,000 Euros
SUS-ECO-02	The system shall have a sustainable end-of-life solution
SUS-ECO-03	The system shall operate autonomously during the navigation and monitoring phases
SUS-ECO-04	The system shall not require more offshore maintenance than once in 4 months

## System Design

From the exploration phase, four architectures were selected. The first is a small autonomous boat. This architecture was not developed further, because of educational constraints. The next architecture, named Puffin, is a morphing wing drone, that can both fly to cover large distances and dive into the water to monitor the seaweed farm. The third architecture is called Hybrid and is a fixed-wing vehicle that flies to the seaweed farm lands on the water surface and takes its measurements from there. This architecture has been discarded because the quality of the measurements from the surface can not reach high precision quality. The final architecture is the Multi-System and consists of two vehicles, one fixed-wing VTOL vehicle that can deploy an autonomous submarine. The submarine is connected with a tether to the flying vehicle, that has landed on the water surface when the submarine is deployed. This architecture has been discarded because it has to stay on the water surface for a long duration and would become too heavy to be feasible. Finally, the Puffin architecture was chosen.

## Configuration

The vehicle has to perform efficiently both in the air and underwater, this generates very different requirements for the configuration of the UAV. A focus also has to be set on designing the drone to be neutrally buoyant underwater to perform the sensing mission.

All components that have to be kept water-tight are integrated within the nosecone, namely the batteries, PCBs and air propulsion motor. The rest of the components are integrated within a fuselage that is completely submerged. The wings are positioned in a high-wing configuration and are open-ended to limit their contribution to the buoyancy of the vehicle. The fuselage is ended by the water chamber, used to propel the vehicle in the air during the water-to-air transition. The tails are fixed to a collar that is bonded to the water chamber. A render of the side-view of the UAV can be seen in Figure 3, the fuselage and nosecone are hidden for visualisation purposes.

An overview of the main budgets of the vehicle can be seen in Table 2.

**Table 2:** Summary of system budgets

Budget	Value
Production Cost	€58,500
Maintenance per month	€1100
MTOM	13.2 [kg]
Power required	300 [Wh]
Power supply	482.4 [Wh]



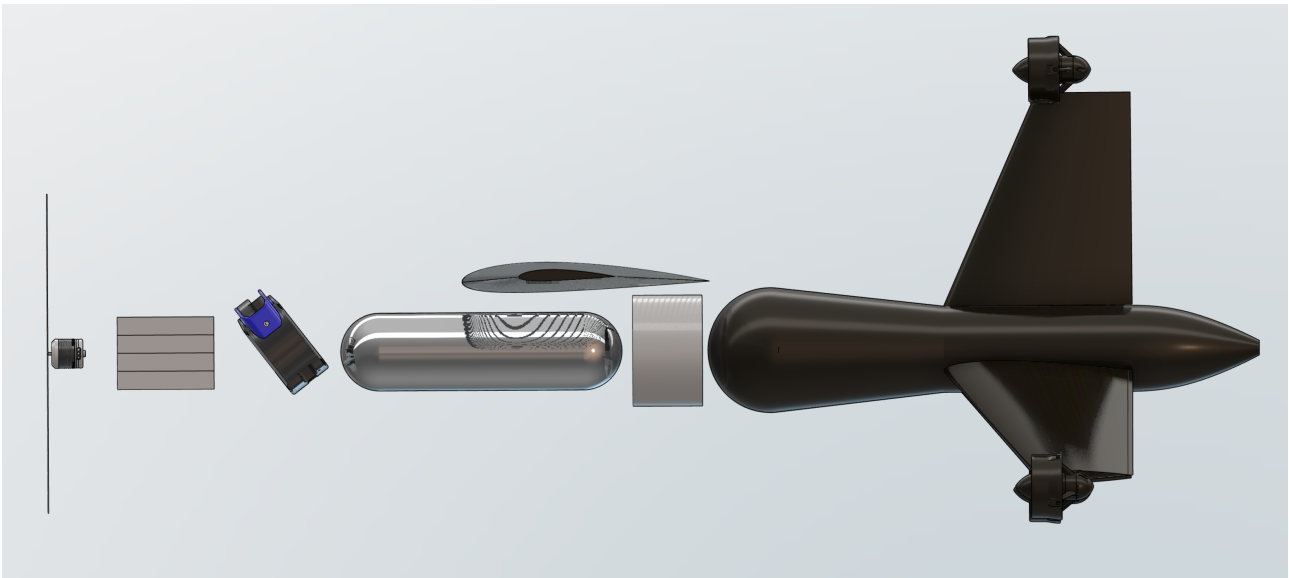


**Figure 3:** Render of the side-view of the vehicle, the fuselage and nosecone are hidden for visualisation purposes

### Risk Assessment and Sustainability Analysis

The SEAMOS team wishes to contribute positively to the environment and thus takes a strong stance on sustainability. The environmental impact of the Puffin has been considered thoroughly in its design. The system will emit no emissions and the material used is mainly recycled CFRP. Further, the system's sonar and cameras ensure that obstacles are avoided and no animals nor flora and fauna are negatively impacted. Moreover, monitoring seaweed growth ensures that it is healthy and can be harvested successfully. This brings the highest quality and largest amount of seaweed to the food market, and hence more people can opt for a sustainable food choice. This encourages a sustainable lifestyle and has a positive impact on society. Sustainability is also considered in the manufacturing of the system. Hence, the philosophy of Lean Manufacturing (LM) is followed. This ensures minimising waste at all levels of the production process. LM encourages the use of renewable energy sources and thereby reduces the carbon footprint of the SEAMOS project.

A technical risk assessment identifies all risks of the design. The most severe risks are the risk of having to rescue the vehicle, failure of the structure, vehicle crashing, mission not being carried out, the inability to come back to base and overlooking errors. The severity decreases for all.

The Puffin design prioritises reliability increasing redundancy. Separate propulsion systems and dual cameras are utilised to reduce the likelihood of failure. Safety measures include obstacle avoidance capabilities, maintaining a safe altitude, and ensuring positive buoyancy for retrieval in case of malfunction. The vehicle's availability is optimised through its ability to operate in various conditions and perform underwater inspections, while maintainability is enhanced by using easily replaceable internal parts and off-the-shelf components.

### Market and ROI

Seaweed farming, currently almost exclusively consisting of near-shore seaweed farming is already a well-established market, with an estimated market value of 15 [bn USD] in 2021, which is expected to grow to 25 [bn USD] by 2028. However, its offshore variant is currently almost non-existent, with a couple of test projects being developed now.

While the growing seaweed market is considered to be a promising market, the performance of the drone is also fitted to be applied to different markets such as general offshore aquaculture monitoring, or offshore energy and infrastructure monitoring. Development for military applications were not considered due to ethical concerns around the potential misuse of the technology, and a divergence from the drone's original intent.

The market study also proposed some design requirements. These included adapting pre-existing requirements set by The Seaweed Company, and the generation of new requirements. An example of the adaptation is the ability to, with the same vehicle, increase the operational range from 30 [km] and monitoring 40 units to 50 [km] and monitoring less units. This has been done to be able to reach more distant wind farms than originally planned. A newly generated requirement is SUS-ECO-03: The system shall operate autonomously during the navigation and monitoring phases. This has been established to provide a competitive advantage over the competition by reducing the need to have a specifically trained operator.

To conclude, it was established that the SEAMOS drone would be a viable solution in the current and future

market, and take advantage of the low maturity of the offshore seaweed farming market.

Additionally, utilising an hourly rental model will provide a return on investment of 91.65% with R&D costs and assuming 15 hours a month at 800 EUR per hour.

## Subsystem Design

Once the mission was clearly outlined, the subsystems were designed in more detail along each phase of the mission

### Sensing

During the airborne part of the mission, the sensors are used for navigation. The vehicle is using GNSS to guide the Puffin the coordinates of the seaweed farm. The IMU allows for correcting any dynamic disturbances. A downward facing camera is used to recognise the seaweed systems in water and allow for finding a splashdown zone, as well as recognising the landing net when returning. It is also used for potential obstacle avoidance.

Once the vehicle dives underwater, sonar becomes the primary navigation sensor. It provides data for the vehicle to recognise the seaweed systems in its field of view. For shorter distances, an upwards facing camera is also used, specifically for detecting the structural elements and navigating along the seaweed systems. It is also the sonar and camera that are used for mapping. A water sampler is used to bring water samples to base and a thermometer to measure the water temperature.

### Air to Water Dive

To ensure a smooth diving entry into the water the impact loads were investigated and a sweeping mechanism. The maximum load the structure will endure is 1700 [N] at a dive velocity of 15 [m/s]. To reduce impact and drag within the water the wings will sweep back using a pneumatic actuator and bevel gears. This will produce a torque of 20 [Nm].

Than minimum angle the system will dive have to dive at is 52 degrees as this will avoid the system from passing through the wave and into the air.

### Water to Air Launch

Water-to-air transition is facilitated by a launch system, leveraging pressurised water as a reaction mass. The launch system is designed to deliver the necessary impulse to bring the Puffin from a submerged position to an aerodynamically stable trajectory in the wind park. All non-structural components are acquired off the shelf with an established high degree of reliability. The water chamber, which is pressurised with high-pressure air from an off-the-shelf tank, is the only component requiring custom manufacturing. Overall, the system delivers an impulsive velocity of 23 [m/s] to the 13.2 [kg] drone.

### Propulsion

The air propulsion unit consists of a single nose-mounted double-blade propeller propelled by a brushless lightweight motor with an electronic speed control unit. The propulsion subsystem has been designed to meet the thrust requirements of 16 [N] at climb and 9 [N] at cruise for 20 [m/s] cruise speed. An off-the-shelf configuration is proposed. The carbon-fibre blades, when not rotating, fold back to limit the water impact. The Puffin needs to have an underwater cruise velocity of 0.5 [m/s] and it should be able to operate in currents up to 1 [m/s]. Furthermore, some thrust in lateral and vertical directions is required to be able to counteract disturbances and monitor in a stable way. The underwater propulsion system comprises three thrusters each mounted on one of the stabilisers of the tail. The three propellers can rotate radially which allows for full body control.



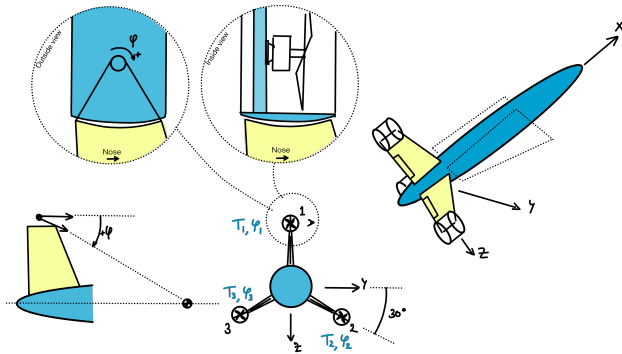


**Figure 4:** The underwater propulsion system where a thruster, with the ability to rotate radially, is mounted on each of the tail blades.

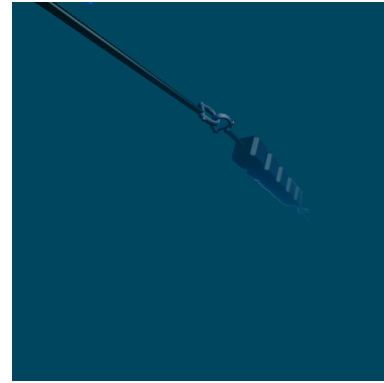


**Figure 5:** The simulated capture of the shackle. It shows a simulation of the turbidity in the north sea.

## Wing and Control Surface

The wing has been designed by first considering airfoils. Based on an aerodynamic analysis and trade-off, the NACA2412 airfoil has been decided on. This airfoil trades off lift and drag characteristics with pitching moments extremely well. Different airfoils either have a too high drag coefficient for given lift coefficients, or providing the required lift performance introduces too big of a moment.

Following this, the wing planform has been determined. This has been optimised for cruise performance, but dive speed had to be taken into account as a limiting factor on the wing size. The resulting wing has a wingspan of 3 [m], with an aspect ratio of 12. Since the Puffin is flying at relatively low speeds, the wing is unswept at the quarter-chord line. The half-wing can be seen in Figure 6.

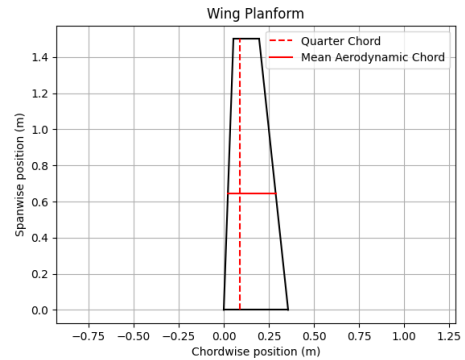


**Figure 6:** Wing Planform

To design the tail different tail configurations were considered for aircraft and submarines. Each configuration was evaluated based on the control authority they provided for their respective mediums. An all-moving Y-tail configuration was chosen due to its superior performance in air and water. The vertical and horizontal fins were sized based on semi-empirical methods from Raymer. The fin sizes were analysed and iterated on for lateral and longitudinal stability and control conditions for the air and underwater. The NACA0012 airfoil was chosen for each tail fin due to its symmetrical shape and high lift performance. Additionally, ailerons were sized and placed on the wings to provide roll control for air operations.

## Structure

Throughout its mission, the Puffin will be subjected to various loads. There are loads induced by the catapult launch, the water launch and the diving impact during the air-to-water transition. Furthermore, the wings and tail are subjected to aero- and hydrodynamic loads during flight and monitoring. To keep all the subsystems together and protect the payload from these external loads, a load-carrying structure has to be designed. The Puffin structure is divided into three groups: The load-bearing structure (fuselage), the wing structure and the tail structure.

The fuselage has a circular cross-section with a 1 [mm] thick skin. Three L-stingers are attached to it to transfer the loads. Including safety margins, the fuselage structure will experience a maximum normal stress of 303 [MPa] and a maximum shear stress of 4.8 [MPa].

To allow for fast water drainage, the wing structure comprises a 1 [mm] thickness shell with an open root and tip chord. The maximum normal and shear stress it experiences due to aero- and hydrodynamic loads are 13.2 [MPa] and 1.7 [MPa] respectively.

Finally, the tail structure is built up from a 1 [mm] thick shell as well. In addition to this, a circular 1 [mm] thick shaft runs through the tail to support the underwater propeller. The maximum normal and shear stresses, due to hydrodynamic loads, the shell undergoes are 5.7 [MPa] and 1.2 [MPa] respectively. The most critical point of the structural design is the circular shaft. It experiences a normal stress of 580 [MPa] due to the water impact.

A recycled carbon fibre-reinforced polymer was chosen as material for the Puffin's structure. It is strong, lightweight, and very corrosion-resistant. Its specifications are listed in the Table 3 below, showing that it can withstand all critical loads.

**Table 3:** List of characteristics of the recycled carbon fibre-reinforced polymer that will be used for the Puffin's structure

Characteristic	Value
Density [ $kg/m^3$ ]	1300
Young's modulus [GPa]	52
Tensile Strength [MPa]	3900
Shear strength [MPa]	115
Compressive strength [MPa]	410

## Flight & Helm Control

The vehicle is controlled by a commercially available flight controller. The firmware for this controller will be adapted to the flight and dive requirements of the Puffin. The sensor data from the camera and sonar sensors will be processed on a companion onboard computer and communicated with the central controller. To verify the usage of a camera and sonar sensor in the navigation around the seaweed farm and the visual inspection of a structural element, a simulation of these sensors in a virtual environment was performed. A capture from the simulation is shown Figure 5. This simulation shows that both the camera and sonar are feasible sensors for use in the high turbidity environment of the North Sea.

## Energy Supply

The battery is made up of eight LiPo battery packs and each pack has the configuration 2S2P and has a capacity of 8000 [mAh].

The battery supplies a total of 482.4 [Wh] to the entire system while the total required power for all subsystems is 300 [Wh], leaving 182.4 [Wh] as a safety margin. The relevant systems requiring power are propulsion, electronics and structures.

## Recommendations on Further Development

Design aspects remain. While the overall feasibility of the architecture is demonstrated, various elements require refinement:

1. In modelling vehicle behaviour, individual components (such as water impact loading) are accounted for, but an integrated simulation is missing. The transition from aerial to aquatic locomotion and vice versa is a novel behaviour, and investigation of dynamics during these phases may have interesting implications. A complete model would incorporate higher fidelity aero-hydrodynamic loading and analysis of (sloshing of) internal fluids.
2. Building on more complete dynamic models, design for and modelling of control and stability should be revisited. Modelling in particular, with constraints on communication and sensor data, should demonstrate that the degree of autonomy required can be executed technically.
3. Component layout and assembly is preliminary, joined by a similarly preliminary structural design. The collection of unique mechanisms (wing sweep, multiple propulsion systems, water impact) drives a complex structure. Efficient integration may achieve significant gains, but inefficient integration may incur heavy penalties.
4. Emission quantification using the Life Cycle Analysis conventions, design hot spot determination, and comparison of possible manufacturing scenarios allowing, should inform design process iterations improving the sustainability of the system.
5. Airfoil optimisation will increase range without incurring extra cost. Currently, a NACA airfoil has been selected, however, NACA airfoils are not optimised for the specific application. Therefore airfoil optimisation has to be done using CFD tools to make the most efficient wing possible.



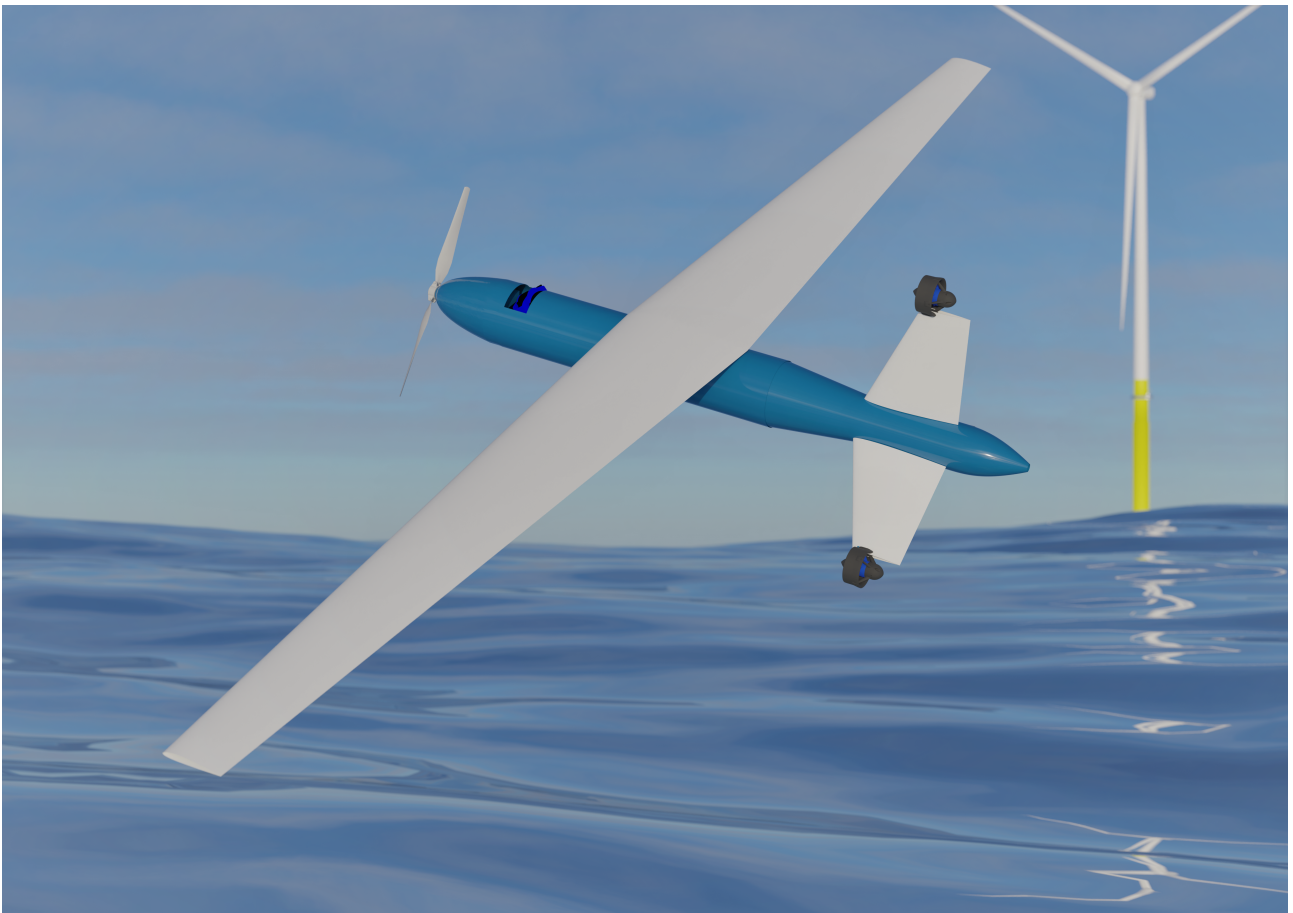


**Figure 7:** Render of final puffin configuration

# Preface

The following report showcases our efforts to find and design a feasible, sustainable and affordable solution for the needs of The Seaweed Company. The task was a part of the Design Synthesis Exercise, a culmination of the Aerospace Engineering Bachelor at the Delft University of Technology.

The SEAMOS DSE posed a fascinating and relevant challenge. The tasks allowed us to utilise the knowledge obtained throughout the Aerospace Bachelor, as well as make us explore unfamiliar concepts. We greatly enjoyed working on the Puffin design, exploring the emerging and exciting area that are diving drones. We believe the project was a suitable end to our Aerospace Bachelor journey.

First and foremost we would like to thank our Tutors, Professor Salua Hamaza and Professor Clemens Dransfeld. We greatly appreciated their help, feedback and the idea behind the SEAMOS DSE. The designed task was challenging but forced us to be creative in exploring our design ideas and solutions. We greatly appreciated our Coaches, Simon van Oosterom and Kherlen Jigjid, for their helpful insight and challenging questions. We would like to thank the SeaEO of The Seaweed Company Joost Wouters. We appreciate the interest and support in our ideas and we wish our best in further expanding the seaweed farming industry. We would like to thank our Teaching Assistant, Korneel Van den Berghe, for his help and feedback. Lastly, we would like to thank André Farinha, for his insightful presentation on his research.

*DSE Group 07 SEAMOS*



# Contents

<b>Executive Overview</b>	<b>i</b>
<b>Preface</b>	<b>viii</b>
<b>1 Introduction</b>	<b>3</b>
<b>2 Project Outline</b>	<b>4</b>
2.1 Project Description . . . . .	5
2.2 Operating Conditions . . . . .	6
2.3 Verification and Validation Process . . . . .	6
<b>I Subsystem Design</b>	<b>8</b>
<b>3 Sensing</b>	<b>8</b>
3.1 Requirements and Assumptions . . . . .	8
3.2 Monitoring Sensors . . . . .	10
3.3 Sonar Outline . . . . .	12
3.4 Telemetry, Tracking, and Command and Data Storage . . . . .	13
3.5 Verification and Validation . . . . .	14
<b>4 Mission Profile</b>	<b>15</b>
4.1 Assumptions . . . . .	15
4.2 Mission Description . . . . .	15
4.3 Launch, Landing, and Ground Operations . . . . .	18
4.4 Mission Planning Considerations . . . . .	20
4.5 Validation . . . . .	21
<b>5 Water to Air Launch</b>	<b>21</b>
5.1 Functional Definition and Design Options . . . . .	21
5.2 Launch Performance Model . . . . .	23
5.3 Propeller Driven Launch Solution $\Delta V$ Scaling . . . . .	23
5.4 High-Power Water Rocket $\Delta V$ Scaling . . . . .	24
5.5 Chamber Pressurization Options . . . . .	25
5.6 Leaping Unit Transfer . . . . .	29
5.7 Launch System Selection and Sizing . . . . .	30
5.8 Wing-integrated Water Chamber . . . . .	32
5.9 Fluid Control and Vehicle P&ID . . . . .	32
<b>6 Air to Water Dive</b>	<b>35</b>
6.1 Requirements . . . . .	35
6.2 Literature . . . . .	35
6.3 Design Options . . . . .	37
6.4 Detailed Design of the Hinge Mechanism . . . . .	38
6.5 Diving Load Impact . . . . .	40

6.6	Verification and Validation . . . . .	42
<b>7</b>	<b>Propulsion</b>	<b>42</b>
7.1	Requirements and Assumptions . . . . .	42
7.2	Aerial Propulsion . . . . .	43
7.3	Water Propulsion . . . . .	48
7.4	Depth Control . . . . .	55
7.5	Iteration on the Underwater Propulsion System . . . . .	57
7.6	Verification and Validation . . . . .	59
<b>8</b>	<b>Wing and Control Surfaces</b>	<b>59</b>
8.1	Requirements and Assumptions . . . . .	59
8.2	Wing Sizing . . . . .	61
8.3	Tail Configuration . . . . .	66
8.4	Tail Sizing . . . . .	67
8.5	Control Surfaces . . . . .	72
8.6	Verification and Validation . . . . .	76
<b>9</b>	<b>Configuration</b>	<b>76</b>
9.1	Design Considerations . . . . .	76
9.2	Nosecone Design . . . . .	77
9.3	Internal Layout . . . . .	78
9.4	Outside Components . . . . .	78
9.5	Mass Budget . . . . .	79
9.6	Center of Gravity . . . . .	80
9.7	Buoyancy System . . . . .	80
9.8	Drainage Model . . . . .	82
<b>10</b>	<b>Structure</b>	<b>84</b>
10.1	Requirements and Assumptions . . . . .	84
10.2	Load-Bearing Structure . . . . .	84
10.3	Wing Structure . . . . .	85
10.4	Tail Structure . . . . .	86
10.5	Take-off and Landing Structure . . . . .	87
10.6	Material selection . . . . .	88
10.7	Verification and Validation . . . . .	88
<b>11</b>	<b>Flight &amp; Helm Control</b>	<b>88</b>
11.1	Requirements and Assumptions . . . . .	89
11.2	Sensor Processing . . . . .	92
11.3	Vehicle Dynamics . . . . .	102
11.4	Controller Architecture . . . . .	102
11.5	Verification and Validation . . . . .	103
<b>12</b>	<b>Energy</b>	<b>105</b>
12.1	Requirements and Assumptions . . . . .	105
12.2	Battery Selection . . . . .	106
12.3	Power Budget . . . . .	106
12.4	Battery sizing . . . . .	107

<b>II System Design</b>	<b>108</b>
<b>13 System Summary</b>	<b>108</b>
13.1 Specification Table . . . . .	108
13.2 System Validation . . . . .	109
13.3 System Sensitivity Analysis . . . . .	109
<b>14 Market Analysis and Return on Investment</b>	<b>111</b>
14.1 Market Analysis. . . . .	111
14.2 Cost Analysis . . . . .	115
14.3 Revenue Generation and ROI . . . . .	117
14.4 Market Absorption . . . . .	118
14.5 The Seaweed Company Analysis . . . . .	119
<b>15 Design overview</b>	<b>119</b>
15.1 Functional Flow and Breakdown Structure . . . . .	119
15.2 Sustainable Development Strategy . . . . .	122
15.3 Technical Risk Assessment . . . . .	123
15.4 Reliability, Availability, Maintainability, Safety . . . . .	129
<b>16 Lifecycle analysis</b>	<b>130</b>
16.1 Goal definition . . . . .	130
16.2 Scope Definition . . . . .	130
16.3 Preliminary Inventory. . . . .	131
16.4 Recommendations . . . . .	131
<b>17 Future Phases</b>	<b>131</b>
17.1 Manufacturing, Assembly and Integration Plan . . . . .	131
17.2 Product Design and Development Logic . . . . .	132
17.3 Project Gantt Chart. . . . .	133
<b>18 Conclusion</b>	<b>135</b>
<b>Bibliography</b>	<b>137</b>



# List of Symbols and Abbreviations

## Acronyms

$\Phi$	bank angle
$C_{l_{\delta_a}}$	aileron control derivative
$C_{l_p}$	roll damping coefficient
ADN	Ammonium Dinitramide
ADS-B	Automatic Dependent Surveillance–Broadcast
AUV	Autonomous Underwater Vehicle
BVLOS	Beyond Visual Line of Sight
C.G.	Center of Gravity
CFRP	Carbon Fibre Reinforced Polymer
COPV	Carbon Overwrapped Pressure Vessel
COTS	Commercial Off The Shelf
CP	Controllable Pitch
EASA	European Union Aviation Safety Agency
ESC	Electronic Speed Control
Eth	Ethernet
FAA	Federal Aviation Administration
FBD	Free-body Diagram
FC	Flight Controller
FP	Fixed Pitch
GNSS	Global navigation satellite system
HPA	High Pressure Air
HYBRID	Hybrid Fixed-Wing VTOL
IMU	Inertial Measurement Unit
LCA	Lifecycle Analysis
Lion	Lithium-Ion
LiPo	Lithium-Polymer
MHD	Magnetohydrodynamic
MSE	Mean Squared Error
MULTI-SYSTEM	Fixed-Wing VTOL with External Payload
NACA	National Advisory Committee for Aeronautics
P	Roll Rate
POI	Point Of Interest
PUFFIN	Peace Upon Fellow Fellowship Incompetent Nerds

PUFFIN	Sweptback Wing Diving Drone
RD	Research and Development
ROC	Rate of Climb
RPM	Revolutions per Minute
TT&C	Telemetry, Tracking and Command
UAV	Unmanned Aerial Vehicle
VTOL	Vertical Take-Off and Landing

### Symbols

$\alpha$	Angle of Attack	[rad]
$\alpha$	Angular acceleration	[rad/s <sup>2</sup> ]
$\Gamma_Y$	Tail Anihedral	°
$\lambda$	Taper Ratio	[-]
$\Lambda$	Sweep Angle	[°]
$\omega$	Angular speed	[rad/s]
$\rho$	Density	[kg/m <sup>3</sup> ]
$\sigma$	Normal Stress	[Pa]
$\tau$	Shear Stress	[Pa]
$a$	Acceleration	[m/s <sup>2</sup> ]
$b$	Wing Span	[m]
$CO_2$	Carbon Dioxide	
$C_2H_2$	Acetylene	
$C_d$	Drag Coefficient	[-]
$C_l$	Lift Coefficient	[-]
$CaC_2$	Calcium Carbide	
$Ca(OH)_2$	Calcium Hydroxide	
$D$	Drag	[N]
$E$	Young's Modulus	[GPa]
$f$	Frequency	Hz
$H_2O$	Water	
$I$	Second Moment of Inertia	[m <sup>4</sup> ]
$J$	Polar Moment of Inertia	[m <sup>4</sup> ]
$K$	Kelvin	[-]
$K_{tail}$	Tail Correction Factor	[-]
$L$	Lift	[N]
$M$	Bending Moment	[Nm]
$m$	Mass	[kg]
$M_r$	Rotational torque	[Nm]

$O_2$	Oxygen	
$P$	Power	[W]
$p_c$	Water Chamber Pressure	[Pa]
$Q$	First Moment of Inertia	[m <sup>3</sup> ]
$Q$	Shaft Torque	[Nm]
$Re$	Reynolds Number	[-]
$S$	Surface Area	[m <sup>2</sup> ]
$S$	Surface Area	[m <sup>2</sup> ]
$S_V$	Vertical Tail Surfaces Area	[m <sup>2</sup> ]
$S_{HPROJ_V}$	Horizontal Tail Projection Area	m <sup>2</sup>
$S_{VTail}$	Tail Fin Area	m <sup>2</sup>
$S_{Y_V}$	Vertical Tail Projection Area	m <sup>2</sup>
$T$	Thrust	[N]
$V$	Shear Force	[N]
$V$	Velocity	[m/s]
$V_c$	Water Chamber Volume	[m <sup>3</sup> ]
$V_H$	Horizontal Tail Volume Coefficient	[-]
$V_V$	Vertical Tail Volume Coefficient	[-]

# 1 Introduction

The final report encompasses all detailed designs of the chosen architecture, the Puffin. This morphing wing diving drone is a unique design that tackles the problem of offshore monitoring, specifically, for offshore seaweed farms. 'The Seaweed Company' commissioned a group of 10 students to research and develop an autonomous system that could monitor an offshore seaweed farm within a 10-week time period. This offshore seaweed farm is situated in Borssele wind park within the North Sea. Its waves, currents and wind turbulence, caused by the wind turbines, make it a challenging environment to operate in. The system should be sustainable and cost-effective in the long term.

Prior to this report, the midterm report [1] explained the process of achieving the concept of the Puffin. Four main architectures were undergoing the trade-off and are displayed below in Figure 1.1.

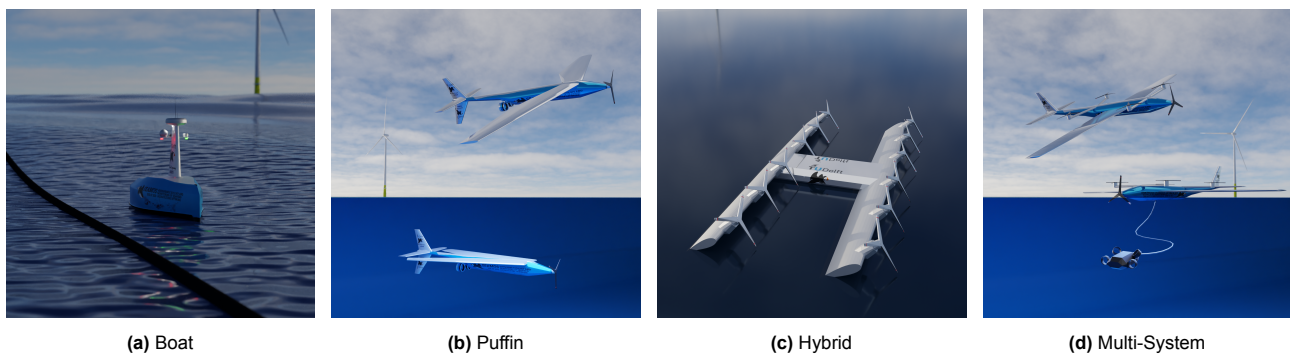


**Figure 1.1:** Impression of all designs, showing preliminary ideation of the four concepts [1]

The architecture was selected through a thorough trade-off process. The process included both quantitative and qualitative elements as well as a sensitivity analysis. Each architecture was ranked based on the parameters energy (30%), cost (30%), reliability (25%), and market (15%). A sensitivity analysis was then carried out to understand the influence of each weight where energy was the only parameter that really influenced the leading architecture. After evaluating all results and having a group discussion it was decided that the Puffin architecture won.

The report investigates all the different subsystems within the Puffin design which includes: sensing, air-to-water dive, water-to-air launch, propulsion, wing and control surfaces, structure, flight and helm control, and energy supply. Together the mission profile and its top-level requirements are achieved. The puffin architecture entails a unique mission profile: the Puffin must fly 30 kilometres from shore in a fixed-wing fashion. It then proceeds to dive into the sea at the desired location and acts like a submarine. It monitors the units of the seaweed farm consecutively until it has completed its maximum and it ejects itself out of the water. It opens its wings and flies back to shore where it will be retrieved by company employees.

The system requires a specific payload for the monitoring of seaweed farms. The client requested that for the payload it should be able to observe the structural integrity of the seaweed net as well as the growth of the seaweed and a water sample to be tested back on shore. This could be done with a variety of different sensors and is investigated in Chapter 3.

The transition phases are also thoroughly researched, having considerations for the mass of the structure, the type of propellant used and the height at which the system must enter and exit the water or the sweeping mechanism of the wings. All these considerations are discussed in the two chapters: Chapter 5 and Chapter 6.

Another important aspect of the design is the way it propels itself above and below water. This has a significant impact on the mass of the batteries and the range of the system. Seeing as there are two different environments the system must act in, two options will be considered, a morphing propulsion system, or two separate. This works closely with control surfaces to enable all maneuverability within its environment. All these factors are explored in Chapter 7 and Chapter 8.

It is compulsory for the system to be autonomous which is a difficult task to tackle as TT&C (telemetry, tracking, and control) solutions are heavily limited by the operating conditions. The system must move by itself from onshore. The path the system follows must move, while taking in relevant data of its surroundings, and must follow the farm using the objects and their relative distance from them. The autonomous system works in three phases: perception, state estimation and path planning. This problem remains in state estimation and a problem that is solved in Chapter 11.

Finally, the configuration and the structure such as the wing and the fuselage are discussed in Chapter 9, Chapter 10 and Chapter 8. Material consideration and loading at attachment points are discussed as well as the aerodynamic loads.

All of the subsystems are summarised within Chapter 13 which concludes part 1 of the report. In part 2, more of the non-technical aspects are discussed. This is then followed by a market exploration and the system's application to other uses and so increasing the profit margin. Together with the market analysis, the return on investment is found in Chapter 14. In the risks involved and the sustainability plan is explored. There is also an exploration into RAMS (reliability, availability, maintainability and safety). The LCA (lifecycle analysis) is described within Chapter 16 and highlights sustainability at later stages of the system development. The final chapter, Chapter 17 indicates elements after R&D (research and development). This includes a manufacturing flow diagram, product design and development logic and a project Gantt chart which indicates the timeline after DSE activities. The budgeting of resources, such as energy, mass and cost are throughout the report. Chapter 18 contains the conclusion.

## 2 Project Outline

In this chapter, an outline of the entire project as well as the structure of the report is described. This chapter contains the project description, compliance matrix, operating conditions and the verification and validation method.



## 2.1. Project Description

Seaweed-based products are a sustainable alternative for various applications in the food industry, pharmaceuticals, and agriculture. Seaweed farming is the fastest-growing aquaculture industry thanks to its multidisciplinary use, this induces the need to expand seaweed farming to off-shore environments. To be financially viable, the farm has to be monitored autonomously.

Hence the purpose of this project is to design a solution that can autonomously and sustainably monitor the structural integrity and seaweed growth in offshore aquacultures. The system has to monitor an entire seaweed farm, thirty kilometres offshore on a monthly basis. The farm comprises forty, 100-meter-long nets on which the seaweed grows. The system has to collect a water sample, monitor how the seaweed grows and observe whether the structural elements of the units are still intact.

**Table 2.1:** Top-Level Requirements and Compliance Table

ID	Requirement	Puffin	Compliance	Verification
<b>Operations</b>				
OPR-NAV-01	The system shall monitor an area that is at least 30 km distant from the shore	30 [Km]	Yes	See Section 7.2.2 and Section 12.4
OPR-ENV-02	The system shall be able to operate at windspeeds of 5 [m/s]	5 [m/s]	Yes	See Section 7.2
OPR-ENV-03	The system shall be able to operate in sea currents of 1 [m/s]	1 [m/s] and more	Yes	
PROP-AQUA-02	The system shall have an underwater cruise velocity of 0.5 [m/s]	0.5 [m/s] and more	Yes	See Section 7.5
OPR-ENV-04	The system shall be neutrally buoyant in the water		Yes	See Section 9.7
<b>Sensing</b>				
PLD-STRC-04	The system shall perform unit structural integrity monitoring at least once every 30 days		Yes	See Section 4.2
PLD-SWG-04	The system shall perform unit seaweed growth monitoring at least once every 30 days		Yes	See Section 4.2
PLD-WTR-01	The system shall perform repeated water quality monitoring of TBD seaweed production units		Yes	
<b>Control</b>				
CTRL-SEN-04	The helm control system shall determine the path of the vehicle to the target underwater		Yes	Chapter 11
OPR-NAV-05	The system shall execute an emergency procedure with direct communication with the base.		Yes	Section 4.4
PLD-INS-04-02	The system shall follow the seaweed unit within 5 m	2 m	Yes	Section 11.2.4
SUS-ECO-03	The system shall operate autonomously during the navigation and monitoring phases		Yes	Chapter 11
<b>Sustainability</b>				
SUS-01	The minimum complete system life cycle duration shall be 10 years			
SUS-ECO-01	The system shall have a life cycle cost below €320,000.	€230,000	Yes	See Section 14.2
SUS-ECO-02	The system shall have a sustainable end-of-life solution	TBD	Depends on LCA outcome	See Chapter 16
SUS-ECO-03	The system shall operate autonomously during the navigation and monitoring phases		Yes	

Continued on next page

Table 2.1 – continued from previous page

ID	Requirement	Puffin	Compliance	Verification
SUS-	The system shall exhaust zero emissions during its mission	TBD	Depends on LCA outcome	See Chapter 16
<b>Structures</b>				
SUS-	The system shall be able to withstand 1636 [N] of impact loads.	12 [kN]	Yes	See Section 10.2
SUS	The system shall be able to withstand 850 [N] of launch loads	12 [kN]	Yes	See Section 10.2
SUS	The system shall not be critically damaged by corrosion within one year of operation	TBD	Has to be tested	See Section 10.6
<b>Power &amp; Propulsion</b>				
SUS-	The system's batteries shall have a capacity of 300 [Wh]	482 [Wh]	Yes	See Section 12.4
SUS-	The system shall be able to generate 16 [N] of thrust in air	27 [N]	Yes	See Section 7.2.2
SUS-	The system shall be able to generate 18 [N] of thrust in water	100 [N]	Yes	See Section 7.5
LNC-03	The preliminary launch system shall deliver a $\Delta V$ of 21 m/s	21 [m/s]	Yes	See Chapter 5

## 2.2. Operating Conditions

The operating conditions are one of the biggest challenges for the system. Performing a mission in the offshore environment means you will encounter, high waves, windspeeds and sea currents. Furthermore, wind turbines make the air in the park turbulent and unsuitable for flight. This limits the envelope available for flight in the park to the range between 2 and 33 meters from sea level.

The North Sea current tends to always occur in the same line of trajectory. The seaweed system's units will be aligned with these currents which can be used in a beneficial way for the operations. The system will be designed to operate in currents up to 1 [m/s].

In the most critical conditions, the wind velocities on operating days can rise to 10 [m/s]. The wave height can increase to 1.8 [m]. However, most of the time the wind velocities are lower than 0.4 [m/s] and the wave height stays below 0.6 [m].

## 2.3. Verification and Validation Process

Developing a complex system requires one to answer the following questions: 'Are the requirements met by the system?' and 'Has the correct system been designed?'. The former aims to tackle verification which is defined as the 'proof of compliance with design solution specifications and descriptive documents' [2]. The latter focuses on validation, which is the 'proof that the product accomplishes the intended purpose based on stakeholder expectations' [2].

The SEAMOS project's verification and validation process is split into four parts: requirement validation, model validation, product verification, and product validation. Requirement validation encompasses checking if the requirements comply with the acronym VALID [2]. VALID stands for:

- **V**erifiable
- **A**chievable
- **L**ogical
- **I**ntegral
- **D**efinite

When writing requirements, the team carefully made sure that the acronym was met. A model is everything that predicts and/or describes system behaviour [2]. Model validation looks at the correctness of the models and ensures that they support the design and verification. Models may be validated by:

1. Experience - looks at similar models and their applications in comparable conditions

2. Analysis - ensures that all parts of a model are integrated correctly and are correct by itself
3. Comparison - compares the model to actual test data or other, independent models that have been proven to be valid

Product verification involves four main methods [2]:

1. Inspection: Either documentation or the product itself can be looked at to see if the requirement complies
2. Analysis: Analysis techniques, such as mathematical ones, are used to establish if the product meets the requirement
3. Demonstration
4. Test: The product is tested in a simulated environment under similar conditions to see if the requirement is fulfilled

Throughout the following report, every chapter that focuses on the design of a subsystem of the Puffin starts with a verification table. It outlines which of the above mentioned method is used to verify each requirement. The table outline can be seen below:

**Table 2.2:** \*Example Table\* Verification methods for the relevant requirements. D: demonstration, A: Analysis, I: Inspection, T: test

Requirement	Verification Description	Method
ABC-DEF-01	Description Here	T,A

Lastly, product validation is considered. Several techniques exist and, starting with the least severe, are as follows:

- End-to-End Information System Testing: aims to demonstrate the compatibility of the project information system such as data, timing, etc.
- Mission Scenario Tests: aims to show that flight hard - and software can execute the system's mission under flight-like conditions without a having the real timeline
- Operations Readiness Tests: show that the system can operate int the real environment
- Stress-Testing and Simulation: analyse the robustness of the system while exposing it to variations in performance and fault conditions

# PART I

## SUBSYSTEM DESIGN

### 3 Sensing

#### 3.1. Requirements and Assumptions

In order to choose the sensors for the PUFFIN, several assumptions were made. They are:

- Fouling<sup>1</sup> of the shackles is insignificant for monitoring
- The Puffin can move under the seaweed farm
- The turbidity is such that a camera's horizontal visibility is at least 1 m

Requirements on the sensing system are collected in Table 8.1, carried forward from the system definition in the baseline report [3]. The sensing system is designed in accordance with these requirements; requirements on other (sub)systems emergent from sensing design are collected in Table 3.2.

**Table 3.1:** Sensor Incoming Requirement Table. These requirements have been generated during the initial design and guide the design of the sensing system.

ID	Description	Traceability	Rationale
CTRL-01	The flight control system shall map its surroundings with sufficient detail to navigate.	From discussion	Collision avoidance -
DET-POS-03	The system shall be able to determine when it is at the surface of the water	From discussion	Communication and GNNS can be established only at the surface
DET-POS-05	The system shall be able to determine its depth with 0.01 m accuracy while underwater	From discussion	For position tagging of the scan data
DET-POS-06	The system shall determine its position relative to the seaweed net with 0.01 m accuracy while underwater	From discussion	Higher accuracy relative to unit, collision avoidance
DET-POS-07	The system shall determine its global position with 10m resolution while submerged	From discussion	Submerged navigation, positioning relative to unit is finer
OPR-NAV-03-01	Mission signal transmissions shall adhere to regulation put forth by the Rijksinspectie Digitale Infrastructuur (RDI)	From discussion	Regulatory stakeholder
PLD-STRC-02	The system shall perform structural monitoring at 6 POI per unit	From TSC, drawing of typical unit	Measurement location rel unit, new data from TSC

Continued on next page

<sup>1</sup>Fouling: unwanted material deposition or formation on the surface of an object



Sensor Incoming Requirement Table 3.1 – continued from previous page

ID	Description	Traceability	Rationale
PLD-STRC-03	The system shall inspect each POI with sufficient detail to make a maintenance decision	From TSC	Specification of the measurement data
PLD-SWG-02	The system shall perform unit seaweed growth monitoring with sufficient resolution to model the seaweed growth	From TSC	Specification for a portion of the unit that should be monitored
PLD-WTR-01	The system shall perform water quality monitoring once during every mission	From TSC	Specification on sufficient sample size for seaweed growth monitoring
PLD-WTR-02	The system shall monitor the water quality at specifiable positions relative to the unit	From TSC	Specification for a portion of the unit that should be monitored
PLD-WTR-05-01	The system shall measure the unit current within 0-10 m/s with 0.1 m/s accuracy	From TSC	Specification of the measurement data
PLD-WTR-05-03	The system shall measure the unit photon flux at specifiable positions relative to the unit	From TSC	Specification of the measurement data
PLD-WTR-05-04-01	The system shall measure the unit volumetric nutrient concentration of NO3	From TSC	Specification of the measurement data
PLD-WTR-05-04-02	The system shall measure the unit volumetric nutrient concentration of NO2	From TSC	Specification of the measurement data
PLD-WTR-05-04-03	The system shall measure the unit volumetric nutrient concentration of PO4	From TSC	Specification of the measurement data
PLD-WTR-05-04-04	The system shall measure the unit volumetric nutrient concentration of Si	From TSC	Specification of the measurement data

**Table 3.2:** Sensor Outgoing Requirement Table. Requirements on other systems imposed by the sensing system

ID	Description	Traceability	Rationale
CTRL-POS-03	The system shall be able to maintain its position relative to the seaweed system with a precision of 0.5 m	Need to stay within sensor range	
DET-POS-04	The position of the system with respect to the seaweed unit shall be known with a precision of 1 m	Need to be able to find the unit again. This is just the position wrt the general position unit, not the net during monitoring.	
PLD-INS-01	The system shall provide 4 GB of data capacity per unit planned in the mission	From PLD instrument options	Sensors generate data that needs to be stored while performing mission
PLD-INS-01-01	The system shall provide 225 x 190 x 98 mm for the sonar sensor		
PLD-INS-02-01	The system shall provide 20 W to the Sonar sensor.	From PLD instrument options	Some instruments require power

Continued on next page

Sensor Outgoing Requirement Table 3.2 – continued from previous page

ID	Description	Traceability	Rationale
PLD-INS-03-01	The system shall be able to attain any roll angle with an accuracy of 0.1 degrees	From PLD instrument options	PLD options require pointing
PLD-INS-03-02	The system shall be able to attain any pitch angle with an accuracy of 1 degree	From PLD instrument options	PLD options require pointing
PLD-INS-03-03	The system shall be able to attain any heading angle with an accuracy of 1 degree	From PLD instrument options	PLD options require pointing
PLD-INS-04-01	The system shall approach a structural element to within 0.5 m	From PLD instrument options	PLD options have specific range requirements
PLD-INS-04-02	The system shall follow the seaweed unit within 5 m	From PLD instrument options	PLD options have specific range requirements
PLD-INS-05	The system shall accommodate the submersion of water quality monitoring instrumentation to a depth of 5 m	From PLD-WTR-05-04 instrument options	Water quality must be measured at depth, WTR-05-04 cannot be measured without submersion
PLD-INS-07	The system shall provide a local downlink to offload the mission data when at the base	Delivery of the data to the operator/client	Open-ended as of now

### 3.2. Monitoring Sensors

The sensors used for the monitoring of the seaweed water quality, growth and shackle structure will be described in this section.

#### 3.2.1. Underwater Monitoring and Navigation

Within the underwater phase, navigation and monitoring sensors need to be traded off. Monitoring can be done through visible inspection or by a specialised sensor. Hence, the following sensors were considered:

- **Visible light (VL) camera** - A camera that utilises visible light to take pictures.
- **Ultrasonic (US) testing** - A contact sensor that sends out an acoustic vibration that can detect defects within the material.
- **X-ray** - An X-ray sensor uses X-ray wavelengths to produce an image that allows examination of the interior of a material.
- **Eddy currents** - Through the variation of induced eddy current patterns defects within the material are detected.
- **Sonar** - Sonar uses sound waves to produce a 3D image.
- **LiDAR** - A sensor that produces 3D images through the use of laser beams.

There are several obstacles when it comes to monitoring underwater. Firstly, an important factor is the turbidity of water in the North Sea. R.Wilson and M.Heath [4], investigated the SPM (suspended particulate matter [ $\text{gm}^{-3}$ ]) is high in the zone of the Borssele wind park with a value of around 10 [ $\text{gm}^{-3}$ ]. This can be seen in Figure 3.1.

Therefore, the choice of sensors is evaluated through the criteria of range, mass and turbidity. The table with these specifications is shown in Table 3.3.

**Table 3.3:** Sensors range, mass and turbidity specification

Sensor	Range	Mass	Turbidity
VL Camera	~10[m]	~100[g]	Dependent
US testing	~5[cm]	~200[g]	Independent
X-ray Camera	<1[m ]	<9[kg]	Independent
Eddy Currents	<5[cm]	~250[g]	Independent
Sonar	<50[m]	~1.5[kg]	Independent
LiDAR	<50[m]	<7[kg]	Dependent

The environment in which the drone is operating in is consistently moving which may make monitoring difficult if it has to be nearby. From the table we can observe that US testing, eddy currents would make the significantly more complex due to its minimal range consequently these options are discarded.

In terms of turbidity, the VL camera and LiDAR will have large issues underwater. They are very dependent on the clarity of the water and through research, as explained prior and can be seen in Figure 3.1, the North Sea in the area of Borssele has high turbidity. These options can therefore be discarded.

The final sensor options are the sonar camera and the x-ray camera and the final factor to compare is mass. The aim of the payload is to be as light as possible to ensure that fixed-wing flight is feasible and a larger mass budget can be applied to complex systems such as water tanks or the battery. The X-ray sensor also has a minimal range for the 100 [m] net.

In conclusion, *the best sensor would be sonar*. Sonar can be applied to seaweed observation and structural integrity through pattern recognition of the seaweed farming unit. This sonar sensor will be used in combination with an upward-facing camera, where the sonar will be used for navigation and biomass estimation and the camera will be used for detailed inspection of individual structural elements.

**Water sampling** According to the requirement PLD-INS-06 the system must take a water sample for the seaweed company to analyse or alternatively analyse the water on-site. The system needs to maintain its cost budget and mass budget therefore, reducing the amount of payload is preferable. This is why the water sample will not be analysed onboard. Taking a water sample back also allows for market flexibility as each client can perform their own unique tests.

The water sample will be taken by a small system in the fuselage of the vehicle, consisting of multiple 100ml water reservoirs that operate as a syringe to take the water with the vehicle back to the base. There will be four water reservoirs, one for each measurement, as measurements sometimes need preservatives already present in the reservoir for accurate nutrient measurement [5]. By separating all four measurements, the most flexibility is preserved to change the measured quantities later. The syringe will be operated by a single servo, that actuates the sample-taking mechanism. A schematic of this system can be seen in Figure 3.2. There will also be a temperature and photon flux sensor on the top of the vehicle, next to the sonar and camera sensors.

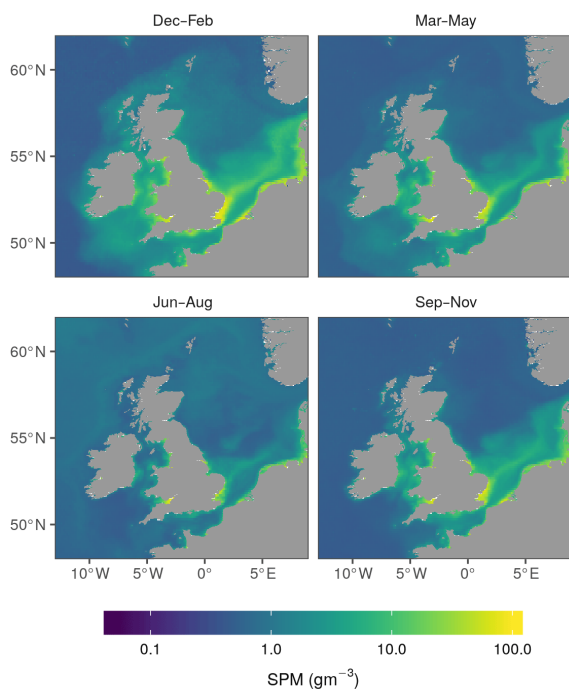


**Figure 3.1:** "Seasonal climatologies of non-algal suspended particulate matter at the water surface for the period 1997–2017. SPM was calculated from Copernicus GlobColour estimates, which are derived from remote sensing data using the Gohin (2011) algorithm." [4]

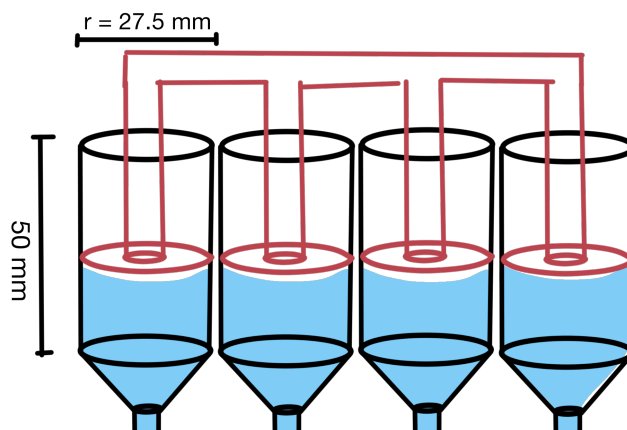


**Figure 3.2:** Schematic of water sample system, located in the fuselage. There is a sampling reservoir for each individual measurement. A single reservoir is approximate 100 [mL] and is 50 [mm] high with a radius of 27.5 [mm]

### 3.3. Sonar Outline

The sonar that will be used is the TriTech Gemini 1200ik multibeam imaging sonar<sup>1</sup>. It is ideal as it can be used for navigation, i.e. obstacle avoidance, and imaging. Its weight in water is 0.44 [kg] and 1.46 [kg] in air. It can monitor the seaweed in detail by creating multibeam images at a frequency of 1200kHz at a short range of 0.1 [m] up to 50 [m]. It does so by swimming beneath the net and pointing the device upwards. The field of view amounts to 120 ° beam width in a horizontal direction and 12 ° beam width in a vertical direction. Furthermore, the sonar can operate at a second, lower frequency of 720 [kHz] for a longer range of 0.1 [m] up to 120 [m]. This will be mainly used for navigation. Here the FOV attests to 120 ° horizontal and 20 ° vertical.

**Table 3.4:** Key specifications for the Gemini 1200ik multibeam imaging sonar

Sonar Specifications	High frequency	Low frequency
Frequency	1200 [kHz]	720 [kHz]
Range	0.1 [m] - 50 [m]	0.1 [m]-120 [m]
Weight	air: 1.46 [kg] water: 0.44 [kg]	idem
Angular Resolution	0.12°	0.25°
Nr. of beams	1024	512
Horizontal beam width	120°	120°
Vertical beam width	12°	20°
Range resolution	2.4 [mm]	4 [mm]
Power	9.5 [W] - 27 [W]	idem

#### 3.3.1. Sonar Resolution

The Trittech Gemini 1200ik sends out 1024 beams every pulse. This results in an angular resolution of 0.12°. When approaching a structural element, like a shackle, at a distance of 0.5 [m], from trigonometry, the sonar has a resolution of approximately 1 [mm] in the horizontal direction. From the information of the sonar, general depth maps of the element can be generated. At this distance, the sonar can inspect objects of approximately 0.8[m] by 0.1 [m]. These dimensions can also be seen in Figure 3.3a. During the seaweed monitoring, the vehicle will follow the unit below and to the side, at an angle to point the sonar towards to farm. The sonar will

<sup>1</sup>TriTech Gemini 1200ik

have a resolution of 10 [mm] at this distance.

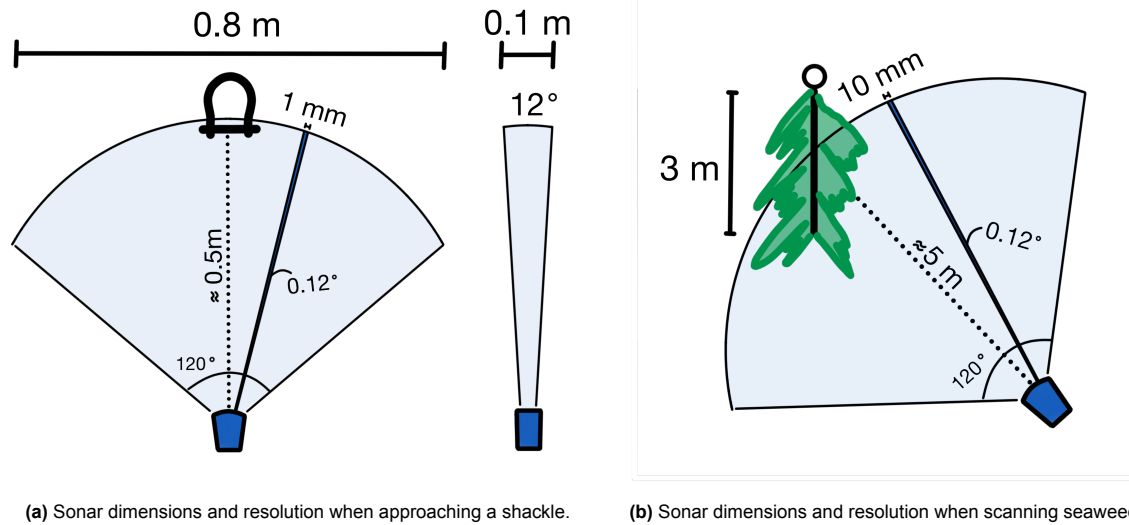


**Figure 3.3:** Sonar scanning dimension and resolution. The sonar will be used at different distances. For the structural elements, a resolution of approximately 1 mm can be achieved. For the seaweed scanning, a resolution of approximately 10 mm can be achieved.

### 3.4. Telemetry, Tracking, and Command and Data Storage

While the vehicle is above water, a reliable connection to the shore can be made. Using this connection, various telemetry signals will be sent to the operator while the vehicle is not submerged. From below the water's surface, creating a reliable connection to the shore is very hard, since the radio waves used do not travel in water well. Creating this connection is not considered to be necessary. All data generated by the monitoring of the unit will be stored on the vehicle until it returns back to the shore, where the data will be downloaded using a local wired or wireless connection. For a typical unit inspection of 50 points of interest, where a photo is taken at each POI, will require 2.5 [GB], when each photo is 50 [MB]. To store the data generated during a seaweed unit scan, 0.6 [GB] is required. To store the entire data range of the sonar from 0 to 50 [m] in its native depth resolution of 2.4 [mm], 20833 levels are needed. This can be stored in 16 bits. Another 32 bits are reserved for the position data of each point. For this initial estimate, every point has a position tag. This can be compressed later, by combining data points taken from the same location and only storing the necessary difference information of the position.

If a unit would have 50 POI and has to be scanned from both sides, a data storage of approximately 4 [GB] per unit would be needed. This is a worst-case scenario, as most units only need structural monitoring and only some need the seaweed scanning. Seaweed scanning can also be done from one side. Data storage is cheap and available, so these storage demands are not a limiting factor.

The European Union Aviation Safety Agency implemented regulations regarding autonomous UAV operating Beyond Visual Line of Sight (BVLOS) [6]<sup>1</sup>. The system has to communicate its location and avoid any interference with other flying units. The ADS-B [7] system is required for the mission conditions by both EASA and FAA<sup>2</sup>, Figure 3.4b. The ADS-B receives and communicates the locations of the ground stations and other active units utilising a GNSS satellite connection. The ADS-B coverage covers the flight path for the mission. A new addition to UAV TT&C requirements is the need for a Remote ID transmitter [8]. The Remote ID is currently only required by the FAA but is expected to be a worldwide identification standard. A Remote ID transmission unit is included in the configuration. Due to the limited coverage of radio and cellular solutions, a satellite transmitter-receiver<sup>3</sup> is implemented in order to allow for status data transmission and ground station emergency inputs. As satellite, radio and cellular transmission is not possible when fully submerged at the monitoring depth, the system will not transmit data or location during monitoring. The system will use the Inertial Navigation system for underwater position tracking, as further explained in Chapter 11. A proposed configuration for the air TT&C can be seen in Table 3.5 and Figure 3.4b<sup>4 5</sup>. The units will be placed in the fuselage. As the carbon fibre structure of the nose and fuselage would cause high attenuation and absorption of the GNSS signals, an outer carbon-fibre antenna will be implemented.

<sup>1</sup>BVLOS OPERATIONS: EXPANDING THE FRONTIER

<sup>2</sup>Automatic Dependent Surveillance - Broadcast (ADS-B)

<sup>3</sup>RockBlock 9603

<sup>4</sup>E-identification idME Data sheet & User manual

<sup>5</sup>Receiver AERO Datasheet & User manual

**Table 3.5:** Power, mass and cost of the TT&C elements

Suggested product	Power [W]	Mass [kg]	Cost [Euro]
E-identification idME	0.075	0.006	175
Receiver AERO	0.35	0.006	200
RockBLOCK 9603O	2.2(maximal in flight)	0.036	263



(a) The suggested configuration of a Remote ID receiver, GNSS ADS-B and satellite transmitter-receiver



(b) ADS-B required by FAA for different mission conditions

**Figure 3.4:** The configuration of the TT&C elements and the ADS-B requirements

### 3.5. Verification and Validation

#### Verification

**Table 3.6:** Verification methods for the relevant requirements of the sensing system. D: demonstration, A: Analysis, I: Inspection, T: test

Requirement	Verification Description	Method
CTRL-01, DET-ATT-03, DET-POS-06, DET-POS-07	Place a weighted ball in a pool (at least 10m) with known coordinates. Do several measurement tests with the sensor and compare results.	T
PLD-WTR-01	Write a simulation in python to see if the system has time to take a water sample during one mission	A
PLD-WTR-02	Test in a pool. Show that the buoyancy system can hold a water sample up to 5 m depth	T
PLD-WTR-05-01	Emerge the sonar underwater, indicate a target. When it resurfaces, see if the IMU, GNSS and sonar managed to announce their position being the same as the specified target	T
PLD-WTR-05-03	Place the camera system underwater and determine its light intake	D,T
PLD-WTR-05-04-01, PLD-WTR-05-04-02, PLD-WTR-05-04-03, PLD-WTR-05-04-04	Take a water sample and show that the asked concentrations can be found	T
DET-POS-03, DET-POS-05	Gradually lower the system in water and measure depth. Compare measurements with known depth.	T
OPR-NAV-03-01	Check documents or call the responsible person	I
PLD-01, PLD-INS-02, PLD-STRC-02, PLD-STRC-03, PLD-SWG-02	Do a demonstration on a unit and inspect recordings.	D



**Validation** The goal of the sensor package is to produce useful data for client analysis and navigation of the system. To validate that the client's needs are fulfilled the data can be shown to the client and they can supply feedback.

To ensure that the navigation works, a simulation can be formulated to investigate whether the perception data encompasses sufficient detail to satisfy the first phase of the autonomous system. For example, this can be done through software like Simulink, ROS, etc...

## 4 Mission Profile

In this chapter, the mission profile is described. The chapter is split into subsections on Assumptions, Mission Description, Launch, Landing and Ground Operations, Mission Planning Considerations and Validation.

### 4.1. Assumptions

In the design of the Mission Profile, several assumptions were made. They are:

- Wind velocity is lower than 11 [m/s] [1].
- Water current velocity is lower than 0.9 [m/s] [1].
- Wave height is below 1.8 [m] [1].
- The GNSS coordinates of the seaweed farm are known.
- The current is largely parallel to the seaweed systems.
- Seaweed scanning ground speed is 0.5 [m/s].
- Transfer velocity ground speed is 1.0 [m/s].
- The vehicle inspects 40 seaweed system within one journey.

### 4.2. Mission Description

This section outlines the mission profile, beginning after launch and ending with recovery. Figure 4.1 visualises the mission of the vehicle and is elaborated upon in the list below the figure. The full mission duration is estimated at 385 minutes, with 65 minutes in the air and 320 minutes underwater. The assumed paths are though straight, the velocities do not take into account potential disturbances and the maneuvers are assumed ideal every time. That would though not always be the case. In order to accommodate the sub optimal mission conditions, a safety factor of 1.2 is put on top of the total mission time. The total mission time is 7 hours 40 minutes and thus fits within a working day of 8 hours.

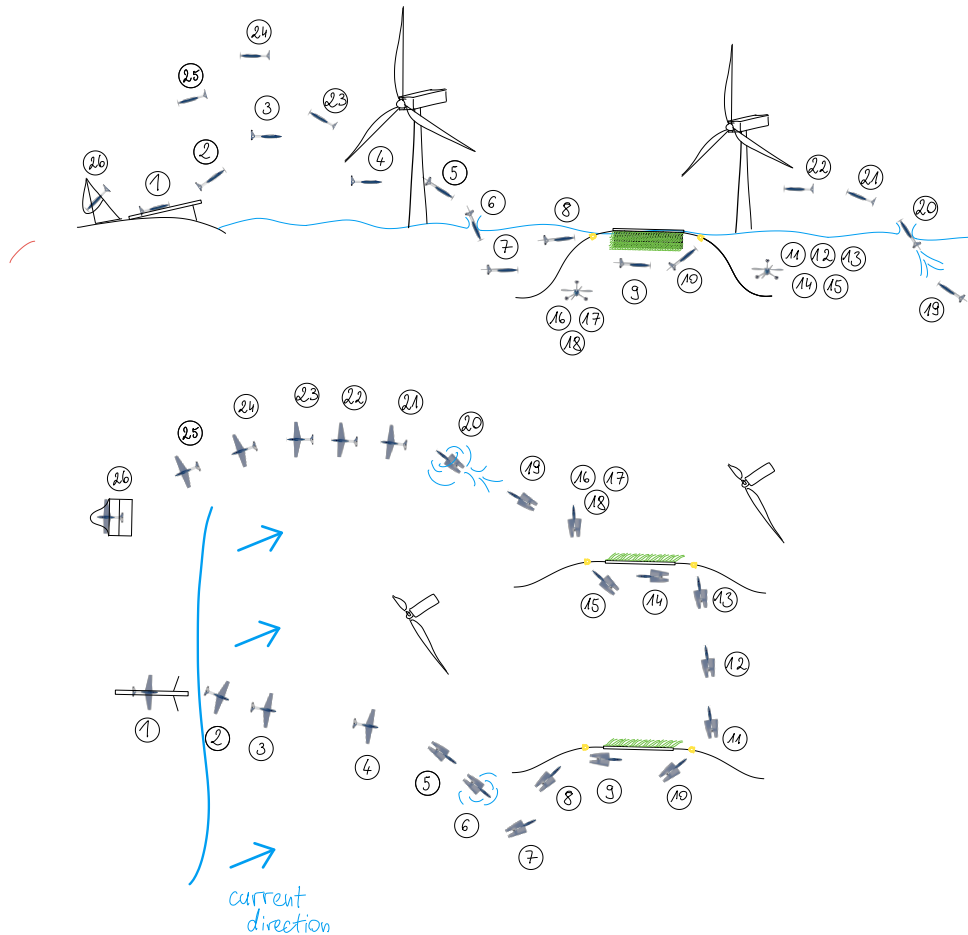


Figure 4.1: Mission outline

1. **Launch** – The mission begins with the vehicle being launched from its land base with a pneumatic catapult. The vehicle is accelerated to the cruise velocity of 20m/s and begins its flight with wings fully extended.
2. **Climb** – The vehicle gains elevation to reach its cruise altitude of 120m within 2 minutes.
3. **Cruise** – The vehicle cruises to Borselle using GPS at the cruise altitude and cruise velocity of 20 [m/s]. It does so until it gets within the visual range of the wind park. The Borselle wind park is at a distance of 30km from the base, giving a flight time of 25 minutes.
4. **Passage under wind turbines** - The vehicle decreases its altitude to 17.5 [m], the middle of the range under the wind turbine blades and the sea surface. This way collisions with the turbine blades and the most significant part of the turbine wakes are avoided. The vehicle flies at this altitude for about 5 minutes.
5. **Approach** - Once the seaweed systems get within visual range, the vehicle loiters above them until the position of all the systems relevant to the mission is known. The optimal path for carrying out the underwater surveying is calculated. A suitable place for splashdown is devised, such that it is upstream from the seaweed systems, around 10m from its end. A path of approach is devised, and the vehicle adjusts its position and heading. The positions of the observed seaweed systems are saved in the memory in the global coordinate frame.
6. **Air to water transition** – the vehicle decreases the altitude to around 7 [m] and the velocity to 17 [m/s] so just above the stall speed of 16m/s. Then, as it approaches its splashdown zone, the vehicle pitches down, sweeps its wings back, turns off its motor and folds its propeller. It dives into the water using its visual system to splashdown as close to the designated spot as possible, adjusting the course with the tail control surfaces.
7. **Reorientation** - Once underwater, the vehicle reaches a stable horizontal position, turns on its underwater navigation and propulsion systems. Then orients itself facing where the first seaweed system to be surveyed is and attempts to recognize it in the sonar and or camera data, within 2 minutes. If it does not, it starts sailing<sup>1</sup> in an expanding spiral until it does.
8. **Structural monitoring upstream** - Using a combination of sonar and camera data, the vehicle navigates to the upstream end of the seaweed system and after recognizing the structural elements of interest, takes

<sup>1</sup>Sailing is used to describe swimming underwater

a sufficient amount and types of images. While carrying out the maneuvers, the vehicle collects the IMU data to characterize the current and water behaviour. The maneuver takes around 1 minute.

9. **Seaweed monitoring** - The vehicle sails under the seaweed system to its downstream end, potentially aided by the current. The velocity with respect to the seaweed system is 0.5 [m/s]. The sonar and camera are pointed at the seaweed above the vehicle and their data is recorded. The travel takes around 4 minutes.
10. **Structural monitoring downstream** - Using a combination of sonar and camera data, the vehicle navigates to the downstream end of the seaweed system and after recognizing the structural elements of interest, takes pictures of them. The maneuver takes around 1 minute.
11. **Preparation for travel to the downstream end of the next system** - Using the characterization of the current and the position of the next seaweed system to inspect, the vehicle calculates an optimal path to the next seaweed system. Due to the fact that the seaweed system will not be in the range of the sonar for the first part of the travel, the vehicle aims at the downstream one-third of the seaweed system, rather than at its very end. This way any errors in the navigation are accounted for. Then the vehicle sets off on that path.
12. **Travel to the next system** - the vehicle travels to the next seaweed system while pitching downwards every 15 seconds, so as to attempt to 'catch' the next seaweed system with the sonar. Once it 'catches' the seaweed system, it corrects its path so as to reach the downstream structural elements to be monitored. With a velocity of 1.0m/s, the travel takes around 2 minutes.
13. **Structural monitoring downstream** - Using a combination of sonar and camera data, the vehicle navigates to the downstream end of the seaweed system and after recognizing the structural elements of interest, takes pictures of them. The maneuver takes around 1 minute.
14. **Seaweed monitoring** - The vehicle swims under the seaweed system to its upstream end. The velocity with respect to the seaweed system is 0.5m/s. The sonar and camera are pointed at the seaweed above the vehicle and their data is recorded. The travel takes around 4 minutes.
15. **Structural monitoring upstream** - Using a combination of sonar and camera data, the vehicle navigates to the upstream end of the seaweed system and after recognizing the structural elements of interest, takes pictures of them. The maneuver takes around 1 minute.
16. **Preparation for travel to the upstream end of the next system** - Using the characterization of the current and the position of the next seaweed system to inspect, the vehicle calculates an optimal path to the next seaweed system. Due to the fact that the seaweed system will not be in the range of the sonar for the first part of the travel, the vehicle aims at the upstream one-third of the seaweed system, rather than at its very end. This way any errors in the navigation are accounted for. Then the vehicle sets off on that path.
17. **Travel to the next system** - The vehicle travels to the next seaweed system while pitching downwards every 15 seconds, so as to attempt to 'catch' the next seaweed system with the sonar. Once it 'catches' the seaweed system, it corrects its path so as to reach the downstream structural elements to be monitored. The maneuver takes around 2 minutes.
18. **Monitoring of eight more seaweed systems** - steps from 8 to 17 are repeated four more times on the next seaweed systems so as to reach a total of 40 systems. The monitoring of 40 systems takes around 318 minutes in total.
19. **Preparation for launch** - The vehicle swims away, in the direction parallel to the seaweed system it has last surveyed. It aligns itself parallel to the seaweed system and pitches up. The maneuver takes around 1 minute.
20. **Water to air transition** - Using the gas in the high-pressure tank, the vehicle ejects the water stored in its chamber and shoots out of the water.
21. **Stabilisation in air** - With the impulse from the water ejection the vehicle gets to the altitude of 15 [m] and has a velocity of 12 [m/s]. It then opens up its wings, turns on the in air motor and opens up the propeller. It gains speed until it reaches the cruise velocity and reaches an altitude of 17.5 [m], stabilising there. The maneuver takes around 2 minutes.
22. **Passage under wind turbines back** - The vehicle remains under the wind turbine blades, flying at altitude of 17.5 [m] at the cruise velocity in the direction of the base for around 5 minutes.
23. **Climb** - once out of the windpark, the vehicle climbs to the cruise altitude and reaches the velocity of 20 [m/s].
24. **Cruise** - Using GPS, the vehicle navigates back to base. It remains at cruise altitude and velocity. Cruise takes around 25 minutes.
25. **Preparation for landing** - The vehicle seeks the landing zone using cameras, once it spots it, it calculates a path of approach and takes it. The maneuver takes around 3 minutes.
26. **Landing** - The vehicle lands in the net.

## 4.3. Launch, Landing, and Ground Operations

### 4.3.1. Launch

#### Requirements

**Table 4.1:** Incoming requirements for take-off

ID	Description	Traceability	Rationale
TO-IN-01	The vehicle shall reach a take-off velocity of no less than 16 [m/s]	Quantity is preliminary stall speed estimate	Stall speed is a conservative initial estimate vs. controllability and stability conditions
TO-IN-02	The vehicle shall have a take-off angle of at least $6^\circ$ .	Quantity is the required climb angle.	Conservative estimate to not use more power than needed during climb
TO-IN-03	The take-off system can launch a vehicle of 13.8 [kg]	Follows from Puffin take-off weight	The catapult has to be able to launch the Puffin's mass

**Table 4.2:** Outgoing requirements for take-off

ID	Description	Traceability	Rationale
TO-OUT-01	The vehicle's structure shall be able to withstand an acceleration of 40 [ $m/s^2$ ]	Quantity follows from the catapult length and take-off velocity	This is the acceleration the Puffin needs to meet its required take-off velocity.
TO-OUT-03	The launch site will have a cleared area of at least 15 $m^2$	Quantity follows from the size of the catapult and the launch angle	This allows for a 5 [m] area of cleared space with a width of the wing span.

#### Launch Description

The Puffin will be launched from land with a pneumatic catapult launcher. Landing and launching in a conventional way was excluded as adding landing gear to the Puffin significantly increases its weight. Furthermore, a runway would be required. Hand launching wasn't feasible either since the vehicle is too heavy for that. Finally, taking off vertically was excluded as it requires a high amount of power which would induce too much battery weight. All these considerations led to using a catapult for launching the Puffin.

The following pneumatic catapult, shown in Figure 4.2 will be used to launch the Puffin. Table 4.3 below the figure displays a list of specifications of this catapult.



(a) PL-40 pneumatic catapult that will be used to launch the Puffin



(b) Customised carriage to be mounted to the catapult that will be designed to specifically carry the Puffin

**Figure 4.2:** PL-40 pneumatic catapult and an example of a personalised carriage to launch a specific vehicle [9]

**Table 4.3:** Specifications of the pneumatic catapult that will launch the Puffin [9]

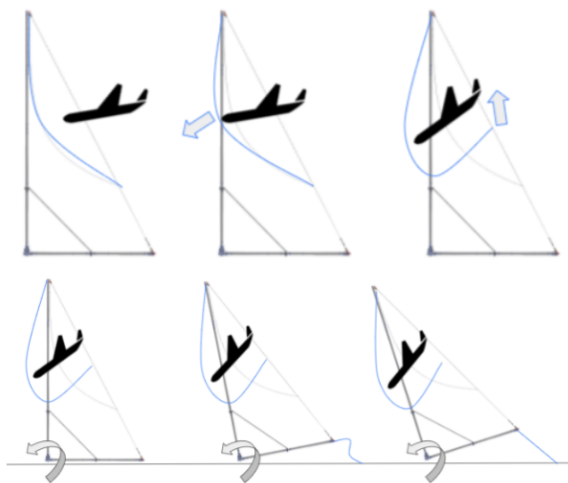
Parameter	Value(s)
Launch angle	11°
Length when deployed	5 m
Max. allowed launch velocity	25 [m/s]
Max. launch mass	40 [kg]
Launcher mass	56 [kg]
Costs	€18,500

The launch system can be set up in five minutes and is hence very efficient in terms of operations.

#### 4.3.2. Landing

Upon returning to the base the system has to safely land. Several landing scenarios have been considered and evaluated in terms of operational feasibility and cost, the added weight to the structure and safety. A runway solution is discarded due to its ground infrastructure needs and the structural need to incorporate landing gear, leading to a higher system mass. The need for a runway would heavily impact the system's universality, and increase maintenance and logistics costs. This landing solution negatively impacts the universality of the design. A parachute retrieval option was considered. Products such as Fruity Chute <sup>1</sup> offer solutions allowing drones. The option has been discarded due to the inability to precisely control the landing location and the need for an additional chute, deployment mechanisms and mass and space occupied by the main chute. The Fruity Chute configuration would add 0.93 kilograms to the structure, excluding the retraction mechanism. Additionally, the wing sweep-back mechanism would only allow for chute deployment at full wing deployment.

A retrieval net, such as the Recovery Net RN86 designed by Embention <sup>2</sup> has been deemed as the most feasible solution. The principle behind the retrieval net mechanisms can be found in Figure 4.3a, the system slows down to the stall speed, glides and gets captured by the net. The net structure minimises the impact forces by absorbing the impact using structure rotation and net shaping. In order to further minimise the impact the Puffin would pitch up before the impact to ensure the landing impact loads are concentrated on the bottom side of the fuselage. As the plane would glide toward the net, the front propeller blades would not be rotating as no torque would be applied. As further explained in Chapter 7 the blades would sweep back for the landing configuration, minimising impact. The blades will not penetrate the net, ensuring no entanglement. The system can be intercepted by the net while flying at stall speed with no inflicted damage on the structure. The Embention net can safely capture units of up to 60 kilograms of mass and 28 [m/s] approach speed. The RN86 can be retracted to form a working net structure of 9.5 [m] in width and 6 meters in height. The net can be easily transported and reused. The downside of this solution is the need for ground space of 14 by 4.5 meters and the cost of 29000 euros per net unit. The development of a new net structure should be considered for a possible significant cost reduction, the system has proven however to be a feasible and universal solution for the needs of the design. The solution has the potential to be sized to the needs of the Puffin system.



(a) The net capturing mechanism



(b) The Embention net fully deployed

<sup>1</sup>Fixed wing recovery bundle

<sup>2</sup>Recovery Net RN86

## Ground Operations

In terms of the operations surrounding launching and landing of the vehicle, the driving idea is that there shall be no permanent base of operations in Scheveningen. Rather, the launch catapult, net operations tent and communication equipment shall be set up close to the coast every time a mission takes place. One day before the mission, operators will set-up the catapult and launch tower at the launch site.

Once the vehicle lands, it first has to be removed from the net. Once that is done, the battery is removed. Then data gathered is retrieved. The drone is cleaned, its state is then checked. Whether the structure is in good shape, parts have no visible damage, propellers are free spinning. Any necessary fixes are carried out. The drone can be then stored or deployed again.

For deployment, a charged battery is inserted, new mission targets loaded and the vehicle is put on the catapult. The catapult is armed and the vehicle is ready to be launched.

The retrieved data is analysed by relevant specialists.

While the vehicle is in the air, there shall always be an operator at the base. They would monitor the operation of the drone and order a dispatch of a rescue boat in case of malfunction.

## 4.4. Mission Planning Considerations

Areas requiring further research can be identified. Most notably:

1. **Seaweed system recognition from air** - In order to carry out the mission, the vehicle will have to have access to a map that includes the position of all seaweed systems to be surveyed. In a dynamic offshore environment a GNSS position of the seaweed systems would not be enough, which is why cameras are used to aid with the navigation. To navigate successfully though, robust recognition algorithms will have to be applied to estimate the positions of seaweed systems visually and compare it with their positions assumed before the mission.
2. **Emergency system** - In case of a malfunction, the vehicle has to be recoverable. The vehicle is positively buoyant and so in case of loss of power it will rise to the surface of water and float. To ensure that, the valves with the high pressure tank are a fail closed system - in case of the loss of power, the valve remains closed, such that the water cannot fill the tank. In case of malfunction but with the power and TT&C subsystem working, a distress signal is sent to the base. In case of loss of power, the communication system at the base will raise an alarm, providing the last known location of the vehicle. In both cases a boat will be sent to retrieve the vehicle.
3. **Position estimation underwater** - determining the position of the vehicle with respect to a seaweed system. At distances beyond the camera range, the vehicle would have to rely on the positions of the seaweed system taken from air and sonar data, both requiring recognition algorithms. Once the vehicle gets close to the system, such that the camera can see it, a recognition algorithm will also be run on the camera images. Most importantly it will be used for the structural elements identification, aided by the sonar inputs. Issues might arise, regarding the reliability of the recognition systems, especially with the turbidity of the camera.
4. **Coping mechanisms** - Given the low visibility, harsh conditions imperfections or potential damage to the sensors, it is possible that the vehicle is unable to recognise the seaweed system with sonar and or camera. When that happens during reorientation phase, the vehicle shall sailing in an expanding spiral path to hopefully find the seaweed system. It shall conduct the same maneuver if it loses the seaweed system while conducting the seaweed monitoring. If the vehicle is unable to locate the next seaweed system during transfer in between systems, it shall emerge to the surface to get its GNSS position and correct its course. If neither of the coping mechanisms work within 15 minutes, the vehicle shall send information failure to conduct the mission to base and return.
5. **Maneuverability** - carrying out the necessary maneuvers might be problematic, especially in high currents. The most complicated maneuvers that the vehicle will need to carry out will be getting in position to take the structural elements, where the vehicle will then need to remain stationary for some time to take the measurement, During the approach of the structural element, complexity is added because of the sonar facing forward and upwards. To 'see' the seaweed system, the vehicle would need to point the sonar at the system. To do that, the vehicle would need to pitch down once in a while, to 'catch sight' of the seaweed system and correct heading, returning to sailing horizontally afterwards as can be seen in Figure 4.4. What is more, the vehicle will need to correct for any disturbances, caused by waves or the current and also follow the system as it sways due to waves.



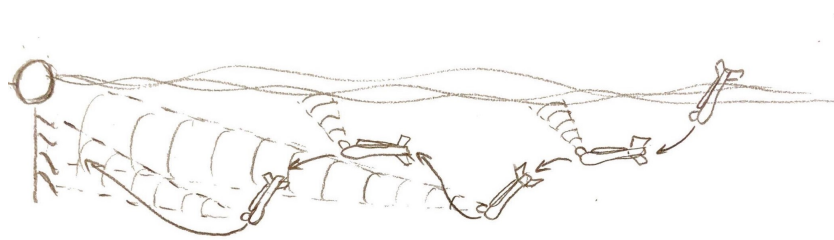


**Figure 4.4:** Visualisation of maneuver to be made to get the seaweed system in sight. Pitching down once in a while, to 'catch sight' of the seaweed system and correct heading.

6. **Avoiding collisions** - In the mission planning, only the seaweed and wind farms are considered potential obstacles. It is possible though that other unexpected objects appear in the area of operation, such as boats or animals. It is also possible that a seaweed system or a wind turbine behaves in unexpected ways. Safety of the drone, animals and infrastructure is of primary importance and so it is critical that the vehicle doesn't come into contact with any objects. Applicable decision-making systems need to be designed, possibly including a human in the loop. Furthermore, the vehicle needs to be designed such that if it comes into contact with something, neither get damaged.

#### 4.5. Validation

The most definitive way of checking whether the design can fulfil its mission or not would be to build a prototype and test it. That is though not very feasible within the DSE constraints. Half measures therefore have to be taken to verify and validate the vehicle.

To validate the whole mission planning, control and subsystem design to some extent, a simulation of the whole system shall be carried out. A simulation like that could be run in a robotics simulator like Gazebo<sup>1</sup>. There the most important features of the physical world such as winds, currents and density changes upon transition could be simulated. With the subsystems designed, and the structure and propulsion systems characterized, the control and mission planning could be run, offering a good understanding of how the vehicle would behave in the actual world.

Such a large simulation would also not be very feasible within the time constraints, given how much time had to be spent in the beginning on the general architecture of the design. What will thus be performed, is a simulation of mission planning, taking into account parameters such as wind speeds, current speeds and density. This shall allow for estimating the time needed to carry out the mission and quantify the efficiency of mission planning.

In terms of verification, for the code written, unit and system tests shall be performed. Also, things that can be checked with hand calculations shall be checked.

## 5 Water to Air Launch

The Puffin launches itself out of the water to execute the water to air transition. Design options, following from a functional definition, are discussed in Section 5.1: sustained (propeller driven) and impulsive options are considered. Of the top level concepts, a most feasible solution is selected in a water rocket motor. Aspects substantiating such a system, being pressurant selection, structural sizing, system integration, and fluid control are discussed in this chapter.

### 5.1. Functional Definition and Design Options

The function of the launch system is to sufficiently energise the vehicle to follow a desired aerodynamic trajectory for climb. Pending insights into vehicle control and stability, the target velocity is set to the stall speed (15 [m/s]), to be achieved at an altitude in the middle of the flight envelope (15 [m]).

<sup>1</sup>Gazebo

**Table 5.1:** Water Launch Incoming Requirement Table. Initial performance requirements for launch architecture selection and initial sizing

ID	Description	Traceability	Rationale
LNC-01	The vehicle shall have an aerodynamic velocity of at least 15 m/s at the end of the water-air transition trajectory	Quantity is preliminary stall speed estimate	Stall speed is a conservative initial estimate vs. controllability and stability conditions
LNC-02	The vehicle shall attain an altitude of 15 m at the end of the water-air transition trajectory	Quantity is half of the flight ceiling of the on-site envelope (30 meter)	Conservative estimate, 15 meters is high
LNC-03	The preliminary launch system shall deliver a $\Delta V$ of 23 m/s	From LNC-01 & LNC-02 via ballistic model	Synthesis of LNC-01 & LNC-02 into an actionable form
LNC-04	The launch system shall launch at least twice per mission	Launch risk mitigation	Redundancy, as necessitated by the risk map [1]

Three propulsion domains are distinguished: **submerged** propulsion, providing thrust while underwater and inoperable in air, **trans-medial** propulsion, providing thrust independent of medium, and **airborne** propulsion, providing thrust while in air and inoperable in water. The systems are not mutually exclusive, combinations are expected. Four combinations are distinguished for evaluation: see Figure 5.1.

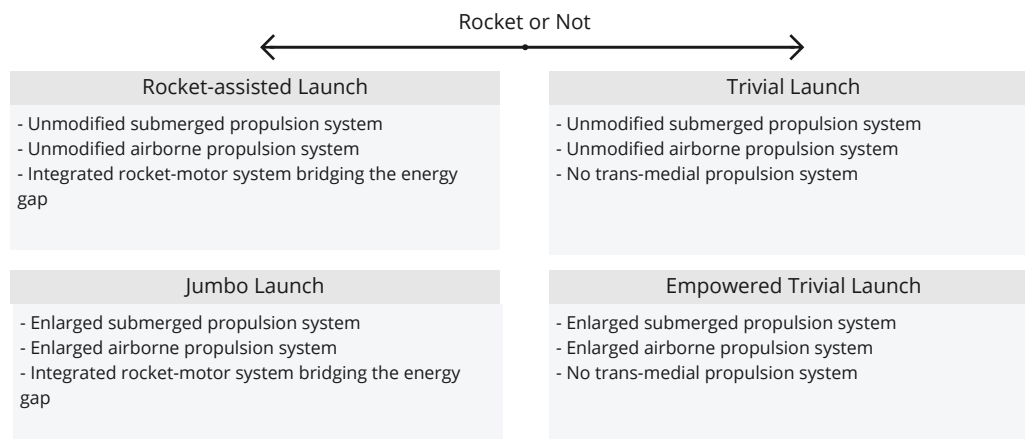


**Figure 5.1:** Launch Architecture Design Options. A top level overview of the possible (combinations of) propulsion systems in facilitating a water-air transition

The energy gap, loosely speaking, is the degree of inadequacy of the trivial launch configuration. Airborne and submerged propulsion systems are already present in the design. The launch configuration then answers two questions:

1. Does a system fulfilling requirements on navigation and monitoring propulsion suffice to execute a successful water launch? (Trivial solution)
2. In the case that the trivial solution is insufficient, are launch requirements met most efficiently by an auxiliary launch system or by scaling up existing options?

Airborne and submarine system options are developed in Chapter 7. Section 5.3 investigates the feasibility and efficiency of modification for launch. In considering auxiliary launch system options, water rocket-type systems are selected for further development. This class of propulsion systems acts by expelling water at high pressure from a reinforced chamber in the vehicle. The water is pressurised by some pressurant. As per Figure 5.2, these are the most relevant for the application: solid rocket motors are a promising alternative, but are discarded on

the basis of cost and handling concerns. Water rockets of various forms have been demonstrated in similar applications [10] [11]. The choice of pressurising mechanism is explored in Section 5.5.

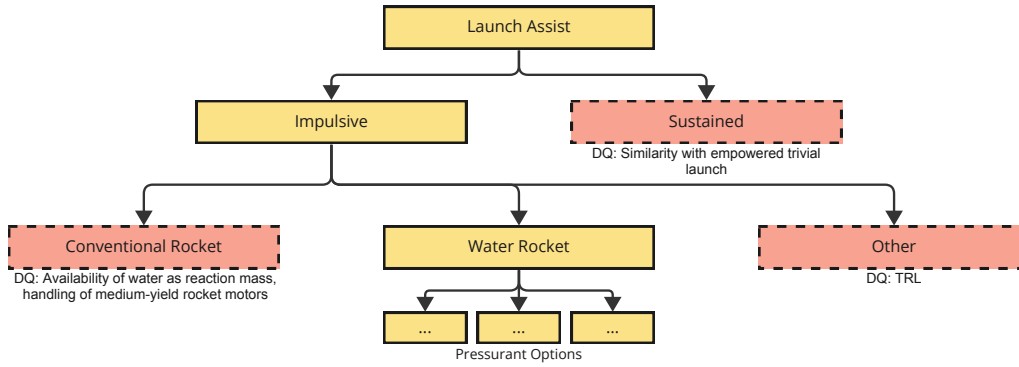


**Figure 5.2:** Auxiliary Launch Propulsion System Design Options. Overview of design options and exclusion logic in selecting water rockets for detailed exploration. DQ indicating disqualified

## 5.2. Launch Performance Model

A  $\Delta V$  model facilitates launch performance comparison. Input requirements are translated into a required launch  $\Delta V$ , to be provided by the propulsion system(s). As a combination of systems may be leveraged, a  $\Delta V$  model provides a way to isolate contributions and explore their relative efficiencies.

The model serves to inform launch propulsion sizing. As contributions are considered by summation, a more accurate (non-linear) model should be developed for final launch performance estimation while the underlying dynamics combine non-linearly.

This section describes the synthesis of the target  $\Delta V$ . The performance of submarine and airborne systems is explored in Section 5.3, the performance of the auxiliary system in Section 5.4 and Section 5.5.

### 5.2.1. Ballistic Component

The ballistic component describes the required initial (impulsive) velocity to overcome gravity losses in reaching the desired launch-end state required by LNC-01 and LNC-02. This initial velocity is the ballistic  $\Delta V$  component. Solution of energetic or kinematic formulations yields the initial ballistic velocity:

$$\text{Energetic: } v_0 = \sqrt{v_1^2 + 2gh} = 22.8[m/s] \quad (5.1)$$

$$\text{Kinematic: implicitly solve for } v_0 \text{ in } v_1 = v_0 \cos \left( \arcsin \left[ \sqrt{\frac{2gh}{v_0^2}} \right] \right)$$

### 5.2.2. Wave, Water, and Air Drag Components

Hydro-aerodynamic losses are not incorporated into the model. The complexity was not warranted in initial sizing, instead  $\Delta V$  requirement quantification is made conservative in LNC-02. An altitude of 15 [m] before climb is very high: the actual lower bound would stem from wave collision margin, with an average wave height of only 1 meter [3]. Relaxation of this requirement to e.g. 2 [m] would reduce the required  $\Delta V$  by 40%. Final propulsion system sizing should be iterated with more precise launch models.

## 5.3. Propeller Driven Launch Solution $\Delta V$ Scaling

The efficacy of (empowered) trivial launch solutions is assessed by the solution of power requirements under relevant drag effects. Energy (drag loss) was also assessed but found to be of negligible relevance when expressed as a mass contribution.

$$P_{prop} = \frac{1}{2} \rho S C_d (\Delta V)^3 \quad (5.2)$$

- The **submerged** propulsion system accelerates to a final velocity, assisted by a buoyancy force. As this propulsion system can only act underwater, it must attain its  $\Delta V$  contribution before breaching. Resolu-

tion of required submarine propulsive power, by Equation 5.2 using typical values, reveals a steep dependency:  $P_{prop}$  for  $\Delta V = [1.0, 5.0, 10.0]$  [m/s]: [150, 3800, 15000] [W]. Buoyancy forces contribute insignificantly at higher velocities ( $>1.0$  [m/s]). Translated into powerplant mass, the total system mass of [16 kg] is quickly exceeded by only this component.

- The **airborne** propulsion system must overcome gravitational forces to accelerate in air. Fulfilling this condition, it can provide essentially unlimited  $\Delta V$  (in the scope of this model). Initial estimation performed by optimization of 1D EOM, iterated in Section 5.3.1. A very large rotor is required.

### 5.3.1. VTOL Propeller Sizing

A VTOL configuration propelled purely by a single nose-mounted propeller should be considered. The model has only included the need to reach the stall speed of  $15[m/s]$ , all the values are heavily underestimated as they do not account for the water interaction drag. The sizing method follows the methodology established in Chapter 7. The relation between the required thrust and the estimated propeller diameter have been estimated and presented in Figure 5.3. The diameter of the propeller of around 1.35 [m] is not feasible, the scale is too large for the system, and the diameter has to be limited to be able to withstand the water impact loads. A thrust requirement above 200 [N] would result in the need for a powerful motor, the lightweight UAV motors are not able to generate the required performance parameters. The limitations are further explained in Chapter 7. The estimated air propulsion unit required was deemed too unfeasible, and the performance of the system would be even worse if all the downward-acting forces were included. For a single front-mounted propeller configuration, an off-the-water take-off is unfeasible and unrealistic. Multiple propellers were considered but were discarded due to high energy consumption, high mass, and architecture limitations.

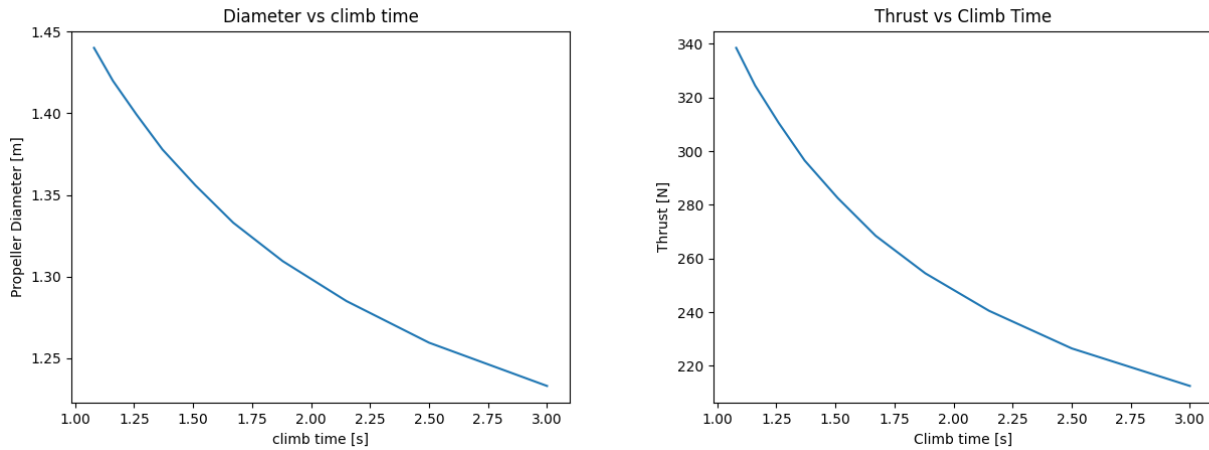


**Figure 5.3:** The diameter of the twin-blade propeller against the climb time with the chosen RPM value of 5000 1/min (left), Thrust required against the climb time(right)

### 5.4. High-Power Water Rocket $\Delta V$ Scaling

A rocket ejects some (onboard) reaction mass at high velocity, providing thrust. An ideal rocket is modelled by the Tsiolkovsky rocket equation:

$$\Delta V = v_e \ln \frac{m_0}{m_f} \quad (5.3)$$

The reaction mass in the case of a water rocket is the water in the chamber. Final mass  $m_f$  is expressed as the empty weight  $m$ , and initial mass  $m_0$  as the sum of empty and propellant (water) mass  $m_p = \rho_w V_w$ .

In the case of a water rocket, the incompressible flow may be assumed as heating is insufficient for vaporisation, and water is approximately incompressible. This simplifies the initial design, as flow behaviour is adequately modelled by Bernoulli's equation. Incompressible flow through an arbitrary orifice (chamber exit) is governed by  $\dot{m} = C_d A \sqrt{2\rho \Delta p}$ , where the discharge coefficient  $C_d$  is neglected ( $=1$ ) in an ideal formulation. The mass flow ( $\dot{m}$ ) is conserved (Bernoulli).

Equation 5.3 is rewritten with these insights, yielding an expression of  $\Delta V$  as a function of chamber pressure and volume:

$$\Delta V = \sqrt{\frac{2\Delta p}{\rho_w}} \ln \left( 1 + \frac{\rho_w V_w}{m_{sys}} \right) \quad (5.4)$$

As the water is not self pressurising a pressurising mechanism must be provided: options are presented in Section 5.5.

#### 5.4.1. Spherical Chamber Mass Model

Generally, pressure vessel mass can be modelled as a linear function of pressure energy,  $m_{PV} = m_0 + C_1 pV$  [12]. The constants  $m_0$  and  $C_1$  are derived, describing the chamber as an aluminium sphere, with a safety factor of 2.0 on yield:

$$\sigma_{hoop} = SF \cdot \sigma_{yield} = \frac{pr}{2t}, \quad V = \frac{4\pi r^3}{3}, \quad S = 4\pi r^2, \quad m = \rho_{mat} St$$

Combining these equations yields Equation 5.5. Coefficients become:  $m_0 = 0$ ,  $C_1 = \frac{3}{2} SF \frac{\rho_{mat}}{\sigma_{yield}}$

$$m = \frac{3}{2} SF \frac{\rho}{\sigma_{yield}} pV \quad (5.5)$$

This is a conservative estimate of chamber mass. The mass model will be updated in future iterations, but serves as an upper bound on chamber mass (and preliminary estimate to aid other subsystem design). Approximate proportionality with pressure energy is an important insight: Figure 5.4 explores the  $\Delta V$ -chamber pressure curves for configurations of constant water chamber 'cost' (mass).

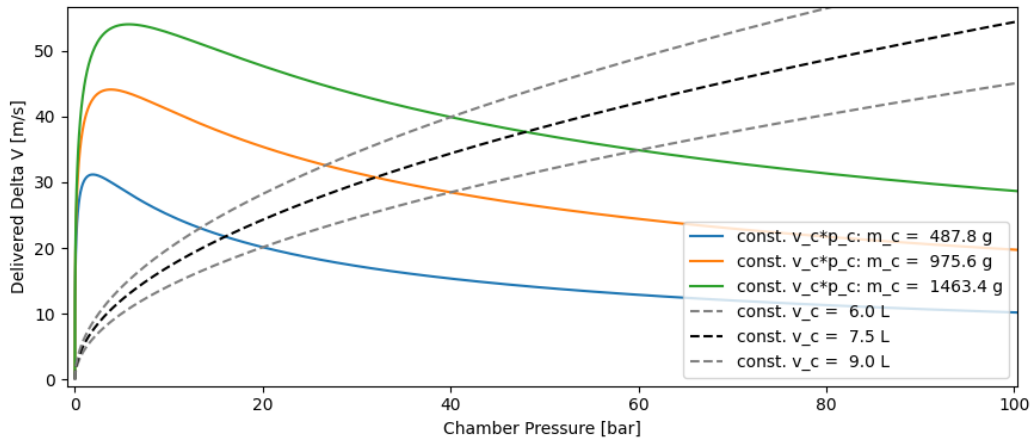


**Figure 5.4:**  $\Delta V$ -chamber pressure curves. The solid lines have constant pressure energy ( $pV$ ): travelling along these lines, the structural mass of the chamber remains constant. The dashed lines plot the  $\Delta V$ - $p$  relationship for a fixed chamber volume.

Optimal chamber pressures, the peaks of the solid lines in Figure 5.4, are impractical requiring very large volumes. Various factors push a real best solution further along the curve (i.e. to higher pressures):

- **High volume** is impractical because:
  - System integration is challenging, driving drag losses.
  - Very high volumes entail very low wall thicknesses, which are more expensive to manufacture and more prone to failure (less robust in other loading).
- **Low pressure** limits your mass flow rate (and thereby your thrust), hampering the vehicles ability to overcome drag and gravity.

Chamber volume requirements will be quite high, irrespective of chamber shape. The chamber will be a defining feature of the design, and opportunities for integration should be explored.

## 5.5. Chamber Pressurization Options

To facilitate expulsion, the chamber must be pressurised by a source, the pressurant. Three methods are outlined: pressure regulated blowdown (Section 5.5.1), water reactive combustion (Section 5.5.2), and a sustainable solid propellant grain (Section 5.5.3).

In preliminary exploration, all pressurants are assumed to act as a constant pressure reservoir. Hence, the variables relevant to modelling are an expression of the expected deliverable chamber pressure level, and the ability of the pressurant to sustain said pressure level (pressure energy).

Assumption of constant pressure will inflate the reported performance water reactive combustion, whose chamber pressure would decrease isentropically as the gas expands.

### 5.5.1. Pressure Regulated Blowdown

The simplest solution is presented by a pressure regulated gas blowdown system. The TRL of this solution is very high; COPV (Carbon Overwrapped Pressure Vessel) and regulator can be purchased for 300 euro at paintball shops<sup>1</sup>. Industrial COTS tanks are also available, offering higher volumes<sup>2</sup> and pressures<sup>3</sup>. A controllable valve would have to be added, as well as an injector head to distribute the gas in the chamber.

Calculation of the pressure energy provided by such a configuration is relatively straightforward:

- The reservoir "storage" pressure is set to the target chamber pressure by the regulator (i.e. the chamber pressure will be constant throughout blowdown)
- The combined volume of the chamber and reservoir are calculated such that isentropic conditions are met (i.e.  $p_c(V_r + V_c)^\gamma = p_r V_r^\gamma$ )

The deliverable  $\Delta V$  of a set of pressurant tanks is plotted in Figure 5.5, alongside the  $\Delta V$ - $p$  relationship for a reference water chamber. The critical takeaway is that a 1.5 [L], 300 [bar] reservoir (a large but standard size paintball tank) provides adequate pressure energy to fulfill the launch  $\Delta V$  requirement. Higher pressure and higher volume configurations are also presented; these are more performant but also more expensive.

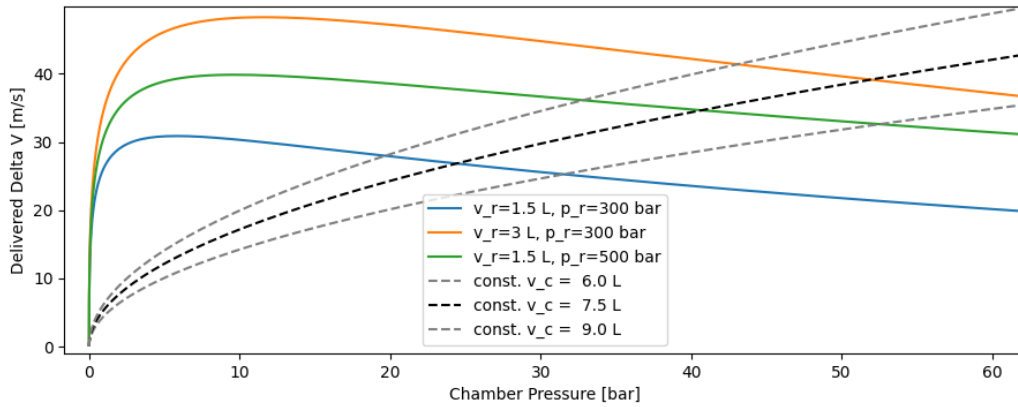


**Figure 5.5:**  $\Delta V$ -chamber pressure curves for a set of reservoir sizes. Chamber pressure is set by a pressure regulator (x axis), expelling mass from a water chamber. The size of the water chamber is limited by the pressure energy of the reservoir and sized accordingly. Here the reservoir is fully exhausted for one expulsion. The dashed lines plot the  $\Delta V$ - $p$  relationship for a fixed chamber volume.

A rough reservoir mass estimate is made by relation of pressure energy to mass: extrapolating from an average of 0.0015 [kg/L/bar] (see Meyers' range of tanks), the plotted tanks mass 0.675, 1.35, and 1.125 [kg]. In Figure 5.5 a reservoir suffices to perform a single expulsion (a single launch). It is interesting to extend analysis to multiple expulsions on a single reservoir:

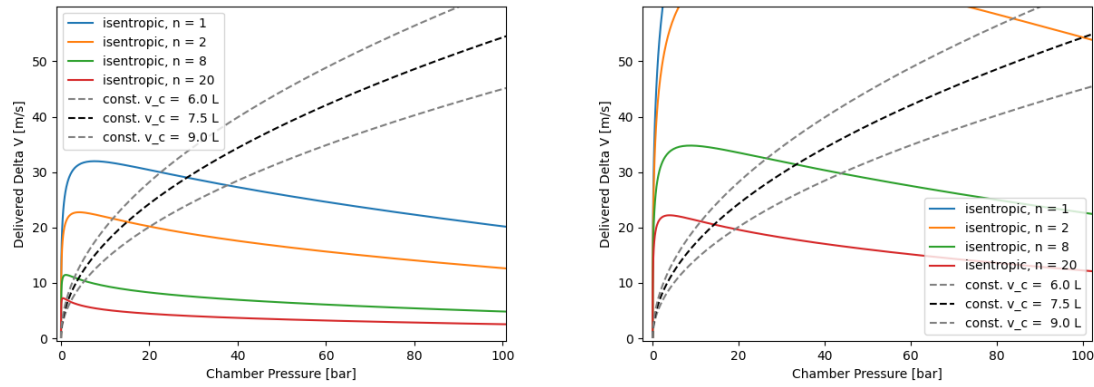
$$\text{Entropy conserved for } n \text{ expulsions: } p_r V_r^\gamma = \sum p_i V_i^\gamma = n p_c V_c^\gamma + p_c V^\gamma \quad (5.6)$$

<sup>1</sup>Ansgear 320 bar / 1.14 L paintball tank

<sup>2</sup>Meyer COPVs

<sup>3</sup>SteelHead Composites COPVs





(a) Standard large paintball tank: 1.5 liters of HPA at 300 bar, fulfilling launch  $\Delta V$  requirement for 2 expulsions (b) Enlarged reservoir, industrial supplier: 7.5 liters of HPA at 300 bar, fulfilling launch  $\Delta V$  requirement for 20 expulsions

**Figure 5.6:**  $\Delta V$ -chamber pressure curves, for a single reservoir performing multiple ( $n$ ) expulsions. The dashed lines plot the  $\Delta V$ - $p$  relationship for a fixed chamber volume.

Per Figure 5.6a and Figure 5.6b, pressure regulated blowdown is extensible to multiple expulsions (and thereby multiple hops) on a single reservoir. The (mass) efficiency in facilitating multiple launches is of interest: should this prove competitive with the performance delivered by the underwater propulsion system, it may be preferable to navigate on-site by repeat launching. A 7.5 [L] reservoir at 300 [bar], estimated as outlined before, masses approximately 3.4 [kg]. Comparing to the mass of the 1.5 [L] (at 300 [bar]) reservoir, the added mass per hop is approximately 0.1 [kg]. Since the  $\Delta V$  requirement sets chamber volume and pressure, the mass of the water chamber is independent of the number of expulsions.

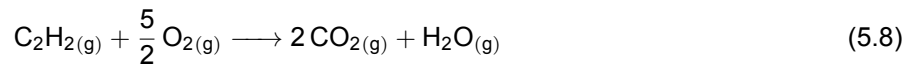
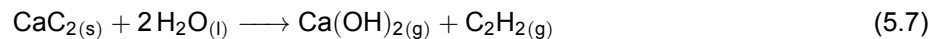
### 5.5.2. Calcium-Carbide Water Reactive Combustion

An alternative solution to generate pressure is through a chemical reaction. A UAV developed by the Imperial College London utilises a chemical reaction of calcium carbide ( $\text{CaC}_2$ ) and water to generate pressure and impulsively launch their UAV out of water [13]. A similar solution will be investigated in this section. The solid chemical chosen for this purpose is calcium carbide, different chemical compounds have been investigated but  $\text{CaC}_2$  displayed the best volumetric properties which is considered a critical parameter to avoid enlarging the UAV and was therefore chosen for the initial sizing [14], [15]. A sketch of the layout of the propulsion system can be seen in ??, the chamber containing the solid  $\text{CaC}_2$  can be seen in the rightmost UAV sketch. Water is injected into the chamber through a pump connected to the fuselage, this reaction generates gas which enters the combustion chamber and is then ignited.

The reaction happens as follows:

- Calcium carbide reacts with water to create Acetylene and calcium hydroxide, which does not have a negative impact on the environment [16]
- The acetylene is ignited and generates carbon dioxide and water vapour

The balanced stoichiometric equations of  $\text{CaC}_2$  reacting with water and the resulting combustion of acetylene are shown in Equation 5.7 and Equation 5.8.



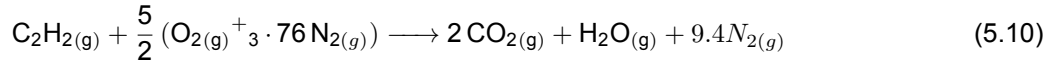
In order to initially size the mass and volume of calcium carbide necessary to generate a pressure of 25 [bar] in a chamber volume of 6.5 [L] taken from Figure 5.9, a simulation model was built in Python. The model assumes a lossless combustion of acetylene and a 100% efficiency of the reaction of  $\text{CaC}_2$  with water. The number of moles of gas generated by both consequential reactions is 3 moles of gas per mole of Calcium Carbide as can be seen in Equation 5.7 and Equation 5.8. An initial guess of the mass of  $\text{CaC}_2$  is made, and the resulting number of moles of gas is calculated. The increase in pressure is then calculated using the ideal gas law, the equation is shown in Equation 5.9.

$$PV = nRT \quad (5.9)$$



With the  $R$  being the ideal gas constant ( $R=8.314 \text{ J}/(\text{mol}\cdot\text{K})$ ),  $T$  the combustion temperature estimated at 3000 [K] from literature [17].

In order for combustion to occur, the acetylene gas needs to be oxidised. This is done by simply keeping the gas in contact with air, which contains oxygen. This means that the water chamber will require either a mechanical system to keep the upper part of the chamber water-tight or that air has to be stored on board. In both cases, this will generate some very strict requirements on the actuation timing sequence of either the opening of a valve or opening the chamber itself. But, regardless of where the oxygen comes from, the required volume of air on board required for the complete combustion of acetylene can be calculated. In order to accurately estimate the amount of oxygen present in our current configuration, the amount of oxygen present in the air should be calculated instead. The modified chemical equation can be seen in Equation 5.10.



The number of moles of reactant oxidiser is then calculated, and using the fact that one mole of gas occupies 22.4 [L] of space, the minimum required volume is calculated. A plot of attainable pressure for increasing masses of reactant calcium carbide can be seen in Figure 5.7. The dashed vertical lines are lines of minimum volume of air required for complete combustion of acetylene.

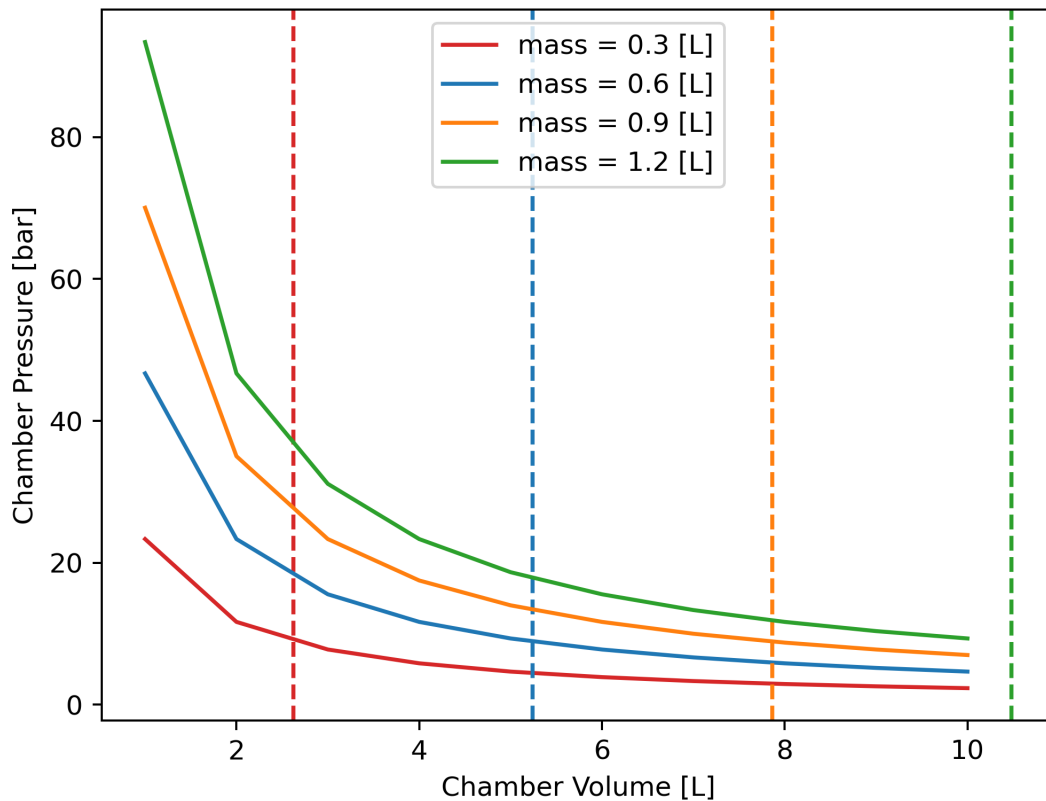


**Figure 5.7:** Plot of attainable pressure for different masses of calcium carbide. The dashed vertical lines are the lines of minimum volume of air required for complete combustion of acetylene.

This solution to generate pressure for the water-to-air transition will not be pursued for the following reasons. The volume of air in the water chamber required for combustion is too high compared to the volume of the chamber itself (6 [L]). This would also require an alternative solution to store air on board or make the upper section of the water chamber water-tight which generates undesirable mechanical requirements on the system.

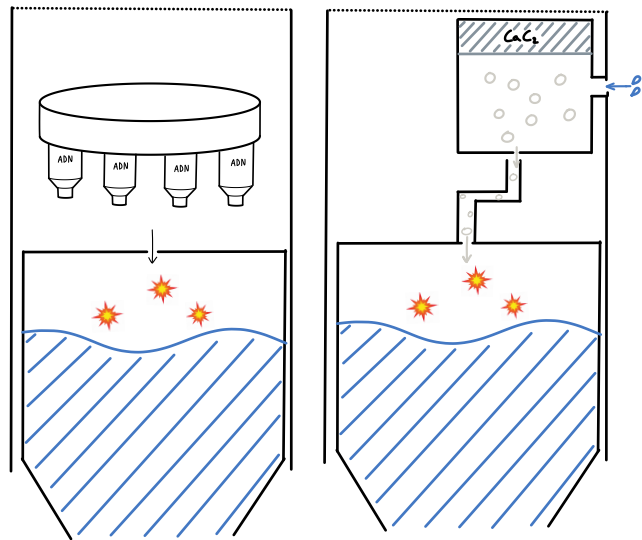


**Figure 5.8:** Schematic of the solid propulsion architectures, on the left an Ammonium Dinitramide-based propellant system is shown. On the right, Calcium Carbide reacts with water and generates Acetylene which is then ignited.

### 5.5.3. Sustainable Solid Propellant Grain

An alternative solution involving the direct combustion of a solid propellant was also considered. Due to the importance of sustainability in this project, "classic" solid propellants had been disregarded due to their negative impact on the environment. Ammonium dinitramide (ADN) is an oxidiser, which used in combination with a binder creates a new option of "green propellant" which presents positive attributes for our purposes [18].

An initial sketch of the configuration used for the combustion of ADN-based propellant can be seen in Figure 5.8. ADN cartridges are positioned on a plate and put in contact with the upper orifice of the combustion chamber before ignition, potentially allowing for multiple take-off maneuvers.

Unfortunately, the combustion of a solid propellant generate issues that were deemed too critical to pursue this design. The combustion of solid rocket propellant is dirty and would require extensive cleaning and maintenance of the combustion chamber between each flight. Additionally, the pressures generated by the combustion of a solid propellant greatly exceed the pressure needed for our purposes. This would also require a heavy combustion chamber that can withstand those pressures.

## 5.6. Leaping Unit Transfer

With a sufficiently efficient launch system, maneuvering between units by launching becomes feasible. A 'leaping unit transfer' may realise efficiency gains as underwater drag is avoided. This entails launching multiple times on site, driving the required reservoir pressure energy. There are other practical considerations next to mass efficiency:

**Table 5.2:** Advantages and disadvantages of designing for leaping or underwater transfer. Underwater propulsion figures sourced from Chapter 7

Advantages	Disadvantages
<ul style="list-style-type: none"> <li>• Makes use of heavy 'fixed' cost (chamber, 1 [kg])</li> <li>• Navigation between units does not need to be performed underwater (no dead reckoning or advanced sensors)</li> <li>• Better equipped for launch failure (more redundant launches)</li> <li>• More versatility in measuring locations (measuring locations may be further apart)</li> </ul>	<ul style="list-style-type: none"> <li>• Makes use of heavy 'fixed' cost (underwater motors, 1.2 [kg])</li> <li>• Scales less efficiently than additional batteries: 0.1 [kg] of pressurant tank vs 0.05 [kg] of batteries per unit surveyed</li> <li>• <b>System becomes more buoyant</b></li> <li>• Better equipped for underwater turbulence (more redundant battery capacity)</li> <li>• More high-risk, highly energy events (dive, launch)</li> <li>• Decreased on-unit endurance (reduced capability at a given location)</li> </ul>

On the basis of increased buoyancy, underwater unit transfer is selected for further development. While other aspects are discussed, buoyancy considerations drive the decision. The increased (albeit pressurised) air volume reduces the average density of an already too buoyant system. Adding air volume, then having to offset said volume with denser components elsewhere, is ill-advised. Adding dense batteries alleviates the buoyancy issues while providing the necessary endurance to complete the mission.

It is challenging to address all aspects of this trade-off. The aspect of efficiency is specific to the Seaweed Company mission profile, though it is interesting how competitive both maneuvers are: If TSC units were twice or three times as far removed from each other (i.e. 200 or 300 meters), re-launch may be more efficient. The tradeoff of on-unit endurance vs unit separation is an interesting consideration for market analysis: perhaps a client prefers to visit many, further removed sites? Here, re-launch offers a unique advantage. Or perhaps the market is more interested in an exhaustive examination of a particular site, choosing a SEAMOS drone for the quick response time.

## 5.7. Launch System Selection and Sizing

The launch system is sized for initial system integration, taking preliminary values (in particular, a system mass of 16 [kg] as per [1]). Evaluated on aspects of performance, complexity, cost, sustainability, and safety, a pressure regulated blowdown system is favoured.

- **Performance and Complexity** of the pressure regulated blowdown system is moderate but definite: an added mass of  $+/- 1$  [kg] + 0.1 [kg/unit]. The performance of combustive solutions is potentially improved but more nebulous: the water reactive system delivers low pressures (difficult to take off) and requires a large supply of oxygen (complexity) while potentially lighter. The efficacy of the solid propellant charge could not be computed.
- **Cost** of the pressure regulated blowdown system is low if common paintball components can be leveraged. Other solutions have specialised components which may incur heavier costs.
- **Sustainability** of all solutions is moderate. Air compression on the base (for paintball) has some energetic cost, water reactive combustion produces some of CO<sub>2</sub>, and the solid propellant could cause acoustic pollution.
- **Safety** requires adequate on-base handling. The combustive systems will require explosives handling licenses and training (the solid propellant cartridge in particular). Principally, high pressure systems are more energetic and a higher risk. This still holds but is mitigated by standardised safety features of paintball hardware.

Due to the difficulty in demonstrating the viability of combustive solutions (water reactive and solid propellant cartridge) a more exhaustive, formal trade-off process is disregarded. Combustive options are underdeveloped, and their performance is too indefinite, to be considered for further development. Pressure regulated blowdown presents a feasible, safe solution, which can be modelled without undue computational expense.

The system then comprises a pressurant tank, some piping, and a water chamber. The water chamber cross section is cylindrical, with the center axis (and the chamber exit) pointing through the center of gravity of the vehicle. The water chamber is of significant size; with chamber diameter constrained by the outer diameter of the fuselage, the chamber length contributes significantly to overall vehicle length. To enhance system integration, a teardrop-shaped water chamber is proposed. Acting also as a structural connection to the empennage, the water chamber is long and slender. This is illustrated in Figure 5.10b.

Commercially available paintball tanks are cheap and readily available. There is a strong design incentive to select an available tank rather than acquiring a custom one from an industrial supplier. The largest available standard size paintball tanks (by pressure energy) have a capacity of 124 cubic inches (2.03 [L]) at a rated pressure of 4500 PSI (310 [bar])<sup>1</sup>. Per the methods introduced in Section 5.5.1, this is the smallest possible reservoir sufficing for at least two launches (one redundant, per LNC-04). The pressure regulators designed for these tanks, though adjustable, cannot be set below 15 [bar]. This is an acceptable constraint, it preserves the safety critical compatibility of off the shelf components. A water chamber design space can be synthesised by combining the reservoir pressure energy, regulator minimum pressure, and LNC-03  $\Delta V$  requirement: see Figure 5.9.

The design thrust must be set to fully constrain the water chamber (setting  $d_t$  in Figure 5.10b). In delivering thrust, the water chamber aims to overcome gravity and drag (and reach the target velocity). In the context of the ballistic simulation, drag is surmised as aerodynamic drag. The design thrust is then obtained by optimising the thrust force minimising the energy lost to gravity and drag while accelerating to the target velocity. This serves as a sizing estimate to be iterated once more sophisticated models are developed. Explicitly:

---

<sup>1</sup>First Strike Hero 2 124/4500

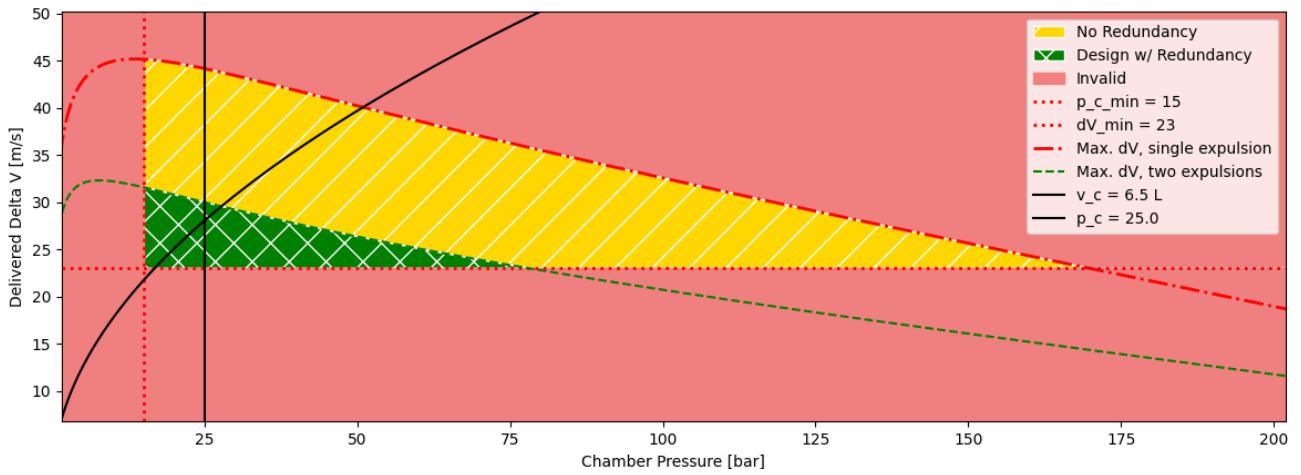


**Figure 5.9:** The viable design space of the pressurised water chamber (green/cross hatched area), with performance ( $\Delta V$ ) on the y axis and pressure on the x axis. For each point in the space, a corresponding chamber volume  $V_c$  may be obtained by solving Equation 5.4. The design space is restricted by a required redundant launch, a minimum performance requirement, and a minimum deliverable pressure. The design point is set at a chamber volume  $v_c$  of 6.5 [L] and chamber pressure  $p_c$  of 25 [bar].

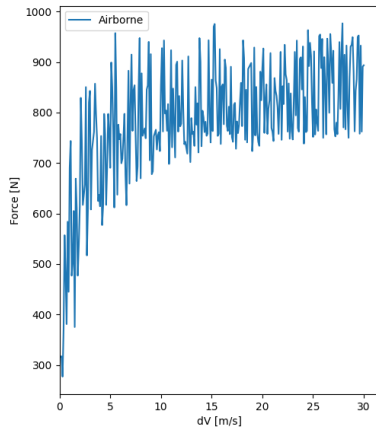
$$F_{T_{design}} = F_t \text{ s.t. } E(F_t) \text{ is minimised for } E = \int_{t_0}^{t_f} (\frac{1}{2}\rho V^2 S C_d + mg) ds \quad (5.11)$$

where range  $t_0 \rightarrow t_f$  presents is the time solution interval of 1D EOM Equation 5.12

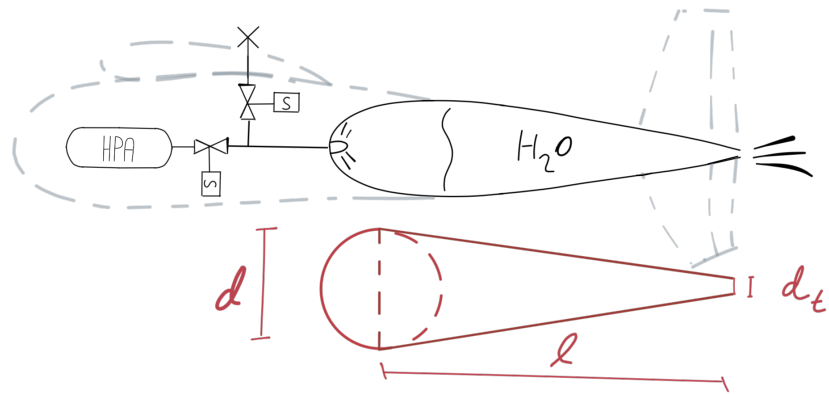
$$m \frac{d^2}{dt^2} x = F_t - (\frac{1}{2}\rho (\frac{d}{dt} x)^2 S C_d + mg) \quad (5.12)$$

with boundary conditions  $x_0 = 0$ ,  $v_0 = 0$ ,  $v_f = v_{target}$

The solution of Equation 5.11 and Equation 5.12 is plotted in Figure 5.10a. Simple forward-euler time integration is combined with an optimiser. The optimum thrust appears to converge to 850 [N] for moderate  $\Delta V$ , setting initial design point. Water (incompressible propellant) thrust is calculated by  $F_T = \dot{m} A_t$  [12], where  $\dot{m} = C_d A \sqrt{2\rho \Delta p}$  (Section 5.4). This provides a relation for chamber exit area, yielding a (circular) throat exit diameter of 14.7 [mm] at 25 [bar] chamber pressure to deliver a thrust of 850 [N].



**(a)** Optimised thrust for a vehicle minimising energy while accelerating in air. Solution of the 1D EOM Equation 5.12 for a body having  $S = 1.25$  [m<sup>2</sup>],  $C_d = 0.05$  [-],  $m = 16$  [kg]



**(b)** Launch system configuration. A teardrop shaped chamber provides a structural connection for tail (empennage) elements. The chamber is filled with water while submerged, and ejected at high velocity during launch to provide thrust. The chamber is pressurised by a commercially available paintball tank. P&ID legend in Figure 5.12

The water chamber is decomposed into a hemisphere and truncated cone (see Figure 5.10b). Constraining the outer diameter of the chamber,  $d$ , by the current fuselage diameter (e.g. 20 [cm,] dependent on iteration), and taking the chamber exit area as above, standard expressions for volume can be reversed. This yields the taper length  $l$ : for the values described, the water chamber size is described by  $l = 575$  [mm,]  $d = 200$  [mm],  $d_t = 7.35$  [mm], having a volume  $v_c$  of 6.5 [L].

In structural modelling of the chamber, two limiting loading modes are considered:

- **In axial loading**, the most extreme stresses occur during water impact and underwater propulsion: these are both compressive loads. As air propulsion is a tensile load, and expected to be lower in magnitude than water impact, it is not considered. Water impact is modelled as a point load at the bulkhead (the closed end of the hemisphere), having a magnitude  $(m_{TC} + m_c) \cdot a_{WI}$ , where  $m_{TC}$  is the tail cone mass,  $m_c$  the chamber mass, and  $a_{WI}$  the peak vehicle deceleration during water impact. The tail end (chamber exit) is fixed. Underwater propulsion is modelled by a point load (equal to the underwater drag) acting at the chamber exit, and a fixed constraint at the bulkhead. Both are conservative models, as the mass of the chamber is not distributed but instead contributes to the point loads.
- **In pressure loading**, the full chamber is subjected to the chamber pressure  $p_c$ . The hoop stress (see Equation 5.5) is evaluated in the most critical plane: with chamber thickness constant (manufacturing), this corresponds to the cylindrical cross section with the greatest diameter (i.e. the end of the spherical section). Stress concentrations are not considered: the chamber would be rounded (Figure 5.10b).

The conservative simplification is made that both cases may be considered in isolation. The assumption follows from a relevant rule of thumb: “The biaxial state of stress lowers the axial stress levels of the various critical events”<sup>1</sup>. Furthermore, in the literature considered, correction factors are introduced for the combined loading case that increases the critical loads (i.e. the structure gets stronger)[19].

Buckling loads are evaluated according to NASA methods outlined in published documentation on the truncated cone and cylinder buckling ([19],[20]). When evaluated, the pressure loading case was found to be  $\approx 10x$  more limiting (in terms of thickness) in sustaining the outlined loads. A wall thickness of 0.29 [mm], for a material having a maximum allowable stress of 435 [MPa] (low estimate for CFRP strength, with a safety factor of 2), is computed. This initial estimate is iterated with eventual material selection: critically, the thickness requirement is not driving in material selection: there is some margin for less performant materials.

## 5.8. Wing-integrated Water Chamber

Buoyancy is identified as a driving vehicle requirement: should the vehicle have a hollow, waterproof wing, it would not be submersible. Hence, the wing must either be flooded or otherwise have drastically reduced empty volume. If the wing is flooded, it is pertinent to evacuate the water in a predictable and rapid fashion during launch Section 9.8. As the wing is structurally underutilised, per Chapter 8, it is interesting to propose unifying the wing and water chamber structural elements.

No research of immediate relevance was found. Utilising the wing as a pressure vessel entails a non-cylindrical cross section; an unconventional practice with no analytical models. Though a rudimentary estimate may be made by the hoop stress formula, this is hardly representative: in a cylindrical cross sections, shear flow does not ‘accumulate’ as local tangential contributions are always in opposition. Having found no relevant literature on the feasibility of eccentric (non-cylindrical) pressure vessels, Finite Element Modelling (FEM) in COMSOL Multiphysics is leveraged. See Figure 5.11.

From Figure 5.11, the impracticality of axially eccentric pressure vessels is apparent: stress concentrations accumulate rapidly (Figure 5.11b) with greatly increased stresses at little shape benefit. A full wing chamber is over 125 times heavier than a tapered chamber with circular cross section (Figure 5.11c).

In this iteration of the design, it is elected to continue with separated wing and water chamber. Structural integration may still be possible, though it is apparent that pressurised elements should have minimal eccentricity. As drainage is still an issue, the wing design must accommodate this (see Section 9.8).

## 5.9. Fluid Control and Vehicle P&ID

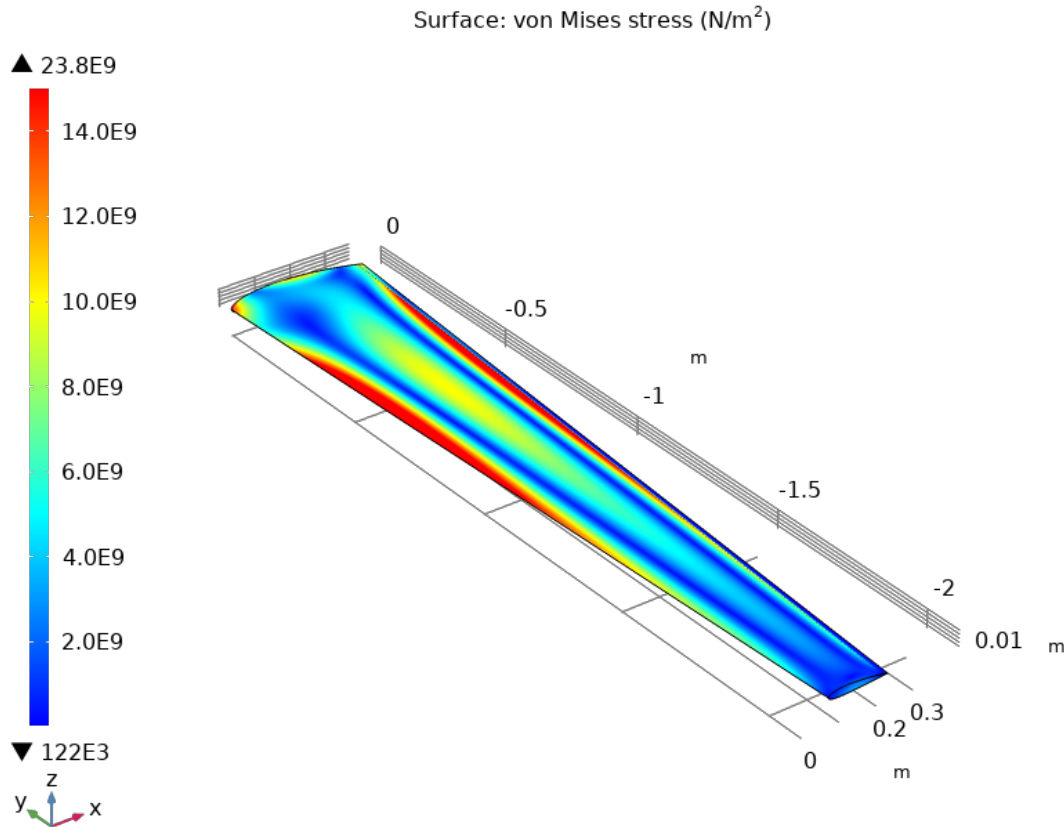
An overview of piping and instrumentation is presented in Figure 5.12. The (pressure) system comprises a singular HPA tank at 310[bar], a water chamber, a wing mechanism actuator, a pressure regulator, two solenoid valves, and various piping (flexible and rigid). The pressurant tank is described in Section 5.5.1, the water chamber in Section 5.8, and the actuator in Section 6.4. COTS options for the pressure regulator and solenoid valves are discussed in this section. Detailed design of fittings and piping was not conducted.

A range of COTS paintball regulators are available. An example regulator has a mass of 0.115 [kg] with an adjustable output range of 20 to 60[bar]<sup>2</sup>. In selecting a regulator, a consistent set pressure and sufficient volumetric flow rate ( $> 15$  [L/s]) are required. For the presented regulator, pressure is set by a less convenient but more robust shim system (preliminarily satisfying consistency); a similar regulator reports volumetric flow rates of 40 [ $ft^3/min$ ]<sup>3</sup> or 19 [L/s]. The selected regulator claims to improve on this by another 30% (est. 25 [L/s] satisfying flow rate). The compliance of these regulators should be validated experimentally.

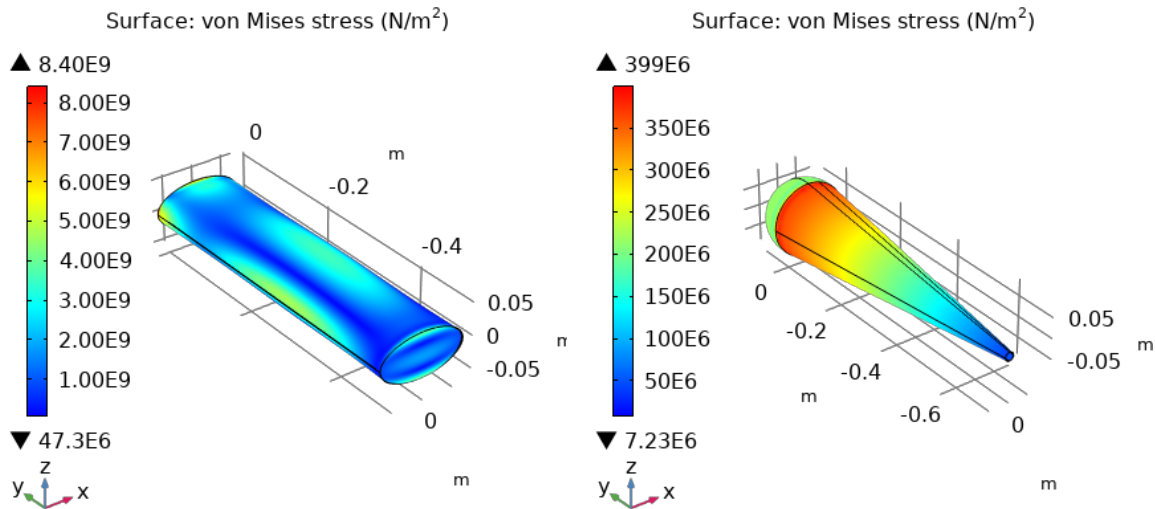
<sup>1</sup>Mechanics of Offshore Pipelines: Buckling and Collapse, Vol. I

<sup>2</sup>Ninja 4500PSI Paintball Regulator

<sup>3</sup>Power Tank Regulators



(a) A static study of the proposed wing water chamber shell. The shell has a thickness of 2[mm], with a mass of 7.5[kg]. A heavier wing is infeasible. Study boundaries are a fixed wing root, and applied pressure loads of 25[bar] (internal, outwards) and 1 bar (external, inward). The simulated stresses are well in excess of what is allowable with current materials: concentrations of 15,000+[MPa] are observed consistently along the leading and trailing edges. In addition to prohibitive stresses, large deflections accumulate at the wing tip ( $\approx 1$  meter, not rendered). A 5mm thick shell experiences theoretically feasible stresses ( $\approx 2,500$ [MPa] peak), with a mass of 15[kg] per wing.



(b) The same boundary conditions as in Figure 5.11a are applied to an elliptical pressure chamber of thickness 1[mm] (eccentricity 0.5[-]). Stress is concentrated at the vertex and co-vertex seams of the chamber: contrasting cylindrical chambers, which exhibit a uniform distribution. An equivalent cylindrical chamber experiences 100[MPa] of hoop stress (simulation result). Stress concentration magnitude increases with eccentricity, and is already significant at low values (830[MPa] at 0.1 eccentricity)

(c) The water chamber outlined in Figure 5.10b is simulated, having a thickness of 0.5mm (same BC's as Figure 5.11a). An axially uniform stress distribution emerges, validating the hoop stress model. The boundary between spherical and conical tank sections is evident, with a factor of 2 difference in magnitude, matching analytical models. Taking a material density of 1750[kg/m] for CFRP, the simulated chamber has a mass of 0.242[kg]: 0.8% the mass of 5[mm] wing shells (which further require 43 times greater allowable material stresses)

**Figure 5.11:** Finite Element Model studies in COMSOL Multiphysics, exploring the feasibility of eccentric pressure vessels



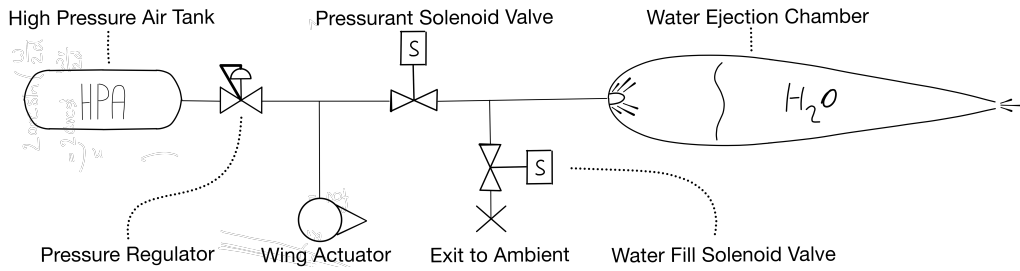


**Figure 5.12:** P&ID (Piping and Instrumentation Diagram) of the final architecture. Air pressure is reduced from storage (max 310[bar]) to a common pressure (25[bar]), which energises the wing sweeping mechanism and water chamber. A path to ambient facilitates filling of the chamber when submerged.

Fluid control is achieved by twin solenoid valves. At a design pressure of 25 [bar], industrial COTS options are available<sup>1 2</sup>. COTS valves have some power requirements to operate, though the primary criteria driving selection are fitting size and corrosion resistance. Fitting size is a practical consideration, as suppliers may not always anticipate demand on the scale of the desired use case. Corrosion resistance must be considered as the valve will be exposed to salt water. Detailed selection of a COTS valve should be performed in tandem with fittings and piping design.

**Table 5.3: Components Overview:** summary of all launch system components. Size is generally height by width by depth. Power is peak power draw, energy is energy draw over the whole mission. A - field indicates nonzero but negligible. TBDs follow from work before final submission

Component	COTS	Mass [kg]	Size	Cost [EUR]	Power [W]	Energy [J]
Pressurant Tank	Yes	1	2.4 [L]	300	0	0
Pressure Regulator	Yes	0.115	5x5x10 [cm]	50	0	0
Solenoid Valve (2x)	Yes	0.2	10x10x5 [cm]	150	15	-
Water Chamber	No	0.5 <sup>3</sup>	9x9x79 [cm]	1000	0	0

### 5.9.1. Future Work

The following developmental areas remain. These topics serve to further develop the dependability of the design. Their non-inclusion should not undermine the feasibility of the concept.

- **Detailed launch dynamics model** to refine performance estimates (replacing the ballistic  $\Delta V$  model) and sensitivity to aspects such as sloshing. This entails trajectory simulation, requiring a time-dependent thrust model, and a breaching water drag model. In addition to refined performance estimates, the study of unique vehicle dynamics and corresponding control insights are of particular interest.
- **Pressurant injector design** and modelling is an aspect of detailed design that should not be neglected. Though unlike chemical rocket engines there are no mixing considerations, a lightweight solution to ensure a uniform pressure field in the chamber is needed.

### 5.9.2. Verification and Validation

**Table 5.4:** Verification methods for launch system requirements. D: demonstration, A: Analysis, I: Inspection, T: Test

Requirement	Verification Description	Method
LNC-01, LNC-02, LNC-03	Develop a time-dependent launch motion simulation to confirm target trajectory.	A
LNC-03	Conduct static testing of the water launch system to confirm sufficient thrust and total impulse.	T
LNC-01, LNC-02, LNC-03	Conduct fully integrated system test of water launch sequence to confirm target trajectory is followed and sufficient for airborne transition.	T

<sup>1</sup>SV5225 25 bar Solenoid

<sup>2</sup>TORK T-SW Submersible Solenoid



**Validation** of the launch system, insofar that the client need is met, is achieved by demonstrating (by a series of field tests) the dependability of water to air transition and operation of the drone as a whole. The ability to execute the maneuver in a predictable and performant manner while around wind park assets is a of high interest.

## 6 Air to Water Dive

In this chapter, the load impact of diving is analysed. The hinge mechanism is explored, researched and designed.

### 6.1. Requirements

**Table 6.1:** Diving Requirements Table. Initial performance requirements for diving architecture selection and initial sizing

ID	Description	Traceability	Rationale
DV-01	The vehicle shall have an aerodynamic velocity of 16 m/s when diving into the water	Quantity is above the preliminary stall speed estimate	Stall speed is a conservative initial estimate and diving just above this still allows for controllability
DV-02	The system shall be able to resist a maximum impact load up to 1700 [N] during the dive operation	Simulating load impacts through a Python code	Is based on area hitting the water and all loads acting on the system e.g. drag
DV-03	The system shall have a dive entry angle at a minimum of 52 degrees	The most critical angle a wave is capable of	It is a conservative angle as this only occurs in the worst conditions
DV-04	The system shall sweep back the wings 90 degrees in 1 second	The minimum angular velocity the sweeping mechanism must accomplish	The time left after ejecting out of the water to the top of the trajectory

As a more general requirement list for the design to abide by the following should be considered:

- Must deploy and fold the wing during the flight in a time duration of 1 second
- A locking mechanism must be established to ensure the wings stay open/closed
- Must be as lightweight as possible.
- Must minimise complexity to decrease failure rate or need for maintenance

### 6.2. Literature

Through research, existing options were found that could be adapted to our design. An investigation was also carried out on the advantages and disadvantages of rigid vs flexible wings.

#### 6.2.1. Flexible Wing vs Rigid Wing

Flexible wings and rigid wings have several advantages and disadvantages where the choice to have one or the other is based on the mission profile.

Firstly, flexible wings are a new technology and are used commonly on MAV designs utilising a flexible membrane wing. The wing is used in low Reynolds number conditions (laminar flow; high lift, low drag) and has high aerodynamic efficiency. It can adapt to different operating conditions e.g. gusts, high angles of attack and density media. They also allow for a more lightweight structure and easy collapsing abilities. However, the flexible wing has a low lift-to-drag ratio due to problems with lift generation and flow attachment; at high speeds, the wing may experience flutter.

On the other hand, a rigid wing operates well at high speeds with great maneuverability. A rigid wing obviously encompasses higher structural integrity helping with safety, minimising the likelihood of crashing and having better, more precise control. However, rigid wings are much heavier and are more expensive to manufacture. Finally, a rigid wing requires more maintenance and inspection which adds to the overall budget.

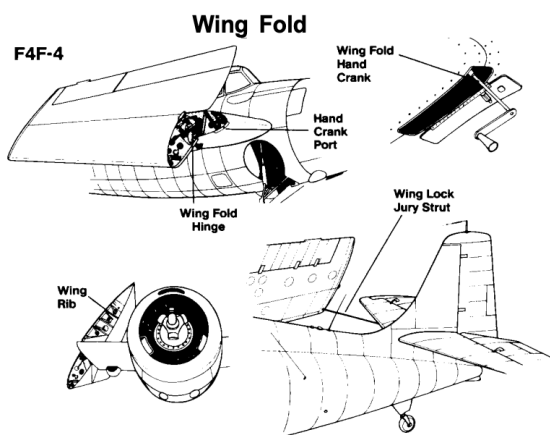
### 6.2.2. Existing Options

There are several existing options that can be adapted to our requirements and design. The STO-wing as displayed in Figure 6.1a, was designed to meet the storage space requirements of the US Navy; this allowed the transport of more military aircrafts. This was a unique solution as it was the most successful folding mechanism at the time. It also allows the wings to be very close to the fuselage and so reduces drag.

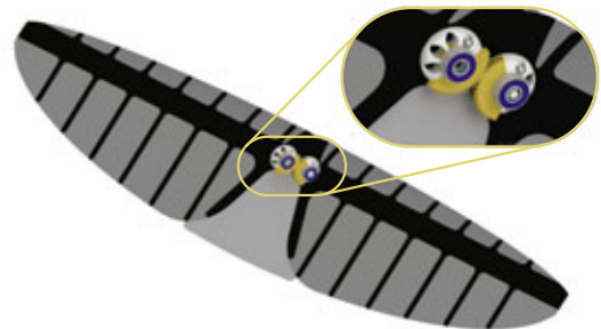
The AquaMAV in Figure 6.1b also has a folding mechanism using a gear linkage that would fold the flexible wing membrane. This allows the wings to be completely folded back with minimal protruding area. Further, it is a lightweight design.

A combination of different mechanisms is seen in Figure 6.1c [21]. A rotary mechanism moves the wings through gears and a linear actuator uses a linear force to pivot the wing. The rotary mechanism transfers the input torque (by a servo) to the gears allowing for high efficiency. It is also a flexible design as the rotation speed can be changed through the power of the servo and the gears transmission ratio. The servo is also very lightweight. Having this linear mechanism is simple and easy for manufacturing and maintenance.

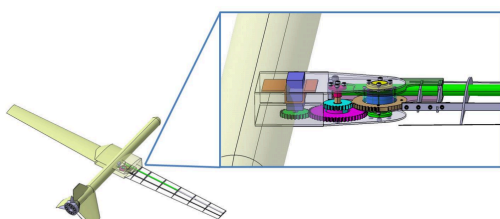
A horizontal fold was also presented within the research investigation shown in Figure 6.1d. this is a lateral folding of the wing so that they end up parallel to the fuselage. This however will create more drag in comparison to the aforementioned techniques.



(a) STO-Wing[22]



(b) AquaMAV folding mechanism[21]



(c) Linear folding mechanism[21]



(d) Horizontal fold[23]

**Figure 6.1:** Figures displaying existing folding mechanisms of the wings

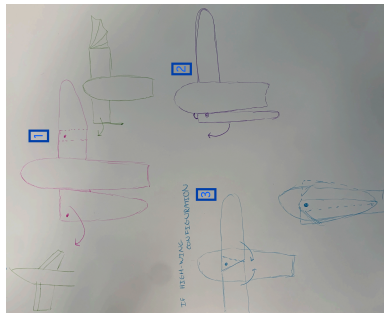


**Figure 6.2:** Sketched out design options

## 6.3. Design Options

Different design options were investigated to gain inspiration for the mechanism within the Puffin design.

### 6.3.1. Option Exploration

A couple of ideas were sketched, as seen in Figure 6.2 which took inspiration from literature.

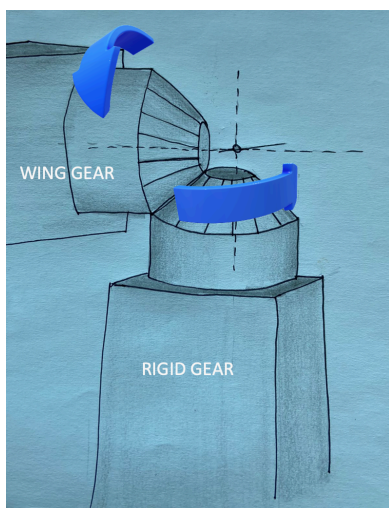
Some ideas can already be eliminated on the basis of the control surfaces. Any fully flexible wings made from the membrane cannot be used as ailerons and must be applicable to the design. Good maneuverability/control is essential to the design for diving and launch.

Consequently, the three options that will be investigated are (using Figure 6.2 as reference):

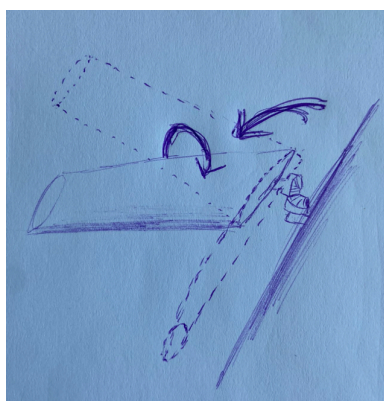
- 1 - Horizontal fold
- 2 - Parallel fold
- 3 - Singular hinge sweep

#### Horizontal Fold

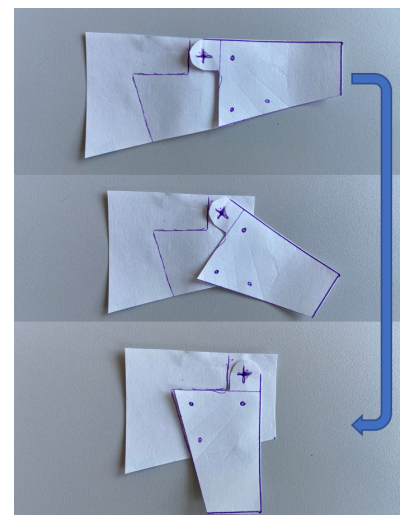
In the case of the horizontal fold, the wings both have a spring-loaded hinge. It is kept in place by a pin-locking mechanism which, when released, sweeps part of the wing backwards where it is again locked in place by a pin. A motor will wind up the wing to its original position during launch. An important consideration is that the wings will need a cut-out to allow them to overlap. This is depicted in Figure 6.3c by the blue line on the left section.



**(a)** Gear mechanism rotating in two degrees of freedom for the singular hinge mechanism



**(b)** Depiction of wing movement for the singular hinge mechanism



**(c)** Sweep back of the horizontal wing fold

**Figure 6.3:** Mechanisms for the horizontal wing fold and the singular hinge fold

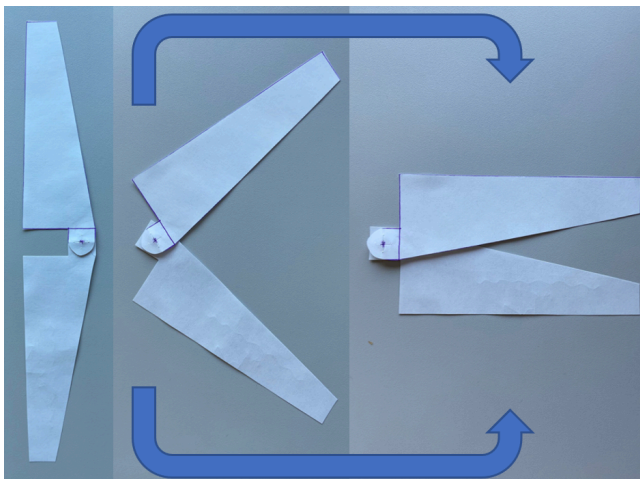
#### Parallel Fold

The parallel fold utilises gears to rotate in two degrees of freedom. The wing rotates 90 degrees till the wing is vertical (with the trailing edge pointing upwards). It then rotates about the root 90 degrees till it is parallel with the fuselage. To enable this movement two gears are used, where one stays rigid and the other moves along

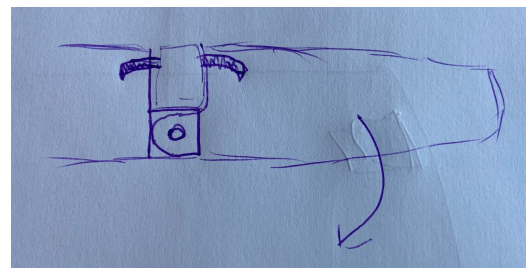
it. This is shown in Figure 6.3a. It will move 90 degrees along the rigid gear while also turning the wing 90 degrees as seen by Figure 6.3b. A servo will supply the power to the gears.

### Singular Hinge Fold

This design is a simple mechanism as it only involves one hinge and assumed a high-wing configuration. The idea is to place a load pivot hinge on the root of the high-configuration wings which are locked in place by hooks. At the moment of sweeping back, the hooks release the wings and due to the spring load, the wings immediately sweep back. There will be a rubber block to stop the blow as well as a dampener to reduce impact. To put the wings back in place, a motor will wind the wings back up. Depending on the airfoil, a cut-out in the wing may be necessary to let them overlap. This mechanism is demonstrated in Figure 6.4b.



(a) Sweeping-back mechanism for a singular hinge



(b) Hooking mechanism for a singular hinge

Figure 6.4: Singular hinge fold mechanism

### 6.3.2. Trade-off Sweeping Mechanisms

The considerations in the trade-off will be the following: These ideas will be investigated and assessed on the following criteria:

- Additional mass
- Logistics
- Complexity
- Drag value

Due to the structural configuration of the Puffin, particular options can be eliminated. The back of the architecture is made up of an inverted-Y tail with underwater propellers placed on top of each tail blade. The parallel fold would therefore not be feasible as it would collide with the propellers behind when it folds.

Out of the last two options, horizontal fold and singular hinge fold, both are feasible for the system. However, when observing mass and drag there is a clear winner. The horizontal fold contains 5% more area when folded meaning it will produce more drag; drag is proportional to area. In addition, the mass of the horizontal fold is higher than that of a singular hinge. It contains two hinges with several locking mechanisms and a motor to rotate the wings back to unfold. In comparison, the singular hinge contains one hinge, one locking mechanism and one motor and so, would be a lighter option. Finally, the complexity of the mechanisms differs slightly. The singular hinge is more simple a design as it is all focused around one point whereas the horizontal fold needs an individual mechanism per wing. *Overall, the decision was made to use a singular hinge mechanism.*

## 6.4. Detailed Design of the Hinge Mechanism

In this section, there will be an investigation into the detailed design of the sweeping back of the wings. There was a process in finalising the final mechanism. Initially, a hinge with adjustable torque was researched however, there was not a spring that was small enough in dimension and delivered enough torque to complete the task. The following idea was to use a bi-stable mechanism with a pneumatic actuator; the bi-stable mechanism would deliver enough angular momentum to successfully complete the mission however, on reflection, with a large enough actuator there would be no need for the bi-stable mechanism and it would be a more simple design. Hence the decision was made.



### 6.4.1. Hinge Mechanism Description

On investigation, there was further thought on the aerodynamic consequences of cutting part of the trailing edge of the wings. An irregular and non-symmetrical shape on the wings will cause the flow over the wing to potentially separate and the non-symmetric wings will cause a loss of control. To resolve this issue, two hinges were established; this is still an improvement in comparison to the horizontal fold as it maintains a lower drag. This movement is portrayed in Figure 6.5b.

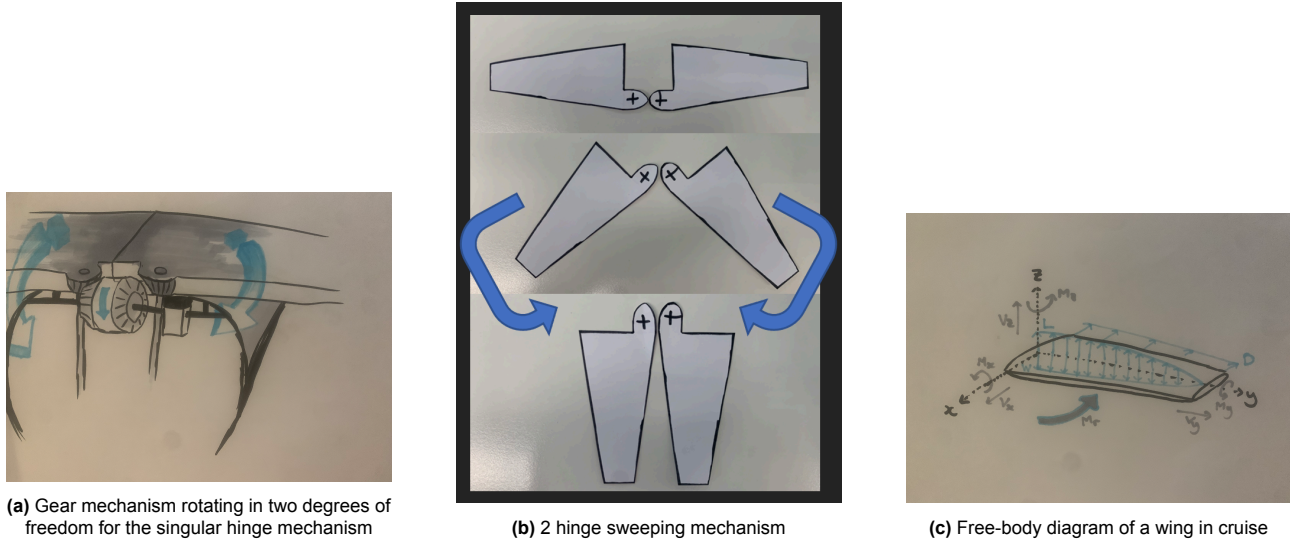


Figure 6.5: Hinge mechanism diagrams

The mechanism will rotate the wing through a pneumatic actuator with some relevant gears, activating both wings in a 90-degree rotation in the preferred direction. The setup is shown in the Figure 6.5a. The idea is to use the actuator to rotate the wings and deliver the necessary linear momentum to rotate the wing quickly. Due to the nature of water-to-air propulsion, the wing must completely empty itself of all water before it can be pivoted into the desired fixed-wing position. The leftover time after expelling the water and reaching the maximum height of the trajectory is approximately one second.

Firstly, using the FBD in Figure 6.5c and relevant equations below, the moment necessary ( $M_r$ ) for the rotation of 90 degrees in one second was calculated. One second is left after ejecting all water and the time to achieve the maximum height in the trajectory. The most critical moment of the mission profile, when reviewing the sweeping back mechanism, is the launch out of the water. It was assumed that the puffin is travelling vertically upwards so weight and drag are acting on the wings.

$$\sum F_n + \leftarrow: m\omega r_G = O_n \quad (6.1)$$

$$\sum F_t + \downarrow: m\alpha r_G = -O_t + m_{wing}g + \frac{1}{2}C_D\rho V^2 A \quad (6.2)$$

$$\sum M_G + CW : I_G\alpha = O_t R_G + M_r \quad (6.3)$$

Where:

- Angular velocity:  $\omega = \frac{\pi/2}{1} = 1.6 \text{ [rad/s]}$
- Angular acceleration:  $\alpha = \frac{\Delta\omega}{\Delta t} = 1.6 \text{ [rad/s}^2\text{]}$
- Mass moment of inertia,  $I_G$ : modelled as a rod

Which resulted in:  $O_n = 3.65 \text{ [N]}$ ,  $O_t = 25.55 \text{ [N]}$ ,  $M_r = -18.5 \text{ [Nm]}$ .

Therefore, the pneumatic actuator must produce a minimum of 18.5Nm to successfully complete the mission profile. A pneumatic actuator of 8 bar will be used and attached to the existing air tank. A depiction of the mechanism is displayed in Figure 6.5a.

As can be seen, the wings will rotate simultaneously as they will be attached to the same gear; this will aid in maintaining control of the system. To ensure that the wings stay locked in place during aerial flight a hooking mechanism will be used, while allowing for a quick release. The pneumatic actuator will also hold the wings in place. During the underwater phase, a locking mechanism is not necessary as the drag and the actuator are substantial.

The pneumatic actuator selected is the 'Festo Double Action Pneumatic Rotary Actuator, 90° Rotary Angle<sup>1</sup>'. It sizes by 13.33x6.85x10 [cm] and weighs 1.3 [kg]. It requires 8 bars of pressure to produce 29.2 [Nm] of torque and costs €101.72. The gears themselves will add an extra 300-500 [kg].

#### 6.4.2. Hinge Sizing

There are multiple stresses acting at the hinge and it must be able to withstand them all. The most critical stress that would occur is during fixed-wing flight and the ejection out of the water. The first observation will be done for fixed-wing flight. As seen by Figure 6.5c there is lift, drag and weight acting on the wing. This produces both shear and normal stresses mostly due to the bending moment around the x-axis (65 [Nm]) and the shear force in the z-direction (100 [N]).

Some python code was utilised to observe the relationship between stress and area (specifically the dimensions). The width and height thickness of the hinges was limited by the maximum thickness of the airfoil and a quarter the root chord. This allows for space for the locking mechanism and minimizes the width of the folded wings and so also drag. The stress that had the most influence over the sizing of the hinge was the thrust vector, specifically its moment. For a width and height of 0.042 [m] and 0.09 [m] respectively a normal stress of 23 [MPa] was calculated.

The yield stress of stainless steel is 205 [MPa] so it will be able to resist all stresses acting at this point. It will be attached to the main root chord and the rear spar of the wing. The rear spar will transfer all loads to the hinge.

A CAD drawing of the hinge is shown in Figure 6.6. It shows the hinge with and without the sized volume for the hinge.

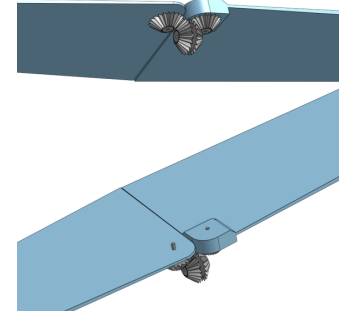


Figure 6.6: CAD drawing of the hinge mechanism

#### 6.5. Diving Load Impact

Another consideration is the loads that the system will experience when diving into the water. This will influence the dive angle and the velocity at which the system will execute the mission. To determine this, three graphs were produced showing the relation of force with time, angle of approach, and velocity. All methods and information were taken from the work 'Slamming dynamics of diving and its implications for diving-related injuries[24]' and the 'Swimming, flying, and diving behaviours from a unified 2D potential model'[25].

The system will experience a slamming force which is a high-impact force produced in a short time interval. This force entails inertial, viscous, surface tension, and gravitational forces. The inertial and gravitational forces are balanced by the dimensionless numbers: Reynolds number ( $Re > 10^4$ ), Weber number ( $We > 10^3$ ) and the Froude number ( $Fr \approx 1 - 10$ ). The slamming force is mainly caused by an unsteady hydrodynamic force defined by:

$$F_h = V^2 \cdot \frac{dm_a}{dz} \quad (6.4)$$

Where  $V$  is the entrance velocity and  $m_a$  is the added mass; the mass that is penetrating below the water level. Von Karman simplified model was utilised to assess the added mass term by assuming it is a hemispherical liquid volume where the radius is equivalent to the cross-sectional radius at the water surface. Consequently, the equation is:

$$F_h = \alpha \rho V^2 r^2 \frac{dr}{dz} \quad (6.5)$$

Where  $\alpha$  is the constant of proportionality which defines the flow field around the body,  $\rho$  is the density of water and  $r(z)$  is the radius in relation to penetration depth. It assumed that there is constant velocity so  $z = Vt$ .

The front of the system is assumed to have a paraboloid shape where  $r = (z/k_m)^{1/2}$  and  $k_m = 2H_s/R_s^2$  is the mean curvature at the snout.  $H_s$  and  $R_s$  are the height and radius of the paraboloid. The equation then becomes:

$$F_h = \alpha \rho V^{5/2} k_m^{-3/2} t^{1/2} \quad (6.6)$$

<sup>1</sup>Pneumatic actuator

Through literature,  $\alpha$  was found to be  $4\sqrt{2}$ . This whole process occurs before an air cavity is formed.

**Impact force vs. angle of approach** In the case of the angle of approach, the same force equation was used with the addition of the weight of the system. The velocity is again assumed to be 15 [m/s]. The impact with the water, therefore, becomes a function of theta and is evaluated along the  $x'$  axis. The equation would be as follows:

$$\sum F_{x'} : F_s = F_h + W \cdot \cos(\theta) \quad (6.7)$$

From the graph you can see that the maximum slamming force would occur when the system is completely parallel with the weight however, the more plateaued the system dives the less additional force would be supplied. However, the waves must also be considered. To avoid the system travelling through the wave into the air a minimum slope must be implemented. The critical conditions the system will be designed for are wave heights of 1.8 [m] and a time period of 6.2 [s]. If the waves are assumed to look like a sinusoidal wave and the derivative is calculated, there is a slope of 52 degrees. Consequently, the slamming force will be a fraction of the maximal impact force that would happen under vertical entry.

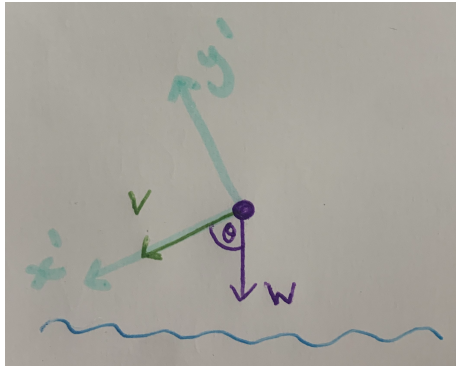


**Figure 6.7:** Dynamics diagram of the Puffin approaching the water

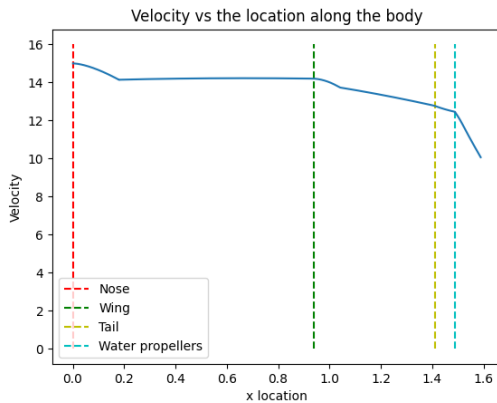
**Impact Force** In order to determine the loads acting on the structure due to the water impacts a numerical model has been developed. The model accounts for the change in the velocity caused by the impact force, water drag and buoyancy in a vertical free fall with an initial velocity of 16 [m/s]. The change of velocity can be found in Figure 6.8a. The impact force acts on the flow-facing surfaces. In order to quantify the impact force, the structure has been simplified following a developed water impact model. The nose has been modelled as a paraboloid. The added mass coefficients have been estimated by simplifying the wing and tail airfoil by ellipses. The water propellers have been modelled according to the used configuration as variable radius discs. The impact loads are shown in Figure 6.8b. The blade impact is not involved as the impact will not cause a velocity change of the structure, the impact force will cause

the blade bending, as further explained in Chapter 7. The model accounts for a vertical water entry, an angled entry will result in lower loads.

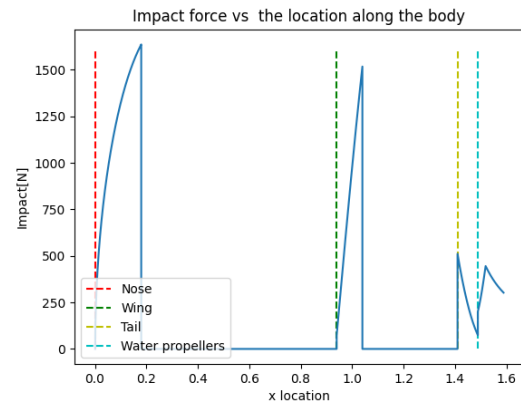
$$m \cdot a = m \cdot g - F_{buoyancy} - F_{water\,drag} - F_{impact} \quad (6.8)$$

$$F_{buoyancy} = V_{underwater} \cdot \rho_{water} \cdot g \quad (6.9)$$

The water drag estimation follows directly from the methodology established in Chapter 7.



(a) The change of entry velocity along the body of the system



(b) The impact force acting at different locations of the body

**Figure 6.8:** Entry velocity - and impact force along the body



## 6.6. Verification and Validation

**Table 6.2:** Verification methods for the relevant requirements of the sensing system. D: demonstration, A: Analysis, I: Inspection, T: test

Requirement	Verification Description	Method
DV-01,	A test will be carried out to observe the control and load impact from diving at this velocity	D
DV-02	A material will be used that can resist up to the required load with a safety factor	I
DV-03	Demonstrate the manoeuvre with a prototype to observe the control of the system	D
DV-04	The mechanism will be tested and timed	T

**Validation** A demonstration will be performed along with the control system to observe the manoeuvre and ensure all calculations have been done correctly. The air-to-water transition test on the prototype will show if the structure can withstand the mission conditions transition loads. The sweep-back mechanism should be tested in flight to ensure the wing is not unfolded during the water entry. The hinge, air propulsion unit blade connection, and the water propeller mounting should all be examined for failure loads.

# 7 Propulsion

In this chapter, the Puffin's propulsion system is sized for both air and water. After establishing the assumptions and incoming requirements on the propulsion system, the aerial propulsion system is sized. This is followed by the choice and sizing of an underwater propulsion system and a section on depth control. Then, the underwater propulsion system was iterated onto a completely new configuration. Finally, the chapter is concluded with verification and validation of the sizing tools, the requirements and the design.

## 7.1. Requirements and Assumptions

Assumptions that were made to size the propulsive systems are listed below. Table 7.1 establishes all the incoming requirements regarding the propulsion systems.

- It was assumed that the Puffin has to move at 2.5 [km/h] underwater to be able to monitor 10 units in an hour.
- It was assumed that the Puffin would have an underwater acceleration of 0.1 [ $m/s^2$ ].

**Table 7.1:** Incoming requirements driving the propulsion system selection and sizing

ID	Description	Traceability	Rationale
SUS-CL-PROP-01	The engine shall deliver a thrust force of 16 [N] during climb	SYS-CL-PERF-01, SYS-CL-PERF-02, SYS-CL-PERF-03	This thrust force is required to meet the performance requirements
SUS-CL-PROP-02	The engine shall deliver a thrust force of 10 [N] during the cruise	SYS-CL-PERF-01, SYS-CL-PERF-02, SYS-CL-PERF-03	This thrust force is required to meet the performance requirements
PROP-AQUA-01	The system shall be able to operate for at least 1.5 hours in currents of 1 [m/s]	PLD-STRC,PLD-SWG,PLD-WTR,OPR-ENV,OPR-NAV	This incorporates 1 hour to monitor the farm and half an hour to swim in and out of the farm

Continued on next page

name unfilled Table 7.1 – continued from previous page

ID	Description	Traceability	Rationale
PROP-AQUA-02	The system shall have a minimum underwater cruise speed in still water of 0.5 [m/s]	PLD-STRC,PLD-SWG,PLD-WTR,OPR-ENV,OPR-NAV	To monitor 10 units of the seaweed farm in an hour, the system has to move at 0.5 [m/s].
PROP-AQUA-03	The system shall have a minimum underwater acceleration of $0.05[m/s^2]$	PLD-STRC,PLD-SWG,PLD-WTR,OPR-ENV,OPR-NAV	At this acceleration, the puffin can reach its cruise speed in 10 seconds which is desired.
PROP-AQUA-04	The system shall be able to attain an underwater heave velocity of at least 0.5 [m/s]	PLD-STRC,PLD-SWG,PLD-WTR,CTRL-POS,CTRL-ATT	The system must be able to vertically translate with a minimum speed to comply with payload and control requirements
PROP-AQUA-05	The system shall be able to attain an underwater sway velocity of at least 0.5 [m/s]	PLD-STRC,PLD-SWG,PLD-WTR,CTRL-POS,CTRL-ATT	This is how fast the UAV should go on average to monitor 10 units in an hour
PROP-AQUA-06	The propulsion system shall be able to deliver at least 16[N] of thrust	PROP-AQUA-4	This is the thrust the system needs to overcome the drag and obtain the required velocities.

Due to the large difference in geometry of aircraft and marine propellers and the performance requirements for both air and aquatic operation individual air and propulsion systems are designed and considered.

## 7.2. Aerial Propulsion

The air propulsion subsystem has to provide sufficient thrust throughout the flight stage of the mission. The thrust requirement is a driving requirement behind the subsystem design. The design of the propulsion subsystem is limited due to the Puffin structure having to accommodate all the subsystems. As established in the Midterm report the aerial propulsion system shall be electric, limiting the feasible propulsion designs to a DC motor powering the propellers [1]. A ducted electric fan design option has been discarded due to lower efficiencies and higher structure weight[26]. An Electronic Speed Controller (ESC) will be used in the system allowing for constant adjustments to the motor settings based on the throttle data [27].

As explained in Chapter 6, the wings are swept back for medium transition and underwater motion. The placement of the propellers on the wings has been determined to be too restricting and structurally complex for the configuration to be beneficial. Placement behind the structure was deemed highly limiting for the integration of the underwater propulsion and air-to-water transition subsystem. The blades have to be retracted for the air-water media transition and underwater motion, to limit the effect of the impact loads and the underwater drag. The blades, attached to the spinner, will fold back onto the fuselage to minimise the water impact loads. The blades will fold when no torque is applied due to the drag forces in movement, and fully deploy in the air with the torque applied. The range of movement of the propellers will be limited in order to avoid blade interference and inflicted damage due to contact with the fuselage upon impact. A single foldable twin-blade propeller on the Puffins' nose has been deemed the most feasible and sized for the needs of the mission.

### 7.2.1. Sizing

**Thrust estimation** The thrust needed to be delivered by the system depends on the drag force acting on the structure. Drag in cruise conditions has been estimated for a cruise velocity of 20 [m/s]. The aerodynamic parameter has been obtained during structure sizing in Chapter 10. Drag is estimated using Equation 7.1 and Equation 7.2.

$$Drag = 0.5 \cdot \rho \cdot C_D \cdot S_{wing} \cdot v_{airspeed}^2 \quad (7.1)$$

$$Drag_{climb} = Drag + W \cdot \sin(angle_{climb}) \quad (7.2)$$

Where  $\rho$  is the air density,  $v_{airspeed}$  is the flight velocity and  $S_{wing}$  is the wing surface area. The highest drag experienced in flight happens during the climb due to the weight contribution, as seen in Figure 7.1.

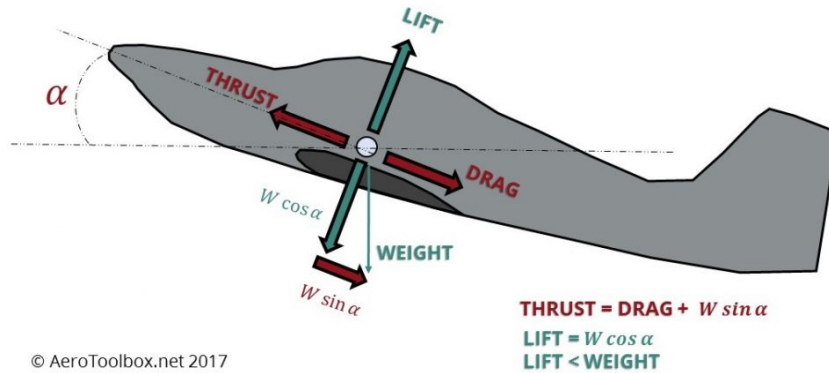


Figure 7.1: Forces on an aircraft in climb climb[28]

The magnitude of the weight contribution is dependent on the climb angle. The steeper the climb, the higher the rate of climb and climb angle. The cruise drag is adjusted for the weight contribution. The final estimated values obtained are found in Table 7.2.

**Propeller sizing** The propeller sizing is an iterative process, the parameters are codependent and oftentimes limited by the performance of the off-the-shelf components. An estimation is performed with the mission profile, component availability and low mass requirement taken into consideration. The required operational revolutions per minute (RPM), the propeller diameter, flight altitude, and the rate of climb (ROC) need to be optimised for the performance of the system. The diameter of the propeller is directly related to how much thrust the system can deliver.

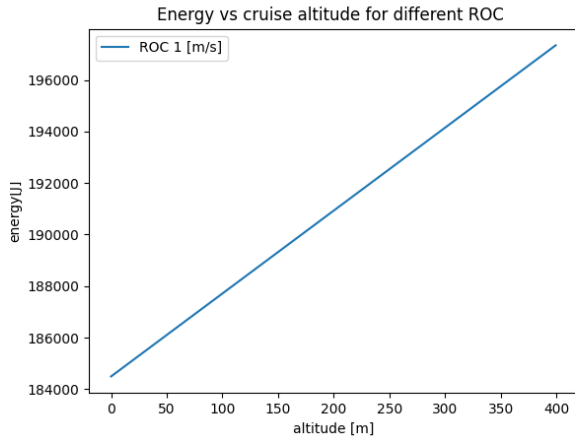
$$T = 0.5\rho \cdot \frac{\pi D_{prop}^2}{4} \cdot \eta_{rotor} \cdot (v_{exit}^2 - v_{airspeed}^2) \quad (7.3)$$

$$D_{prop} = \sqrt{\frac{8 \cdot T}{\eta_{rotor} \cdot \pi \cdot \rho \cdot (v_{exit}^2 - v_{airspeed}^2)}} \quad (7.4)$$

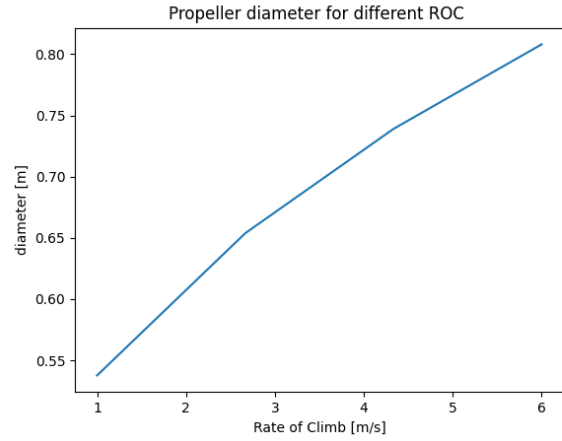
$$Power = \frac{Drag_{climb} \cdot v_{airspeed}}{\eta_{motor}} \quad (7.5)$$

$$Torque = \frac{Power}{RPM} \quad (7.6)$$

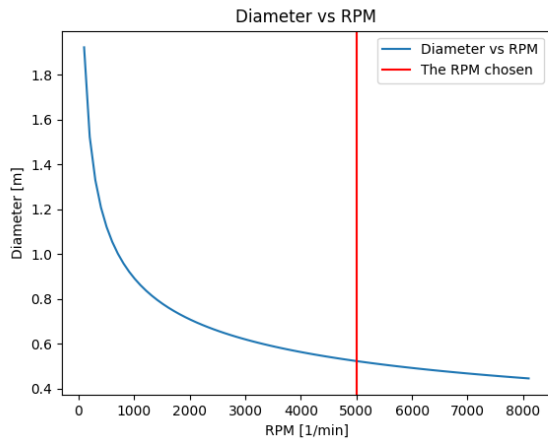
T is the required thrust,  $D_{prop}$  is the diameter of the propeller,  $\eta_{rotor}$  is the propeller efficiency,  $\eta_{motor}$  is the motor efficiency and  $v_{exit}$  is the exit airflow velocity. The exit velocity has been estimated to be a vector sum of the propeller tip velocity and the airflow velocity.



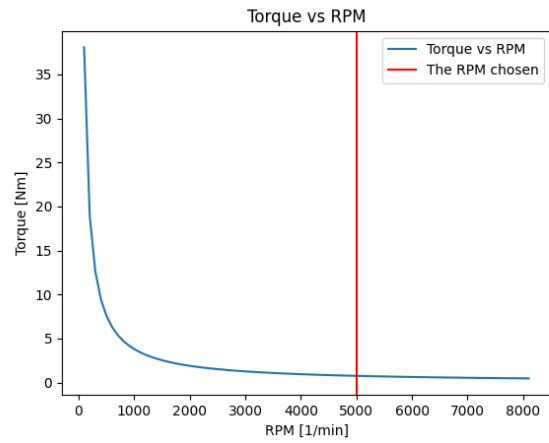
(a) The energy required per one one-way flight to the seaweed farm vs the cruise altitude for different rates of climb



(b) The estimated required propeller diameter vs the rate of climb



(a) The diameter of the twin-blade propeller against the RPM with the indicated chosen RPM value of 5000  $1/min$



(b) The environment seen from underwater, with the turbidity simulation and the example ROV.

As seen in Figure 7.2a the diameter heavily relies on the motor RPM, similarly to the required torque (Figure 7.2b). The commercially available lightweight UAV brushless motors have a limited RPM and generated torque. The available motors are mostly operating around 3000  $[1/min]$  RPM, with the highest performing motors achieving 5000  $[1/min]$  RPM. The available motors mostly allow for the generation of torque up to 1  $[Nm]$ . The diameter is to be minimised due to impact loads and mass required. With those aspects considered, the RPM of 5000  $[1/min]$  has been chosen in order to minimise the torque and diameter requirements. The following assumption led to a diameter estimation of 0.52  $[m]$ , as presented in the Table 7.2. The estimation assumed the rate of climb of 1  $[m/s]$ , this flight characteristic will be revised at a later stage in order to obtain the most beneficial configuration.



**Figure 7.4:** Propeller efficiency vs diameter for various RPM, for estimated required diameter the propeller efficiency is 0.7, the efficiencies increase with decreasing rpm and increase with the increasing diameter. Increasing the diameter is to be avoided for impact performance.

With the diameter established, the propeller efficiency can be evaluated. The relation between the efficiency,

diameter and RPM can be seen in Figure 7.4. The efficiency of the propeller blades for the configuration is around 0.7. Although the efficiency increases with decreasing RPM, low RPM is not desired due to torque and diameter requirements. The ROC has to be established in order to evaluate the requirements for the system. As the rate of climb impacts the climb angle, the required thrust increases. This relation can be seen in Figure 7.3a and Figure 7.3b, the higher the rate of climb the higher the required propeller diameter. The rate of climb of 1  $[m/s]$  has been deemed the most feasible for the needs of the design, allowing for a low diameter and acceptable flight energy consumption. The system will be modelled for an altitude of 120  $[m]$ . This altitude is the highest certified altitude for STS-02 vehicles according to EASA<sup>1</sup>. This altitude will allow for avoiding obstacles along the flight path, and provide the highest realistic necessary energy estimate.

**Table 7.2:** Flight specification estimation

Velocity [m/s]	Altitude[m]	Max thrust required [N]	Rate of climb [m/s]	RPM	Torque [Nm]	Blade diameter[m]	Motor power [W]
20	120	16	1	5000	0.76	0.52	399

### 7.2.2. Final Configuration

The initial sizing resulted in a propeller diameter estimation for a maximal thrust required for an RPM of 5000. Based on the final thrust, power, torque and RPM requirements a configuration of compatible, able to deliver the required thrust, off-the-shelf components has been chosen. The configuration includes blades of 0.47  $[m]$  diameter, lower than the initial estimation. Having a lower blade diameter is beneficial for the fuselage design and for the blade durability given the blades will be subject to loads upon water entry. The blades are made out of carbon fibre, a strong, corrosion, resistant material. The blades will be connected to the propeller adapter with a stainless steel connection. A carbon-fibre spinner will cover the mechanism. An estimation of the deflection and stresses has been performed on the blade to ensure the blades can withstand water entry and underwater movement. The blade material is a 3K carbon fibre.

The specifications of the elements can be found in Table 7.3<sup>2</sup>, Table 7.4<sup>3</sup>, Table 7.5<sup>4</sup>. The components are shown in Figure 7.5a, Figure 7.5b and Figure 7.5c.

**Table 7.3:** Motor specification

Motor name	Max Throttle Power [W]	Motor length [m]	Motor diameter [m]	Max RPM	Max torque [Nm]	Max thrust [N]	Motor mass [kg]	Cost [Euro]
KDE3520XF-400 Brushless	344	0.045	0.042	4920	0.9	25.8	0.245	130

**Table 7.4:** Blade configuration specification

Blade name	Number of blades	Propeller diameter [m]	Blade material	Blade total mass [kg]	Blade cost [Euro]
KDE-CF185-DP 18.5" x 6.3	2	0.470	Carbon-fiber 3K	0.038	144

**Table 7.5:** ESC specification

ESC name	ESC length [m]	ESC width [m]	ESC mass [kg]	ESC cost [Euro]
KDE-UAS35HVC	0.063	0.035	0.084	145

<sup>1</sup> Cover Regulation to Implementing Regulation (EU) 2019/947

<sup>2</sup> KDE3520XF-400

<sup>3</sup> KDE-CF185-DP

<sup>4</sup> KDE-UAS35HVC



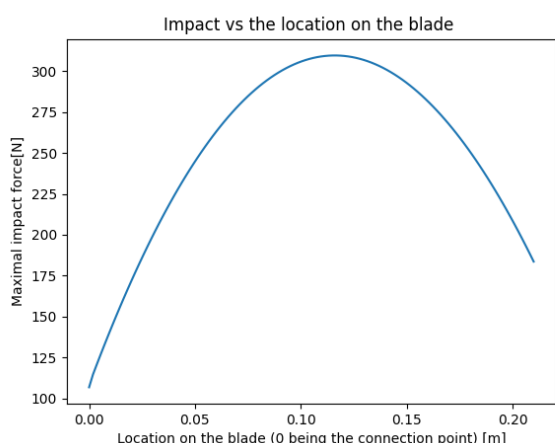
(a) KDE3520XF-400 motor

(b) KDE-CF185-DP 18.5" x 6.3 blades

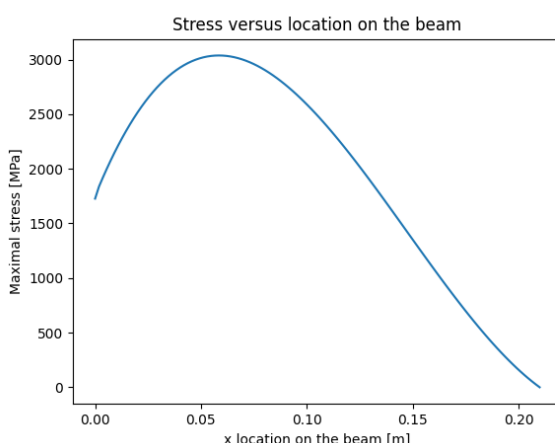
(c) KDE-UAS35HVC ESC

### 7.2.3. Nose Propeller Configuration

The water impact has been modelled and explained in Chapter 6. As established in the model, the surface entering the water shall be angled, and the blades will sweep back as seen in Figure 7.7a. Considering the geometry of the nose and the yoke width of 5 [cm], the maximum sweep back angle of 30 degrees is designed for. Such deflection limits the water impact while not allowing for the blades to hit the fuselage structure. The blades are free to rotate, the full retraction happens due to the blade momentum when the torque is applied to the shaft. The blade has been modelled as a beam. The blade has been simplified to a triangular front surface carbon-fibre beam with one end fixed support. The estimated effect of the water impact on the water structure can be found in Figure 7.6a. The critical load acting on the blade with a magnitude of 310 [N]. It is to be noted that the stresses and loads are overestimated, the impact model only takes into account the vertical free-fall at the stall velocity of 15 [m/s], and the loads at an estimated entry angle of 52 degrees would significantly decrease. The estimation does not account for the propeller pitch, the propeller has been modelled as a flat flow-facing plate, so the actual loads would decrease as the impact performance of angled surfaces is much better. The calculations prove that the blades can withstand the most critical impact. The maximum created stress in the modelled beam is 2% of the allowable stress. The final configuration includes a carbon-fibre spinner and stainless steel blade stopper<sup>1</sup>, as shown in Figure 7.7b. If the aforementioned off-the-shelf blades are used a stainless steel connection should be 3D printed, allowing for the folding back as shown in Figure 7.7a. The blade stopper limits the blade orientation changes from perpendicular to the shaft axis to the folded 30 degrees back impact configuration. The total energy estimated for the flight both ways is 438712 [J], having taken into account a 20% safety factor. The maximum thrust able to be generated by the air propulsion unit is 26 [N], a thrust margin allows for emergency. The maximum thrust in the climb configuration with the negative effect of the expected wind is 25 [N], the air propulsion is able to generate the necessary thrust at all expected flight conditions.



(a) The impact force acting along the blade



(b) The estimated stresses within a single blade against the position

<sup>1</sup>Aeronaut 2-Blade Black Spinners for Folding Propellers





(a) The blades folded onto the fuselage, mounted to the adapter.



(b) The proposed configuration: carbon-fibre spinner, blade stopper limiting the movement to 30 degrees off fully expanded.

## 7.3. Water Propulsion

### 7.3.1. Propulsion Architecture Selection

From Section 7.3.2, initial performance values were calculated that the system must fulfil. To find a propulsion system that can adhere to the performance values and requirements an investigation was done on various marine propulsion systems. The most commonly used propulsion systems for marine vessels are propeller based. Other non-propeller-based solutions exist such as magnetohydrodynamics and superconducting motors however these are not as commonly used within naval engineering. The efficiency of a magnetohydrodynamic drive (MHD) is proportional to the flow speed of the vehicle meaning this system is only efficient at high speeds. For a MHD system to be efficient at lower speeds a stronger magnetic flux intensity is needed by using stronger magnets. Given the weight required for an MHD system to achieve a similar efficiency to propeller-based propulsion at the vehicle's target speed, the MHD is eliminated from consideration. Superconducting motors are still in the early phase of design and require an operating temperature of 35-40 [K]. To maintain these temperatures an extensive cooling system is needed which increases the weight and worsens the performance of the Puffin [29]. Therefore the final marine propulsion system is chosen to be propeller based. Propellers work Different types of propeller-based propulsion systems exist within marine engineering each with their own strengths and limitations. The most commonly used system is a fixed pitch propeller due to their simplicity, robustness and efficiency [30].



**Table 7.6:** Overview of marine propeller-based propulsion systems [31]

Propulsion System	Description
Fixed pitch propellers (FP)	Most commonly used propulsion system. The position of blades is fixed for mission, heavy weather will negatively impact the performance and power requirements of this system
Controllable pitch propellers (CP)	The pitch of the propellers can be adjusted through a hydraulic system within the hub of the propeller. A larger hub also lowers the efficiency of the propeller.
Tandem propellers	Tandem propellers consist of multiple propellers mounted on a single shaft. These ease the loading on each of the propellers and do not experience cavitation-induced thrust breakdown. However, they have large bending moments which increases the size and weight of the stabilizing system.
Cycloidal propellers	Cycloidal propellers are a set of vertical vanes that are mounted on a rotating disc. This system provides high maneuverability, and reliability and also avoids the need for a rudder in an aquatic environment. However, cycloidal propellers have a high degree of mechanical complexity and are very large in size and weight.
Water jet propulsion	This system has an inlet of water and then accelerates the fluid through a propeller or impeller. It then ejects the accelerated fluid causing a thrust in the opposite direction of ejection. This offers high maneuverability, high efficiency at larger speeds and avoids cavitation. However, the system has a large weight and power requirements.
Azipods	This system is a propeller-based thruster that can rotate about its vertical axis. Normally, 360 degrees of revolution can be done with azimuth thrusters and it provides excellent maneuverability. Podded thrusters are chosen as they will be electrically powered. This system has a high cost, and weight and requires a significant amount of power for the propeller and its rotation relative to other propulsion systems.

To determine which propulsion system is feasible multiple systems from Table 7.6 will be investigated. However, certain systems can not be implemented as their inherent properties are not suited for amphibious operations. Tandem propellers are commonly used in large vessels and are impractical and generally too inefficient for small AUVs.

Cycloidal propellers are eliminated from consideration as they require significantly heavier, more complex systems and have high power to provide the given level of thrust required. While they provide high maneuverability the extra power needed for the flight to compensate for the weight, drag, and battery of the cycloidal system makes this propulsive system infeasible given the better alternatives [31].

Water jet propulsion creates thrusts by utilizing a propeller or impeller to accelerate fluid and eject it. The ejection requires a nozzle and potentially a bucket to utilize thrust vectoring properties. This system provides high maneuverability but low efficiencies, high power and high mass requirements for the speed of operation of the Puffin. Additionally, controllable and fixed-pitch propellers offer significantly better performance, mass and power qualities for propulsion [32].

Controllable pitch propellers offer many benefits and the high maneuverability could be very beneficial for the operating environment. However, given that the control surfaces in our system will also have to operate in the air, they may be oversized for aquatic operations proving a high level of controllability in the water with fixed-pitch propellers. However, they have lower efficiency, larger size, more complex and higher cost relative to fixed-pitch propellers.

Fixed-pitch propellers and water jet systems could be used as a propulsion system for an AUV. They are reliable, cost-effective and have the best mass and power properties compared to the other propulsion systems in Table 7.6. However, they have low maneuverability and a more extensive maneuvering system is required. At an operational speed range of 0.5 – 2[m/s] FP propellers have high efficiencies. [30]

### 7.3.2. Drag Model of the Submerged Puffin

To make a first estimate of the propulsive forces needed to meet the requirements underwater, the Puffin was modelled as a smooth sphere with a diameter of 0.4 [m]. The Reynolds number of the seawater at a flow speed of approximately 2 [m/s] equals  $2 \cdot 10^6$ . For a smooth sphere, this results in a drag coefficient of 0.3<sup>1</sup>. Applying the balance of linear momentum to the body as shown in Figure 7.8, with an acceleration of 0.1 [m/s<sup>2</sup>], the required thrust was calculated. Subsequently, the power required was found by multiplying this resulting thrust force with the flow velocity. The Puffin needs 45 [N] of thrust and 67 [N] of power to meet the requirements.

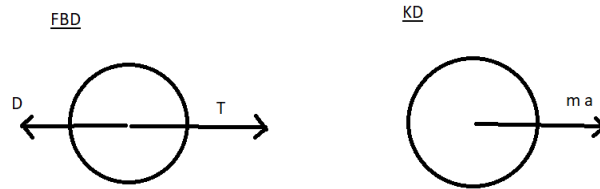


**Figure 7.8:** Free body diagram and kinetic diagram of the Puffin showing thrust (T), drag (D) and acceleration

Later in the design process, the underwater drag estimation was refined. To estimate the underwater drag of the system the hull, wing and control surfaces are considered. To estimate the hull skin friction coefficient Equation 7.7, the hull is modeled as a cylinder with a diameter 0.18 [m] and total length of 1.76 [m] with two hemispheres at each end.

$$C_{F_{flat}} = \frac{0.067}{(\log_1 0R_e - 2)^2} \quad (7.7)$$

The drag force caused by the hull skin friction is then calculated with Equation 7.8:

$$D_{F_{hull}} = C_{F_{flat}} \frac{1}{2} \rho V^2 S_{wetted} \quad (7.8)$$

Similarly, the drag caused by the skin friction from the wings and control surfaces can be calculated using Equation 7.9. Where  $S_{front}$  represents the frontal area exposed in the direction of motion.

$$D_{F_{control}} = C_{D_{frac12}} \rho V^2 S_{front} \quad (7.9)$$

Another source of drag is in the form of pressure drag. This is caused by vortices forming due to disruptions in the fluid flow. First, the pressure drag coefficient is calculated using Equation 7.10:

$$C_{F_{pressure}} = \frac{0.075}{(\log_1 0R_e - 2)^2} \quad (7.10)$$

The pressure drag is computed using Equation 7.11.  $\eta_{hull}$  represents a form factor which is dependent on the shape of the hull. For modern submarine shapes, this value is set to 5.  $\frac{L}{D}$  is the slenderness ratio which is the length of the system divided by the diameter.

$$D_{F_{pressure}} = \eta_{hull} \left(\frac{L}{D}\right)^{-1.7} C_{F_{wake}} \frac{1}{2} \rho V^2 S_{wetted} \quad (7.11)$$

The total drag felt by the system is computed with Equation 7.12.

$$D = D_{F_{hull}} + D_{F_{control}} + D_{F_{pressure}} \quad (7.12)$$

The drag was calculated in the longitudinal and lateral by adjusting the Reynolds number, the area exposed and velocity for both cases. The resultant drag

<sup>1</sup>Drag coefficient of a sphere

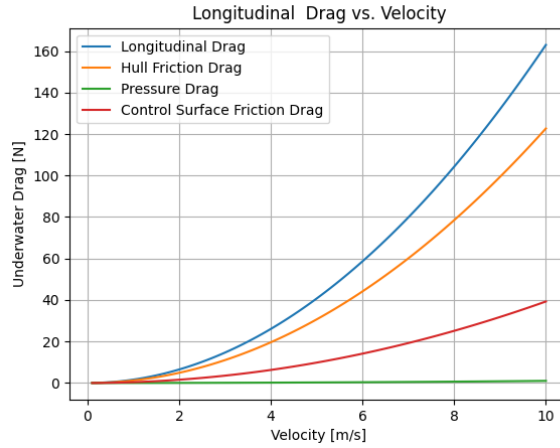


**Figure 7.9:** Longitudinal drag contributions over different velocities

From Figure 7.9 the majority of drag originates from the hull skin friction and then the pressure drag.

### 7.3.3. Estimates of Initial Parameter

Firstly the propeller will be designed to meet the requirements of underwater propulsion. The motor and subsequently battery selection will follow from new requirements that arise from the propeller sizing.

As a starting point for designing the fixed-pitch propeller, a couple of parameters were estimated based on reference literature and propeller design textbooks. The angle of attack ( $\alpha$ ) was assumed to be  $5^\circ$  and the pitch angle ( $\phi$ ) was assumed to be  $10^\circ$  [33]. Furthermore, the free stream velocity is modelled to be 1.5 [m/s] as it incorporates the 0.5 [m/s] velocity coming from the requirements and an additional 1 [m/s] of current velocity. The parameters can be seen in the schematic drawing in Figure 7.10 below where  $V_r$  is the free stream velocity.

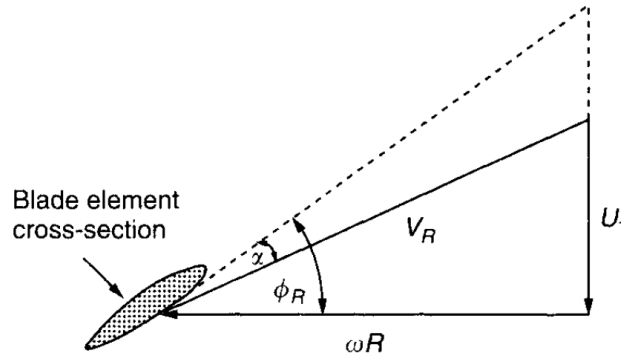


**Figure 7.10:** Schematic drawing of a propeller blade showing the pitch angle, the angle of attack and the free stream velocity [33]

The propeller diameter ( $d$ ) was varied between 0.05 [m] and 0.4 [m]. Propellers smaller than 5 [cm] are not applicable for this design whereas propellers with diameters larger than 40 [cm] would be hard to integrate with the overall design. With these input parameters and Using Equation 7.13, Equation 7.14, and Equation 7.15, the rotational velocity ( $\omega$ ), shaft torque ( $Q$ ) and power required to drive the propeller ( $P_{drive}$ ) were calculated [33]. The value of  $a$  in the formulas is 2 for open propellers [33].

$$\omega = \frac{2V}{d \cdot \tan(\phi - \alpha)} \quad (7.13)$$

$$Q = \frac{a \cdot \tan(\phi - \alpha)}{4} T d \quad (7.14)$$

$$P_{drive} = \sqrt{\frac{a}{\rho \pi}} \frac{T^{\frac{3}{2}}}{d} \quad (7.15)$$

From the formulas, it can be seen that for increasing propeller diameter, the angular velocity and required driving power decrease, which is advantageous. However, the shaft torque increases rapidly with larger diameters. Following Table 7.7 shows the calculated values for propeller diameters of 0.05 and 0.4 [m].

**Table 7.7:** Ranges of angular velocity, driving power required and shaft torque for propeller diameters ranging from 0.05[m] to 0.4[m]

Diameter [m]	Driving power [W]	Shaft torque [Nm]	Angular velocity [rpm]
0.05	130	0.074	6549
0.4	16.3	0.590	820

This first sizing helps to gain a better understanding of the orders of magnitude of the final propeller size. The next step is to use Matlab's OpenProp software to find the best design point and optimise the propeller design for that point. Additionally, the OpenProp software allows for the validation of the first sizing.

### 7.3.4. OpenProp Propeller Sizing

Now that a substantiated idea of the range of propeller and motor sizes was gained, OpenProp sizing software was used to optimise the propeller design within this range. Once a propeller geometry is chosen, the motor can be sized by researching reference motors. The OpenProp sizing is done in 2 phases. Firstly, based on a couple of input parameters, propeller efficiencies are generated for various numbers of blades and angular velocities. Once the most efficient combination of the number of blades, diameter and angular speed is determined, the propeller design can be optimised for these parameters. This results in a final propeller layout and specifications. Following Table 7.8 establishes the input of the first parametric sizing step.

**Table 7.8:** Different input parameters for the first estimation of propeller efficiencies based on the number of blades, diameter and angular velocity

Parameter	Value(s)
Required thrust	50 [N]
Flow speed	1.5 [m/s]
Hub diameter	0.05 [m]
Fluid density	1023 [kg]/m <sup>3</sup>
Number of blades	1 - 5
Rotational speed	100 - 1000 [rpm]
Rotor diameter	0.1 - 0.4 [m]

The results of this first parametric sizing are shown in Figure 7.11 below. Larger propeller diameters lead to better efficiencies but are not convenient for the design as they are harder to integrate, result in more drag and require stronger structures. Hence, looking at the graphs, a three-blade propeller with a diameter of 0.2 [m] was chosen. At an angular speed of 850 [rpm] this configuration has an efficiency of 64 % which is sufficient.

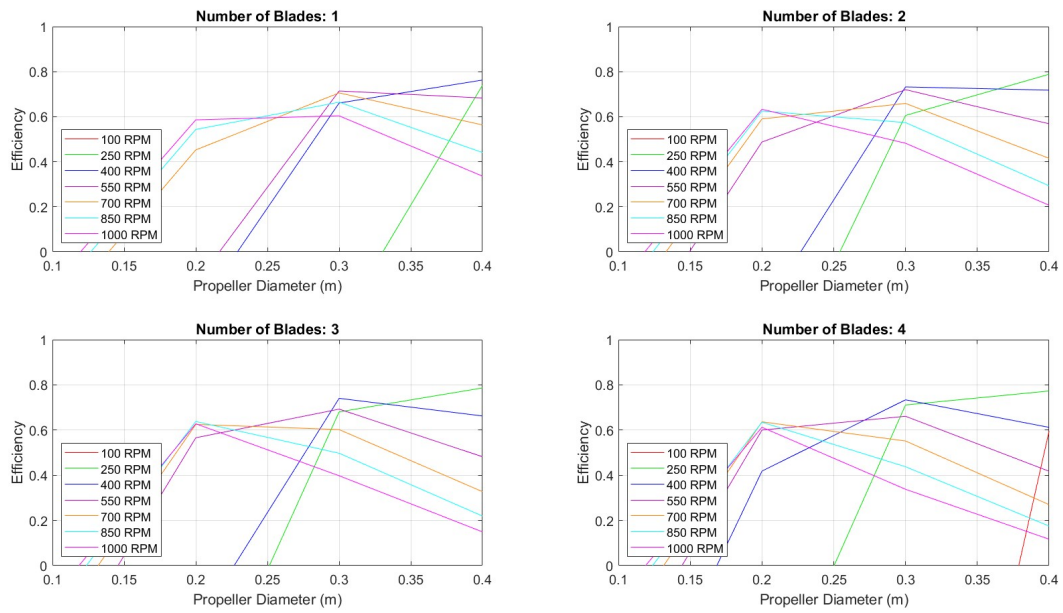


**Figure 7.11:** Propeller efficiencies for various angular velocities, number of blades and diameters

Secondly, the propeller design was optimised using the selected diameter, angular velocity and number of blades in addition to the parameters listed in Table 7.8. The final propeller design is shown in Figure 7.12. Its more detailed performance parameters can be found in Table 7.9.

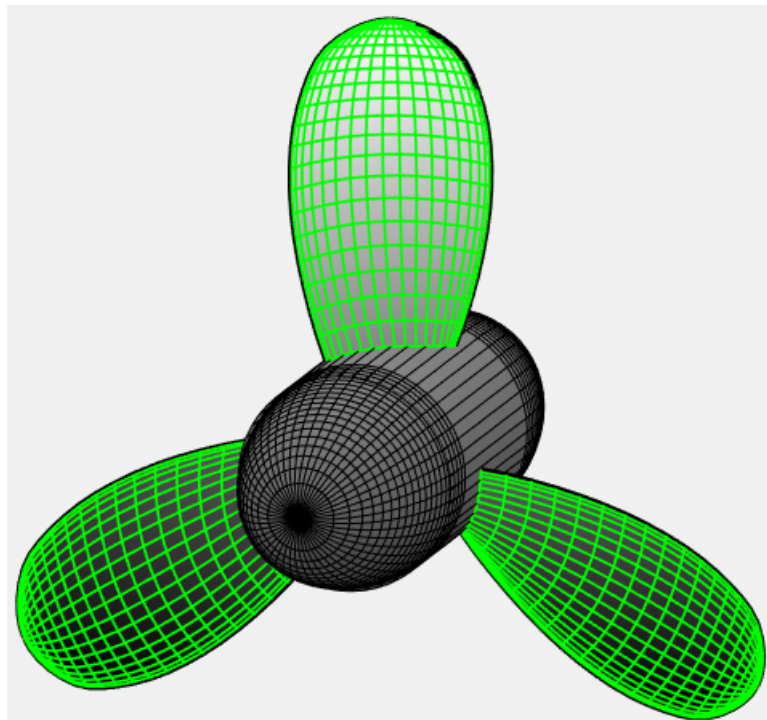


**Figure 7.12:** A 3D visualisation of the final propeller design with a diameter of 0.2 [m], an angular velocity of 850 [rpm] and an efficiency of 64 %

**Table 7.9:** Different input parameters for the first estimation of propeller efficiencies based on the number of blades, diameter and angular velocity

Parameter	Value(s)
Efficiency	0.64 [-]
Torque	1.32 [Nm]
Required power	117.2 [W]
Advance ratio	0.53 [-]

The next step is to find a motor that matches this propeller's specifications.

### 7.3.5. Motor Selection

Motors have to be found that can deliver the required power, rotational speed and torque the propeller needs to deliver sufficient thrust. None of the lightweight motors with masses between 0.1 [kg] and 0.5 [kg] can deliver a torque of more than 1 [Nm]. Hence, a heavier motor with a built-in gearbox will have to be used.

A suitable motor gearbox combination was found that meets the requirements. A brushless EC motor and internal rotor with planetary gearhead Performax 63<sup>1</sup>.

**Table 7.10:** Specifications of the motor selected to drive the underwater propulsion system

Parameter	Value(s)
Output power	230 [W]
Output torque	2.7 [Nm]
Output speed	800 [rpm]
Mass	1.15 [kg]
Voltage	24 [V]
Rated current	12.3 [A]
Efficiency	0.78

When re-optimising the propeller design with this new rotational speed of 800 [rpm], the propeller parameters do not change significantly. The efficiency and power remained the same, and the torque slightly increased to 1.39 [Nm]. Hence, the selected motor is still suited.

### 7.3.6. Lateral Propulsion

Besides the main underwater propulsion system, additional thrusters have to be foreseen to be able to counteract perpendicular currents during the visual monitoring of the seaweed and shackles. The thrust required to counteract current and remain stationary is 21 [N] and was calculated with the method explained in Section 7.3.2.

An off-the-shelf thruster was found that satisfies the requirements. The Blue Robotics T200 thruster can deliver 36 [N] of forward thrust and 28 [N] of reverse thrust, allowing the puffin to have only one T200 thruster that can control the lateral drifting in both directions. The following table provides the specifications of the thruster.

**Table 7.11:** T200 thruster performance specification table

Parameter	Value(s)
Forward thrust [N]	36
Reverse thrust [N]	28
Mass [kg]	0.344
Diameter [m]	0.1
Length [m]	0.113
Input power required [W]	205

The puffin only has to counteract perpendicular current when it has to be stationary to take a picture of a shackle. It is assumed that the puffin has to monitor 5 shackles per unit and that it will need 30 seconds of lateral position control during this manoeuvre. Some margin is incorporated so the propulsion system will be sized such that it has the capacity to maintain its position for 3 minutes in total per unit. This adds up to 30 minutes when

<sup>1</sup>Brushless motor with gearhead

monitoring 10 units resulting in 102.5 [Wh] of energy. As the energy density of lithium polymer batteries is about 200 [Wh/kg], this can be translated to a battery mass of 0.513 [kg].

### 7.3.7. Sizing of the Entire Water Propulsion System

Based on the total power required to monitor 10 units of the seaweed farm, the battery size and mass can be determined. Three manoeuvres can be distinguished: One where the Puffin follows a unit downstream, one where the puffin travels from one unit to the next, perpendicular to the current, and one where it follows a unit against the current, just as is shown in Figure 4.1. The ground speed and acceleration for each manoeuvre follow the requirements. The flow speed and required thrust are calculated with the model explained in Section 7.3.2. Finally, the propeller required power and efficiency are calculated in the OpenProp software. Table 7.12 provides an overview of the characteristics of these manoeuvres that will be used to calculate the entire required battery power.

**Table 7.12:** Characteristics of moving through the farm in different directions

	Move with current	Transfer	Move against current
Flow speed [m/s]	0.5	1.44	1.5
Ground speed [m/s]	0.5	1	0.5
Acceleration [ $m/s^2$ ]	0.1	0.1	0.1
Thrust [N]	6.4	42	50
Propeller required power [W]	11.5	91	117
Propeller efficiency	0.30	0.64	0.64

The motor efficiency is 0.78. Taking into account the propeller and motor efficiencies, and the time every manoeuvre takes based on the ground velocity of the puffin, the total required energy was found. For moving with current, transferring and moving against current, the required energies are 2.7 [Wh], 5.1 [Wh] and 13 [Wh] respectively. This leads to a total required energy of 124.6 [Wh] to monitor 10 units of the seaweed farm. Lithium polymer batteries have an energy density of around 200 [Wh/kg][34]. This leads to a battery mass of approximately 0.65 [kg].

The propeller will be made out of carbon fibre reinforced polymer (CFRP). This light, strong and waterproof material is very suited for this application[35]. The density of CFRP is two [ $g/cm^3$ ]. Modelling a propeller blade as a 20 [cm] by 3 [cm] plate with a 0.4 [cm] thickness, it has a mass of approximately 0.05 [g]. Furthermore, the propeller hub is made from galvanised aluminium which has a density of 2.7 [ $g/cm^3$ ]. To calculate its mass, the hub is assumed to be a cylinder with a diameter of 0.05 [m], a length of 0.13 [m] and a thickness of 0.005 [m]. This leads to a hub mass of 0.302 [kg]. The following table summarises the sizing of the propulsion system:

**Table 7.13:** Overview of the sized propulsion system

	Propeller blades	Propeller hub	Motor	Battery
Mass [kg]	0.15	0.302	1.15	0.65
Dimensions [mm]	200 Dia. x 30 x 4 t.	50 Dia. x 130 x 5 t.	63 Dia. x 200.5	0.415 [L]

After verifying and validating the design of the propulsion system, the investigation of how to incorporate it in the final Puffin configuration can begin.

## 7.4. Depth Control

From the requirements, the system needs to be able to control its position and depth level. From the control and positioning requirements, the system shall be able to control its attitude at different depths. To achieve this a buoyancy control system is needed for the system to attain neutral buoyancy for the system to remain underwater. To be able to have a high level of buoyancy control multiple AUV, UUV and submarine buoyancy control systems were investigated to research how these systems achieve buoyancy control. From this two main architectures were discovered, static and dynamic control systems. Static control systems take the form of ballast tanks and dynamic control systems are thrusters and propulsive methods. Within static control systems, multiple solutions exist such as piston, hydraulic and pressurised air ballast tanks.



There are two major categories that can be identified: static and dynamic systems. Static systems are systems that control their depth by adding/removing ballast to their system in order to increase the weight of the system. Dynamic systems are systems that use propulsion to control their depth and/or keep themselves submerged. In the static category, there are three main types, pressurised air, piston, and hydraulic ballast tanks. The dynamic category uses thrusters to keep itself at a certain depth.

Pressurised air systems use pressurised air to fill up a bladder to increase the volume of the submerged vehicle. When the volume needs to be decreased, the bladder releases the air into the environment. This has a major downside as the system can run out of air and the buoyancy control is limited. One major advantage is the energy efficiency of the system. The reliability of the system is also high but if the bladder is not air-tight, the system will not work. This system also only works with negatively buoyant vehicles.

Piston ballast tanks use pistons to open up a valve depending on the buoyancy required. The advantages of this system are its reliability and its accuracy. The major downside of this technology is the weight of the system and the power required to move the water around with the piston.

Hydraulic ballast tanks fill up tanks with water to control their buoyancy. This can be done using pumps. The advantages of this system are its relatively low weight, accuracy, and versatility of location. The downside is the power required to pump the water.

The general equation for Buoyancy control:

$$F_b = -\rho V_s g$$

EOM:

$$m \cdot a = m_{uav} \cdot g + T - \rho_{water} \cdot g \cdot V_s - D$$

To determine the optimal choice of buoyancy control system initial sizing was done to quantitatively investigate each parameter of the trade-off criteria and evaluate the performance of both architectures. A combination of off-the-shelf component specifications and first principle engineering concepts were used to size the systems.

## Thrusters

To investigate the thruster performance as a buoyancy control system the Maxon thruster 20 was chosen <sup>1</sup>. This product was chosen due to high-performance relative to its weight

For a dynamic buoyancy control system the thrust needed was calculated using the EOM equation. Following this using a propeller from literature, the number of propellers needed and power requirements were found. Based on an underwater operating time of 1.5 hours and the energy density of a battery, it was found that a 0.04 [kg] battery is needed to power the thrusters. This value begins to increase as the density of the system diverges from one indicating as the less water the system displaces relative to its mass the more power and thrust is required to achieve a state of neutral buoyancy. The total system mass was found by summing the required battery mass and mass of the propellers. It was found to achieve 4[kg] of thrust a battery mass of 0.04[kg] and propellers with a mass of 0.84 giving a total system mass 0.88 is needed.

## Ballast Tanks

To size the ballast tank system an acceleration following from requirements/assumptions is inputted. Based on the EOM equations, the V is calculated as required to have a positive and negative acceleration. In this calculations T = 0 and D = 0. Based on this volume calculated, the difference with the original volume can be looked at, thus giving the size of the tanks needed to control buoyancy.

To estimate the mass of the system, different materials were researched with various material properties. These materials are commonly used in ballast tanks for submarines and AUVs [36]. The tank was assumed to be a cube with a thickness of 3 millimeters, from this the volume was multiplied by the density of the material and the total tank mass was found. The mass of the pump, coating and additional systems were estimated based on off-the-shelf components and added to the tank mass to find the total mass. A tank mass of 0.72[kg] was found to generate 4[kg] of buoyancy which includes, pumps, tank skin and additional battery mass for the pumps.

Both static and dynamic systems are feasible solutions for the Puffin architecture. Thrusters can provide a thrust force to keep the system below water but may lead to a higher battery mass if the thrust force is too large. Ballast tanks are also a possible solution that is lightweight and can provide large amounts of buoyant force but requires a large volume. A combination of both is also possible but will determine on the more detailed structure and configuration design. The buoyancy design is further elaborated on in Section 9.7

<sup>1</sup>Maxon Thruster 20

## 7.5. Iteration on the Underwater Propulsion System

While configuring the layout of the Puffin, the size and layout of the selected water propulsion system were very inconvenient to integrate into the overall design. Hence, this subsystem was iterated to find a new configuration.

In the new design, three propellers are mounted on each stabilizer of the inverted-Y tail as is depicted in Figure 7.13. The propellers are podded and can rotate radially. This mechanism makes that they can provide sufficient forward thrust to the puffin when moving forward, but it also allows for lateral and vertical position control.

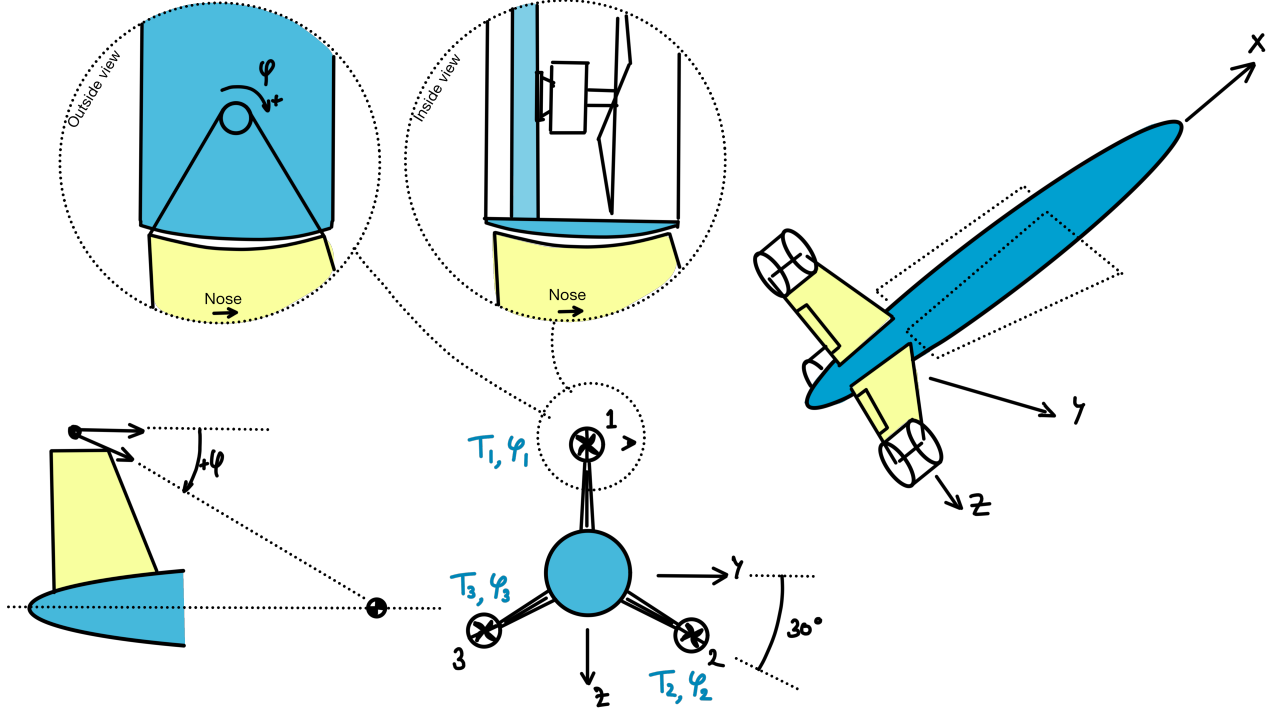


**Figure 7.13:** Iterated water propulsion system, where a propeller is mounted on each tailplane, by radially rotating these propellers, the Puffin is able to move forward, sideways, and vertically

By having all the propellers at an angle of  $0^\circ$ , the Puffin is purely propelled forward. The thrust and angle settings required to deliver a certain thrust in the lateral or vertical direction are calculated with the following equations:

$$\begin{cases} T_X = T_1 \cos \psi_1 + T_2 \cos \psi_2 + T_3 \cos \psi_3 \\ T_Y = -T_2 \cos 30^\circ \sin \psi_2 + T_3 \cos 30^\circ \sin \psi_3 \\ T_Z = -T_1 \sin \psi_1 + T_2 \sin 30^\circ \sin \psi_2 + T_3 \sin 30^\circ \sin \psi_3 \\ M_X = 0 \\ M_Y = T_1 (-w_{tm} \cos \psi_1 - x_{tm} \sin \psi_1) + \\ \quad T_2 (w_{tm} \cos \psi_2 \sin 30^\circ + x_{tm} \sin \psi_2 \sin 30^\circ) + \\ \quad T_3 (w_{tm} \cos \psi_3 \sin 30^\circ + x_{tm} \sin \psi_3 \sin 30^\circ) \\ M_Z = T_2 (w_{tm} \cos \psi_2 \cos 30^\circ + x_{tm} \sin \psi_2 \cos 30^\circ) + \\ \quad T_3 (w_{tm} \cos \psi_3 \cos 30^\circ + x_{tm} \sin \psi_3 \cos 30^\circ) \end{cases} \quad (7.16)$$

In these equations, the thrust and angle settings are given by  $T_1$  and  $\psi_1$ ,  $T_2$  and  $\psi_2$ , and  $T_3$  and  $\psi_3$  according to Figure 7.13.  $x_{tm}$  is the position of the tail motors with respect to the C.G. in the x-direction and  $w_{tm}$  is the distance of the motor from the centre of the fuselage. These equations do not include the contributions of the control surfaces that are present on each tail and assume the C.G. is on the x-axis, i.e. the vehicle is rotationally symmetric. These simplifications will be addressed in the system design. Using the control surfaces, also a roll moment can be achieved. By setting the moment equations equal to zero, they can be solved for the desired thrust and angle settings to move in any direction.

The thrusters that are used for the underwater propulsion system will nominally deliver a thrust of 20 N each. At

higher voltages, they can deliver thrusts up to 50 N which might be needed for some of the lateral and vertical control manoeuvres<sup>1</sup>

The thrusters will be mounted on a CFRP hollow shaft located within each tail surface. Two cables connected to a servo run through the tube to control the rotational motion of the podded thrusters. The schematic drawing in Figure 7.14 visualises the layout of this mechanism.

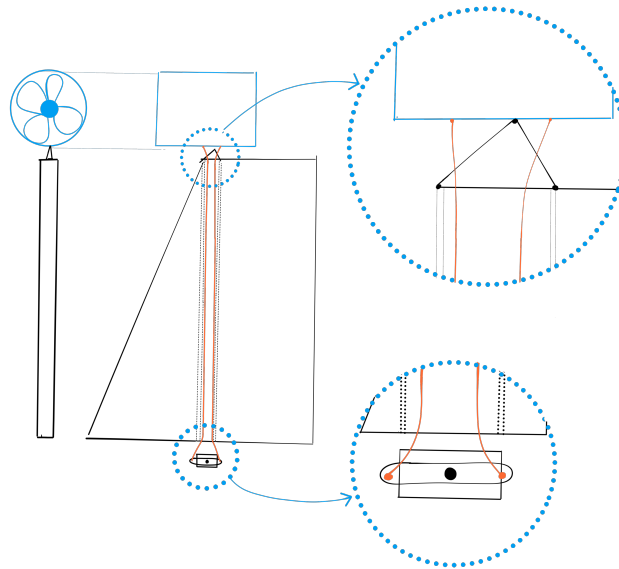


**Figure 7.14:** Schematic drawing of the thruster rotation mechanism showing the thruster mounted on a hinge, being controlled with two cables connected to a servo, running through a CFRP tube

To find a servo that can deliver sufficient torque, a moment equilibrium around the hinge point can be set up. Assuming the cable run straight down to the servo, the motor will have to provide a torque of 3.75 Nm. A 9 grams, 2 by 2 by 2-centimetre servo was found that generates enough torque to control the propellers<sup>2</sup>.

The batteries powering the propulsion can now be sized again. Table 7.14 below establishes characteristics of certain manoeuvres and their associated battery mass. All quantities in the table are regarding the entire propulsion system so for the three thrusters. The drag on the third row was calculated with the new drag estimation method as explained in Section 7.3.2. Subsequently, the required thrust was calculated, taking into account the acceleration and the angle of the propellers, i.e. for the lateral position control, the thrust is not completely pointed in the direction of motion. Then, using a safety factor of 1.5, the required power was found in the thruster specifications<sup>3</sup> From the duration of each manoeuvre, the total required energy was found, followed by the battery weight as lithium polymer batteries have a density of approximately 200 [Wh/[kg]]<sup>4</sup>

**Table 7.14:** Iteration on characteristics of moving through the farm in different directions

	Move with current	Transfer	Move against current	Lateral control
Flow speed [m/s]	0.5	1.44	1.5	1
Ground speed [m/s]	0.5	1	0.5	0
Drag [N]	1.81	4.4	6.52	2.25
Acceleration [ $m/s^2$ ]	0.1	0.1	0.1	0.1
Thrust [N]	2	4.6	6.8	18
Duration for 1 unit [s]	200	100	200	30
Power required [W]	6	15	21	48
Energy required per unit [Wh]	0.33	0.42	1.16	0.4
Battery mass [kg]	0.0017	0.0021	0.0058	0.002

The total battery mass to monitor 10 units of the farm is equal to 0.058 [kg].

<sup>1</sup>T200 water thruster

<sup>2</sup>Water propeller servo

<sup>3</sup>T200 water thruster

<sup>4</sup>Lithium Polymer battery

## 7.6. Verification and Validation

Verification and validation were performed on the tools and Python code used to size the different propulsion systems. Pytests, external software and real-world data were used to verify and validate the different functions in the scripts. Additionally, potential solutions to verify the requirements dictating the aquatic and aerial are presented.

### 7.6.1. Sizing V&V

To verify and validate the sizing methods different operations were performed. For verification, unit tests were created for each function and tested against pre-calculated values using pytest. Additionally, certain parts were plotted against each other to ensure they had the correct relationship i.e (Power vs RPM, Torque vs RPM, and efficiency vs diameter. For validation, the sizing code was tested against OpenProp, an open-source propeller sizing simulation made for optimized designs of marine propellers [37]

### 7.6.2. Requirements V&V

In Table 7.1, the requirements that the propulsion system must comply with were presented. For each requirement, a verification test is given in Table 7.15. Given that these are requirements for propulsion systems only analysis or test methods are considered for verification [38].

**Table 7.15:** Verification methods for the relevant requirements of the propulsion system. A: Analysis, T: test

Requirement	Verification Description	Method
PROP-AQUA-01,	Write code in Python to simulate the system operating in currents up to 1.3 m/s and investigate how long it can remain operational.	A
PROP-AQUA-02, PROP-AQUA-03, PROP-AQUA-04, PROP-AQUA-05	Place the system in a pool and test how fast it can move under cruise conditions and on the heave and sway axis. Measure the distance it covers and time and or use accelerometers and velocity sensors.	T
PROP-AQUA-06	Mount the motors on a propeller testing device to measure the thrust they can deliver.	T
SUS-CL-PROP-01	The thrust generation shall be verified using a standard thrust stand, the actual thrust will be measured for the climb configuration	T
SUS-CL-Prop-02	The thrust generation can be verified using a thrust stand, using the established air propulsion cruise parameters	T

**Validation** The water propulsion system can be validated by a number test in a bath. Once a prototype of the system is made, tests should be performed in a bath to see if the required velocities are met. The thrust vectoring principle can be tested by mounting three propellers on a simple frame and measuring the resultant forces. For the air propulsion, a flight test should be performed for the prototype, ensuring that the propulsion correctly counteracts the drag and weight forces and allows for achieving the desired performance. The flight test would validate the drag estimations and thrust performance data.

## 8 Wing and Control Surfaces

In this chapter, the wings and control surfaces of the Puffin design will be discussed. This will start with the sizing of the main wing, where the whole planform of the wing will be designed. Following this, the tail will be sized in order to guarantee a stable system. Stability is an important consideration, but the system should also be controllable, which will be ensured by the control surfaces on the wings and tail.

### 8.1. Requirements and Assumptions

**Table 8.1:** Incoming Requirements for the Wing and Control Surfaces Sizing Table. <Caption here>

ID	Description	Traceability	Rationale
ID	Description	Traceability	Rationale
SYS-PERF-02	The system shall have a rate of climb of 1 [m/s]	Mission profile	See traceability
SYS-PERF-03	The system shall have a cruise velocity of 20 [m/s]	Mission profile	See traceability
CTRL-ATT-01	The system attitude shall be controllable in an unstable aerodynamic environment	From OPR-ENV-03, with OPR-ENV-01	Placeholder logic, necessary to ensure collision avoidance in the operating conditions
CTRL-ATT-02	The system attitude shall be controllable in an unstable maritime environment	From OPR-ENV-03 and OPR-ENV-02, with OPR-ENV-01	Placeholder logic, necessary to ensure collision avoidance in the operating conditions
CTRL-ATT-03	The system shall be able to attain a minimum roll rate of 20 degrees per second	From CTRL-ATT-01 & CTRL-ATT-02	Makes sure the system has enough maneuverability to make sudden changes to its position and attitude. The system can react to any disturbances it encounters
CTRL-ATT-04	The system shall be able to attain a minimum yaw rate of 10 degrees per second	From CTRL-ATT-01 & CTRL-ATT-02	Makes sure the system has enough maneuverability to make sudden changes to its position and attitude. The system can react to any disturbances it encounters
CTRL-ATT-05	The system shall be able to attain a minimum pitch rate of 5 degrees per second	From CTRL-ATT-01 & CTRL-ATT-02	Makes sure the system has enough maneuverability to make sudden changes to its position and attitude. The system can react to any disturbances it encounters
CTRL-ATT-06	The system shall be able to return to its inherent neutral orientation	From CTRL-ATT-01 & CTRL-ATT-02	If the system lands upside down it should be able to flip itself over and be in the correct orientation
CTRL-ATT-07	The system shall have 6 degrees of freedom while underwater	Allow us to understand the maneuverability of the system	See traceability

Continued on next page

Incoming Requirements for the Wing and Control Surfaces Sizing Table 8.1 – continued from previous page

ID	Description	Traceability	Rationale
CTRL-ATT-08	The system shall be able to attain a minimum angular velocity of up to 2 <i>deg/s</i> for rolling while underwater	This will allow for determining how quickly the system can change direction or, in an emergency situation, how to escape quickly	See traceability
CTRL-ATT-09	The system shall be able to attain a minimum angular velocity of up to 2 <i>deg/s</i> for yawing while underwater	This will allow for determining how quickly the system can change direction or, in an emergency situation, how to escape quickly	See traceability
CTRL-ATT-10	The system shall be controllable around its yawing axis in horizontal flight	From CTRL-ATT-01	See traceability
CTRL-ATT-11	The system shall be controllable around its pitching axis in horizontal flight	From CTRL-ATT-01	See traceability
CTRL-ATT-12	The system shall be controllable around its rolling axis in horizontal flight	From CTRL-ATT-01	See traceability
CTRL-ATT-13	The system shall be controllable around its yawing axis in vertical flight	From CTRL-ATT-01	See traceability
CTRL-ATT-14	The system shall be controllable around its pitching axis in vertical flight	From CTRL-ATT-01	See traceability
CTRL-ATT-15	The system shall be able to attain a minimum angular velocity of up to 2 <i>deg/s</i> for pitching while underwater	This will allow for determining how quickly the system can change direction or, in an emergency situation, how to escape quickly	See traceability
CTRL-ATT-16	The control surfaces shall assist to a successful landing maneuver	The drone shall not be damaged	The system is reusable, thus has to remain functional
CTRL-POS-01	The system position shall be controllable in an unstable aerodynamic environment	From OPR-ENV-03, with OPR-ENV-01	Placeholder logic, necessary to ensure collision avoidance in the operating conditions
CTRL-POS-02	The system position shall be controllable in an unstable maritime environment	From OPR-ENV-03 and OPR-ENV-02, with OPR-ENV-01	Placeholder logic, necessary to ensure collision avoidance in the operating conditions

## 8.2. Wing Sizing

The wing is the main lifting body of the drone, and is therefore of key importance to the design. An efficient wing design will provide enough lift for the drone to fly, while minimising drag. Minimising drag will result in a lower thrust requirement, and therefore less battery has to be allocated to cruise, meaning more battery energy can be used for measurements taken at the seaweed farm. Firstly, an airfoil will be selected and analysed that

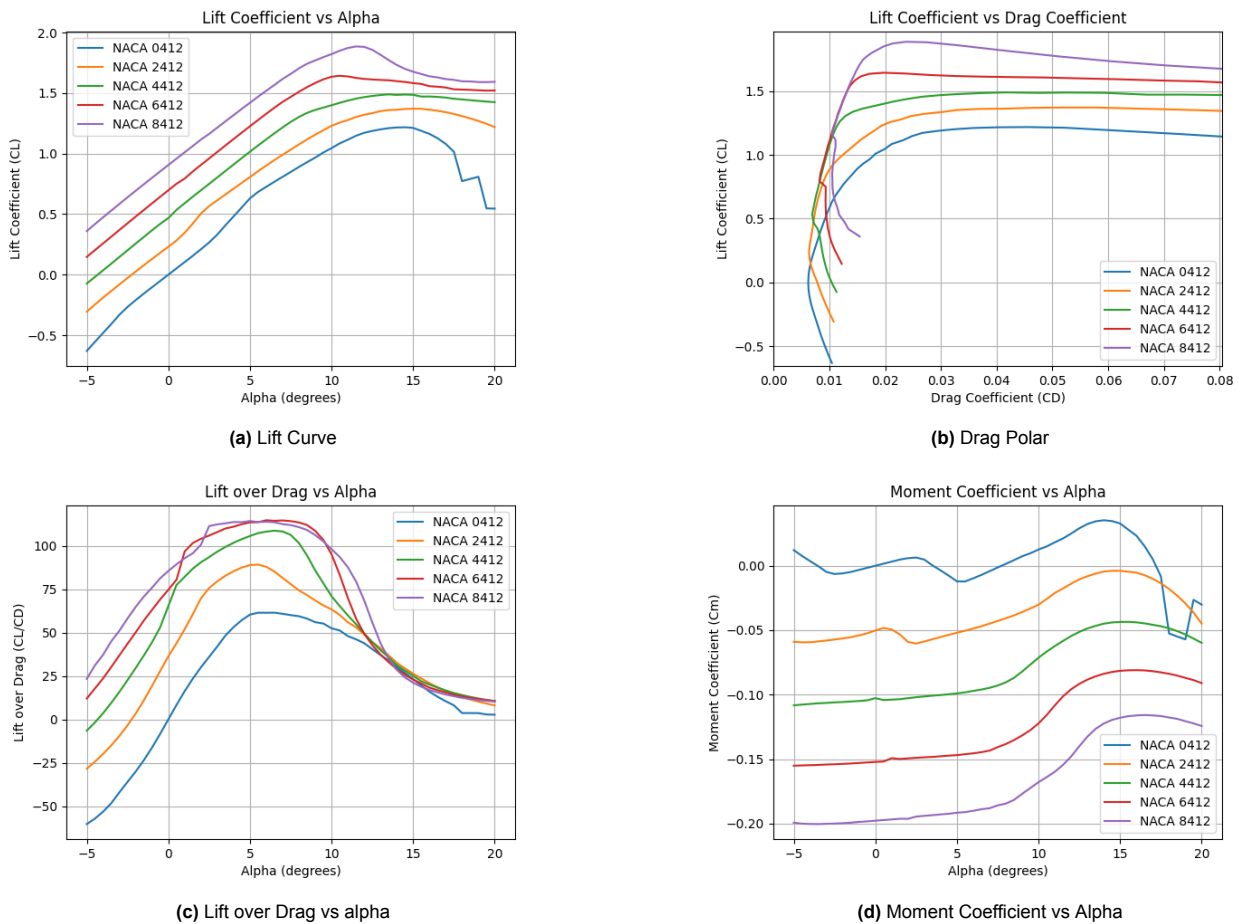


**Figure 8.1:** Comparison of aerodynamic properties for different airfoils

can be used for the wing. This can be seen in Section 8.2.1. This will give a first estimate of the performance of the airfoil and the wing. Following this, the wing surface area will be determined, which is the minimum surface area required for the drone to fly. This will be discussed in Section 8.2.2. Based on the airfoil selected and the wing area, the wing geometry will be optimised for the specific mission profile in Section 8.2.3. This wing will then be analysed further to iterate the previously found wing surface area and planform design. Techniques to optimise the airfoil for the specific mission will also be inspected in Section 8.2.5

### 8.2.1. Airfoil Selection

The first step in wing design is the airfoil selection. The airfoil is the basis of the lifting capabilities of the wing, and is critical, as the whole size of the wing of the wing will be determined by its performance. The main philosophy for airfoil selection would be to design an airfoil that provides a high lift coefficient, at relatively low angles of attack, and that has good stall characteristics. All off this should be done while considering the drag and pitching moment of the airfoil as well. If the drag and pitching moment were to be too large, the propulsion system and stability design would become more complex.

A good and well-established airfoil database is the NACA airfoil database. It is a database with airfoils that have often been used over a wide range of applications. However, since these airfoils have been developed without the use of strong computational tools, NACA airfoils are not always optimised for specific design applications. However, they provide a solid baseline for the wing sizing.

Using Xfoil, an aerodynamic analysis of the lift, drag and moment coefficients of the airfoil is performed. These are then plotted against each other, such that a trade-off can be made between the airfoils.

The comparison between some selected airfoils can be seen in Figure 8.1. A baseline of four airfoils has been selected, namely NACA0412, 2412, 4412, 6412, 8412. Based on this comparison, an ideal airfoil will be selected

In Figure 8.1, it can be seen that a higher-cambered airfoil, has a lower drag coefficient for a given lift coefficient than a lower-cambered airfoil. However, the minimum drag is lower for less cambered airfoils. Based on the lift and drag requirements, a high-cambered airfoil should be selected. However, since high-cambered airfoils



have a more negative moment coefficient, this will lead to a bigger tail size, and therefore a heavier drone. The trade-off has to be made between an airfoil with a high lift coefficient and high moment, leading to a lighter wing, but a heavier tail, and an airfoil with a lower lift coefficient and a lower moment, with a lighter tail, but a heavier main wing.

In order to balance both considerations, the NACA2412 airfoil has been chosen, This airfoil provides enough lift for the required constraints, and limits the moment generated. This airfoil can later be optimised for specific puffin applications.

### 8.2.2. Wing Surface Area

The next step in the wing sizing is determining the surface area of the wing. In order to do this, a wing loading has to be determined. This can be done by creating a wing loading vs power loading diagram, to then choose a design point. The wing loading diagrams are based on the critical flight phases. These critical phases are the stall or dive speed, the rate of climb requirement during cruise, and the maximum cruise speed.

The wing loading for the stall or diving speed can be seen in Equation 8.1.

$$(W/S)_{stall} = C_{L_{max}} \frac{1}{2} \rho V_{stall}^2 \quad (8.1)$$

This will give an upper limit for the wing loading.

The next step is to develop the loading diagram for the max cruise speed. The max flight speed is assumed to be 35 [m/s]. Equation 8.2 gives the relation between power loading and wing loading for a certain velocity.

$$\frac{W}{P} = \frac{\eta_p}{\frac{1}{2} \rho V^3 C_{d0} \frac{S}{W} + \frac{2k}{\rho V} \frac{W}{S}} \quad (8.2)$$

Another critical flight requirement is the rate of climb. This has been determined to be 1 [m/s]. The equation that describes the relation between the wing loading and power loading for the rate of climb can be found in

$$\frac{W}{P} = \frac{1}{\frac{ROC}{\eta_p} + \sqrt{\frac{W}{S} \frac{2}{\rho_{cruise} \sqrt{3C_{d0}/k}}}} \quad (8.3)$$

The last case to be looked at is the power required to fly at the service ceiling of our design. This can be seen from Equation 8.4

$$\frac{W}{P} = \frac{(L/D)_{max} \eta_p \sigma_{cruise} \rho_{cruise} \sqrt{3C_{d0}/k}}{1.155 \sqrt{2W/S}} \quad (8.4)$$

Based on these requirements, the wing loading vs power loading graphs can be made. An original estimate for the stall speed was assumed to be 12 [m/s], however, this limited the design point very strongly. Adjusting it to 15 [m/s] allowed for a smaller wing, while still keeping an acceptable speed to dive at.

The final design wing loading diagram can then be seen in Figure 8.2

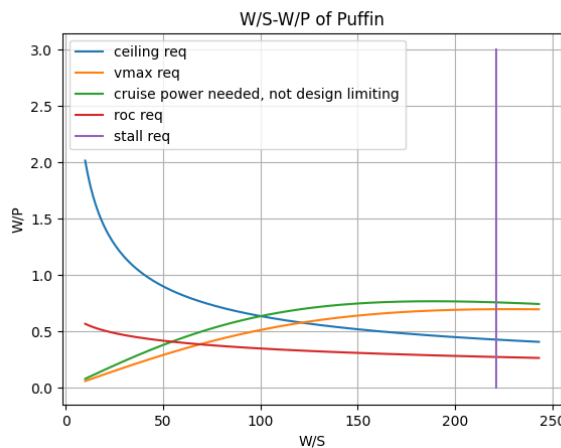


Figure 8.2: Wing Loading Diagram of Puffin

This will then result in a total wing area of 0.75 [m<sup>2</sup>].

### 8.2.3. Wing Planform Design

The wing area has already been determined in Section 8.2.2. However, this is not the only parameter to be decided on when sizing the wing. In this section, the exact shape of the wing planform will be designed. This will include determining the sweep and taper ratio.

The ideal wing shape for aerodynamic performance is an elliptical wing shape, as this will have the lowest lift-induced drag. However, an elliptically shaped wing adds quite some challenges from a manufacturing point view. Most aircraft use a trapezoidal wing to overcome these manufacturing challenges. This will have a negative effect on the aerodynamics, but considering the budget available, and the complexity of the puffin, a trapezoidal wing will have good enough aerodynamic performance. Adding sweep and a taper ratio will allow to approach the lift distribution of a trapezoidal wing as a the lift distribution of an elliptical wing.

According to [39], sweep is mostly used to reduce the net velocity over a wing at high-speed flight, and therefore reduce the effects of transonic airflow such as transonic wave drag. However, since the design will only be used at relatively low speeds up to around 20 [m/s], sweeping is unnecessary. The quarter-chord sweep angle will therefore be 0°.

The next step in the wing planform design is the decision on the taper ratio. The taper ratio is used to modify the lift distribution over the wing. The goal is to let the trapezoidal wing have the same or similar lift distribution over the wing as an elliptical wing. According to [40], this can be achieved by having a taper ratio of around 0.4. Note that this is only true for unswept and untwisted wings

An additional parameter that influences the aerodynamic performance of the wing is the aspect ratio. A higher aspect ratio will lead to better lifting capabilities, however, this will be at the cost of lower maneuverability. A higher aspect ratio will also mean that the wingspan increases, and therefore the moment arm increases. An aspect ratio of 12 has been used as a finalised value to allow for good aerodynamic performance while keeping enough maneuverability.

Based on these calculations, the final planform can be designed with Equation 8.5, Equation 8.6, and Equation 8.7.

$$b = \sqrt{S \cdot AR} \quad (8.5)$$

$$c_{root} = \frac{2 \cdot S}{(1 + \lambda) \cdot b} \quad (8.6)$$

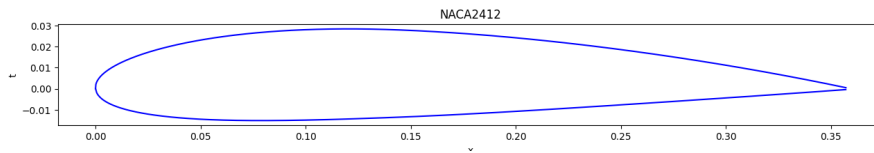
$$c_{tip} = c_{root} \cdot \lambda \quad (8.7)$$

These equations are first used to further analyse other subsystems, and will be iterated upon to come up with the final values based on the detailed design of other subsystems. The final values for the wing planform can then be found in Table 8.2.

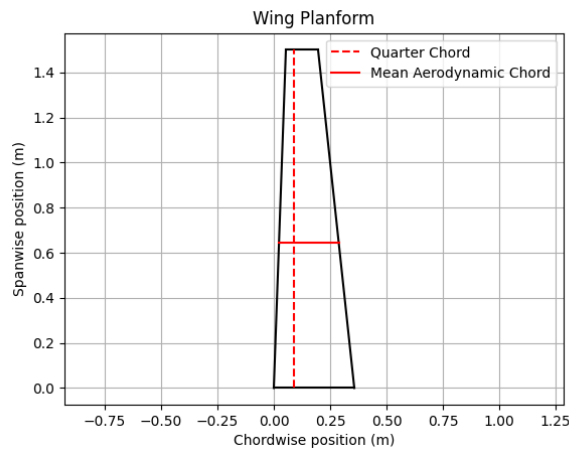
**Table 8.2:** Planform parameters of the main wing

Parameter	Value
Aspect Ratio	12
Taper Ratio	0.4
Wing Area	0.75 [m]
Wing Span	3 [m]
Root Chord	0.337 [m]
Tip Chord	0.135 [m]

A visual of the wing planform can then be seen in Figure 8.3



(a) NACA2412 Airfoil



(b) Wing Planform

**Figure 8.3:** Final Airfoil and Wing sizing

In Figure 8.3, the airfoil used and the wing planform of half a wing can be seen, as well as the quarter-chord line, and the mean aerodynamic chord.

#### 8.2.4. Wing Analysis

Now that the wing has been designed, it can be analysed further to reiterate the aerodynamic coefficients found in Section 8.2.1. This will now give the aerodynamic properties for the whole wing instead of the airfoil. Using the Aerosandbox Python module, the wing can be modelled in Python, and a VLM analysis can be performed. A VLM analysis models the lifting surfaces as an infinitely thin sheet of discrete vortices. This will allow to estimate the lift and induced drag of the wing accurately. However, the model neglects any viscous effects, ignoring the wing's thickness. Therefore, the drag is not really modelled accurately. In later design stages, this will also not be able to analyse fuselage influences either. In order to set up a more detailed analysis, *Aerosandbox's* aero-buildup function has been used. This uses a more extensive breakdown of all airplane elements, and analyses its aerodynamic properties over more extensive sections, instead of a flat plate.

The wing used for the aerodynamic analysis can be seen in Figure 8.4, and an example of a VLM analysis has been visualised in Figure 8.5.

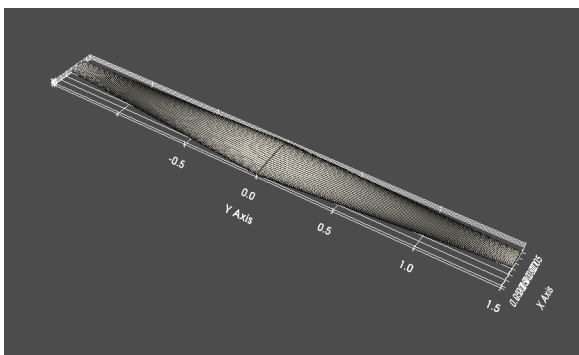


**Figure 8.4:** Wing used for aerodynamic analysis

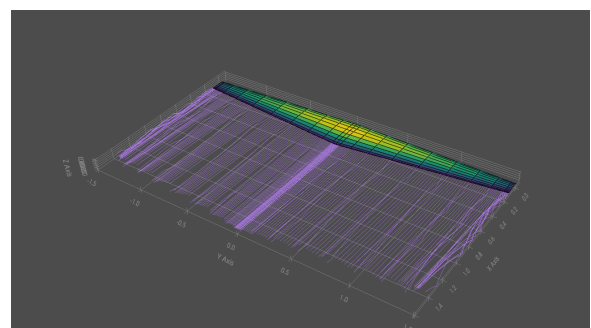


**Figure 8.5:** Visualisation of VLM Analysis for an Angle of Attack of 5°

The aerodynamic properties of the final wing can be seen in Figure 8.6

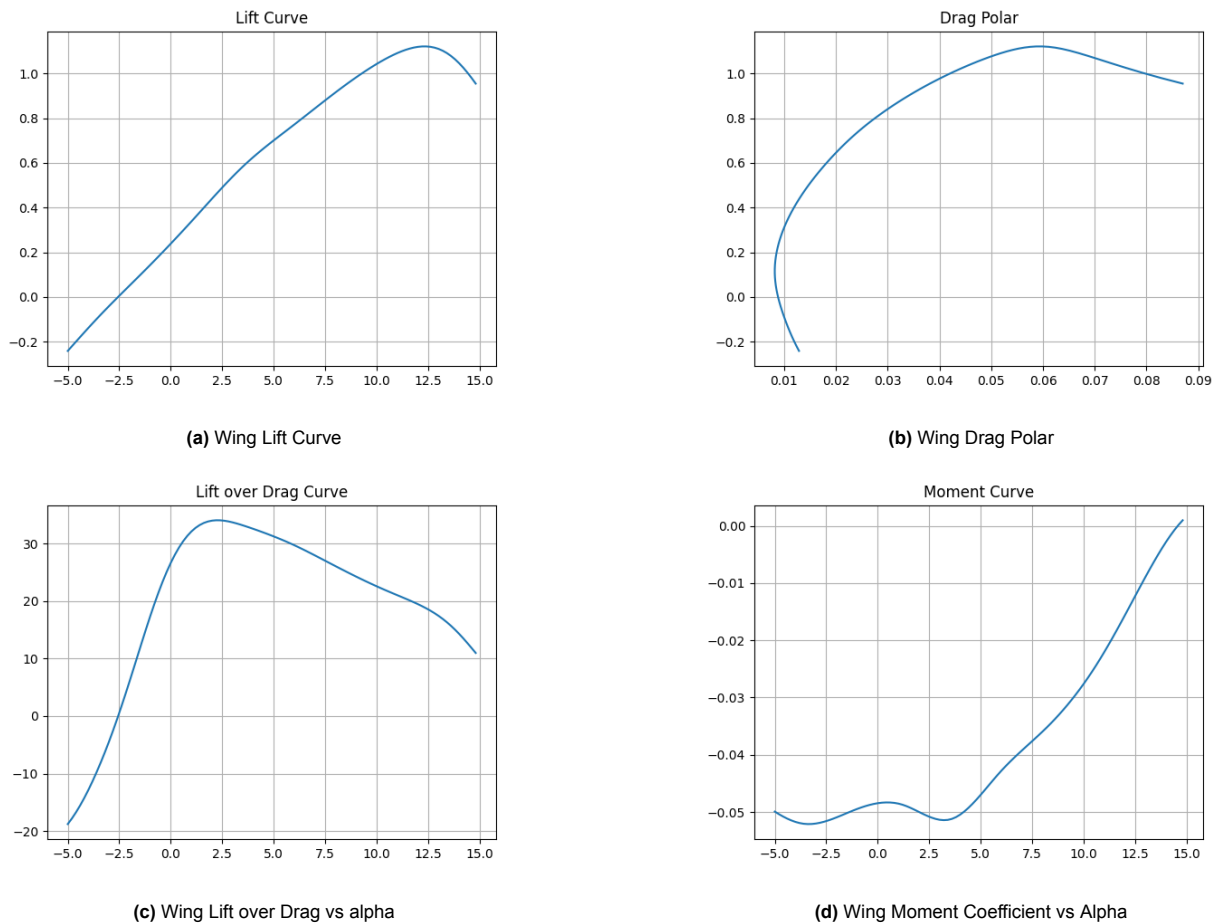


**Figure 8.6:** Aerodynamic Properties of the Wing

Based on the graphs and values found for the whole wing in Figure 8.6, the wing sizing can be reiterated, and a tail sizing can be made to ensure stability.

### 8.2.5. Airfoil Optimisation

NACA airfoils are reliable airfoils that have been used for decades. However, they have been developed before the availability of strong computational tools, and therefore are not always optimised. In order to increase the aerodynamic performance of the Puffin, the airfoil of the main wing should be optimised for its specific applications. However, due to time and computational power constraints, this will be done in the post-DSE phase of the design.

## 8.3. Tail Configuration

The Puffin is expected to be operable both in-air and underwater. This imposes a large challenge on the tail design. The configuration needs to not only be optimized for flight but also for the underwater monitoring of the seaweed farms. Two vehicles that are considered for this analysis are the conventional aircraft and the submarine. The control surfaces have the goal of moving the system in a controlled manner.

The submarine has rudders and stern planes. It encompasses four main configurations: the X-stern or X-form, the cross-form, the inverted Y-tail and the pentaform (see Figure 8.7). The aircraft tail consists of horizontal and vertical components. Figure 8.8 shows different tail configurations for aircrafts.

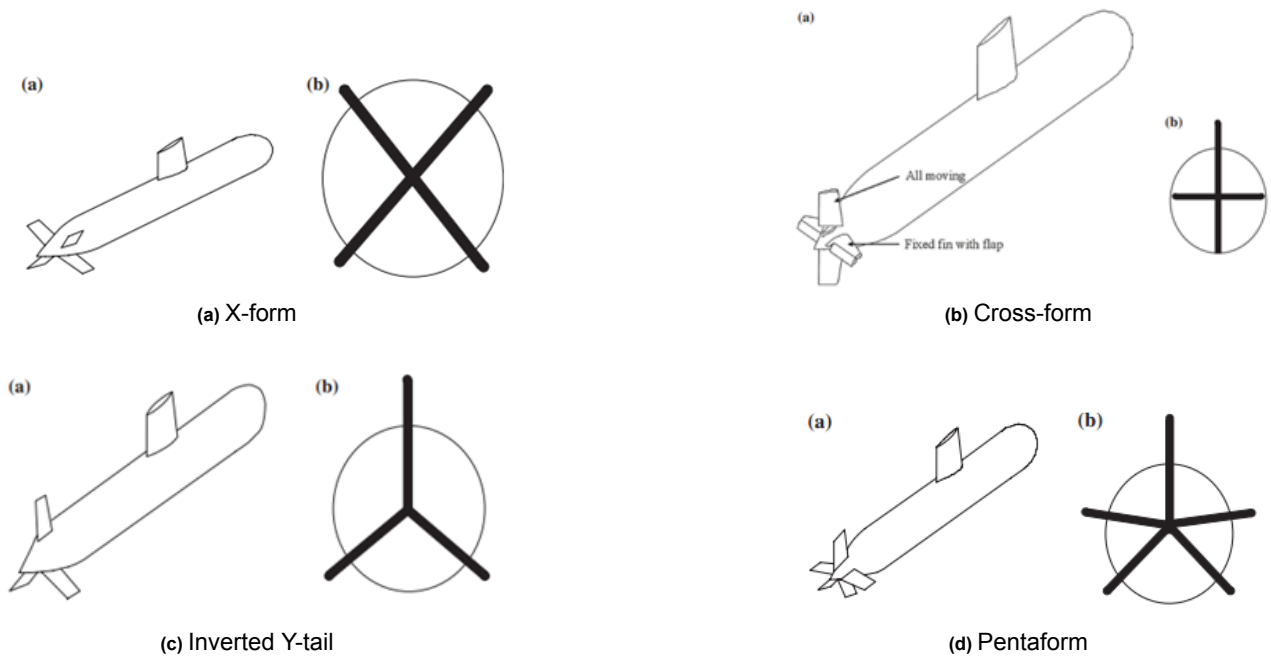


Figure 8.7: Submarine tail configurations

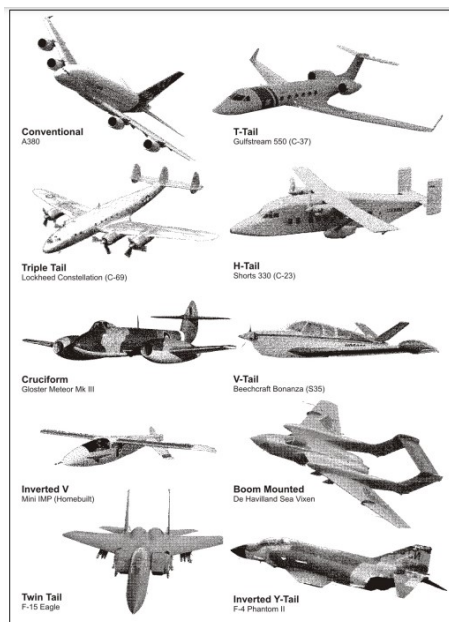


Figure 8.8: Tail Configurations for an in-air vehicle [41]

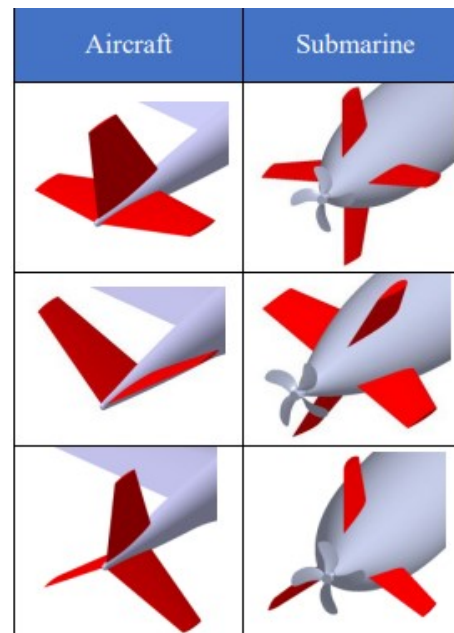


Figure 8.9: Comparable tail configurations for aircrafts vs submarines [42]

Comparing both, the in-air and underwater designs, one can conclude that the cross-form is similar to the conventional tail of the aircraft and that the X-form is comparable to the V-tail on the aircraft. The inverted Y-tail exists for both. Thus, three possible tail configuration for the Puffin are considered as outlined by Figure 8.9. In the end, the inverted Y-tail has been chosen as the final tail configuration of the Puffin. It can accommodate the sweeping wing mechanism, which is a crucial part of the Puffin design. Furthermore, it enhances the system's stability.

## 8.4. Tail Sizing

From Section 8.3 the inverted Y-tail configuration was selected for its advantages in air and water cruising. This configuration composes of three fins, one oriented vertically as the rudder and two below it acting as elevators in an inverted V tail configuration seen in Figure 8.7c. Additionally, all moving tails are selected as they are as effective as generating pitching moments as conventional tails for the same or smaller area and a deflection

of 30 [degrees] is chosen for each fin as a preliminary design value. First, the vertical surface is sized as a conventional vertical tail. From Raymer the vertical tail area  $S_V$  can be estimated as [40]:

$$S_V = \frac{K_{tail} V_V b_w S_w}{L_v} \quad (8.8)$$

Where  $K_{tail}$  is a correction factor for an all-moving tail and is between .90 – 0.85%,  $V_V$  is the vertical tail volume coefficient,  $b_w$  is the wingspan,  $S_w$  is the wing area and  $L_v$  is the vertical tail arm to the center of gravity. The volume tail coefficient is found to be 0.03 for similar-sized UAVs [43]. Additionally,  $K_{tail}$  is set to be 0.85 and the initial  $L_V$  is assumed to be half the fuselage length at 0.75 [m]. With this and information from Table 8.2 the vertical tail area is equal to  $S_V = 0.0765 [m^2]$

For the horizontal tail a similar method is a formula from Raymer is used:

$$S_h = \frac{K_{tail} V_H \bar{c} S_w}{L_h} \quad (8.9)$$

Where  $V_H$  is the horizontal tail volume coefficient,  $\bar{c}$  is the average chord,  $S_w$  is the surface area of the wing and  $L_h$  is the horizontal tail arm to the center of gravity.  $V_H$  is found to be 0.6 for similar UAVs [43] and the horizontal tail arm is equal to the vertical tail arm of 0.75. Using data from Table 8.2 the total horizontal tail area is found to be  $S_h = 0.135 [m^2]$

However, Equation 8.9 sizes a conventional horizontal tail. To transform this value into an inverted Y-tail configuration, the conventional horizontal tail is transformed into an inverted V-tail. The inverted V tail area is assumed to be composed of a projected vertical area contributing to the effective vertical fin and projected horizontal area. Therefore the total vertical tail area from Equation 8.8, is composed of the area from the vertical fin and the projected area from the inverted V-tail fins,  $S_{H_{PROJ_V}}$  [42].

$$S_V = S_{Y_V} + S_{H_{PROJ_V}} \quad (8.10)$$

Where the anhedral can be calculated as:

$$\Gamma_Y = \arctan \left( \sqrt{\frac{S_{H_{PROJ_V}}}{S_H}} \right) \quad (8.11)$$

However, from Section 7.5 the tail must be symmetric about the rudder, meaning the angle between each tail fin component should be 120[degrees] and the anhedral should equal  $\Gamma_Y = 30[degrees]$ . From this, the horizontal projection can be calculated by rearranging Equation 8.11

$$S_{H_{PROJ_V}} = \tan(\Gamma_Y)^2 S_H \quad (8.12)$$

Solving this gives  $S_{H_{PROJ_V}} = 0.0451 [m^2]$  and  $S_{Y_V} = 0.0315 [m^2]$ . Finally, the area of one of the inverted V fins is calculated:

$$S_{V_{Tail}} = \frac{1}{2} \frac{S_H}{\cos^2(\Gamma_Y)} \quad (8.13)$$

This gives a V-tail component area of 0.0901  $[m^2]$ . This value is highly similar to the vertical fin area of  $S_V = 0.0765 [m^2]$ . Through this sizing process, it is found that the vertical and horizontal tail fins can be set to the same size. It is chosen to have the same size fins for the vertical and horizontal fins to simplify the manufacturing and production process as now only a single mold, joint, and fin needs to be designed. Additionally, this simplifies and enables a marine propulsion system to be implemented on the tail.

#### 8.4.1. Longitudinal Stability

After preliminary sizing, the horizontal components of the inverted Y tail, are checked for longitudinal stability. This is done by analyzing the scissor plots where each line represents the stability and control of the aircraft. The stability curve is calculated with Equation 8.14 and the controllability curve is calculated using Equation 8.15

$$\frac{S_h}{S} = \frac{1}{\frac{C_{L_{\alpha_h}}}{C_{L_{\alpha_{A-h}}} \left(1 - \frac{d\epsilon}{d\alpha}\right) \frac{l_h}{\bar{c}} \left(\frac{V_h}{V}\right)^2} \bar{x}_{cg}} - \frac{\bar{x}_{ac} - 0.05}{\frac{C_{L_{\alpha_h}}}{C_{L_{\alpha_{A-h}}} \left(1 - \frac{d\epsilon}{d\alpha}\right) \frac{l_h}{\bar{c}} \left(\frac{V_h}{V}\right)^2} \quad (8.14)$$

$$\frac{S_h}{S} = \frac{1}{\frac{C_{L_h}}{C_{L_{A-h}}} \frac{l_h}{\bar{c}} \left(\frac{V_h}{V}\right)^2} \bar{x}_{cg} + \frac{\frac{C_{m_{ac}}}{C_{L_{A-h}}} - \bar{x}_{ac}}{\frac{C_{L_h}}{C_{L_{A-h}}} \frac{l_h}{\bar{c}} \left(\frac{V_h}{V}\right)^2} \quad (8.15)$$

The final scissor plot is presented in Figure 8.10.

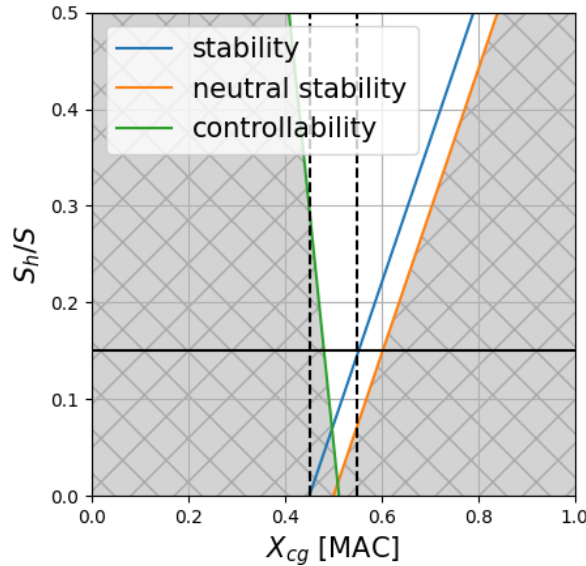


**Figure 8.10:** Stability and Controllability scissor plot

For the current horizontal tail area of  $0.135 \text{ [m}^2\text{]}$  the  $S_h/S$  ratio is at 0.18. From Figure 8.10 it is seen that this ratio can be lowered while still maintaining acceptable amounts of stability and controllability. A new ratio is chosen at  $S_h/S = 0.15$ . This gives a new horizontal tail area of  $0.1125 \text{ [m}^2\text{]}$  and single fin area of  $0.0976 \text{ [m}^2\text{]}$ . From Section 8.4 it is found the vertical fin can be set to the same area. Additionally, a symmetric airfoil NACA0012 with an aspect ratio of 3 is chosen based on the lift and stall angles it can obtain [44]. The overall geometry of each fin in the inverted Y tail is presented in Table 8.3.

**Table 8.3:** Dimensions and geometry of individual fins on inverted Y tail

Tail property	Value	Unit
Half span	0.2905	[m]
Area	0.0562	$\text{[m}^2\text{]}$
Root chord	0.258	[m]
Tip chord	0.129	[m]
MAC	0.200	[m]
Aspect Ratio	3	[-]
Sh/S	0.15	[-]
Tail arm	0.872	[m]
Fin Volume	0.55	[L]

#### 8.4.2. Lateral Stability

To check if the vertical fin satisfies lateral stability two scenarios will be analyzed. The first is to investigate how the rudder performs under crosswind and cross-current operations and the second is to see if the rudder can withstand an engine failure during aquatic operation.

#### Crosswind and Crosscurrent

For air, the maximum wind is predicted to be  $15 \text{ [m/s]}$ ; for aquatic operation, the maximum current is estimated to be  $1.3 \text{ [m/s]}$ . The wind at these speeds will generate drag equivalent to  $13.2 \text{ [N]}$  and  $28.1 \text{ [N]}$  for air and water respectively. The force generated by the rudder can be computed as:



$$Y = C_{L\alpha} \beta \frac{1}{2} \rho V^2 S_v \quad (8.16)$$

Where  $C_{L\alpha}$  is the lift curve alpha slope and  $\beta$  is the sideslip angle for low aspect ratio rudders,  $C_{L\alpha}$  can be approximated as:

$$C_{L\alpha} = \frac{b^2 \pi}{2S} \quad (8.17)$$

resulting in:

$$Y = \frac{b^2 \pi}{2} \beta \frac{1}{2} \rho V^2 \quad (8.18)$$

Using values from Table 8.3, the force generated by the rudder is equal to 17 [N] in air and 35.5 [N] in water, equivalent to moments of 14.8 [Nm] and 30.9 [Nm] in air and water respectively. From this, it is seen that the rudder can withstand the amount of drag high transverse winds cause.

## Engine failure

As the air propulsion unit is located at the nose and acts through the centre of gravity, a failure in this unit will not cause any moments. However, a failure in one of the aquatic propulsion units on the horizontal tails can cause a moment. The moment caused by an engine failure is calculated by:

$$M_{thruster} = 28.63542 \cdot 0.2905 \cos 30 \quad (8.19)$$

This corresponds to a moment of 23.4 [Nm]. The rudder can withstand this moment at roughly 20 [degrees] of deflection. As the rudder was designed to deflect by 30 [degrees] the rudder satisfies this condition.

### 8.4.3. Parameter Stability

The general stability of an aircraft is dependent on multiple parameters such as the centre of gravity, aerodynamic centre and neutral point. These points located along the aircraft have a significant impact on the overall stability, control, and operation of the aircraft. In flight, it is desired to have the aerodynamic centre aft of the centre of gravity. This generates negative pitching moments which correct any gust or external loads the aircraft may experience. Similarly, the neutral point should also be located aft of the centre of gravity for the same reason [45]. For aquatic stability, the centre of buoyancy and centre of gravity locations are critical to the stability of the system. The centre of gravity should be located below the metacentre of the centre of buoyancy to ensure any heeling moments are corrected through righting moments [46]. This ensures a dynamically stable system to any external loads or disturbances.

Additionally, the moment coefficient can also be investigated to see how it changes for increasing angles of attack given the new wing and tail configuration. Figure 8.1d shows the  $C_m - \alpha$  curve clearly showing a negative pitching moment is present. The curve begins to become nonlinear close to 10 [degrees] as this is roughly the stall angle for the mission's Reynolds number. A negative pitching moment indicates dynamic stability that any external loads exerted onto the aircraft will cause the aircraft to return to the equilibrium position.

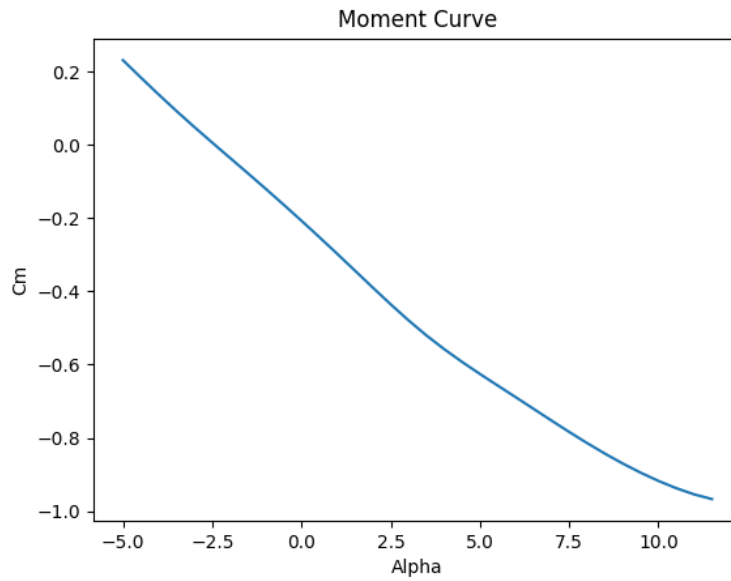


**Figure 8.11:** Moment curve for different angles of attack

#### 8.4.4. Stability Derivatives

To analyze the stability of the aircraft with the wings and newly sized tail, the stability derivatives were calculated using Aerosandbox [45]. At this stage of the design cycle, the signs of each derivative are investigated to ensure that the vehicle's wings, tail and structure provide inherent stability across multiple axis.

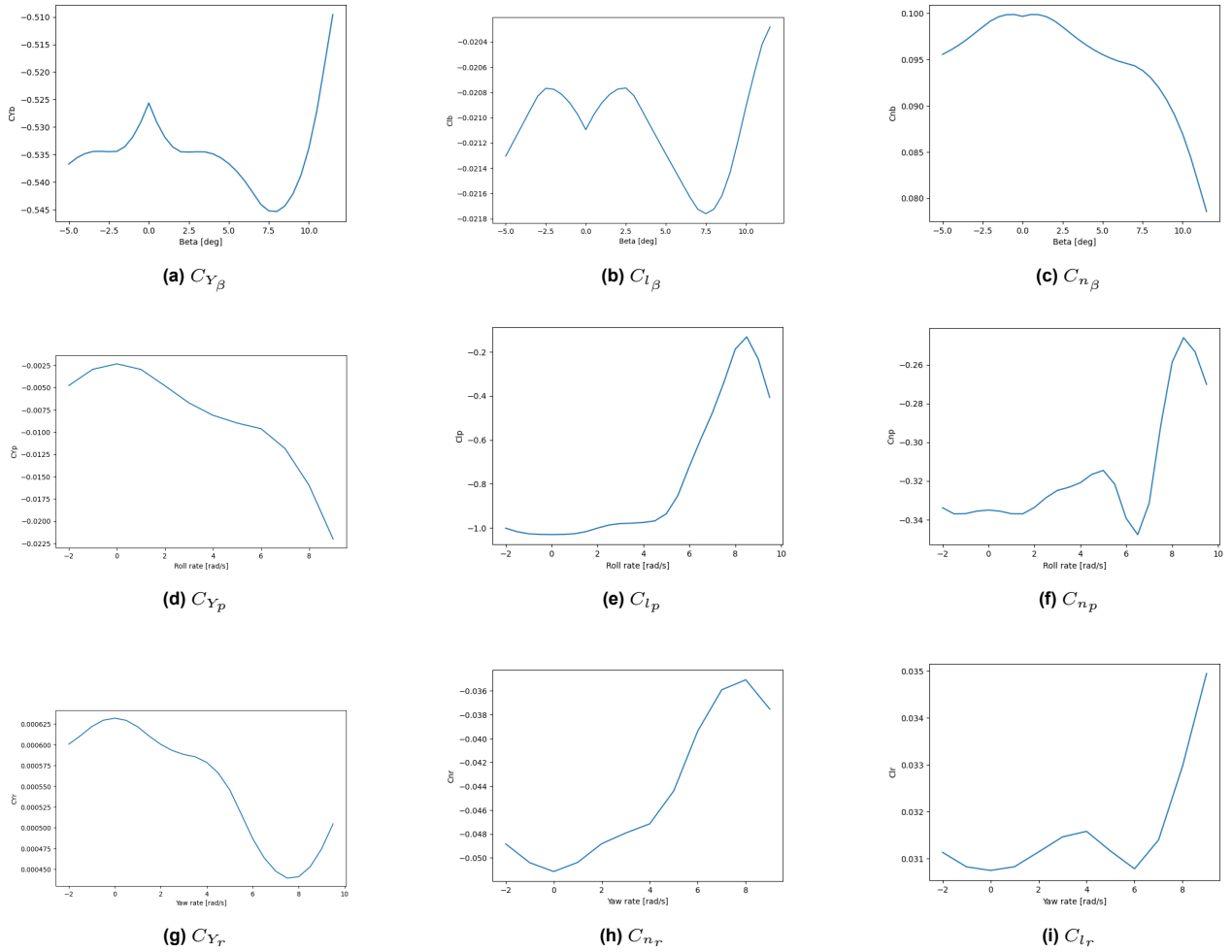


**Figure 8.12:** Stability derivatives for beta, roll rate and yaw rate

From Figure 8.12, plots a-c inclusive show the sideslip, d-f show the yaw rate and g-i visualize the roll rate. Analyzing Figure 8.12a it is seen  $C_{Y_\beta}$  is negative indicating a stable restorative force acting against any sideslip. If the aircraft were to be subjected to sideslip the aerodynamic systems will inherently produce a yawing moment in the opposite direction to return the aircraft to the original position. Looking at Figure 8.12b  $C_{l_\beta}$  is negative indicating that if the aircraft is subjected to sideslip the aircraft will generate a restoring rolling moment to counteract any rolling effects caused by sideslip and bring the wings level. Additionally, Figure 8.12c shows  $C_{n_\beta}$  is positive which is desired as the aircraft will automatically rotate to the direction of velocity thereby eliminating any undesirable sideslip. Looking at Figure 8.12d  $C_{Y_p}$  it is seen this value is negative and small demonstrating that the tail can generate a restorative rolling moment if an undesired rolling velocity is incurred. From Figure 8.12e is negative indicating the wings and tail have restorative roll damping effects. Figure 8.12f is negative demonstrating that a negative restoring yawing moment is generated to counteract unwanted roll rates. Investigating Figure 8.12g it is seen to be small and positive showing that the tail will create a positive restoring force from the sidewash. Figure 8.12i is positive indicating the main wings and tail create a positive restoring rolling moment. Finally, Figure 8.12h is negative showing the tail provides a restorative yawing force.

## 8.5. Control Surfaces

### Ailerons

Ailerons are responsible for the roll of the system. In his book AIRCRAFT DESIGN: A CONCEPTUAL APPROACH, Raymer [40] states that the span of the ailerons can be estimated from the graph seen in Figure 8.13.

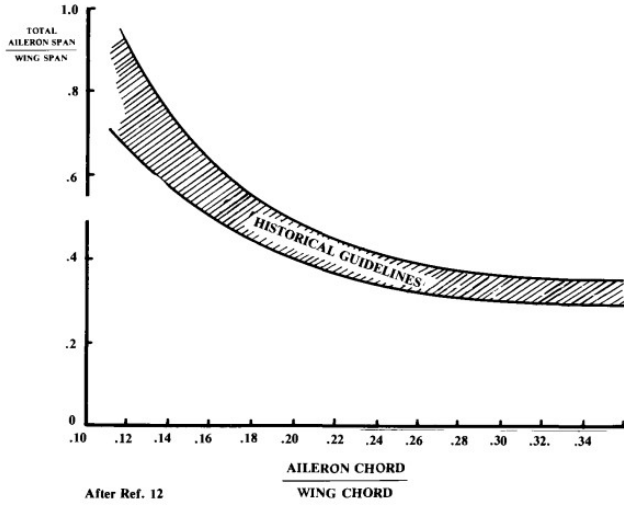


Figure 8.13: Aileron Design Guidelines [40]

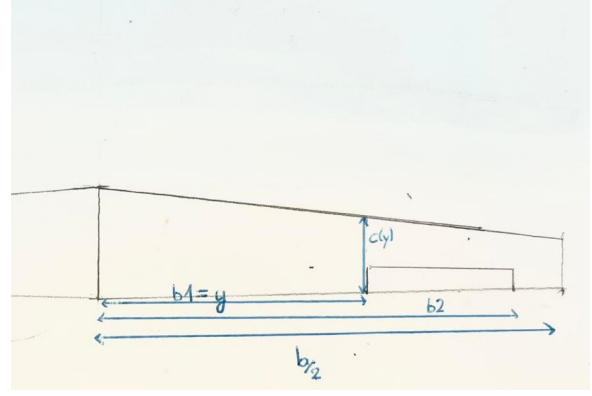


Figure 8.14: Aileron Geometry. b: wing span, b1: start aileron, b2: end aileron, c(y): wing chord at b1

The wing span is 3.04 [m], and the chord ratio is chosen to be 0.32. Thus, from the graph, the aileron span vs wing span ratio is 0.32, which gives an aileron span of 0.97 [m]. Now, in order to size the ailerons, an iterative process has been used. First, the wing geometry is assumed as seen in Figure 8.14. The ailerons are roughly placed along the wing, starting at b1 and extending until b2. with a span determined from the just mentioned aileron design guideline graph.

Next, the goal is to determine the roll rate, P, which is the rate of change of the bank angle with time and the time it takes to reach the maximum bank angle. If the time, t, is too large, the aileron geometry is changed. Reiteration is continued until the time reaches an acceptable value.

The roll rate [47] is calculated using:

$$P = \frac{d\Phi}{dt} = -\frac{C_{l_{\delta_a}}}{C_{l_p}} \cdot \delta_a \cdot \frac{2V}{b} \quad (8.20)$$

Where  $\Phi$  is the bank angle, b is the wing span, V is the cruise speed (20 [m/s]),  $\delta_a$  is the maximum aileron deflection equal to

$$\delta_a = \frac{1}{2} \cdot (\delta_{a_{upper}} + \delta_{a_{lower}}) = \frac{1}{2} (14 + 20) = 17.5^\circ \quad (8.21)$$

$C_{l_{\delta_a}}$  [47] is

$$C_{l_{\delta_a}} = \frac{2c_{l_\alpha} \cdot \tau}{S_{ref} \cdot b} \cdot \int_{b_1}^{b_2} c(y) \cdot y \, dy \quad (8.22)$$

and  $C_{l_p}$  [47] is equal to

$$C_{l_p} = -\frac{4(c_{l_\alpha} + c_{d_0})}{S_{ref} \cdot b} \cdot \int_0^{\frac{b}{2}} c(y) \cdot y^2 \, dy \quad (8.23)$$

The  $c_{l_\alpha}$  and  $c_{d_0}$  are the lift curve slope and the zero drag coefficient of the airfoil. They are found from public NACA2412 data and are equal to 0.0984 and 0.018 respectively.  $\tau$  is the aileron effectiveness and can be determined from Figure 8.15 [47].

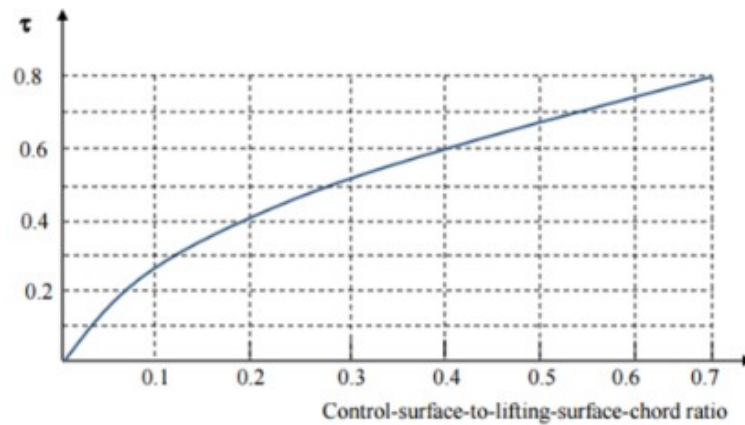


**Figure 8.15:** Aileron effectiveness vs the ratio of the aileron chord over the total airfoil chord [47]

Consequently, after iteration, the aileron design specifications are:

**Table 8.4:** Aileron Placement on Wing

Specification	Value
b1	0.868
b2	1.368
Aileron Span	0.973 [m]
Aileron Chord	0.086 [m]
$\delta_{a_{upper}}$	14 [°]
$\delta_{a_{lower}}$	- 20 [°]
Max bank angle	35 [°]
Roll rate	23.37 [°/s]

The question now arises how to attach the ailerons to the main wing structure. A detailed configuration has been worked out as can be observed in Figure 8.16. A rod runs throughout the aileron right behind the leading edge from one side to other. The rod sticks out slightly and is connected to gears that are powered by a servo. The gears can rotate the shaft so that it may achieve the maximum aileron deflection angle,  $\delta_a$ . The maximum torque that the rod can withstand has been calculated to be 118 [Nm]. The servo thus is not allowed to provide more torque than this as this would break the rod.

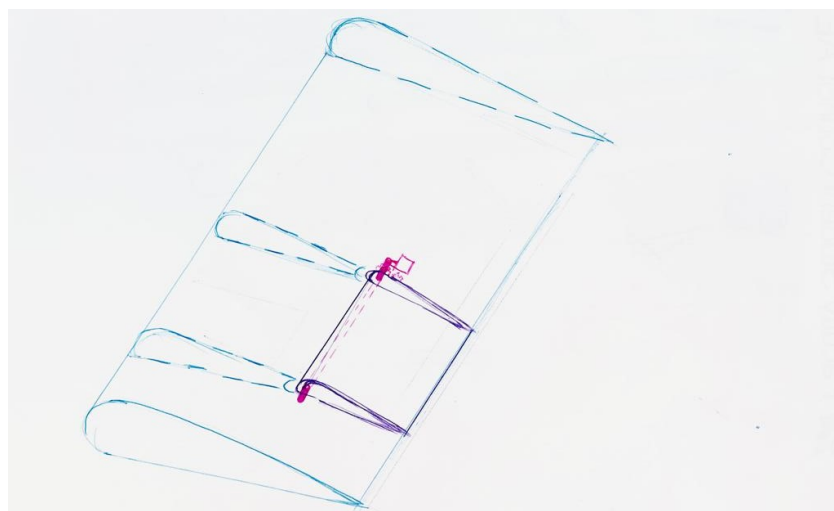


**Figure 8.16:** Aileron attachment mechanism - a circular shaft connects to gears that are turned by a servo

## Elevators

To allow for pitch and yaw control, the tail of the Puffin is equipped with elevators.

As explained before, the entire tail surfaces will rotate to provide pitch, roll and yaw control. Following Figure 8.17 illustrates the mechanism that is used to generate this rotational moment. As the tail incorporates the mounting shaft for the engines, which is not allowed to rotate, a set of gears is used to make the tail rotate around the shaft. The sizing of the motor used for this mechanism is explained below the figure.

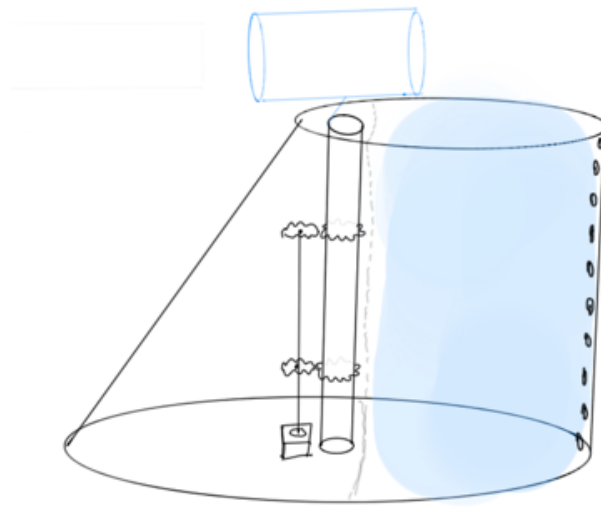


**Figure 8.17:** Schematic drawing of the mechanism consisting of a servo and gears that is used to rotate the tail to allow for attitude control/

The shaft will be located at the thickest point of the airfoil at the tail tip, which is at 30 % of the chord. A conservative approach was used to size the motor that has to provide the torque. The maximum aerodynamic moment coefficients the NACA0012 airfoil experiences lie between -0.05 and +0.05. Using the moment equation, this leads to torques around the shaft of 0.2 [Nm] in air and 0.9 [Nm] in water. A safety factor of 1.5 still has to be added to these values. A 0.06 [kg] servo was found that can provide this torque <sup>1</sup> An overview of the controllability is presented in Table 8.5 along with their corresponding requirements.

**Table 8.5:** Control surfaces controllability speeds for the vehicle

Medium	Control Type	Value [deg/s]	Requirement Satisfied
Air	Roll Rate	23.4	CTRL-ATT-03
	Yaw Rate	25.5	CTRL-ATT-04
	Pitch Rate	12.3	CTRL-ATT-05
Water	Roll Rate	14.2	CTRL-ATT-08
	Yaw Rate	4.2	CTRL-ATT-09
	Pitch Rate	5.2	CTRL-ATT-15

<sup>1</sup>Tail rotating servo

## 8.6. Verification and Validation

**Table 8.6:** Verification methods for the relevant requirements of the control surfaces. D: demonstration, A: Analysis, I: Inspection, T: test

Requirement	Verification Description	Method
CTRL-ATT-01, CTRL-ATT-10, CTRL-ATT-11, CTRL-ATT-12, CTRL-POS-01, CTRL-CSF-01	Expose the system to disturbances in a simulated in-air environment. See if it is able to return to a stable and controllable state	T, D
CTRL-ATT-03, CTRL-ATT-04, CTRL-ATT-05, CTRL-ATT-06	Maneuver the system such to determine the limits of roll, pitch, and yaw respectively	T, A
CTRL-ATT-02, CTRL-POS-02	Expose the system to disturbances in a simulated underwater environment (pool). See if it is able to return to a stable and controllable state	T, D
CTRL-ATT-07	Place system in pool and see if it moves in all directions	I, D
CTRL-ATT-08, CTRL-ATT-09, CTRL-ATT-15	Analyse the angular velocity behaviour of the system in a simulated environment with respect to roll, pitch and yaw	A
CTRL-ATT-16	Perform a landing maneuver and observe if the control surfaces operate successfully	D

# 9 Configuration

Now that most of the components present in the UAV have been defined and sized. It is time to arrange them in an efficient 3-dimensional to define the constraints of the structure of the UAV. The layout requirements related to the different mission phases, as well as the components that have to be positioned within the vehicle will be described in Section 9.1. The components will be positioned within the body of the UAV starting with the design of the nosecone in Section 9.2, then the internal layout of the fuselage in Section 9.3.

## 9.1. Design Considerations

A few considerations have to be kept in mind when constructing this configuration. The different mission phases will generate different design considerations. An overview of the main critical aspects of each phase is listed in Table 9.1.

**Table 9.1:** Overview of the main design considerations of each mission phase

Mission phase	Characteristics
In-air navigation	Aerodynamic efficiency → minimize cross-section, minimize fuselage length, limit surface irregularities, and limit interference with lift-generating surfaces.
In water navigation	Amount of wetted surface, tapering or slenderness ratio (wake drag)
Water-to-Air transition	The difference of cross-sectional area in contact with the water at each time-step.
Air-to-Water transition	Getting to nominal flight condition as soon as possible

Another critical aspect is the components that have to be contained within the fuselage, and the position of the wings, tails and control surfaces with respect to the center of gravity for stability. All the components required for the mission are shown in Table 9.2 including certain positional constraints to take into account.



**Table 9.2:** Components of the UAV including the number of parts and positional considerations when constructing the layout

Subsystem	Component	Amount	Characteristics
Structures	Wing	2	High-wing configuration for folding
	Tail	3	Inverted-Y tail
	Fuselage	1	Non load-bearing skin
	Nosecone	1	Paraboloid shape
	Wing hinge	1	Positioned at the trailing edge of the wing
	Tail hinge	3	Positioned below the midpoint of the tail
Propulsion	In-air motor	1	Positioned in nosecone, not water-tight
	In-air propeller	2	Attached to the in-air motor
	Underwater motor	3	Positioned at the leading edge of the tip of the tail
	Gas tank	1	-
	Water tank	1	Positioned at the end of the fuselage
Electronics	Batteries	8	Not water-tight
	Sonar	1	Positioned at the top of the fuselage, the view should not be obstructed
	Camera	2	One pointing up, one pointing downwards
	Water sample pump	1	-
	Flight controller	1	Not water-tight

## 9.2. Nosecone Design

An easy starting point for the design is the nosecone. It is a component that can easily be made water-tight and therefore contain components that can not be in contact with water. This is coincidentally beneficial since adding weight to the front of the UAV is good for aerodynamic stability since the center of gravity should lie in front of the aerodynamic center of the wing as explained in Section 8.4.3. The nosecone will also contain the PCBs required for navigation and sensing as well as the flight controller as listed in Chapter 11. The final component to be included in the nosecone is the in-air propulsion system. The motor will be contained within the nosecone and the propeller shaft will extend out of the front of the nosecone on which the propellers are attached.

The nosecone is split into two compartments. An outer shell that gives it its aero/hydrodynamic properties and a cylindrical insert surrounded by o-rings that makes it water-tight. An additional container for the batteries has been considered to act as a thermal insulator and a shrapnel box in case of an explosion but the nosecone itself was deemed sufficient if designed accordingly. The cables connected to the batteries are plugged into a connector on the inner wall of the cylindrical insert to remain water-tight.

Finally, the chosen shape of the nosecone is a "full parabola" (namely a parabola tangent at its base). This was selected due to its positive aerodynamic properties at a low Mach number and because it allowed it to fit the internal components of the nosecone efficiently [48].

A sketch of the configuration within the nosecone can be seen in Figure 9.1.

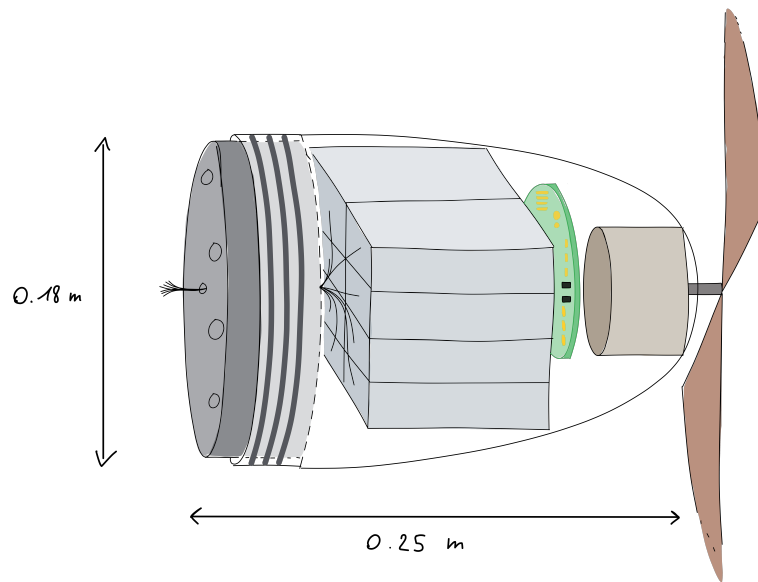


**Figure 9.1:** Sketch of the components housed within the nosecone of the UAV, it is kept water-tight with an inserted cylindrical section and three o-rings. The electrical cables are plugged into a connector within the nosecone that is isolated from the outer surface.

### 9.3. Internal Layout

The remaining components that have to be positioned within the fuselage are the cameras, the sonar, the water sample pump, the wing hinge and the gas tank. The fuselage will be considered non-load-bearing and will simply provide an aerodynamic shape to the vehicle, this decision will be further explained in Section 10.2.

The sonar has to be able to sense above the vehicle, without any hindrance from the material of the fuselage itself. It is also the widest element within the UAV and will therefore be the constraint in the fuselage diameter. The cameras also have to point in specific directions, the sensing camera should point upwards, in the same orientation as the sonar. The navigation camera should point downwards. A rectangular cut-out in the fuselage will be made for the sonar and sensing camera with dimensions as shown in Figure 9.2, for the navigation camera a simple circular hole can be made.

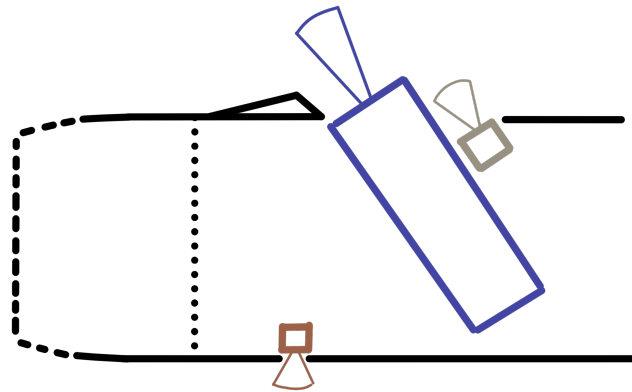


**Figure 9.2:** Visual representation of the position of the sensor and cameras, as well as the cut-outs in the fuselage to allow visibility to the outside

The pump used to sample the water will be positioned in the remaining volume under the sonar. The gas tank containing compressed air for the impulsive water-to-air launch maneuver will be positioned behind the sonar. This is due to the positional requirement of the wing hinge to be positioned at the trailing edge of the wing. The wing hinge will be located behind the gas tank as shown in Figure 9.4, as well as all the internal components within the nosecone and fuselage. The wing hinge is depicted as the grey cylinder in this render.

### 9.4. Outside Components

In this section, the wings, tails and water chamber will be positioned with respect to the main body of the vehicle. The main influencing factors for the wing and tail are the aero and hydrodynamic stability considerations explained in Chapter 8. The water chamber should be positioned at the end of the fuselage, aligned with the

centre of gravity.

The wing is positioned above the fuselage due to the constraints imposed by the hinge of the wing and the fact that the wing can physically not fold within the fuselage. The final dimensions of the fuselage can be seen in Figure 9.5.

The water chamber is positioned at the aft end of the fuselage, connected to the outer wall. Due to the longitudinal positional requirements of the tail, generated by the longitudinal stability requirements outlined in Section 8.1. The tail has to be placed at the same longitudinal position as the water chamber. Since it has to be rotated by the hinge mechanism described in Section 6.4, the wing can not be simply bonded to the water chamber so a collar will be bonded to the water chamber as shown in Figure 9.5 to provide a secure attachment point for the hinge.

The thruster is attached to the top of the tail, per the sketch shown in Figure 7.13. An isometric render of the CAD model made with the software CATIA can be seen in Figure 9.3.

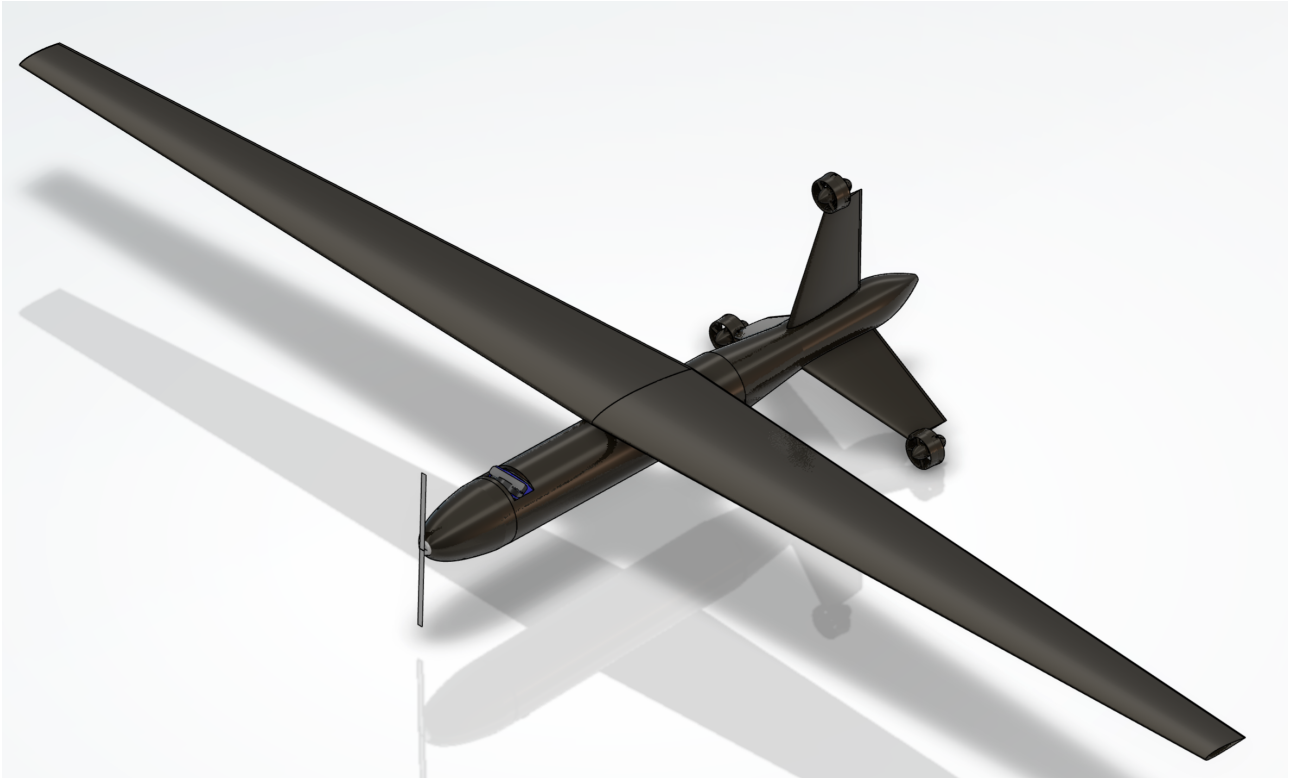


**Figure 9.3:** Isometric view render of the vehicle made in the software CATIA

## 9.5. Mass Budget

In order to calculate the location of the center of gravity of the vehicle, a mass distribution table has been constructed. It can be seen in Table 9.3. The location of the centre of gravity will influence the stability of the UAV and therefore drive the requirement for the longitudinal position of the wing.

**Table 9.3:** Mass budget of the components grouped per subsystem

Group	Component	Amount	Mass [kg]	tot. mass [kg]
<b>Structures</b>	Wing	2	1.08	2.16
	Tail	3	0.065	0.195
	Fuselage	1	0.65	0.65
	Nosecone	1	0.16	0.16
	Wing hinge	1	2	2
	Tail hinge	3	0.029	0.087
	Tail collar	1	0.1	0.1
	<b>Total</b>			<b>5.35</b>
<b>Propulsion</b>	Air motor	1	0.329	0.329
	Air propeller	2	0.019	0.038
	Underwater motor	3	0.344	1.032
	Gas tank	1	1.26	1.26
	Water tank	1	0.26	0.26
	<b>Total</b>			<b>2.9</b>
<b>Electronics</b>	Batteries	9	0.317	2.853
	Sonar	1	1.46	1.46
	Camera	2	0.05	0.1
	Water sample pump	1	0.4	0.4
	Flight Controller	1	0.1	0.1
	TT&C	1	0.048	0.048
	<b>Total</b>			<b>4.96</b>
<b>Total</b>				<b>13.2</b>

## 9.6. Center of Gravity

To calculate the location of the centre of gravity, the location of the centre of gravity of each individual component of the vehicle is found. The location of the c.g. can then be calculated using Equation 9.1.

$$\bar{x} = \frac{\sum_{i=1}^n \tilde{x}_{ii}}{\sum_{i=1}^n i} \quad (9.1)$$

With the sum being over all the components of the vehicle,  $\bar{x}$  being the location of the centre of gravity,  $\tilde{x}$  being the location of the c.g. of the individual component and  $i$  the mass of the individual component.

Due to the sweeping mechanism of the wing, the position of the centre of gravity will change when underwater. This shift in the position of the centre of gravity is shown in Figure 9.4. In this figure, the position of the centre of gravity in the air with the wings deployed is indicated by a "1", and the shifted centre of gravity underwater when the wings are folded is indicated by a "2".

The location of the centre of gravity in all three axes shown in Figure 9.3 can be seen in Table 9.5. The location of the c.g. is shown for the folded and unfolded wing configuration.

## 9.7. Buoyancy System

Since the UAV has to evolve underwater, certain design decisions have to be made to manage the voluminous, water-tight components of the drone. Certain elements such as the fuselage, wings, or tail contain more than 10 [L] of air if kept water-tight and would therefore require an unrealistic downward force from the thrusters to keep the vehicle underwater.

This imposes a new requirement on the system, namely that the water should be able to escape the structure fast enough to not hinder the water take-off. This will be achieved by allowing water to freely enter and leave the fuselage, wings, and a certain section of the tail.

Therefore, the wing will be submerged by keeping the root and tip surfaces open. This greatly reduces the buoyancy force applied on the vehicle while decreasing the structural requirements imposed on the structure of the wing due to the increase of pressure when submerged. A similar decision was made for the fuselage, water is able to enter the fuselage through the hole made for the sonar and the cameras. A model simulating the flow of water through the wing and fuselage will be described in Section 9.8.

The main components that contribute to the buoyancy force are listed in Table 9.4.

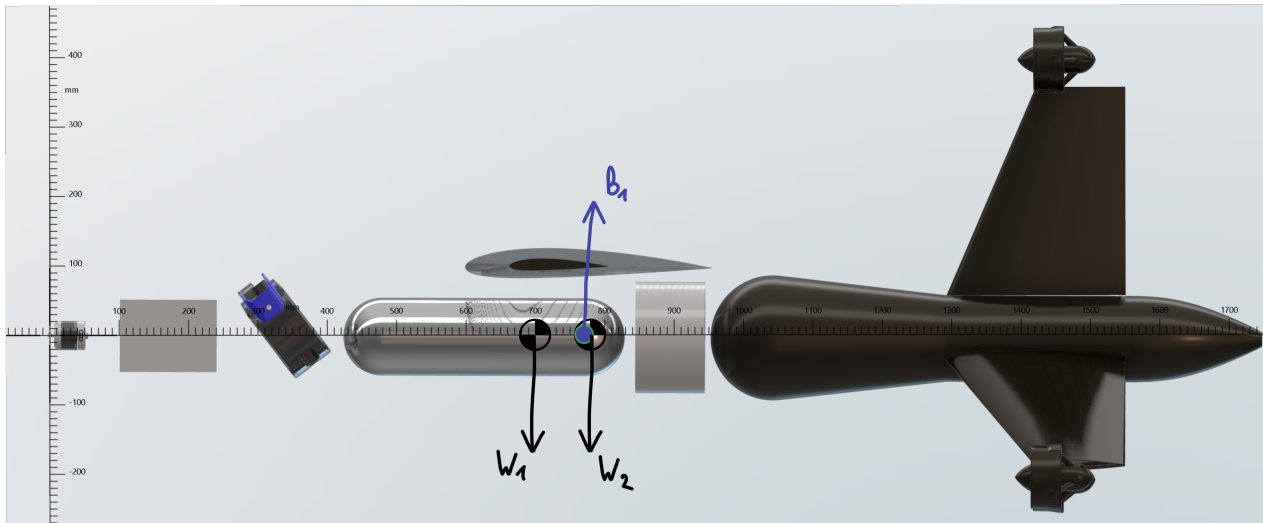


**Figure 9.4:** Center of gravity in air (unswept wings) on the left, c.g. in water (swept wings) on the right, centre of buoyancy indicated as the full blue circle in between the two.

**Table 9.4:** Buoyancy budget of all main components of the vehicle

Group	Component	Amount	Volume [L]	tot. Volume [L]
<b>Structures</b>	Wing	2	0.75	1.5
	Tail	3	0.55	1.65
	Fuselage	1	0.2714	0.2714
	Nosecone	1	3.6	3.6
	Tail collar	1	2.2	2.2
<b>Propulsion</b>	Gas tank	1	2.	2.
	Water tank	1	0.1374	0.1374
<b>Electronics</b>	Sonar	1	1.119	1.119
	Water sample pump	4	0.1	0.4
<b>Total</b>				<b>12.8778</b>

The calculated buoyancy values of each component and their influence on the moment around the c.g. under-water are shown in Table 9.5. These values, as well as a calculated center of buoyancy and the two center of gravity locations (unswept & swept wings) are visualised in Figure 9.4. The center of buoyancy can be visualised by the blue circle positioned between the two centres of gravity.

**Table 9.5:** Location on all three axes of the center of gravity and center of buoyancy of the vehicle, the center of gravity has a value when the wings are folded and unfolded.

	X-axis (unfolded) [mm]	X-axis (folded) [mm]	Y-axis [mm]	Z-axis [mm]
Center of gravity	697	777	0	20.8
Center of buoyancy	-	771	0	14.4

Looking at Table 9.3 and Table 9.4, it can be noticed that the resulting force acting on the system is of  $\approx 2$  [N] upwards and the vehicle is subjected to a "nose up" moment of  $\approx 0.06$  [Nm]. These deviations from a neutrally buoyant UAV can be compensated by the underwater propulsion system.

The geometry of the collar positioned on the water chamber supporting the wing is precisely designed to make the vehicle's buoyancy as close to equilibrium as possible. This results in a geometry of the collar shown in Figure 9.5. The flat part of the collar on which the tail is positioned is labelled by a "1", this part is kept water-tight. The remaining section of the collar is added for aero/hydrodynamic purposes and will be submerged, it has the label "2".

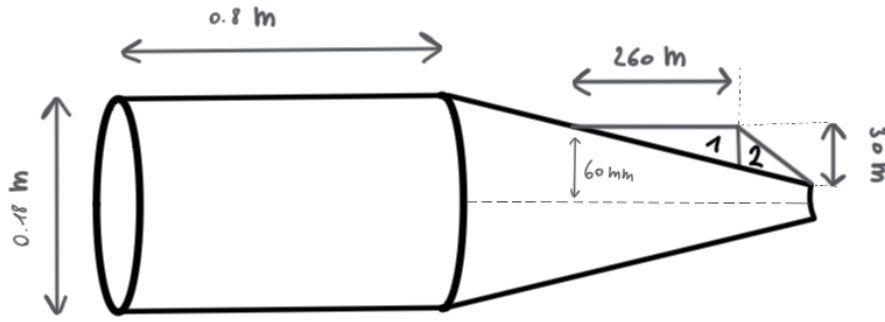


Figure 9.5: Sketch of the dimensions of the fuselage and collar positioned around the tail of the vehicle

## 9.8. Drainage Model

To meet buoyancy requirements, wings, fuselage, and other elements are flooded when submerging. On launch, these volumes must be rapidly drained. An analytical model is developed, experimentally validated, and applied to major elements (wing and fuselage).

### 9.8.1. Analytical Model

Mass flow through an orifice (such as a drainage port) may be modelled by Equation 9.2, where the discharge coefficient  $C_d$  is an efficiency between zero and unity (ideal case). Per Figure 9.6a a reference volume is defined, for which the acting pressure difference is obtained (Equation 9.3). The pressure difference arises from the hydrostatic pressure exerted by the weight of the column of water over the exit area. The difference in ambient (air) pressure between upstream and downstream is assumed to be negligible. During launch, the vehicle accelerates rapidly (5.5 [g]), see Chapter 5); this is the acceleration considered when calculating hydrostatic forces. Considering a finite mass of water [m] in the reference volume, Equation 9.2 and Equation 9.3 combine to yield the time derivative of said finite mass, Equation 9.4. For some initial mass ( $m(t = 0) = m_0$ ) the time solution of Equation 9.4 is Equation 9.5.

$$\dot{m} = C_d A \sqrt{2\rho \Delta P} \quad (9.2)$$

$$\Delta P = (p_a + p_{hydrostatic}) - (p_a) = \frac{mg_0 n}{A_R} \quad (9.3)$$

Rephrasing as a differential equation:

$$\frac{dm}{dt} = -\dot{m} = -C_d A_t \sqrt{\frac{2\rho m g_0}{A_R}} \cdot m \quad (9.4)$$

Time domain solution:

$$m(t) = \frac{a^2 t^2}{4} + \frac{c_1 a t}{2} + \frac{c_1^2}{4} \text{ where } a = -C_d A_t \sqrt{2\rho \cdot \frac{1}{A_R} \cdot g_0 \cdot n}, \text{ and } c_1 = \sqrt{4m_0} \quad (9.5)$$

$$\text{where } a = -C_d A_t \sqrt{2\rho \cdot \frac{1}{A_R} \cdot g_0 \cdot n}, \text{ and } c_1 = \sqrt{4m_0}$$



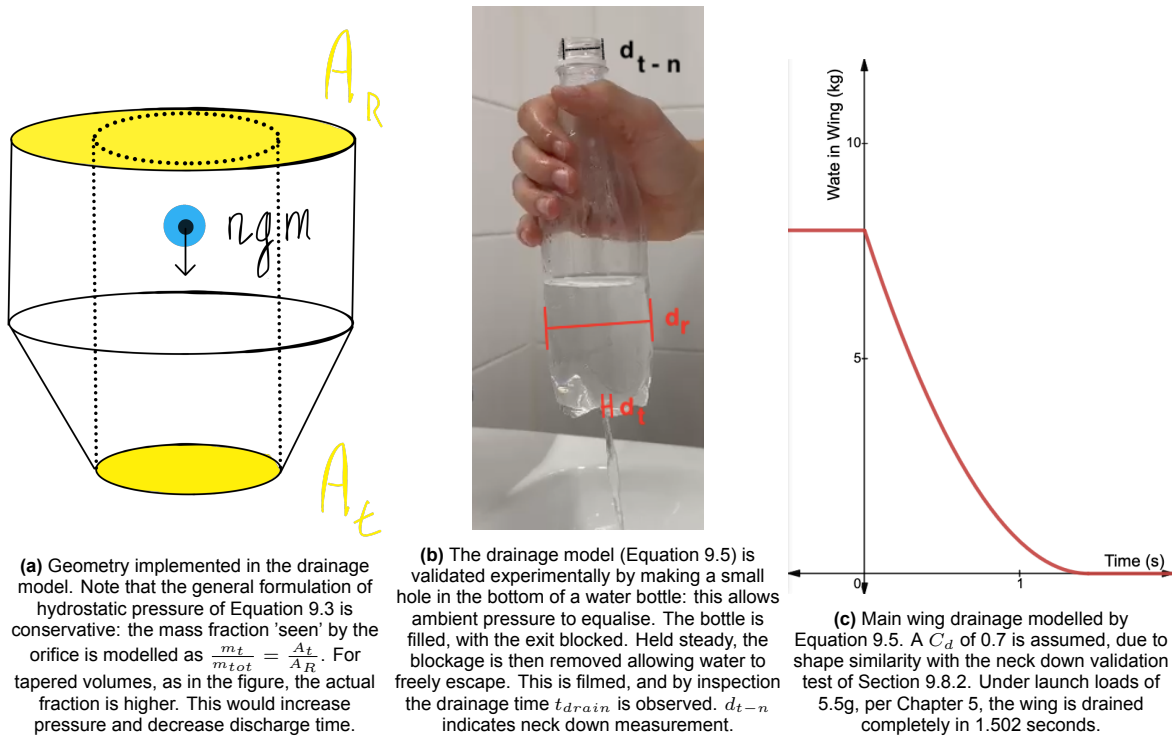


**Figure 9.6:** Water drainage model for the wing and fuselage, validated experimentally

### 9.8.2. Model Validation

The model is validated experimentally: the test setup is presented in Figure 9.6b. Relevant calculation parameters and validation test results are presented in Table 9.6. Circular areas  $A_R$  and  $A_t$  are calculated from the diameters  $d_R$  and  $d_t$  in the table. In the neck up measurement, the remaining water is assumed to be about 5% of the mass, and this is the model time displayed. The model appears to predict drainage duration well, and should provide a decent estimate for drainage design.

**Table 9.6:** Drainage model validation input parameters and results. Two measurements were made for each orientation, with neck down measurements having a drain time variation of 0.25 [s] and neck up measurements a variation of 1.0 [s]. A discharge coefficient of 0.5 is assumed: fitting to the data, a coefficient of 0.56 [-] is calculated for neck up and 0.73 [-] for neck down.

	Model Input Parameters						Discharge Time [s]	
	m_0 [L]	rho [kg/m3]	g_0 [kg/s2]	d_R [mm]	d_t [mm]	C_d [-]	Model	Actual
Bottle Neck Down	0.33	997	9.81	76	24	0.5	2.4	1.5
Bottle Neck Up	0.33	997	9.81	7	7	0.5	22.3	20

### 9.8.3. Effect on Design

Wing drainage is estimated by assuming an open ended shell structure: wing structure is sized accordingly. The reference area ( $A_R$ ) is then the wing root area (0.010524 [m<sup>2</sup>]), the throat area ( $A_t$ ) is the wing tip area (0.00168 [m<sup>2</sup>]), the initial water mass ( $m_0$ ) is the product of water density and enclosed wing volume (8 [L]), and the load factor ( $n$ ) is set by launch acceleration (5.5 [g]). The time dependent result is plotted in Figure 9.6c: the wings are found to drain completely in 1.5 seconds.

Fuselage drainage ports are designed for the same drainage time as the wing: the total drainage port area is found by inverting Equation 9.5 to solve for  $A_t$ . Other model input parameters are a conservative estimate of  $C_d = 0.5$ ,  $A_R$  as the cross-sectional area of the fuselage with diameter  $d_R = 180$  [mm], and fuselage water volume of  $20 - 3.2 = 16.8$  liters. Solution yields a required drainage port area of 0.00531 [m<sup>2</sup>] (equivalent to a circle of 82.2 [mm] diameter) for a drainage time  $t_{drain} = 1.5$  [s].

These drainage holes will be positioned at the bottom of the fuselage around the spherical endcap of the water chamber. The exact geometry of those holes will be further analysed in the final version of this report to minimise their aero/hydrodynamic impact. A preliminary visualisation of the drainage holes can be seen in Figure 9.7.

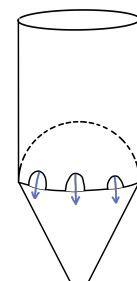


**Figure 9.7:** Preliminary visualisation of the drainage holes positioned at the bottom of the fuselage

# 10 Structure

The Puffin's structure will provide support and connections between all the subsystems. Furthermore, it has to protect the payload from externally applied loads. This chapter starts off with establishing a list of the most important requirements regarding structural sizing. Then the fuselage, wing and tail structure are sized to withstand all the loads. Finally, a suited material is selected to then validate and verify the suitability of the entire structure with the mission objective.

## 10.1. Requirements and Assumptions

Following Table 10.1 establishes all the requirements that will be driving the structural sizing. They can be traced back to higher-level requirements or requirements induced by other subsystems.

**Table 10.1:** Incoming requirements for structures

ID	Description	Traceability	Rationale
STR-FUS-01	The nose cone structure shall withstand 1636 [N] of impact loads.	DV-01, DV-03	The diving manoeuvre induces severe loads on the Puffin's structure. These will be the critical loads in sizing.
STR-FUS-02	The fuselage structure shall withstand 850 [N] of launch loads	Follows from launch sizing	To successfully perform the mission the structure has to sustain the loads exerted upon it during launch.
STR-WI-01	The wing structure shall withstand 100 [N] of aerodynamic loads.	Follows from wing sizing	To perform the mission the wing has to withstand the aero- and hydrodynamic loads it will experience in flight and underwater.
STR-WI-03	The wing shall withstand 1636 [N] of impact loads	DV-01, DV-03	The diving manoeuvre induces severe loads on the Puffin's structure. These will be the critical loads in sizing.
STR-TAIL-01	The tail shall withstand 94 [N] of aerodynamic loads	Follows from tail sizing	To perform the mission the tail has to withstand the aero- and hydrodynamic loads it will experience in flight and underwater.
STR-TAIL-02	The tail shall withstand 800 [N] of impact loads	DV-01, DV-03	The diving manoeuvre induces severe loads on the Puffin's structure. These will be the critical loads in sizing.
STR-TAIL-03	The shaft in the tail shall withstand 120 [N] of impact loads applied on the underwater thrusters.	DV-01, DV-03	The diving manoeuvre induces severe loads on the Puffin's structure. These will be the critical loads in sizing.
SYS-STR-04	The system's structure shall not be critically damaged by corrosion within 1 year of operation		

## 10.2. Load-Bearing Structure

The main load-bearing structure of the airframe is the fuselage. This will be a non-watertight structure that connects the watertight nosecone with the wing and the tail. In order to size the load-bearing structure, some

assumptions have to be made. The first one is that the structure is modelled as a beam, carried by lift loads, and pulled down by its weight. Underwater, the buoyancy force also has to be considered. The cross-section of the load-carrying section is assumed to be modelled as can be seen in Figure 10.1a, with three stringers carrying the main load, and a thin sheet to improve aerodynamic performance. In the sheets, some holes will be made to allow for water drainage. L-stringers are used to carry the loads. The L-stringers can be seen in Figure 10.1b

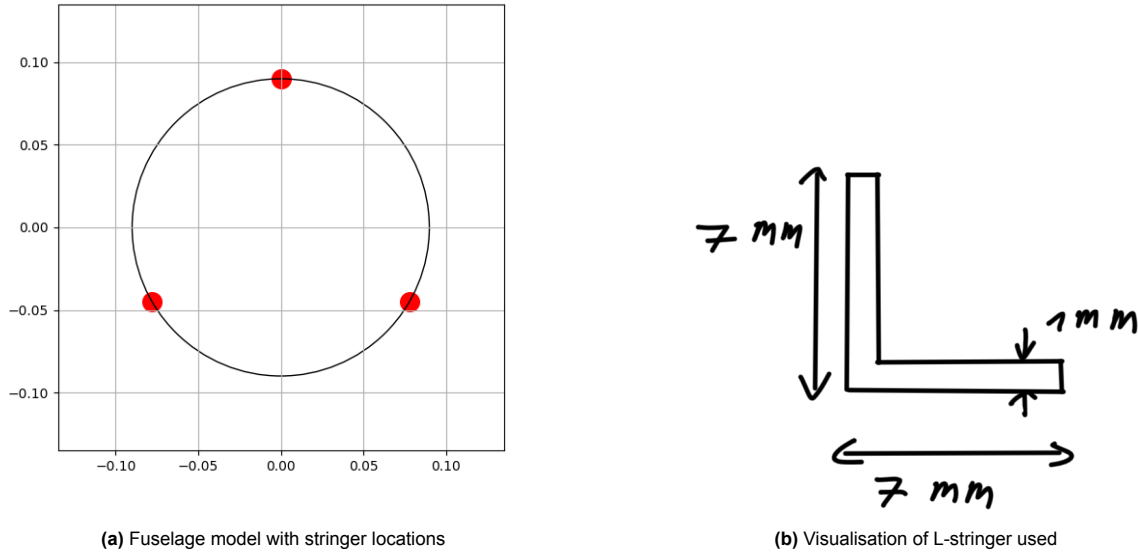


**Figure 10.1:** Figures showing the fuselage cross-section with stringer locations and the L-stringer cross-section including dimensions

The first load is the normal stress due to the normal force exerted on the fuselage during diving and launching. Drag (both in air and in water), could also be considered, however, this will be negligible compared to the impact loads. By knowing the applied load and the surface area, the normal stress can be calculated. The next load is the normal stress due to the bending of the fuselage. Since the lift, weight, and buoyancy all introduce a bending moment onto the fuselage, this is one of the most critical stresses. The bending moment stress can be found using Equation 10.1. Shear stress in the fuselage consists of stress due to the shear force introduced by the lift, weight, and buoyancy, and the stress resulting from torsion of the control surfaces of the tail. These stresses are found using Equation 10.2 and Equation 10.3 respectively. The last failure mode of the fuselage is buckling. Modelling the fuselage as a beam, Euler buckling of beams has to be considered. The critical load at which the structure will buckle is seen in Equation 10.4.

$$\sigma = \frac{My}{I} \quad (10.1)$$

$$\tau = \frac{VQ}{It} \quad (10.2)$$

$$\tau = \frac{Tr}{J} \quad (10.3)$$

$$P_{crit} = \frac{\pi^2 EI}{L^2} \quad (10.4)$$

Using the process described above, a load-bearing structure consisting of three 7x7 [mm x mm] L-stringers will be used. The stringers will have a thickness of 1 [mm]. This will lead to a maximum normal stress (including a safety factor) of 303 [MPa], shear stress of 4.8 [MPa], and a maximum normal force that can be exerted on the fuselage of 12 000 [N], which is largely over the 1666 [N] impact loads. Recycled CFRP will be used to carry these loads, as its failure stress is higher than the maximum stress in the structure. The structure will weigh 0.1053 [kg].

### 10.3. Wing Structure

The wing is a key element in the structural design, as it transfers the lifting loads it generates onto the fuselage. The main loads acting on the wing are the lift loads generated by the wing, the drag of the wing, the pitching moment introduced by the wing, and the weight of the wing. A key consideration in the wing structural design is the effect of the wing on the buoyancy of the whole drone. A fully closed wing will be structurally stronger, but it will limit the ability to fill itself with water to become neutrally buoyant. Even a wing with water escape holes has to deal with problems such as slow water escape and potentially trapped water. A first solution would be to make a fully solid wing, as this would neglect any need to store water, and would not cause any drainage problems. However, this would result in a wing that is massively overdesigned for the loads it would

have to carry, resulting in a high mass. Another solution that does not have major drainage problems is a shell structure. If the shell is opened at the root and tip chord, water can easily flow in and out without any risk of it being trapped. Even though not an ideal solution weight-wise, the water drainage performance outweighs the increase in weight.

In order to ease up the design process, some assumptions have to be made. The first assumption is that the wing is modelled as a cantilever beam with a length of half the wingspan. A second assumption is that the loads on the wing only consist of lift, drag, pitching moment, and weight of the wing. It is assumed that these loads act through the centroid of the wing, and therefore will not introduce any additional moments.

The lift and weight can be modelled as a distributed force. The lift can be assumed to be an elliptical distribution along the wingspan given by Equation 10.5. The weight of the wing can be defined based on the thickness of the wing shell structure, the perimeter of the airfoil at a specific chord length, and the density of the material. The wing mass can thus be structured as seen in Equation 10.6

$$L(x) = -\frac{4L}{\pi b} \sqrt{1 - \left(\frac{2x}{b}\right)^2} \quad (10.5)$$

$$W(x) = \int_0^x \rho t_{shell} p(c(x)) dx \quad (10.6)$$

The visualisation of these loads can be seen in Figure 10.2. Based on this, the shear force and moment force can be found, using Equation 10.7

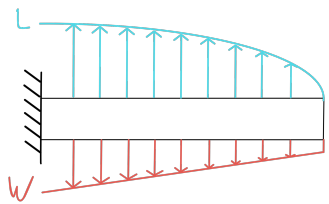
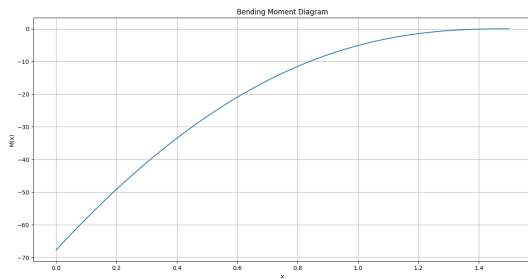


**Figure 10.2:** Lift and weight distribution

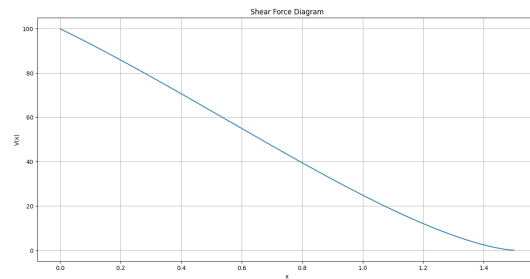
The loads on the wing can be seen in Figure 10.3

$$V = \int w dx$$

$$M = \int \int w dx^2 \quad (10.7)$$



**(a)** Bending moment on the main wing



**(b)** Shear force on the main wing

**Figure 10.3:** Bending moment and shear force on the wing

Due to these loads, shear stresses and normal stresses are introduced. The shear stress is given by Equation 10.2. Which is calculated based on the shear stress,  $V$ , the first ( $Q$ ) and second ( $I$ ) moment of area, and the thickness  $t$  of the structure in the load direction. The normal stress due to the bending moment is given by Equation 10.1, based on the maximum distance of the airfoil from the neutral axis  $y$ . Additionally, a torsion force acts on the wing due to the pitching moment. It is not possible to model the pitching moment along the wingspan, therefore it is assumed the pitching moment acts equally on the whole wing. The shear stress introduced by torsion is given by Equation 10.3. The maximum stresses in the wing due to aerodynamic loads are thus 13.2 [MPa] normal stress and 1.7 [MPa] of shear stress.

## 10.4. Tail Structure

The most important loads the tail structure will be subjected to are considered below to find the critical load and size of the tail structure. Firstly, the aerodynamic, hydrodynamic and impact loads on the tail as a whole will be analysed. Secondly, the bending loads on the circular shaft that supports the propellers are analysed. These are the consequence of thrust and diving impact.

## Loads on the Tail Shell

It is assumed that the tail will be a shell structure with a thickness of 0.001 [m], without additional structural elements. If the strength of the structure turns out to be insufficient, additional structural elements can be added. The tail is modelled as a cantilevered beam. The cross-section is simplified to a thin-walled rectangular beam for the calculations.

The main aerodynamic load on the tail planes will be the lift. The lift was calculated taking into account the large dihedral angle of the inverted Y-tail. The lift on each of the tailplanes is equal to 7.5 [N] in air and 63 [N] underwater in cruise conditions. The lift is assumed to be constantly distributed over the tail surface.

Next to the lift, the impact load will be of importance when sizing the tail. Following the calculations in Section 6.5 the impact force at the moment that the tail hits the water is equal to 800 [N]. This load is assumed to be equally distributed along the three leading edges of the Puffin hitting the water. The two load cases and the tail's simplified cross-section are shown in Figure 10.4.

As the lift underwater is higher than the one in the air, only that case will be looked at in terms of aerodynamic loads. The maximum normal stress and shear stress the tail will experience are calculated with the following formulas:

$$\sigma_{z,max} = \frac{M_{max}y_{max}}{I_{xx}} \quad (10.8)$$

$$\tau_{max} = \frac{V_{max}h^2}{8I_{xx}} \quad (10.9)$$

The resultant normal and shear stresses due to aerodynamic forces are 11.8 [MPa] and 0.3 [MPa] respectively.

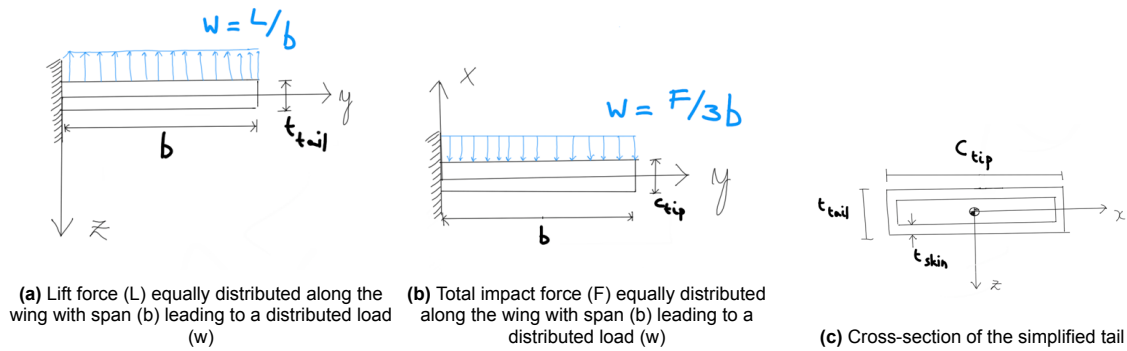


**Figure 10.4:** Simplified model of the tail being subjected to aerodynamic and impact forces and its cross-section used for determining the internal stresses

In a similar fashion, the impact loads on the tail structure can be calculated. The model assumes that the leading edges of the three tails strike the water surface all at once. This leads to a constant distributed load of 889 [N/m]. In the same way as was done for the aerodynamic loads, using  $I_{zz}$  instead of  $I_{xx}$  the maximum normal and shear stresses were calculated to be 5.7 [MPa] and 1.2 [MPa] respectively.

## Shaft Bending

Each of the thrusters will produce at most 50 [N] of thrust during operation. This will induce a bending moment and normal stresses in the shaft where the motor is mounted on. However, the force each thruster experiences during impact is around 120 [N]. The second case is hence the limiting one. The structural element in the tail carrying the thrusters is sized to carry those loads. The tube is a thin-walled circular rod.

Constrained by the thickness of the airfoil, the rod can have an outer diameter of 0.01 [m]. The maximum moment occurs at the root of the rod and is equal to 45.6 [Nm]. Using Equation 10.8, the maximum normal stress in the rod was calculated to be 580.6 [MPa]. A safety margin of 1.5 still has to be applied.

## 10.5. Take-off and Landing Structure

No additional structural elements have to be foreseen for take-off. The Puffin is launched with a customized carriage on which it simply rests. However, the launch loads need to be considered. During the launch, the puffin is accelerated at 40 [ $m/s^2$ ]. With its 13.8 [kg], this means that it has to withstand a launch force of 552 [N]. The carrier applies the launch loads on the fuselage structure. This force is still lower than the 1666 [N] of impact loads and will hence not be driving for the fuselage structural design.

## 10.6. Material selection

The Puffin's structure will be made out of recycled carbon fibre-reinforced polymer (CFRP). Table 10.2 below list some specifications of the material:

**Table 10.2:** List of characteristics of the recycled carbon fibre-reinforced polymer that will be used for the Puffin's structure

Characteristic	Value
Density [ $kg/m^3$ ]	1300
Young's modulus [GPa]	52
Tensile Strength [MPa]	3900
Shear strength [MPa]	115
Compressive strength [MPa]	410

The fuselage structure experiences maximum shear and normal stresses of 4.8 [MPa] and 303 [MPa] respectively. The wing experiences maximum shear and normal stresses of 1.7 [MPa] and 13.2 [MPa] respectively, whereas these are 1.2[MPa] and 11.8 [MPa] for the tail. Finally, the maximum normal stress the shaft experiences is 870 [MPa].

All these stresses are more significantly lower than the ultimate strength of the recycled CFRP. Hence, the material can be used for this application and might even seem overdesigned in terms of load-carrying capacity. However, as CFRP is very corrosion-resistant and light, it is very suited as a material for the Puffin.

## 10.7. Verification and Validation

Pytests were used to verify the code that was written to size the Puffin's structures. Furthermore, several input parameters were varied to analyse if they would influence the output values in a logical way. Next to the code, the main structural requirements have to be verified. Methods for doing this are established in Table 10.3 below.

**Table 10.3:** Verification methods for the relevant requirements of the structures. D: Demonstration, A: Analysis, I: Inspection, T: test

Requirement	Verification Description	Method
STR-FUS-01, STR-WI-03, STR-TAIL-02, STR-TAIL-03	Set up a simulation or a finite element analysis to simulate the applied loads. Eventually, test structural parts by letting them dive into a pool.	A, T
STR-FUS-02, STR-WI-01, STR-WI-02, STR-TAIL-01	Mount the structural elements or scaled versions of the elements to a testing machine and apply the maximum loads.	T
SYS-STR-04	Perform an analysis based on knowledge of the behaviour of CFRP in salt water.	A
SYS-STR-04	Put samples of the used material in salt water, investigate degradation rate and extrapolate.	T, A

**Validation** Several prototypes or scaled versions of the Puffin, or of the structural elements separately could be made and tested. Wind tunnel experiments, as well as experiments in a bath, can validate the structure's performance under aerodynamic and hydrodynamic loads. The prototype can be launched with a catapult and thrown in a bath or pool to validate if it can survive the manoeuvres.

# 11 Flight & Helm Control

The Flight & Helm Control system is responsible for the control of the vehicle. It has to analyse the information gathered from the sensors available on the vehicle and make decisions based on the result of this analysis. Then it needs to calculate actions that need to happen based upon these decisions and send commands to

the relevant actuators. The sensor processing is elaborated further with a simulation of the sensors in an underwater environment.

### 11.1. Requirements and Assumptions

From the previous design steps, the following assumptions are made to design the control system.

- The vehicle will have a sonar and camera sensor for navigation and monitoring.
- The vehicle will have a GNSS and IMU sensor for navigating.
- The turbidity is such that a camera's horizontal visibility is at least 1 [m].

From other subsystems, Table 11.1 and 11.2 shows the requirements imposed on the control subsystem.

**Table 11.1:** Flight & Helm Control Incoming Requirements Table. It shows the requirements for the control system imposed by other systems.

ID	Description	Traceability	Rationale
CTRL-ACT-01	The flight control system shall issue commands to actuators		
CTRL-ACT-02	The flight control system shall compute the required commands to follow the mission path		
CTRL-POS-03	The system shall be able to maintain its position relative to the seaweed system with precision of 0.5 [m]	Need to stay within sensor range	
CTRL-SEN-01	The flight control system shall autonomously determine a suitable landing position for the air-to-water transition		
CTRL-SEN-02	The flight control system shall autonomously determine its required flight path from all available sensor and surrounding information while in the air		
CTRL-SEN-03	The flight control system shall process all available sensor information onboard		
CTRL-SEN-04	The helm control system shall determine the path of the vehicle to the target underwater		
DET-ATT-01	The system shall be able to determine its attitude in an aerodynamic environment	CTRL-ATT-01	Control requires some assertion of system state (estimated or measured)
DET-ATT-02	The system shall be able to determine its attitude in a maritime environment	CTRL-ATT-02	Control requires some assertion of system state (estimated or measured)
DET-ATT-03	The system shall have a attitude determination accuracy of 0.1 degrees while underwater	Determines how accurate the monitoring readings should be need to be accurate for sensor tagging	
DET-POS-01	The system shall be able to determine its position in an aerodynamic environment	CTRL-POS-01	Control requires some assertion of system state (estimated or measured)

Continued on next page



Flight &amp; Helm Control Incoming Requirements Table 11.1 – continued from previous page

ID	Description	Traceability	Rationale
DET-POS-02	The system shall be able to determine its position in a maritime environment	CTRL-POS-02	Control requires some assertion of system state (estimated or measured)
DET-POS-03	The system shall be able to determine when it is at the surface of the water	To know when communication is possible	
DET-POS-04	The position of the system with respect to the entire seaweed unit shall be known with precision of 1 [m]	Need to be able to find unit again. This is just the position wrt the general position unit, not the net during monitoring.	
DET-POS-05	The system shall be able to determine its depth with 0.01 [m] accuracy while underwater	For position tagging of the scan data	
DET-POS-06	The system shall determine its position relative to the seaweed net with 0.01 m accuracy while underwater	For position tagging of the scan data	
DET-POS-07	The system shall determine its position up to 10 [m] while underwater	Depth perception is important for navigation and ensuring the navigation is proceeding along the right pathway	
OPR-NAV-05	The system shall execute an emergency procedure with direct communication with the base.		
PLD-INS-03-01	The system shall be able to attain any roll angle with an accuracy of 0.1 [degrees]	From PLD instrument options	PLD options require pointing
PLD-INS-03-02	The system shall be able to attain any pitch angle with an accuracy of 1 [degrees]	From PLD instrument options	PLD options require pointing
PLD-INS-03-03	The system shall be able to attain any heading angle with an accuracy of 1 [degrees]	From PLD instrument options	PLD options require pointing
PLD-INS-04-01	The system shall approach a structural element to within 0.5 [m]	From PLD instrument options	PLD options have specific range requirements
PLD-INS-04-02	The system shall follow the seaweed unit within 5 [m]	From PLD instrument options	PLD options have specific range requirements
PLD-INS-05	The system shall accommodate the submersion of water quality monitoring instrumentation to a depth of 5 [m]	From PLD-WTR-05-04 instrument options	Water quality must be measured at depth, WTR-05-04 cannot be measured without submersion
PLD-INS-08	The system shall be able to carry out measurements at a depth of 5 [m].		
SUS-ECO-03	The system shall operate autonomously during the navigation and monitoring phases	From discussion	A full-time operator falls outside the given budget

Continued on next page

Flight & Helm Control Incoming Requirements Table 11.1 – continued from previous page

ID	Description	Traceability	Rationale
SUS-ENV-02	The system shall be retrievable in case of a malfunction during mission operation	From the TSC	Defining constraint, limit pollution
SUS-ENV-02-02	The system shall receive information during the navigation phase	Ensure SUS-OPS-02	See traceability
CTRL-ATT-01	The system attitude shall be controllable in an unstable aerodynamic environment	From OPR-ENV-03, with OPR-ENV-01	Necessary to ensure collision avoidance in the operating conditions
CTRL-ATT-02	The system attitude shall be controllable in an unstable maritime environment	From OPR-ENV-03 and OPR-ENV-02, with OPR-ENV-01	Necessary to ensure collision avoidance in the operating conditions
CTRL-POS-01	The system position shall be controllable in an unstable aerodynamic environment	From OPR-ENV-03, with OPR-ENV-01	Necessary to ensure collision avoidance in the operating conditions
CTRL-POS-02	The system position shall be controllable in an unstable maritime environment	From OPR-ENV-03 and OPR-ENV-02, with OPR-ENV-01	Necessary to ensure collision avoidance in the operating conditions

**Table 11.2:** Flight & Helm Control Outgoing Requirements Table. It shows the requirements the control system imposes on other systems.

ID	Description	Traceability	Rationale
CTRL-ATT-08	The system shall be able to attain an angular velocity of up to TBD for rolling while underwater	This will allow for determining how quickly the system can change direction or, in an emergency situation, how to escape quickly	
CTRL-ATT-09	The system shall be able to attain an angular velocity of up to TBD for yawing while underwater	This will allow for determining how quickly the system can change direction or, in an emergency situation, how to escape quickly	
CTRL-ATT-15	The system shall be able to attain an angular velocity of up to TBD for pitching while underwater	This will allow for determining how quickly the system can change direction or, in an emergency situation, how to escape quickly	
CTRL-02	The system shall be able to deliver 25 [W] to the control system	There needs to be a minimum power deliverable to the payload to allow it to navigate.	
CTRL-ACT-03	The position during cruise shall be communicated to the control centre		

Continued on next page

Flight &amp; Helm Control Outgoing Requirements Table 11.2 – continued from previous page

ID	Description	Traceability	Rationale
SUS-ENV-02-01	The system shall transmit location and status information during the navigation phase	Requirement to ensure the system can be located to facilitate SUS-OPS-02	See traceability

## 11.2. Sensor Processing

While submerged, the control system cannot make use of GNSS as it does while airborne. Sonar, IMU, and camera sensors as must inform state determination. The processing of the sonar and camera sensor data for this purpose is explored in this section. GNSS and IMU sensor data processing is assumed to be available as a COTS package.

### 11.2.1. Sensors on the Vehicle

In the design, sonar is the key sensor used in navigation underwater. It creates a depth map of the area in front of it by sending out sound signals and measuring the time it takes for them to return. After the analysis of the signal, the vehicle shall be able to recognize the seaweed system in front of the sonar. Sonar will be mostly used for reorientation, seaweed monitoring and Travel to the next system stages as stated in Section 4.2. Travel to the next system and reorientation require a front-facing sonar and the seaweed monitoring requires an upwards-facing sonar. The weight of two sonars would though significantly complicate the design, therefore a decision was made to angle the sonar at 45[°] in order for it to be used for both applications. It does not make seaweed monitoring more problematic. Travel to the next system and reorientation will though necessitate that the vehicle pitches down to recognize what is 'in front of it'.

The sonar chosen for the vehicle is Tritech Gemini 1200ik sonar<sup>1</sup>. It has a field of view of 120 [degrees] in its horizontal plane and 20 [degrees] vertically. Its effective resolution is 0.12[°] and the update rate is between 5 and 65[Hz].

Next to the sonar sensor, two cameras will be used, one facing 45[°] upwards and one 45[°] downwards. The downward-facing camera will be primarily used for navigation during flight, most importantly for the seaweed system and landing zone recognition. The upward-facing camera will be primarily used while underwater, most importantly for structural element recognition and data recording.

Both sonar and camera will be used to scan the seaweed to analyse its growth.

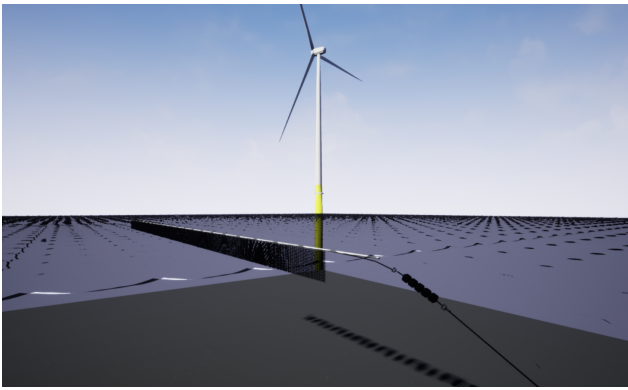
### 11.2.2. Premise of the Simulation

When designing the approach to sensing of the vehicle multiple unknowns emerged, related to underwater navigation and sensing. The critical ones are listed below.

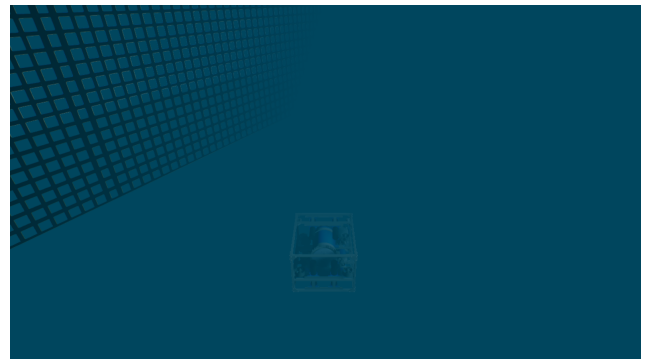
1. **Sonar for navigation** - Usage of sonar for various applications in navigation has been demonstrated before [49]. During the design considerations, it was not clear though whether it would be suitable when navigating with respect to the seaweed system. Most importantly when navigating under the seaweed system in seaweed monitoring but also when approaching the seaweed system from the side travel to the next system and reorientation as stated in Section 4.2. An algorithm to recognise the seaweed system in the sonar data will thus be developed.
2. **Camera for the structural element recognition** - The camera is the main mean of navigation underwater at close distances, where the sonar resolution is insufficient. It is used for taking images of the structural elements, but also for navigating to them. It can be used from a distance of 5m to 1m, depending on the turbidity of the water. It is though uncertain, with what tools and to what extent the camera can be used to recognise the structural elements. An algorithm to recognise the structural elements in the sonar data will thus be developed.
3. **Use of sonar and camera to navigate under the seaweed system** - Once the sonar and camera data are obtained and analysed is still is uncertain if they would be sufficient to navigate successfully. An algorithm to navigate under the seaweed system to the structural element will thus be developed.

The uncertainty in the design decisions above was why a proof of concept was needed. To demonstrate that, a Hovering AUV configuration with sonar was tested in simulation software.

<sup>1</sup>TriTech Gemini 1200ik



(a) The environment seen from the air.



(b) The environment seen from underwater, with the turbidity simulation and the example ROV.

**Figure 11.1:** The environment used for the simulations, made in Blender and Unreal Engine 4. It contains a part of a seaweed farm unit and an anchor line with structural elements that can be inspected.

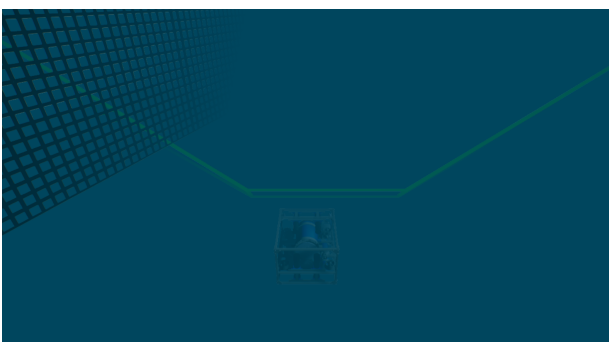
### 11.2.3. Simulation in HoloOcean

To simulate the sonar and camera sensor in a relevant underwater environment, the HoloOcean software package [50] was used. This software is based on HoloDeck, serving to simulate underwater ROV sensor data collection and dynamics. HoloDeck is configured by combining Unreal Engine 4 <sup>1</sup>, a general-purpose game engine, handling graphics and physics, and Python, handling the setup of environments and data collection. The Unreal Engine part is pre-compiled and has an environment that the ROVs can move around in. To make the simulation suitable to our case, a custom environment was made. This environment consists of a part of a seaweed farm unit with an anchor line. The net part of the unit is used to test the navigation part and the anchor line is used to test the inspection of the structural elements. This environment was made in Blender<sup>2</sup> and Unreal Engine. This environment can be seen in Figure 11.1. The simulation is run at 60 ticks per second.

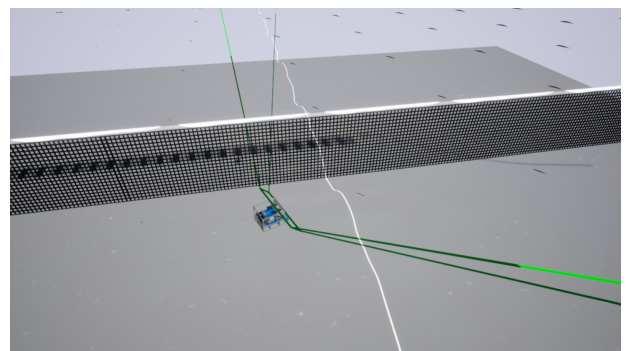
In the simulation software, a configurable UAV with sonar and camera sensors is already implemented. This UAV has a hovering design, that has 8 thrusters giving it 6 degrees of freedom. This is not the same design as the Puffin, but it is still suitable for use in our tests, since it is used as a position-able platform for the sensors, and the vehicle dynamics are not yet considered. The sonar and camera sensors are configured to match the placement and orientation of the Puffin. For the camera, a simple turbidity simulation was created, where the distance to the camera decided the visibility of the object in accordance with earlier assumptions.

### Results of the Sonar Sensor

The aim of this investigation is to assess how feasible it is to use sonar for navigation under a seaweed system. To do that, sonar scans are taken from a representative manoeuvre, which is a drone passing under the seaweed system at an angle of 30 [degrees]. Each level of filtering uses the same sonar data 'image'. The set-up can be seen in Figure 11.2.



(a) View from the water, with the green lines outlining the field of view of the sonar



(b) View from above water, with the green lines outlining the field of view of the sonar

**Figure 11.2:** UAV Passing under the seaweed system

<sup>1</sup>Unreal Engine

<sup>2</sup>Blender

The Gemini sonar has a field of view of  $120^\circ$  and an angular resolution of  $0.12^\circ$  and so 1000 distance data points are created. To allow for a smoother simulation, the simulated sonar is run at 300 data points and 1Hz. The data provided by the sonar is an array of values where every column contains values of intensities of reflected signals along a distance of the sonar's range. The process of analysing the sonar data is visualised in Figure 11.3 and elaborated in the rest of the subsection.

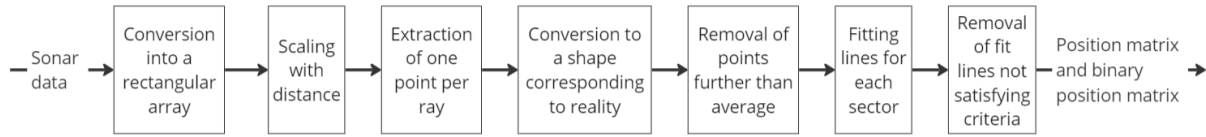


Figure 11.3: The diagram of sonar data filtering and analysis

**Conversion into a Rectangular Array** The data received is 'fan'-shaped as it is formed of straight rays of the same length, originating from the same point. However, the array of data provided by the sonar is received as a rectangular shape. It thus has to be converted to provide a realistic image of what is in front of it, otherwise, it is distorted as can be seen in Figure 11.4. Before that happens though, one useful point per ray has to be extracted.

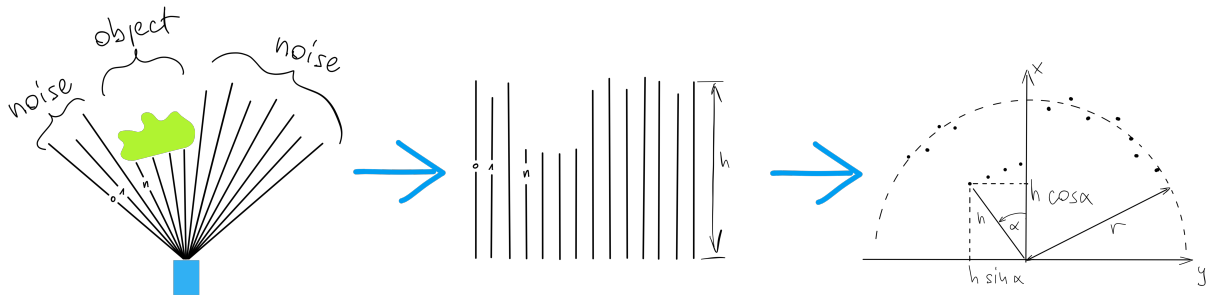


Figure 11.4: Conversion of the sonar data from rectangular to corresponding to reality

That is done because ideally, the only thing visible in the sonar image would be the object in front of it. That unfortunately is not the case. Sonar images suffer from noise due to reflections and scattering making it not trivial to distinguish between noise and the actual objects. Therefore the first step for finding the seaweed system is filtering the sonar data. For every sonar ray, only the first point of reflection is useful, as any points behind it cannot realistically provide information as they come from noise. A ray cannot be reflected from two objects, one behind the other when travelling in a straight, radial path from an emitter and back.

**Scaling with Distance** Due to reflections though, the further from the origin, the more noise there is. There thus has to be some method implemented to distinguish between the rays actually reflected from objects and noise. The primary task of the sonar is to allow for navigation along a seaweed system, within a 5m range of the seaweed system. The noise of the sonar is relatively low at ranges below 20m. It was therefore found promising to scale the brightness of the sonar data pixels with the distance from the origin (which coincides with the sonar), the closer to the origin, the higher the scaling factor. Multiple scaling formulas were tried and can be seen in Figure 11.7. With  $q$  denoting magnitude of the received sonar signal,  $h$  range from the origin,  $r$  max sonar range and  $i$  intensity and scaling factors  $a$ ,  $b$ , the formula describing the magnitude is:

$$q = (r - h)^a \cdot i^b \quad (11.1)$$

The data is from a case where the vehicle passes under the seaweed system, 4 [m] below the water surface.



Figure 11.5: Filtered sonar data

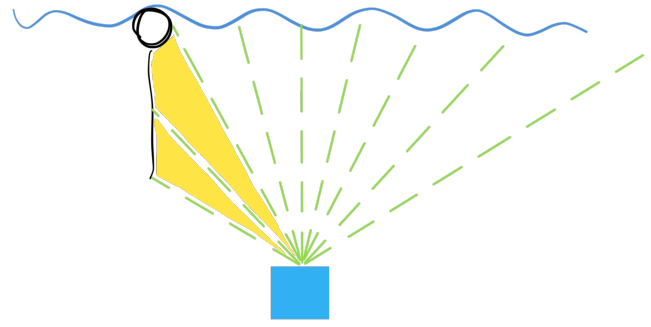
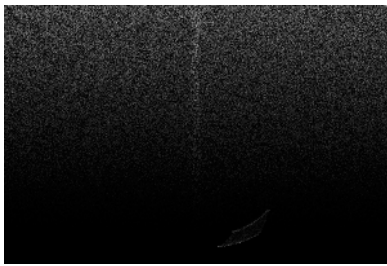
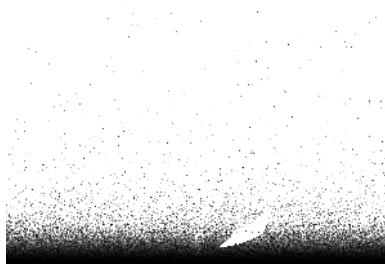


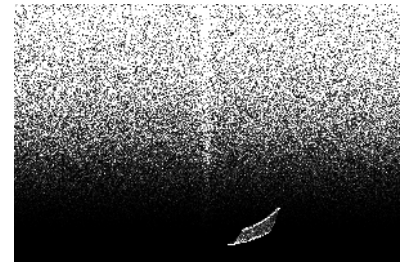
Figure 11.6: Sonar field of view split into sectors, with yellow zones delimiting the sectors in which a satisfying line fit is found



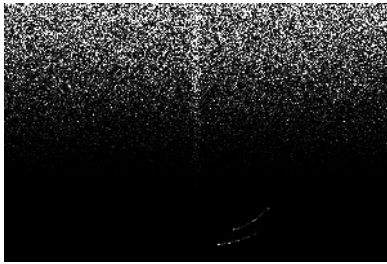
(a) original data



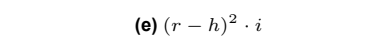
(b)  $(r - h) \cdot i$



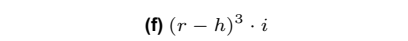
(c)  $(r - h) \cdot i^2$



(d)  $(r - h) \cdot i^3$



(e)  $(r - h)^2 \cdot i$



(f)  $(r - h)^3 \cdot i$

Figure 11.7: Sonar data with different scaling formulas applied.

In the original image, the object is barely visible. After applying  $(r - h) \cdot i$ , it becomes much more apparent but also blends with the noise that gets much brighter. For  $(r - h) \cdot i^2$ , the object is also quite pronounced and the noise moves back. With  $(r - h) \cdot i^3$ , the noise moves back even further but the object is hardly visible. For  $(r - h)^2 \cdot i$  and  $(r - h)^3 \cdot i$ , the noise takes up nearly all of the field of view.  $(r - h) \cdot i^2$  is chosen as the scaling formula as then, the object is most distinguishable from the noise.

**Extraction of One Point per Ray.** Once the filtering is applied to the whole image, the pixels meaningful for the analysis have to be extracted. That is done using the fact that for every ray, only the pixel closest to the origin provides useful information, unless it is coming from noise. Either way, pixels closest to the origin above some brightness have to be extracted. A threshold brightness is manually chosen such that the meaningful pixels are extracted. The resultant image can be seen in Figure 11.5. The pixels describing the seaweed system can be easily distinguished. For it to be usable, a recognition algorithm has to be implemented.

**Conversion to Shape Corresponding to Reality** Before that can be done, the image has to be converted from the array of 'parallel rays' into the geometry corresponding to reality Figure 11.4. This is done with the field of view angle of the sonar  $\Theta$ , total number of rays  $[N]$  and which in turn a given ray is  $n$ . The angle at which a ray is  $\alpha$  from the x-axis of the vehicle is then given by:

$$\alpha = \frac{n}{N} \Theta \quad (11.2)$$

Once that is repeated for every ray, the array of points takes a shape representative of reality and can be seen in Figure 11.8a.



**Removal of Points further away than Average** In Figure 11.5 it can be seen that the points belonging to an object are closer to the origin than a belt/cloud of points originating from noise. Further filtering can thus be carried out by calculating an average distance of the points and removing all points further away than that average. The result can be seen in Figure 11.8b Such an approach runs a risk of removing points belonging to an object if it takes up a large part of the field of view. Such a case is most likely to occur when the vehicle is facing the system perpendicularly and in such a case the remaining points should be enough to navigate reasonably.

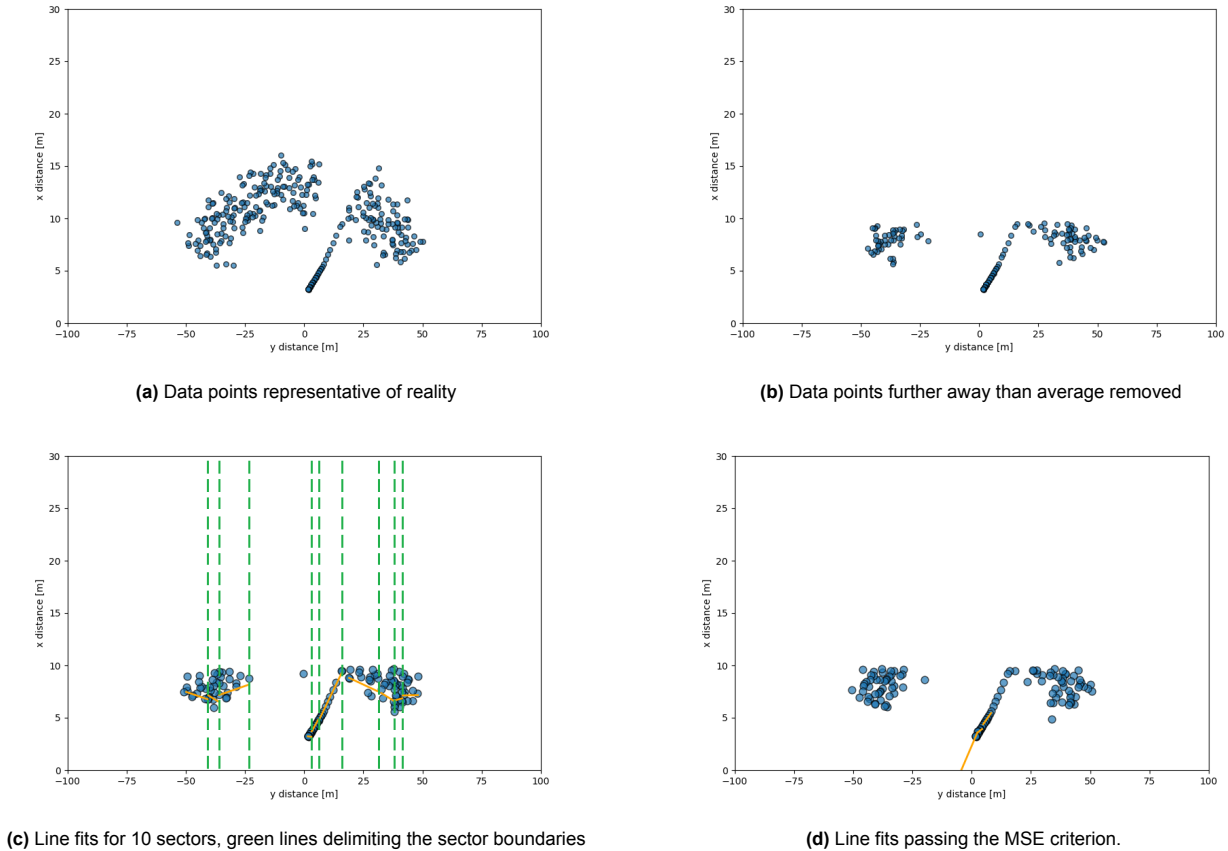


**Figure 11.8:** Steps of filtering of the sonar data representative of reality

**Fitting Lines for each Sector** To be able to use the sonar information, points corresponding to an object have to be determined. As the seaweed system is a plane, its image in sonar data shall resemble a line. Recognition of a seaweed system is therefore done by means of fitting a line to the sonar data points and can be seen in Figure 11.8. A decision on whether they belong to an object is done by measuring the Mean Squared Error (MSE) of the fit.

Fitting a line to all data points makes sense when an object occupies the whole field of view. It is though not enough when it occupies only a small part. Furthermore information such as 'the object runs from the left of the field of view to the middle and ends abruptly', is very important for navigation. To accommodate such situations, the field of view is split into an arbitrary amount of sectors the fit line is calculated separately for each sector. The case of 10 sectors, can be seen in Figure 11.8c and in Figure 11.6.

**Removal of Fit Lines not satisfying Criteria** Not all of the fit lines provide meaningful information, so an MSE criterion was established. If the MSE of the fit line is below the criterion, it is displayed. For a criterion of MSE of 0.01, Figure 11.8d is created. For lines passing the MSE criterion, its middle point is calculated and returned in a position matrix. Every value in the position matrix corresponds to the distance from the observed seaweed system. Additionally, a binary position matrix is created of length the same as the number of sectors. Each value in the matrix is a 0 or a 1, describing whether a seaweed system has been recognized in the sonar view.

For Figure 11.8d the position matrix is: [0. 0. 0. 1.84541473 1.93314016 1.72374915 0. 0. 0. 0.], while the binary position matrix is: [0. 0. 0. 1. 1. 1. 0. 0. 0. 0.]



To give an idea of the sonar data in time, in Figure 11.9 the images produced when the vehicle passes under a seaweed system can be seen. It begins 1m to the side of the seaweed system, at depth of 4 [m], at an angle of  $30^\circ$  to the seaweed system.

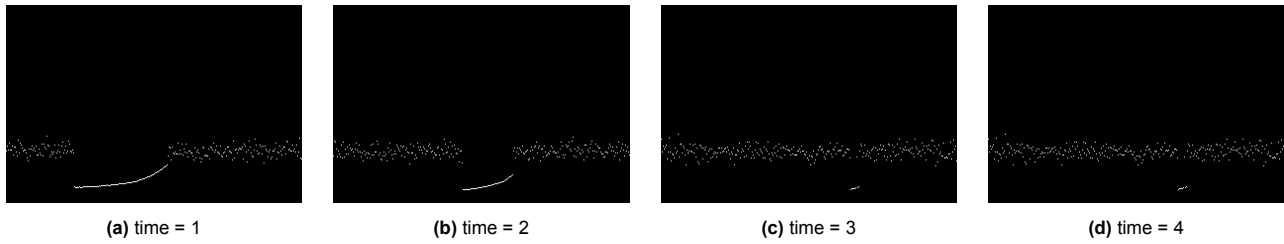


**Figure 11.9:** The sonar data as the vehicle passes under a seaweed system

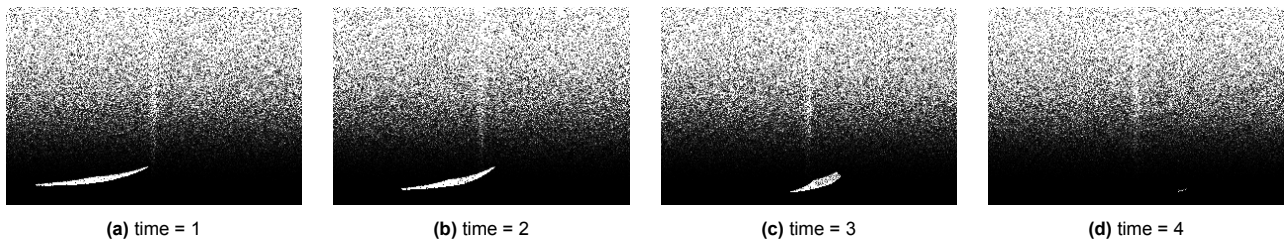


**Figure 11.10:** Filtered data as the vehicle passes under a seaweed system

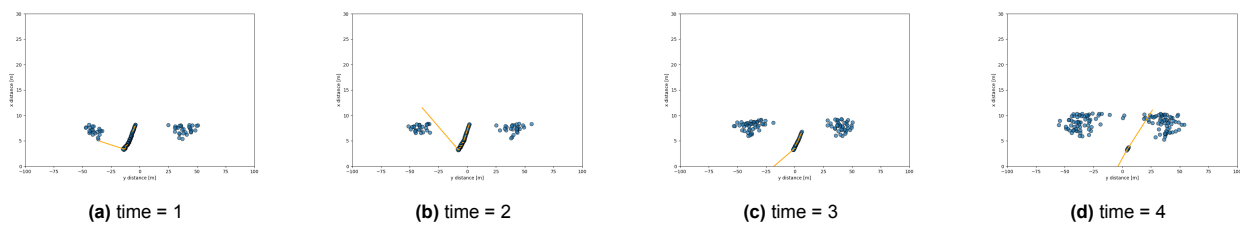


**Figure 11.11:** Fitted data as the vehicle passes under a seaweed system

**Noise Considerations** To better understand the robustness of the application, more noise was introduced to the simulation. HoloOcean, offers a parameter *MultSigma*, which is a factor of multiplication of the standard deviation of the noise that is distributed normally.

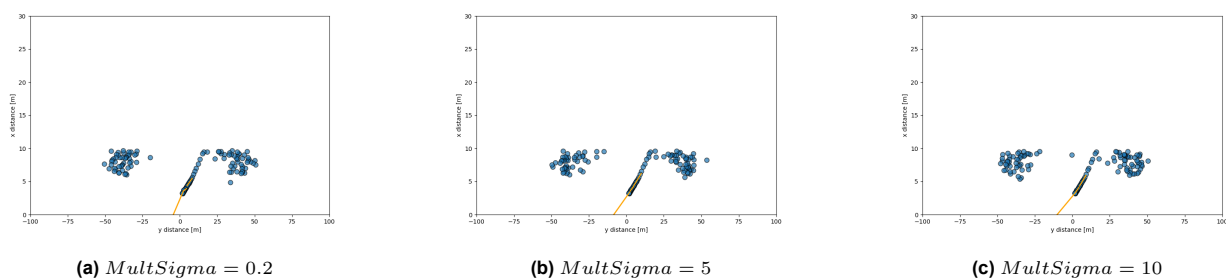


**Figure 11.12:** Line fits at different noise levels

The results of varying *MultSigma* can be seen in Figure 11.12. It can be seen that even for a factor of 10, the line fit is similar to the one for *MultSigma* of 0.2, hinting at high robustness of the method.

**Discussion** The proposed solution is able to suggest areas of sonar data as an object in front of the sonar. Given a relatively low data needs of a line follower robot, the results are deemed satisfying for application in the Puffin.

Potential improvements could include dynamically changing parameters such as the threshold pixel brightness such that the MSE value is minimised. Furthermore, how the image changes over time could be analysed to offer more information. A more refined analysis of the sonar data that can estimate the exact position and orientation of the seaweed unit could be implemented in future work and provide valuable data for an advanced navigation system.

### Results of the Camera Sensor

The second primary sensor used for underwater navigation is the camera. Its main task is the recognition of the structural elements and providing data for navigating to them. The degree to which a camera could be used for underwater navigation and how it would behave was though unknown. It was thus decided to simulate the camera underwater. To simulate visual conditions at Borssele, a simple turbidity simulation was created, where the distance to the camera decided the visibility of the object in accordance with earlier assumptions. Gaussian noise was added on top of that to further complicate the image.

The example images taken by the camera of the seaweed system can be seen in Figure 11.13. Images of the structural elements can be seen in Figure 11.14. Both are taken at a distance of 2 [m] and depth of 1.5 [m].

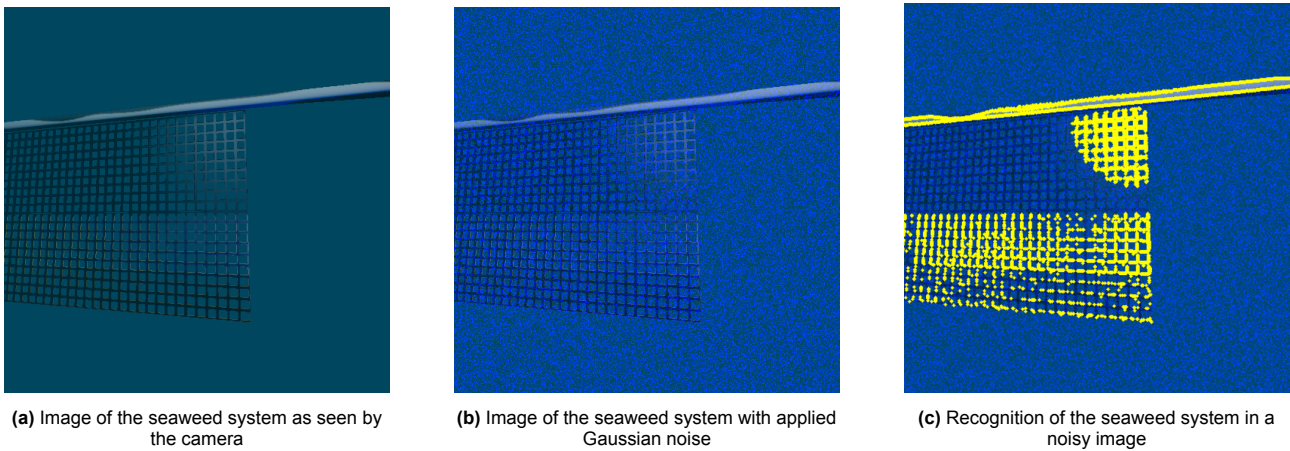


**Figure 11.13:** Image analysis of the seaweed system

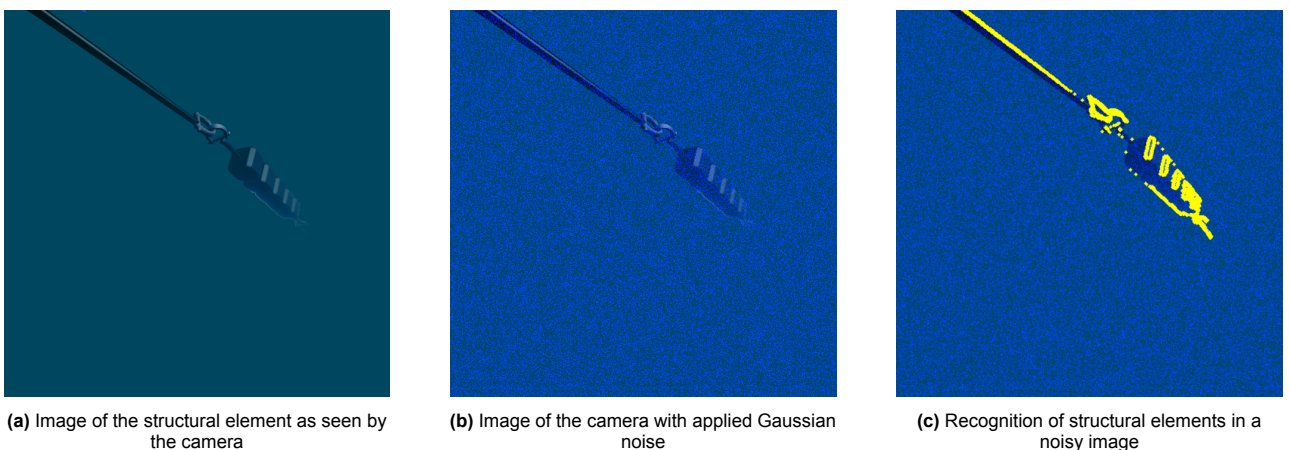


**Figure 11.14:** Image analysis of the structural elements

In order to extract useful information from the images, image processing was used. The visualisation of the process can be seen in Figure 11.15

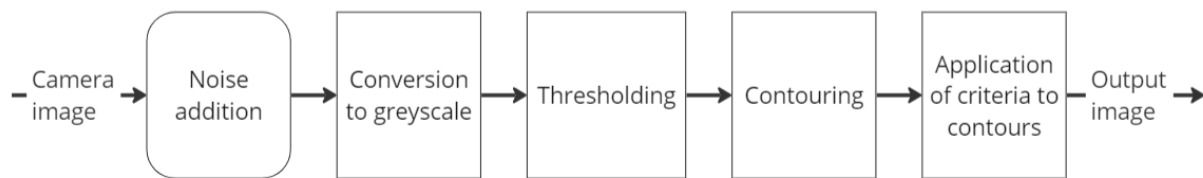


**Figure 11.15:** The diagram of camera data filtering

**Filtering** Figure 11.13a and Figure 11.14a, present images as viewed by the camera. To simulate the turbidity of the water, Gaussian noise was added to the images at mean 0 and standard deviation of 250, the results of which can be seen in and Figure 11.14b.

Then an OpenCV<sup>1</sup> filtering is applied, where first the image is converted to greyscale. after which thresholding is applied to find edges in the image. Then contours are extracted from the list of edges. Finally, a criterion is applied to the contours, such that only contours with more than 4 edges and an area of more than 20 pixels are left. This way images Figure 11.13c and Figure 11.14c are created.

**Noise** To investigate, the robustness of the recognition algorithm, it was tested at noise levels of standard deviation from 100 to 500, with the pixel values between 0 and 255. The results can be seen in Figure 11.16.

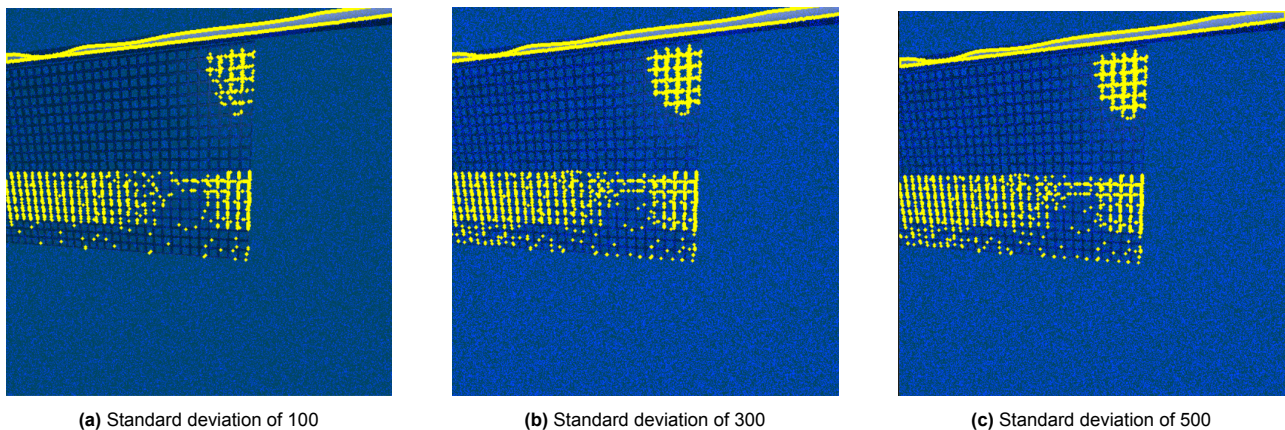


**Figure 11.16:** Varying of the noise standard deviation for an underwater camera

Despite the introduction of quite significant noise, the algorithm is able to recognise the main features of the object in the water quite well

**Discussion** The investigation into using the camera for navigation has given promising results. With the applied distortion, it was possible to recognise the parts of the seaweed system or the structural elements in images using OpenCV. How comparable the applied distortions are to conditions in the Borssele wind park is though unknown. Furthermore, OpenCV by itself does not provide enough capabilities to recognise the structural elements. It would thus be recommended to use an algorithm to the one investigated and incorporate machine learning on top of it to recognise the structural elements of the seaweed system.

#### 11.2.4. Use of Sonar and Camera to Navigate under the Seaweed Unit

**Control** With the sonar and camera data available and analysed, their usage for navigation under the seaweed system can be investigated. The minimum viable product for the case of sailing under the seaweed system is a line-following robot- the UUV shall sail along the system while keeping it in the middle of its field of view. The vehicle begins by sailing parallel to the system, at a depth of 4 [m], 1 [m] to the side of the seaweed system. To simplify the simulation, the vehicle can only be actuated to go to the right or to the left, without attitude change. The depth and forward velocity are kept constant.

To accomplish the task, data from the sonar is used. The field of view is split into 10 sectors. As seen in Figure 11.8, the distances of recognized objects in 10 sectors are returned in a position matrix and binary position matrix.

<sup>1</sup><https://opencv.org>

As the depth is kept constant, only the binary position matrix is used. The first 5 values in the matrix correspond to the objects recognized in the left side of the field of view, while the latter 5 correspond to the right side. For the binary position matrix created in paragraph 11.2.3: [0, 0, 0, 1, 1, 1, 0, 0, 0, 0], in 2 sectors on the left side there was an object recognized and 1 on the right.

The role of the implemented controller is to keep the vehicle as close to the plane of the seaweed system as possible, so decreasing the distance or the imbalance between the sectors recognized to the right and left. The desired state is thus 0. The controller diagram can be seen in Figure 11.17.

For the vehicle to make a decision on where to go, The left part of the field of view is summed and the right part is summed. The right sum is then subtracted from the left. The value obtained describes the confidence that a seaweed system is to the left or to the right. The higher the magnitude of that value, the higher the confidence that the seaweed system is to the left or to the right. That is also the measure of error from the desired state. If the result of subtracting is 0, it is concluded that the system is in the middle of the field of view and no action needs to be taken.

The state of the vehicle is changed by adding or subtracting thrust to the right or left. To translate the confidence into thrust values, proportional and differential blocks are used in the controller. For the proportional block, the higher the confidence, the higher the thrust added. For the differential block, the higher the rate of change of the confidence, the higher the added thrust.

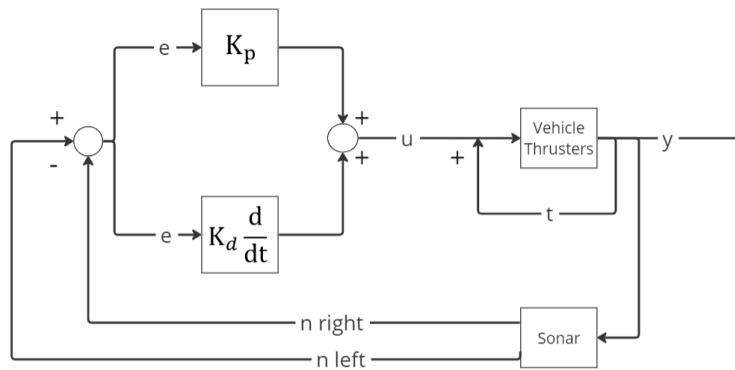


**Figure 11.17:** Control diagram for the seaweed system line following

The variables used in Figure 11.17 are:

- $y$  - output signal: position of the vehicle
- $e$  - error: confidence level that the system is to the right or to the left
- $u$  - control input: thrust value to increase
- $K_p$  - proportional gain
- $K_d$  - differential gain: gain for the rate of change of error
- $t$ : current thrust value
- $n_{right}$ : number of systems recognized in the right part of the field of view
- $n_{left}$ : number of systems recognized in the left part of the field of view

Using gains  $K_p = 7$  and  $K_d = -4$ , the path obtained can be seen in Figure 11.19b. The path does not diverge from the seaweed system, over the course of 15 meters and resembles a sine function. The vehicle remains within 1.5 [m] of the seaweed system plane.

The plot also contains the error data, so confidence levels of whether the system is to the left, right or centre. Every data point describes what is the difference in the number of sectors in which a seaweed system was recognised to the left or to the right. The  $e$ -data is nearly exactly out of phase with the path of the vehicle. This should be the case as when the vehicle is to the right of the seaweed system, it should recognise the system to the left in the sonar data.

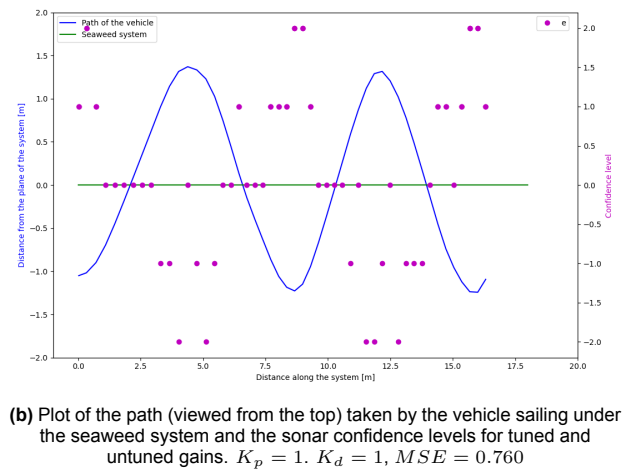
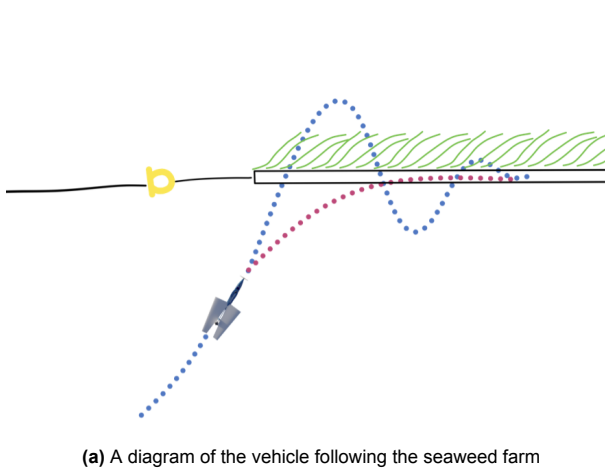


**Figure 11.18:** Diagram and path following for the untuned case

**Gain tuning** The gain chosen for Figure 11.18b were chosen arbitrarily. To estimate the optimal performance of the vehicle in the simulation gain tuning is performed.

A simulation was run for proportional and differential gains in range between -7 and 7, with a step of 1. For each pair of gains, the Mean Squared Error was calculated, as a measure of, on average, how close was the to the seaweed system. The heat map of gains can be seen in Figure 11.19a. The best performance was obtained for gains of  $K_p = 7$ ,  $K_d = -4$ , providing a Mean Squared Error of 0.320, as opposed to 0.760 for the untuned case in Figure 11.18b. The path plot for the tuned case can be seen in Figure 11.19b.

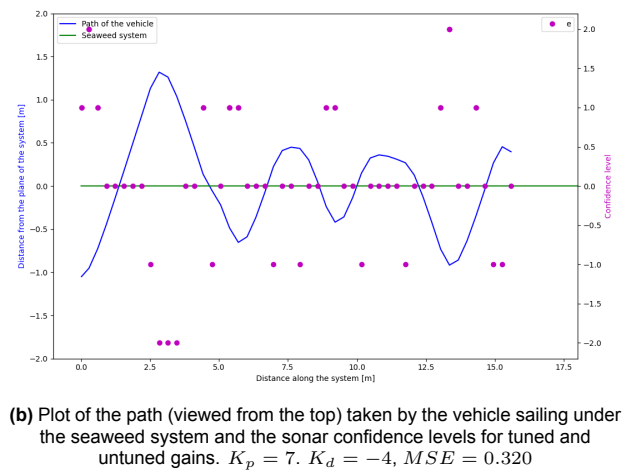
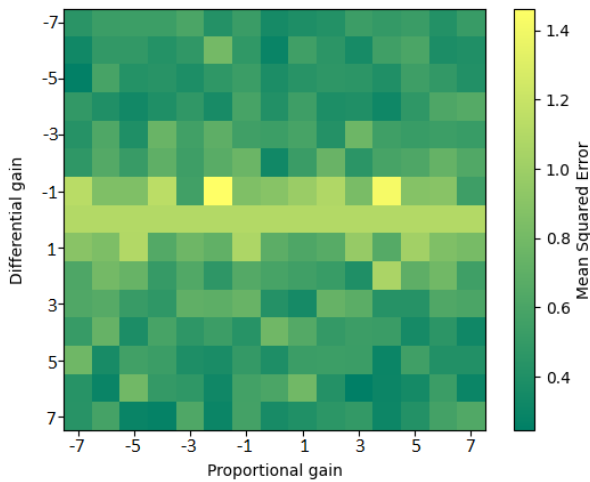


**Figure 11.19:** Heat map of the gain tuning and path following for the tuned case

The gain tuning was performed with a relatively low resolution due to computing time required. The vehicle investigated is also not representative of the Puffin and so any results could not be reused for the final Puffin design. Overall, the vehicle is deemed to follow the path sufficiently well to demonstrate the feasibility of the sonar based navigation.

## Discussion of the Simulation

The aim of the carried-out simulations was the demonstration that the sonar and camera can be used for navigation underwater. It was demonstrated that with the use of sonar and a PD controller, the vehicle shall be capable of sailing underneath the seaweed system.

The conditions in the simulation did not mimic the conditions at Borssele very closely. To provide a better level of validation of navigation with sonar, the simulation should include currents, waves and turbidity of characteristics



similar to the ones at the wind park. Additionally, the vehicle in the simulation is significantly different from the Puffin. To achieve a representative simulation, the model of the Puffin together with all accompanying dynamics should be implemented.

Furthermore, for the final product, a more robust navigation technique would need to be developed. Ideally, using the GNSS data obtained in flight, IMU, sonar, camera and sensor fusion algorithms, the vehicle would be able to determine its position with respect to the seaweed system in 3 dimensions. That would make navigation much more robust but also the vehicle more flexible in terms of applications, increasing the market potential.

### 11.3. Vehicle Dynamics

In Chapter 7 and 8, a configuration of propulsion systems and control surfaces is chosen. In the air, a single propeller on the nose is used in combination with a standard configuration of two ailerons, two elevators and a rudder, with an inverted y-tail. While underwater, the vehicle is propelled by three thrusters on the tips of the tail surfaces, that can be moved in the radial direction. The three tail surfaces are used in a combined manner to generate roll, pitch and yaw control, depending on the attitude of the vehicle.

#### 11.3.1. Dynamics Laws

The vehicle will have 14 command channels to control various parts. These channels range from throttle command to launch jet activation:

- $T_{air}$  Thrust generated by the air propulsion system [0% - 100%]
- $T_1, T_2, T_3$  Thrust generated by the water propulsion system [-100% - 100%]
- $\delta_{a_l}, \delta_{a_r}$  Deflection of the ailerons
- $\delta_1, \delta_2, \delta_3$  Deflection of the tail surfaces according to Figure 11.20
- $\psi_1, \psi_2, \psi_3$  Radial deflection of the water thrusters according to Figure 11.20
- $\theta_{wing}, \theta_{launch}$  Activation of the wing sweep and launch system valves [0,1]

The positive directions of the deflections are shown in Figure 11.20. In Section 7.5, the underwater propeller mechanics have been explored, to show that the thrust vectoring system is able to generate forces in all directions and moments in pitch and yaw. Only for the roll, the control surfaces have to be used underwater. These only work while the vehicle has non-zero velocity. The control surfaces will also be used for pitch and yaw to augment the thrust vectoring system.

### 11.4. Controller Architecture

The control system will read all the sensor data, process it, and calculate the necessary commands to the 14 available command channels. It also needs to command the sensing system to start a measurement. These functions will be performed by a combination of different subsystems. There are multiple options to achieve this functionality, ranging from a complete scratch-build flight controller to a COTS package. The scratch-build system can be adapted completely to our needs and optimised for flight and underwater sailing, but it will be costly to develop. The COTS package will be much cheaper, but the adaptation to our mission will be much harder, if not impossible. For the hardware requirements of the flight controller, there are COTS packages available, like the Pixhawk platform<sup>1</sup>. For the main flight controller, the CUAV Pixhawk V6X<sup>2</sup> is chosen, since it has a powerful processor, has the necessary PWM I/O for all command channels and I/O channels for the sensors. It is also able to communicate over Ethernet, which will be used to communicate with a companion computer for advanced sensor processing and the sonar sensor itself. The firmware and software for the Pixhawk will be adapted for the combined aerial and aquatic mission domains. This is where much of the necessary continued development of the control system is located. A schematic of the wiring of the flight controller can be seen in Figure 11.21.

---

<sup>1</sup>Pixhawk

<sup>2</sup>CUAV Pixhawk V6X

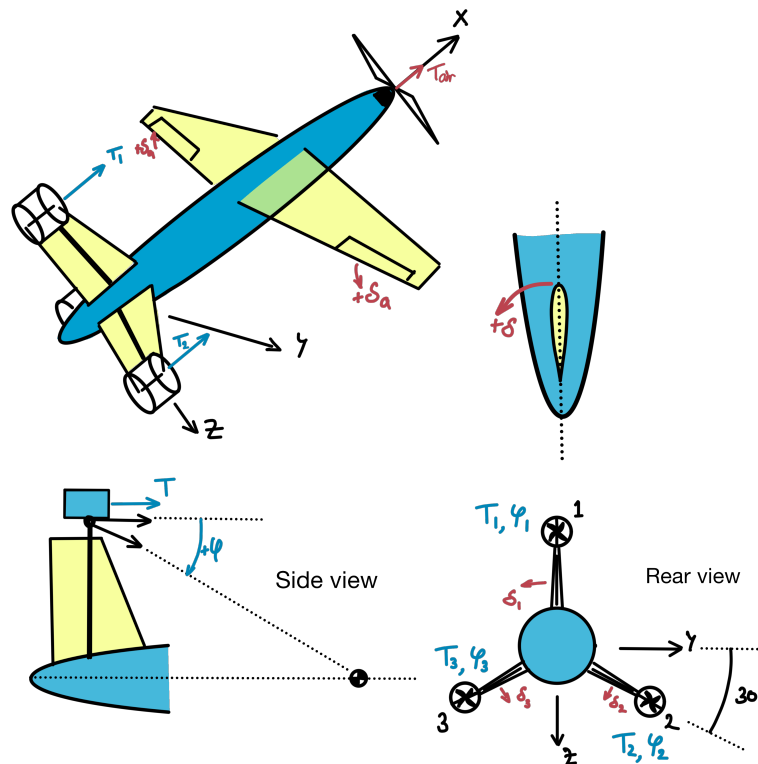


**Figure 11.20:** Axis system and positive direction of the control outputs of the vehicle. There is one main air motor, three water thrusters, ailerons, a combined rudder and elevon system and rotation actuators for the thrusters

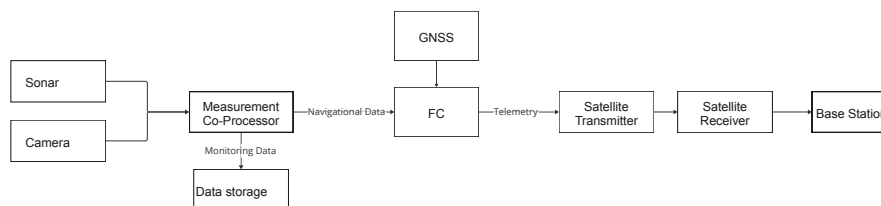


**Figure 11.22:** Communication Flow Diagram

## 11.5. Verification and Validation

The control system will be tested in small-scale, short-distance physical tests at first. When the systems are working according to the specification of the requirements in these tests, these will be scaled until the entire mission distance can be flown and sailed reliably. These tests can be seen in Table 11.3



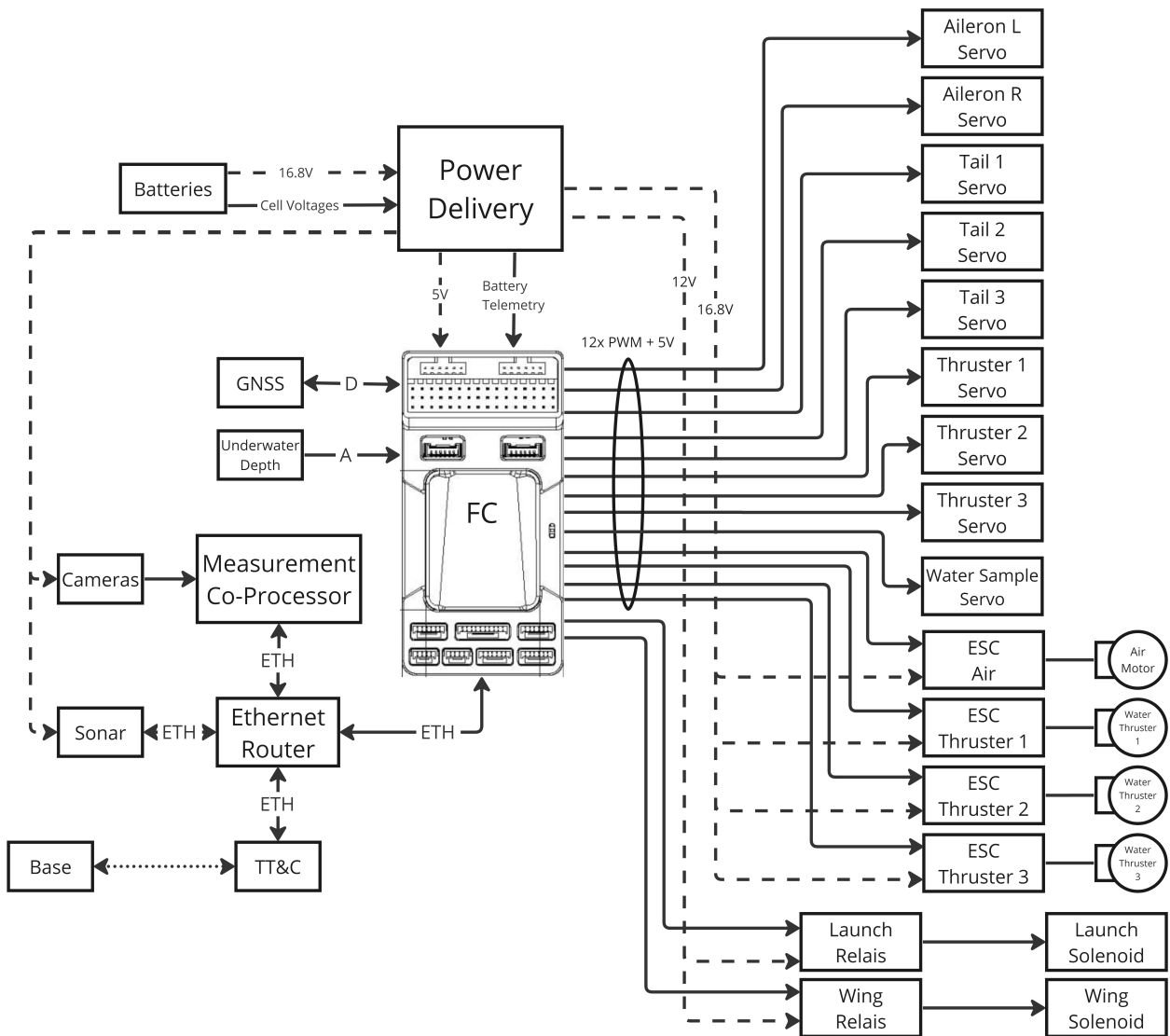


**Figure 11.21:** Electrical Diagram of the Flight and Helm Control system. It shows the Flight Controller (FC) in the centre. It is connected to the Ethernet network, which connects the sonar, measurement companion computer, communications to base, and the FC together. The power delivery system conditions the right voltages for all subsystems from the battery voltage.

**Table 11.3:** Verification methods for the relevant requirements of the flight and helm control system. D: demonstration, A: Analysis, I: Inspection, T: test

Requirement	Verification Description	Method
CTRL-ATT-01, CTRL-POS-01	Short distance unpowered flight test	T
PLD-INS-03-01, PLD-INS-03-02, PLD-INS-03-03	Short distance powered flight test	T
CTRL-ACT-01, CTRL-ACT-02	Long distance powered flight test	T
CTRL-POS-03, CTRL-SEN-01, CTRL-SEN-02, CTRL-SEN-03	Flight navigation test	T
CTRL-SEN-02, DET-ATT-03, DET-POS-01, DET-POS-02, DET-POS-04, DET-POS-05, DET-POS-06, DET-POS-07, SUS-ENV-02-02	Sensor accuracy analysis	A
PLD-INS-05, PLD-INS-08	Water submersion test	T
CTRL-POS-03	Water position hold test	T
CTRL-ACT-02, CTRL-ATT-02, CTRL-POS-02	Underwater travel test	T
CTRL-ATT-02, CTRL-POS-02	Underwater wave and rough environment test	T
CTRL-SEN-04, DET-ATT-02, DET-POS-02, PLD-INS-04-01, PLD-INS-04-02, DET-POS-04	Underwater navigation test	T
CTRL-POS-03, DET-POS-06	Underwater seaweed scanning test	T
PLD-INS-04-01	Underwater structural element scanning test	T
OPR-NAV-05	Underwater Failure test	T
CTRL-01, SUS-ECO-03	Autonomy analysis	A

## 12 Energy

The Energy chapter describes the energy source used to power the vehicle. Section 12.1 describes the requirements relating to the power and energy requirements of critical sub-systems. This is followed by Section 12.2 which analyses various batteries and selects the battery material based on different performance factors. This is followed by Section 12.3 provides power and energy budgets for the different subsystems and components. Finally, Section 12.4 presents initial sizing parameters for the selected battery.

### 12.1. Requirements and Assumptions

The requirements relating to the energy and power system are presented in Table 12.1.

**Table 12.1:** Battery Requirements Table. Initial performance requirements for battery selection and initial sizing

ID	Description	Traceability	Rationale
CRTL-02	The system shall be able to deliver 25 [W] to the control system	There needs to be a minimum power deliverable to the payload to allow it to navigate.	Accurate navigation is vital to the mission profile
ENR-AQUA-01	The system shall be able to deliver 13.1 [Wh] to the underwater propulsion system	There needs to be a minimum power deliverable to the payload to allow it to propel in the required direction.	Manoeuvrability is vital to the mission profile
PLD-INS-01-04	The system shall be able to deliver 60 [Wh] to the payload	There needs to be a minimum power deliverable to the payload to allow it to monitor.	The purpose of the mission is to retrieve data for the client

## 12.2. Battery Selection

To ensure a compact, energy-dense battery the correct configuration and type should be selected. The following batteries are considered:

- Lithium polymer [LiPo]
- Lithium Ion [Lilon]
- Lithium Iron Phosphate [LiFePO4]

These batteries offer different characteristics that may be useful to the drone. The table below lists the relevant details where cost is ranked relative to other options:

**Table 12.2:** Battery characteristics of LiPo, Lilon and LiFePO4

Chemical type	Specific energy [Wh/kg]	Cycle life [no. cycles]	Cost
LiPo	140 - 200+	150–250	Medium
Lilon	100-158	400-1200	Low
LiFePO4	90–160	1,000-10,000	High

A vital part of the design is the conservation of mass as the batteries are placed in the nose cone of the system. More mass may pull the centre of gravity too far forward. In this case, LiPo and Lilon would be preferable with not too high a cost. The disadvantage is that the cycle life is relatively low in comparison to LiFePO4.

When comparing LiPo and Lilon, the main difference as seen in Table 12.2 is the cycle life in which Lilon lasts longer. However, after researching the batteries LiPo is a safer, more stable solution. It is robust and flexible, lower chance of leaking electrolytes and has a low profile. When considering the requirements given by the seaweed company (specifically SUS-ENV-01: The system shall not deposit waste material at the monitoring site) safety and sustainability are top-level requirements. Therefore, *it has been opted to use LiPo batteries and sacrifice lifespan.*

## 12.3. Power Budget

The power and energy consumption of all power-consuming components of the vehicle including the time during which they are active per mission can be seen in Table 12.3

**Table 12.3:** Power budget of all power-consuming components of the vehicle

Group	Component	Power [W]	Energy [Wh]	Time active [h]
Structures	Wing hinge	0.1	-	-
	Tail hinge	9.9	-	-
Propulsion	In-air cruise	123	103.32	0.7
	In-air climb	278	23.35	0.07
	Undewater forward	90	11.55	2
	Underwater control	4.11	1.55	0.375
Electronics	Sonar	20	126.7	6.3
	Cameras	4	14	3.5
	Flight Controller	25	87.5	3.5
	TT&C	2.45	1.715	0.7
<b>Total</b>		<b>566.56</b>	<b>523</b>	

## 12.4. Battery sizing

For initial sizing, a specific energy value of 200 [Wh/kg] was used. Then, for every energy iteration the mass of batteries was used to estimate cg positions as well as buoyancy.

For the final battery selection, the battery must hold 70000 [mAh] to produce a total of 523 [Wh] for all relevant subsystems. However, for market purposes, the battery could be sized to allow for a larger range and therefore more application, as to be discussed in Chapter 14. The battery chosen<sup>1</sup> and its specifications are displayed in Table 12.4.

Therefore, nine of these batteries can be used and placed in parallel which will maintain the correct nominal voltage of 7.6 [V]. For the required power consumption only the total of nine battery packs are necessary which provides a leftover 9 [Wh] as a safety factor.

*In total the battery provides 532 [Wh].*

**Table 12.4:** Battery specification

Specs	Values
Capacity	8000 mAh
Length	138 mm
Width	47 mm
Height	26 mm
Mass	317 g
Configura- tion	2S2P

<sup>1</sup>Battery selction

# PART II

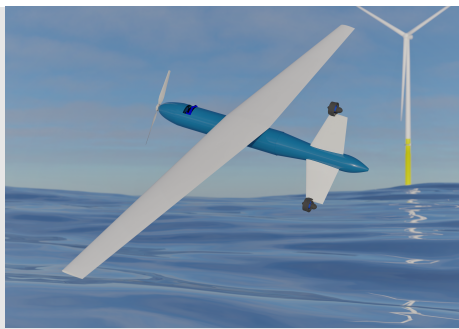
## SYSTEM DESIGN

### 13 System Summary

The following chapter discusses the logistics of the final system design. The Puffin characteristics and specifications are summarised in a detailed table to provide a clear overview. Furthermore, the validation of the completed system is outlined. Lastly, the system sensitivity analysis is described in order to observe the impact of changing parameters on the design. The specifications of the system can be found in Table 13.1.

#### 13.1. Specification Table

**Table 13.1:** Initial specification sheet for the Puffin, comprised of physical, flight, power, monitoring and cost aspects

Specification	Puffin
	
Mission Time	7.5 [hr]
<b>Physical</b>	
MTOM	13.2 [kg]
Propulsion Type	Battery Electric
Max Payload Mass	2 [kg]
Payload Dimensions	150x125x65 [mm]
Wing Surface Area	0.75 [ $m^2$ ]
Wing Span	3 [m]
<b>Flight</b>	
Altitude	120 [m]
Max Thrust	25.8 [N]
Airspeed (Cruise) [m/s]	20 [m/s]
Dive Speed	15 [m/s]
Stall Speed	15 [m/s]
Maximum Speed	33.7 [m/s]
Operational Range	60 [km]
L/D (Cruise) [-]	20
Mission Time Air	85 [min]
Flight Climb Thrust	16.5 [N]
<b>Underwater</b>	
Underwater cruise speed	0.5 [m/s]
Mission Time water	125 [min]

Continued on next page

Specification	Puffin
Underwater drag	6.5 [N]
Underwater Range	10 km
<b>Battery</b>	
Total Battery Mass [kg]	2.853 [kg]
<b>Monitoring</b>	
Units per Mission [-]	40
Sonar frequency	1200 [kHz] (high), 720 [kHz] (low)
Sonar range	0.1 [m] - 50 [m] (high), 0.1 [m] - 120 [m] (low)
Angular Resolution	0.12° (high) 0.25° (low)
<b>Cost</b>	
System	€60,000
Operational [€/month]	€550
Maintenance [€/month]	€1,100
<b>Water to air transition</b>	
Chamber pressure	25 [Bar]
Thrust	850 [N]
Total Impulse	384 [Ns]

## 13.2. System Validation

The system design is finalised, which means that it now has to be verified and validated. Requirement validation and product verification, as outlined in Section 2.3, has been done throughout the chapters.

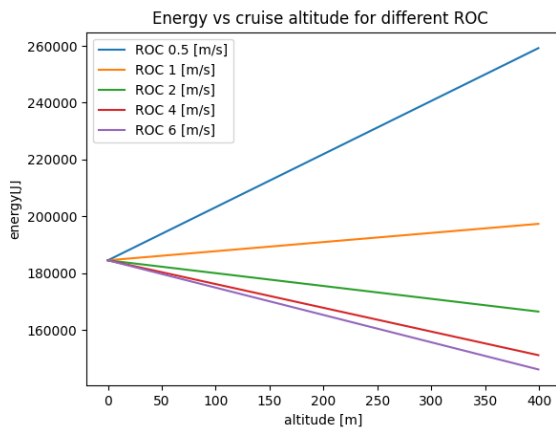
The next steps in the validation process begin with model validation. Throughout the design of the Puffin, models have been made to simulate the functions of the subsystems, as well as to ensure the working of the final, completed system. In order to aid the iteration process, the models have been made in Python. The main method used to validate the models is comparison, which takes already validated models and looks at similarities and compliance between both.

In order to validate the completed, integrated system, several recommendations, still to be fulfilled, will now be outlined. First, a comparison of all specifications of the Puffin with other similar UAVs to see if its performance and its attributes such as MTOM etc. are in believable ranges.

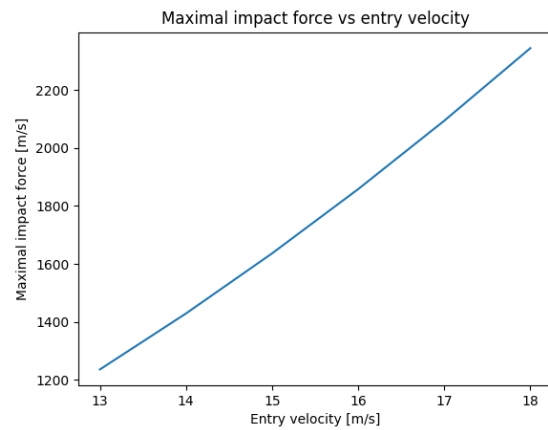
Following model validation, product validation can begin. First, end-to-end information testing [51] is done. Here, it is made sure that the products show compatibility with set operational specifications such as the mission timing. Next, mission scenario tests [51] will be carried out. Here, flight-like conditions thus the conditions on the way to and in the wind farm, and underwater-like conditions that occur in the North Sea are simulated in order to see if the hard- and software can execute the mission successfully. Furthermore, operations readiness tests [51] are performed. Here the full mission, including launch, landing and data retrieval is completed using a real timeline. Finally, the Puffin is subjected to stress-testing and simulations to check its robustness to changes in performance and fault conditions [51].

## 13.3. System Sensitivity Analysis

A sensitivity analysis is performed to observe the effect of changing a singular parameter and its impact on the design. An example of this is displayed below in Figure 13.1



(a) Altitude vs energy graph with various rates of climb



(b) The impact of increasing diving velocity on the load on the structure

**Figure 13.1:** Sensitivity analysis of the whole system

As can be seen in Figure 13.1a, at low ROC there is a significant increase in energy with altitude. The system has to climb for longer, the high thrust motor setting has to be maintained for longer, hence the steep increase. At higher ROC the energy declines with altitude which is counter-intuitive, at higher altitudes there is however more time for gliding which requires no power. The system will achieve the goal altitude in a short duration and naturally glides to the desired location. The energy consumption estimated accounts for possible altitude changes.

Another sensitivity analysis is the diving velocity vs. impact force. The graph in Figure 13.1b shows there is a positive correlation between the two parameters; the higher the velocity the higher the force. At higher velocities the controllability and manoeuvrability are better, particularly to avoid stall. However, if the entry velocity increases the design will have to be iterated to withstand higher loads. The nose cone, load structure, hinge mechanism, and tail specifically will need to be redone. The water entry loads have been modelled for stall speed, the actual entry velocity might be higher. The realistic deviations from the exact values used for estimations should be considered and accounted for. The Puffin design accounts for the possible changes in energy consumption and higher loads by designing with safety factors.

Additionally, the flight range versus the number of farms will be analysed. Based on the requirements and the market analysis, it is required that the drone should fly 60 [km] offshore. The drone is capable of doing this, but the mission will not be able to complete a whole farm in one day. In Figure 13.2, the distance offshore versus the number of farms able to visit is plotted. From these graphs, it can be concluded that the battery capacity is enough to have a large range, and inspect 30 seaweed units at 60 [km] offshore. If a whole farm were to be inspected, multiple operating days would have to be planned.



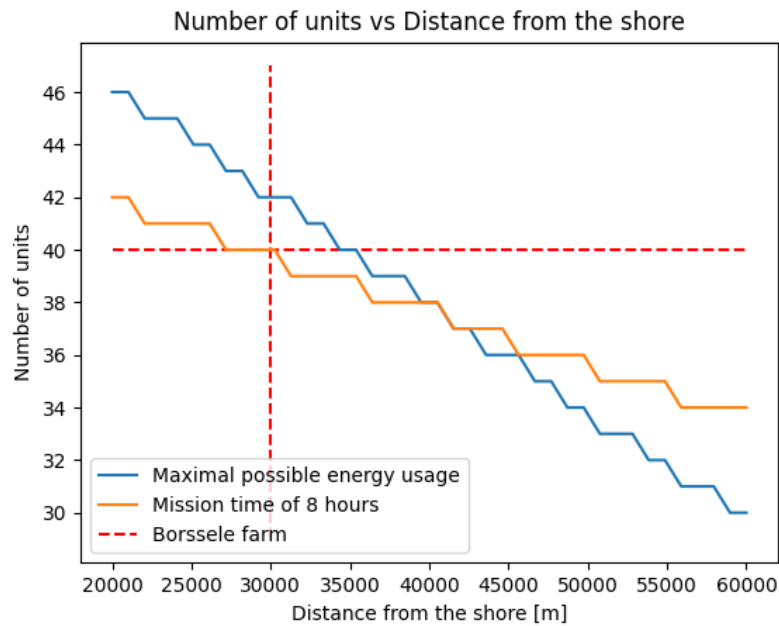


**Figure 13.2:** Possible number of units monitored vs the distance from the shore of the farm. The relation is displayed for a limited mission time of 8 hours and limited total battery capacity.

## 14 Market Analysis and Return on Investment

The financial considerations of a product are a crucial factor during the design phase. If a product is too expensive for its market, or does not provide enough value for the customer, the product will not be economically viable. In this chapter, a market analysis is performed, based on which design guidelines and requirements will be established. Additionally, the costs of the product are analysed, and a selling point will be established. Additionally, the value of the product for The Seaweed Company will be analysed, and areas, where the drone differentiates itself from its competitors, will be identified.

### 14.1. Market Analysis

In this section, the market potential of the drone will be analysed. The SEAMOS group was commissioned to make a design based on the plan of The Seaweed Company to build seaweed farms at the Borssele wind farm. However, a market analysis has to be performed in order to discover if the requirements set by the seaweed company are too constraining, or if the requirements are impractical for additional market applications that could significantly increase selling potential.

Firstly, the currently determined market by The Seaweed Company will be analysed, namely the seaweed farming market and the offshore drone inspection market. This will be discussed in Section 14.1.1. Following this, different markets will be explored to potentially expand the applications of the drone, and acquire more investments and funds with it.

To conclude, in Section 14.1.4, additional requirements that have been determined by the market analysis will be presented. These will then be used to design the drone for the specific market applications defined.

#### 14.1.1. Target Markets

The current market presented to the team, and the main application of the SEAMOS drone is the monitoring of offshore seaweed. This can be split up into two markets to analyse, the offshore seaweed market, and the offshore monitoring market.

The first market that has been identified is the offshore monitoring market. The offshore energy and infrastructure monitoring market has a current market size of 19.2 [bn USD] [52], with a projected value of 26.5 [bn USD] by 2026. Looking at [53], it can be seen that some parts of the offshore monitoring market are already well-established, however, a lot of areas of offshore monitoring are still in their introductory and growth phase. This can also be seen in Figure 14.1.

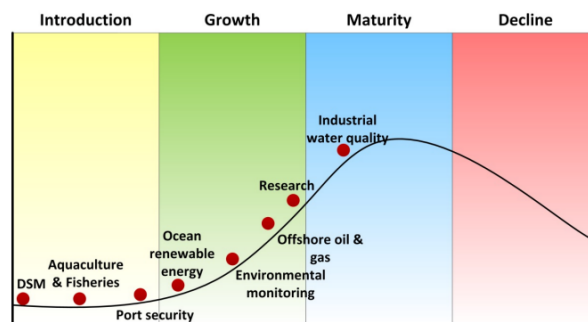


**Figure 14.1:** Market Maturity of Offshore Monitoring Areas [53]

In Figure 14.1, it can be seen that aquacultures and fisheries, under which seaweed farming falls, are still in a very introductory phase. The total aquaculture market has a value of 289.6 [bn USD] in 2021, and a projected value of 421.2 [bn USD] by 2030 [54]. Seaweed farming consists of 15 [bn USD] of that value, and will grow to 25 [bn USD] by 2028. Seaweed farming is already a well-established market, but primarily consists of near-shore farming in Asia which possesses large coastlines, and thus access to shallow water for near-shore farming. Offshore seaweed farming is an emerging market still in early development and is currently in the testing phase [55]. A market with low maturity has inherent risks and opportunities. The opportunities include large growth potential and a high-demand outlook. Additionally, since the market has a highly sustainable impact, a lot of potential investors are present. Risks of an immature market are lack of technological advancements, large initial capital needed, and high development costs. However, since the near-shore seaweed farming market is already a well-established market [56], the risk of clients not having enough funds, or not being able to develop their product is lower.

**Table 14.1:** Segmented Market Overview (Combined and Transposed)

Key Market	Aquaculture [54]	Seaweed farming [57]
Value (2021) [bn USD]	289.6	15.01
Projected Value [bn USD]	421.2 by 2030	25 by 2028
CAGR [%]	5.5	7.51
Use cases / potential clients	Population growth, protein demand	Demand for seaweed-based products, biofuel production, carbon sequestration
Further market segments	Fish farming, seaweed farming, freshwater farming, nearshore farming, offshore farming	Red seaweed, brown seaweed, green seaweed, nearshore farms, offshore farms

Due to the growing nature of the seaweed farming market, and the low maturity of offshore seaweed farming, it can be concluded that offshore seaweed farming can be a viable target market, where profit can be made. However, in order to build some security, offshore aquaculture has been identified as a secondary market. As it has similar applications to the seaweed market and more established firms, the SEAMOS drone will be able to competitively sustain itself. The SEAMOS drone also has a lot of potential in the military field, however, an ethical analysis will have to be performed to discuss if this is wanted. This will be done in Section 14.1.3.

The needs of clients should also be considered. Aquaculture clients will primarily be companies specializing in aquaculture production and specifically seaweed production. They will require a solution that can measure data such as water quality, dissolved oxygen, carbon dioxide levels, and the number of fish/amount of flora, with medium to high accuracy. Additionally, the structural integrity of the mechanical system used for seaweed or aquaculture farming needs to be monitored. Clients are also interested in solutions that can operate in rough

conditions for continuous monitoring. Some critical factors for aquaculture and seaweed farming clients are cost, performance, continuous monitoring capabilities, [58].

Regulatory factors also have a big impact on the design of the drone. Based on [59] [60] [61], limitations on drone operations will be established. Additionally, wind farms also have regulations that will add additional requirements [62].

#### **14.1.2. Current Solutions**

Currently, solutions to the problem of offshore seaweed farming consist of manned specialised vessels traveling to the seaweed farm and inspecting the farm there. This results in a very expensive, slow and weather-dependent operation. Looking at other solutions for underwater monitoring, most systems are not autonomous. Additionally, drones specifically designed to go underwater are usually tethered. This is primarily done to enable communication. The tethering, therefore, requires an additional vessel to support the underwater drone, which is both expensive, slow and limits range capabilities. The Puffin would differentiate itself by providing an autonomous, very flexible solution that can inspect at remote locations and move there, which makes it more weather-resistant. The main advantage of the current solutions is the depth that it can dive to, the Puffin can dive 10 [m] deep, whereas most of these systems are capable of diving deeper.

#### **14.1.3. Ethical Analysis**

In Section 14.1.1, it has been identified that the SEAMOS drone could also have military applications due to its unique design, and bi-modal capabilities. However, providing technology for military operations raises some ethical questions.

The development of the SEAMOS had as its main target to use innovation to design an efficient system for offshore monitoring. These technological advantages were oriented towards making the world more sustainable by allowing for easier monitoring of aquacultural farming. Especially with the raising concerns about climate change, the SEAMOS drone is a development that can majorly impact the future of our planet.

However, when shifting towards military applications, the ethical consequences increase. Drones are already often used in modern military operations, from surveillance and intelligence to direct attack. By allowing the drone to be used for such missions, the team would deviate from the original intent of the drone (encourage environmentalism). Even if not used for direct attacks, the potential of indirect harm is not in line with the ethics of the team.

Another factor to consider is the control of the drone. The drone has been developed to operate autonomously. In the case of seaweed applications, a misjudgment of the drone will have minor implications whereas, in military operations, this could lead to major consequences. Additionally, due to the ease of deployment, there is no need for a specialist operator, which makes the drone accessible to almost everyone, and control over who can operate the drone becomes limited.

To conclude, the application of the SEAMOS drone technology should be limited to civilian applications, as allowing military applications would deviate from the original intent of the drone. Additionally, encouraging military operations is not in line with the ethics of the team.

#### **14.1.4. Market Requirements**

Based on the market analysis, additional design requirements can be identified. A key requirement is an adaptation from the requirement set by The Seaweed Company NAV-OPR-01: The system shall monitor an area that is at least 30 [km] distant from the shore. Based on [63], it can be seen that a lot of additional wind farms can be reached if the range requirement is increased (see Figure 14.2). It is expected that the return of the 30 [km] extra range will outweigh the increase in battery weight. The update requirements can be seen in Table 14.2

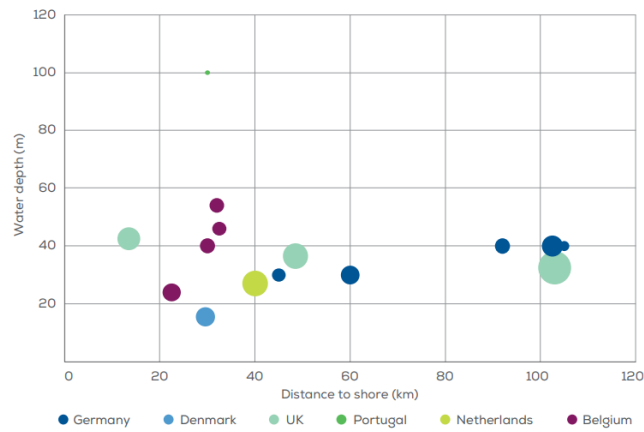


**Figure 14.2:** Average water depth and distance to shore of offshore wind farms under construction during 2019. The size of the bubble indicates the capacity of the site [63]

**Table 14.2:** Additional Requirements Based on the Market Analysis

Requirement Code	Requirement	Justification
OPR-NAV-01	The system shall monitor an area that is at least 60 km distant from the shore	Update on OPR-NAV-01 based on additional windfarms available [63]
OPR-NAV-06	The system shall keep a minimum of 500 [m] distance to any wind farm structure	From [62]
OPR-NAV-07	The system shall have a nominal cruise altitude below 120 [m]	From [60]
SUS-ECO-03	The system shall operate autonomously during the navigation and monitoring phases	Provide competitive advantage

#### 14.1.5. SWOT

A SWOT analysis has been made in [1], and has been adapted, which can be found in Table 14.3. In the table, S stands for the seaweed market, O for the offshore monitoring market, and P for the Puffin performance compared to the market.

**Table 14.3:** SWOT Analysis of Offshore Inspection and Seaweed Market [1]

<p><b>Strengths</b></p> <ul style="list-style-type: none"> <li>• High growth potential (S+O)</li> <li>• High demand outlook (S+O+P)</li> <li>• Many potential investors (S+O)</li> <li>• Versatile applications (S+O+P)</li> <li>• Can grow in a variety of aquatic environments (S)</li> <li>• High rate of carbon sequestration (S)</li> <li>• High yield for unit area (S)</li> <li>• Ease of deployment (P)</li> <li>• Autonomous (P)</li> </ul>	<p><b>Weaknesses</b></p> <ul style="list-style-type: none"> <li>• Immature market (S+O)</li> <li>• Lack of technological advancements (S+O+P)</li> <li>• Large initial capital needed (S+O+P)</li> <li>• Strict regulations (O+P)</li> <li>• High development cost (S+O+P)</li> <li>• Critical dependencies (governments/ investors) (S+P)</li> <li>• Limited scalability (O)</li> <li>• Limited understanding of long-term environmental effects (S)</li> <li>• Limited understanding of optimized farming methods (S)</li> <li>• High dependency on weather and environment (S+O+P)</li> <li>• Lack of monitoring technology (S)</li> <li>• Environmental operating conditions (P)</li> </ul>
<p><b>Opportunities</b></p> <ul style="list-style-type: none"> <li>• New technologies (S+O+P)</li> <li>• New customers (S+O)</li> <li>• New providers (S+O)</li> <li>• Diversification (S+O)</li> <li>• Carbon credit payments potential (S)</li> <li>• Growing in new strategic areas (S+O)</li> <li>• Growing demand for sustainable agriculture (S)</li> <li>• High collaboration (S+P)</li> </ul>	<p><b>Threats</b></p> <ul style="list-style-type: none"> <li>• Maritime environment (S+O+P)</li> <li>• Regulations (S+O+P)</li> <li>• Global economic decline (S+O+P)</li> <li>• Potential maritime pollution (S+O+P)</li> <li>• Lack of collaboration (O)</li> <li>• Potential maritime habit modification/ threat(S+O+P)</li> <li>• Competitor solutions (P)</li> </ul>

## 14.2. Cost Analysis

To determine the potential return on investment the total cost of the product needs to be analysed. The costs are segmented into production and acquisition, infrastructure maintenance, operational, and end-of-life (EOL). Production and acquisition accounts for procuring materials, equipment, and parts and assembling them into the solution while infrastructure is the launching and landing systems needed for operation. Maintenance relates to repairing and maintaining optimal performance of the system and subsystems and operational relates to the cost of operating during the mission. The end-of-life cost relates to the capital needed to safely and sustainably dispose of the product. Table 14.5 shows the contribution of each cost segment to the lifetime cost of the product. To estimate the various costs through the lifecycle of the product a top-down method was employed for the main systems of structure, sensing, propulsion, launching and landing. Each component for every subsystem was identified and off-the-shelf parts were researched. Additionally, assembly costs were estimated to be 15% of the total component cost.

**Table 14.4:** Component cost breakdown for structural, propulsive, sensing, launching, landing systems

Sub system group	Component	Amount	Upfront / Production cost	Maintenance cost per month
Structure	Wing	2	€500.00	€50.00
	Tail	3	€200.00	€50.00
	Fuselage	1	€500.00	€50.00
	Nosecone	1	€500.00	€200.00
	Tail Hinge	3	€200.00	€50.00
	Wing Hinge	1	€408.08	€50.00
Sum			€2,308.08	€450.00
Propulsion	Air motor	1	€275.00	€20.00
	Air propeller	1	€155.00	€20.00
	Undewater motor	1	€236.00	€20.00
	Gas tank	1	€1,000.00	€40.00
	Water tank	1	€1,000.00	€80.00
	Valves	2	€160.00	€10.00
Sum			€2,826.00	€190.00
Sensing	Batteries	8	€560.00	€100.00
	Sonar	1	€22,000.00	€200.00
	Camera	2	€400.00	€10.00
	Water sample	1	€100.00	€20.00
	Flight Controller	1	€1,000.00	€20.00
	TT&C		€638.00	€10.00
Sum			€24,698.00	€360.00
Launching/ Landing	Catapult	1	€18,000.00	€50.00
	Net	1	€3,000.00	€50.00
Sum			€21,000.00	€100.00
Assembly			€7,624.81	0
Total Costs			€58,456	€1,100

## Operational, Maintenance & EOL Costs

The operational costs are estimated using Equation 14.1 where  $n_{mis}$  is the number of days for a mission,  $C_{charge}$  is the hourly wage of the worker,  $n_{hours}$  is the time to arrive at the destination for the worker,  $t_{operation}$  is the length of the mission and  $C_{storage}$  is the cost of the storage container to house the vehicle and is a one time fixed cost.

$$C_{operation} = n_{mis}C_{charge} (1.02_{car}n_{hours} + t_{operation} + 1.025_{car}n_{hours}) + C_{storage} \quad (14.1)$$

The hourly wage is found to be 40 EUR per hour [64],  $n_{hours}$  is estimated to be 1.5 hours from Rotterdam to the coast in Borssele,  $t_{operation}$  is 7 hours and 40 minutes from Section 4.2 and  $C_{storage}$  is equal to 1500 EUR<sup>1</sup>

This gives an operation cost of 550 EUR for one mission with an additional 1500 EUR if a container needs to be purchased.

The maintenance costs were estimated based on the frequency of inspection or replacement needed for each part. Additionally, for off-the-shelf components, their product lifetime/number of usages were taken into account and recalculated for a 10-year use case for the Puffins mission.

The end-of-life (EOL) costs are associated with the costs needed to safely and sustainably dispose of the vehicle. There is cost in dismantling, separating components, and recycling. As most of the vehicle is made from carbon fiber the recycling cost will be determined by that material. For a 13kg drone, the recycling cost discounted back is estimated to be 296 EUR seen in Table 14.5 [65]

## R&D Costs

Before the Puffin can be implemented into the market, research and development need to take place on critical systems. As the Puffin utilises a unique combination of technology, many parts will have to be self-tested and developed. For an electric UAV of similar size an estimated R&D time is 5 years [66]. Over this time, subsystems and multisystem testing will take place as well as certification, outlined in Figure 17.2. Additionally,

<sup>1</sup>Zelfbouw Container

many tax benefits provided by the Dutch government exist specifically for R&D costs for start up and companies [67]. Other tax planning strategies may be employed to mitigate the additional cost such as utilizing benefits for skilled migrant workers, IP box structures and employing start-up deductions. This may lower the total R&D costs depending on the specific corporate and tax structure [68] Based on this and the maximum take-off mass, complexity, assembly, tests and testing environments the R&D cost was estimated to be 500,000 EUR.

**Table 14.5:** Lifetime cost breakdown over different phases

Phase	Section	Cost [EUR]
Research Development		€500,000
Production	Materials + assembly	€37,456
	Infrastructure for operation	€21,000
Total production cost		€58,457
Running costs	Operational	€66,405
	Maintenance	€132,000
	EOL	€296
Total running costs		€211,982
Product lifetime cost (costs discounted back+excluding RD)		€258,423

After calculating the costs for the various phases of the product lifetime, a cost breakdown structure is presented in Figure 14.3. The various post-DSE phases described in Figure 17.2 are used in and are seen in the cost breakdown structure. Yellow blocks represent the main phases of research and development, production and running costs. An estimated cost is present in each box. Below each yellow box are green boxes displaying the specific components and the percentage cost contribution to their respective phase.

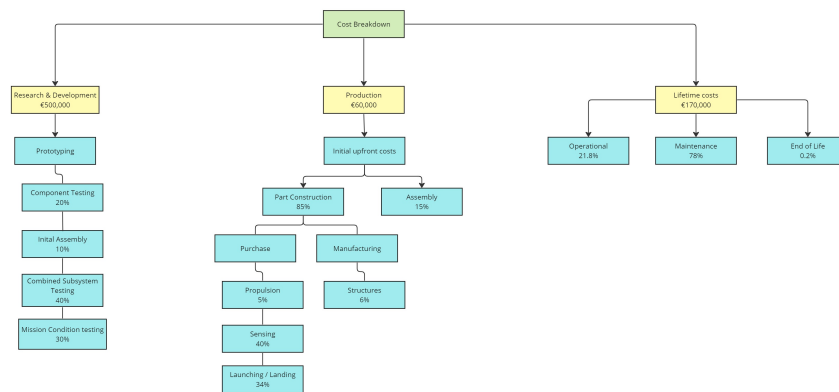


**Figure 14.3:** Cost breakdown structure based on phases from Figure 17.2

### 14.3. Revenue Generation and ROI

To generate revenue the product must be monetized such that it can be competitive in the market and support future operations of the company selling/producing it. From the midterm[1] different selling methods of upfront selling, subscription and rental were discussed. However, from Section 14.1 the majority of customers within the market have either medium to large amounts of capital to invest, immediate needs for monitoring solutions or a combination of both. From this, the most effective ways of monetizing the solution are either upfront selling for firms with enough capital to afford and operate the solution or a rental model for firms with an affordably immediate need for monitoring solutions. The company producing and selling the Puffin solution could employ both methods to increase revenue and be competitive to multiple firms within the market.

Upfront selling encompasses selling the Puffin after producing and assembling it. The buyer would incur all operational and maintenance costs and is freely able to deploy the Puffin whenever it is needed. This selling strategy is targeted towards large firms with enough capital to purchase the architecture and large enough infrastructure and operational capacity to deploy, operate and maintain the solution. With this method, the pro-



ducer of the Puffin foregoes any operational or maintenance costs over the product's lifetime which contributed over 75% of total lifetime costs. To determine an initial price of entry in the market, the Puffin should be sold at a price that at least covers the cost to produce and provide enough capital to produce another unit. From Table 14.5 the cost for production of a single unit is roughly 60000 EUR, meaning a viable selling price range would be at 130000-200000 EUR. This would cover the costs of one unit, provide capital for another unit and also have some margin for additional unforeseen costs and expenses. At this price range, the Puffin remains competitive with current solutions existing in the market while also offering a unique and multifaceted inspection quality compared to competitors. Current AUV that offer similar or more measuring capabilities as the Puffin can range between 300000-500000 EUR [69]. A selling price point of 175000 EUR was chosen for the Puffin as it remains competitive within the market and covers the necessary costs while also accounting for unforeseen expenses. Additionally, with economies of scale and learning curve effects, the production cost and time to produce can be lowered over time. A way to measure the effectiveness of the selling solution is to calculate the return on investment (ROI). This metric measures the profitability of the solution and is found by dividing the net returns by the net cost and multiplying it by 100 to arrive at a percentage. With a production and assembly cost of 60000 EUR and a selling price of 175000 EUR the return on investment for upfront selling is 193%.

For a rental model, an hourly rate is commissioned to any potential clients. This rate would need to be significantly lower than the upfront selling price to be affordable to different firms in the market whose priorities are immediate affordable monitoring solutions. Additionally, a rental model is also for firms who lack the operational capacity and infrastructure to maintain and operate the Puffin. From Section 4.2 a minimum of roughly 15 hours of operation is needed per month. At a rate of 800 EUR/hour the Puffin remains extremely attractive as other competitors charge rates of 1000-1500 EUR/hour [69]. Table 14.6 shows the discounted cash flows over the product's lifetime with R&D costs in the first year. The costs are discounted back at a rate of 2% to account for the time value of money. Assuming R&D costs have been paid before selling begins, after one year of operating the rental model will have generated enough profit to produce another Puffin unit. This gives a lifetime ROI of 412% assuming R&D costs have been paid back before operations begin. If the R&D costs have not been paid back and are incorporated into the total cash flows of the product, at 15 operational hours per month charged at 800 EUR per month gives the ROI is 84.31%. The cost of production is recuperated after 4 months and the break-even point for profitability is after 5 months.

**Table 14.6:** Cash flow breakdown over 10 years for a rental model of one unit of puffin, assuming 15 hours a month every month for a year at 800 EUR/hour

Year	Cost [EUR]	Revenue [EUR]	Rolling Cost [EUR]	Rolling Revenue [EUR]	Profit [EUR]	Cumulative Profit [EUR]
1	-€579,562.39	€144,000.00	-€579,562.39	€144,000.00	-€435,562.39	-€435,562.39
2	-€20,642.06	€144,000.00	-€600,204.45	€288,000.00	€123,357.94	-€312,204.45
3	-€21,054.90	€144,000.00	-€621,259.35	€432,000.00	€122,945.10	-€189,259.35
4	-€21,476.00	€144,000.00	-€642,735.34	€576,000.00	€122,524.00	-€66,735.34
5	-€21,905.52	€144,000.00	-€664,640.86	€720,000.00	€122,094.48	€55,359.14
6	-€22,343.63	€144,000.00	-€686,984.48	€864,000.00	€121,656.37	€177,015.52
7	-€22,790.50	€144,000.00	-€709,774.98	€1,008,000.00	€121,209.50	€298,225.02
8	-€23,246.31	€144,000.00	-€733,021.29	€1,152,000.00	€120,753.69	€418,978.71
9	-€23,711.23	€144,000.00	-€756,732.52	€1,296,000.00	€120,288.77	€539,267.48
10	-€24,547.15	€144,000.00	-€781,279.67	€1,440,000.00	€119,452.85	€658,720.33
ROI with R&D cost	84.31%					

## 14.4. Market Absorption

The versatile Puffin is applicable to the European aquaculture market, performing various missions such as investigating fish farm quality and flora farming. As the market is still experiencing high growth and a combination of established and new customers are present, two different selling solutions of upfront selling and hourly rental are considered.

With the number of existing solutions and their price points, The Puffin can capture a significant market share by offering lower prices compared to existing rented boats and UUVs. Current solutions in the market are typically rented boats or UUVs, requiring on-site deployment and operators, with prices ranging from 15,000 to 50,000 Euros per month. As the Puffin is designed specifically for seaweed monitoring it can be produced and operated at considerably lower price points. Since the Puffin is specifically designed for offshore seaweed monitoring, the determination of an achievable market share will focus on this particular market. Adapting the

solution for other use cases may require extra time and cost. A realistic market share of 0.2% within the first 5 years of operation is achievable, amounting to approximately 3.42 million Euros in net revenue. This revenue can be generated through the sale of 20 units or by renting out 6 units for 15 hours per month over a 5-year period.

### 14.5. The Seaweed Company Analysis

After analyzing the return on investment for a potential producer of the Puffin, an ROI analysis is done for The Seaweed Company. For other firms in the market, the exact return will depend on the use case for the Puffin as that may increase maintenance and operational costs. First, a cost analysis is performed for the Seaweed Company. Currently, specialized marine vessels are planned to be used to travel and monitor seaweed farms. This has an estimated 10-year cost of 320,000 EUR. Firstly, an upfront selling model is considered where The Seaweed Company purchases the solution and maintains and operates the Puffin itself. Assuming The Seaweed Company purchases the Puffin at cost, the 10-year lifetime cost is 260,000 EUR. This is already cheaper than the current solution and has greater operational and data capabilities. With roughly 60,000 EUR in savings, this amount can be reinvested into creating more seaweed farms. Additionally, as the Puffin is able to constantly monitor the farms, accurate data on carbon sequestration levels can be obtained which may enable the creation of blue carbon credits [70]. At 160 Hectors can be produced then an extra 9100 tons of CO<sub>2</sub> is sequestered each year [71]. At this magnitude of carbon sequestration, blue carbon credits can be sold and traded on the carbon credit market as the Puffin allows to the collection of consistent data for verification and validation of these credits. Selling roughly 9100 carbon credits at prices between 16.5 - 26.6 EUR creates an additional potential revenue of 150000-240000 EUR every year per farm [72]. Thus spending 260,000 EUR over 10 years allows for high levels of monitoring of seaweed and saving 60,000 EUR. Additionally, it enables enough data collection to verify and validate the levels of carbon sequestration and generate blue carbon credits [73]. Over 10 years roughly 1,950,000 EUR worth of blue carbon credits can be sold giving an ROI of 733%. This value is for a single farm and is highly likely to increase as more farms are created. However, entering the blue carbon credit market may be difficult or unfeasible for The Seaweed Company, therefore, assuming the savings on investment in the puffin is 23%.

## 15 Design overview

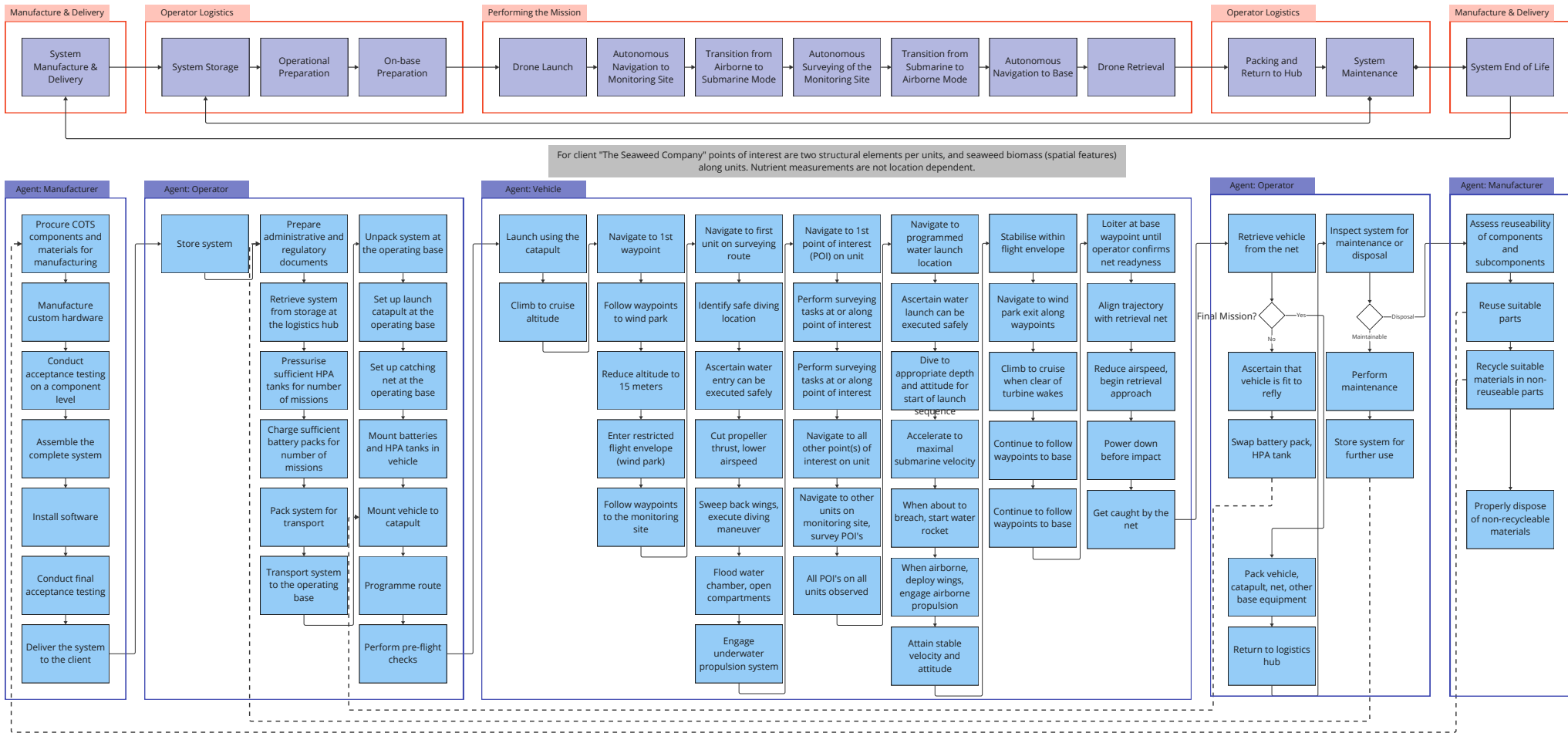
In order to obtain a clear overview of the steps needed to complete the design, as well as the future steps of the implementation of the solution in the market, certain project design tools will be used. A flow diagram of the steps performed during a mission will be described and broken down in detailed action points in Section 15.1.

The sustainability of the design will be assessed and measures will be put in place to limit the environmental impact of the vehicle and the operations necessary for its implementation. This will be described in Section 15.2. The risk associated to the project will be investigated in Section 15.3 and finally a similar investigation will be made for the reliability of the mission in Section 15.4

### 15.1. Functional Flow and Breakdown Structure

The functional flow diagram and breakdown structure of the steps that take place during one mission profile are presented in the following two pages.

## Puffin Functional Flow Diagram

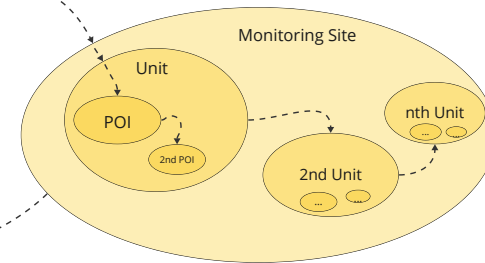


**Logistics hub**

Permant facility accomodating vehicle storage, vehicle maintenance, battery charging, and HPA tank refill

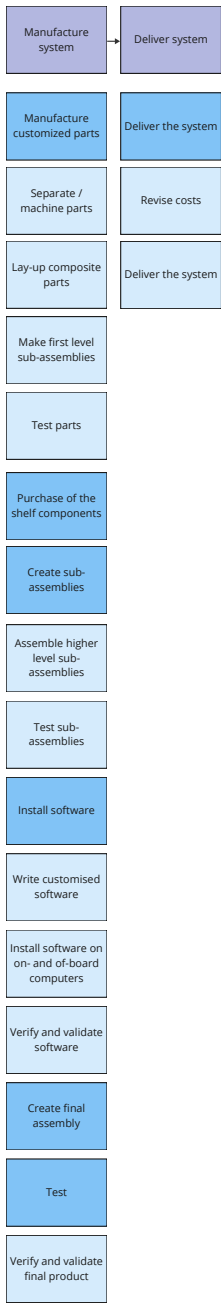
**Operating base**

Launch site location, no permanent fixtures. Vehicle launched and retrieved here.

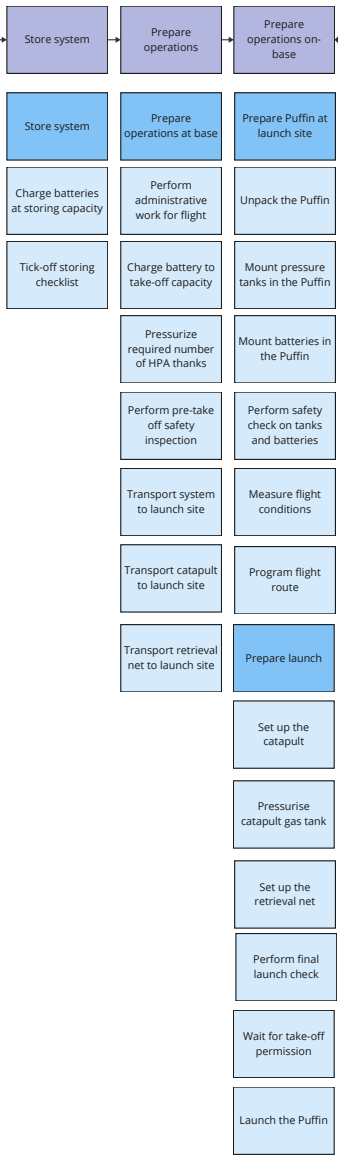


Puffin Functional Breakdown Structure

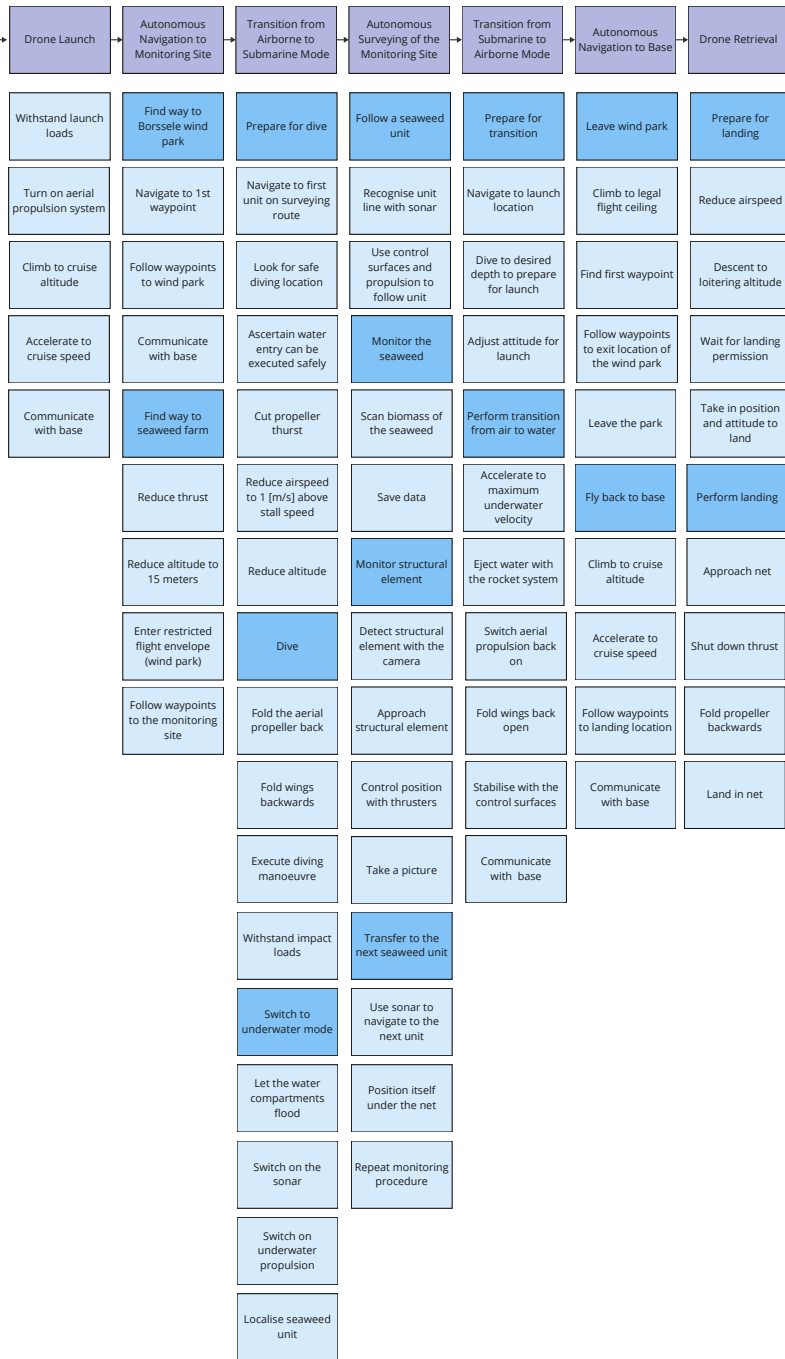
Manufacture & Delivery



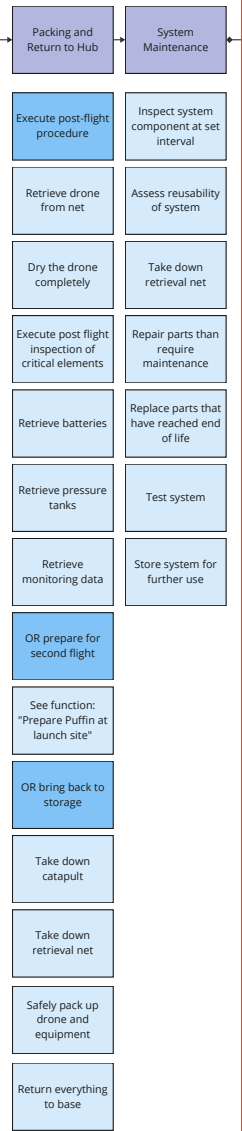
Operator Logistics



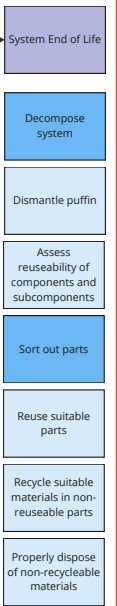
Performing the Mission



Operator Logistics



Manufacture & Delivery



Key

Function

Sub-function 1

Sub-function 2

## **15.2. Sustainable Development Strategy**

The seaweed sector is an upcoming industry that is gaining more and more relevance. The constant growth causes an increasing weight to be put on the importance of sustainability and on ecological designs. The integration of autonomous drones will aid in the realisation of today's relevance in this area.

### **15.2.1. Environmental Impact**

Almost seventy percent of waste produced on Earth ends up in landfills. However, much of it sneaks into the environment. More than 7 million tons of plastic waste enters the oceans every year. SEAMOS wishes to regulate its environmental impact and to protect the Earth.

The system will be designed to be energy efficient. The goal is to use lightweight materials. However, this poses an enormous challenge as the system has to operate both in-air and underwater. It has to be heavy enough in order to sink but for flight, being light is much better. Furthermore, the SEAMOS team aims to use materials that can be recycled. Hence, the Puffin will mainly consist of recycled CFRP (carbon fiber reinforced polymer).

Further, the materials shall be non-toxic. The SEAMOS team strongly believes that no toxicity is allowed to enter the North Sea under any circumstances as this would impose a risk on the animals living underwater. Contact with the seaweed plants or any surrounding fauna is also to be avoided. The goal is to monitor them, not to disturb their growth or harm them in any way.

In its design, the team has considered noise pollution. Noise pollution in air is less important as there will be plenty of sounds due to the rotating wind turbines. However, underwater, the propeller noise can upset the ecosystem and thus any living creatures. In order to prevent this, propellers were chosen with low noise in mind.

### **15.2.2. Manufacturing**

The SEAMOS team wishes to prevent contributing to the increasing amount of waste and wants to ensure a smooth manufacturing process where two things are set to be of the highest priority: recycling and waste management.

Therefore, the philosophy of 'Lean Manufacturing' shall be introduced and followed. Lean Manufacturing (LM) is a way of minimizing waste at every level of the manufacturing process. It involves everyone from workers to managers. The little waste that is left, will be reused or recycled so that it may be part of other products. Collaboration with other drone companies is a desired goal on the SEAMOS team's list. Good communication with other drone developers and knowledge of their manufacturing processes allows us to see if their waste could be an asset to the SEAMOS team or the other way around. If many use the same materials, it might be cheaper to buy them at the same time. There will be an in-detail strategy on how to deal with leftover material. Either reuse it oneself or reuse it efficiently through collaboration with similar or no-similar companies or institutions such as municipalities, governments, universities etc. Lean manufacturing also encourages using renewable energy sources. Green energy can minimise the carbon footprint of the SEAMOS project which is a high priority. Additionally, the entire supply chain can be made more sustainable by collaborating and discussing with suppliers. The suppliers must be convinced that reducing waste in their area, contributes to the reduction as a whole. Consequently, with SEAMOS's own sustainability and the sustainability of other parties (suppliers, governments, other drone designers), a closed loop systems for recycling and sustainability is created.

The water energy during manufacturing shall be minimised. The team will also look into emissions and how to avoid pollution while the drone is made. Finally, human resources are an important part of sustainability and must be considered. Ensuring the safety of workers during the manufacturing process is important to the team.

Although being cost effective is a large part of the project, sustainability also means supporting ones local, national population. Hence, SEAMOS plans to employ local companies where possible.

The transport and storage of materials, tools and final product must be handled efficiently. Transportation vehicles can be chosen to be fuel efficient in order to reduce emissions. Furthermore, delivery routes can be optimized. Packaging is a big source of waste in every industry and it is no surprise that minimising this, has a large impact on the whole sustainability of the project.

### **15.2.3. Life Span**

The drone has an operational lifetime of 10 years. This means that it has to be designed and manufactured in a such a way, that it needs minimal maintenance while having maximum performance. Wear, corrosion, breakage – these are all significant risks for the system. Hence, the design will be optimized for hydrodynamics and aerodynamics in order to move quick and efficient throughout the water. The faster the system can complete

a mission and the smoother the operation runs, the more times the system can be deployed and thus the more efficient and sustainable it is. The team wants to prevent that the drone has to be replaced before its set operational lifetime.

To further solidify the goal of an efficient life cycle, the mission path shall be optimised. With climate change, changing water conditions, and changing tides, wind and weather conditions have to be accounted for. The environmental factors in the North Sea are never fixed and thus the team aims to continuously, throughout the coming years, reiterate on the best route, both safe and efficient, for the system.

Data collection allows to monitor the health of the seaweed farm and the surrounding ecosystems. The collected water samples will be able to determine if the water conditions are optimal. This allows any measures to be implemented if needed. That way, the seaweed grows at an optimal rate. The healthier the seaweed, the better and faster it grows and the more seaweed can be harvested. The end effect is that more seaweed can be used in the food industry and people can opt for a more sustainable alternative than meat.

Maintenance is another large factor impacting sustainability. The system has to be easily maintainable. If a part breaks but is not accessible to the one carrying out the repairs, the whole system has to be thrown out. Hence, the system will be designed and built in such a way that components are easily exchangeable and repairable. Batteries must be exchanged and charged regularly so they must be able to be taken out.

SEAMOS also wishes to contribute to the newest research on sustainable drones. With every completed mission, the system will be analysed to see if and how it can be optimised. To do so, any help is welcome and thus SEAMOS wishes to keep close relations to the universities in its perimeter and the possible improvements they may come up with for the system. The team wishes to keep growing and evolving.

Lastly, the team aims to come up with a sustainable End-of-Life solution.

### 15.3. Technical Risk Assessment

The following section analyses all technical risks that pose a threat to the SEAMOS project. It is reiterated from the Midterm report [1]. The risks are subdivided into the following categories: operational Risks, environmental risks, mechanical risks, power risks, software and control risks, communication risks, instrumentation risks and system integration risks [1].

#### Operational Risks

- TRI-OPR-02: The system needs to be rescued.
- TRI-OPR-03: The systems navigation function contains an error.
- TRI-OPR-05: Damage to the system is not detected during maintenance.
- TRI-OPR-06: Regulation relevant to the system operation changes.
- TRI-OPR-08: The position of an unexpected vessel is conflicting with the mission.
- TRI-OPR-09: More frequent maintenance than anticipated is needed.
- TRI-OPR-10: The system collides with an object.
- TRI-OPR-11: The system cannot be recovered after failure.
- TRI-OPR-14: The launch of the system fails.
- TRI-OPR-15: The landing net fails
- TRI-OPR-16: The propellers fail to stop rotating and entangle in the landing net
- TRI-OPR-17: The catapult fails to launch the system at the right speed
- TRI-OPR-18: The catapult is defect
- TRI-OPR-19: The nose propeller fails to fold before landing and entangles with net/breaks

#### TRI-ENV: Environmental Risks

- TRI-ENV-01: Winds on the way to the seaweed farm are stronger than designed for.
- TRI-ENV-02: Waves at the seaweed farm are higher than designed for.
- TRI-ENV-04: The rate of degradation due to seawater is higher than expected.
- TRI-ENV-05: System pollutes the environment.
- TRI-ENV-06: The system is driven away due to strong sea currents.
- TRI-ENV-07: The system temperatures are lower/higher than designed for.
- TRI-ENV-08: The system disturbs the local marine life.
- TRI-ENV-10: The water has lower visibility than accounted for.
- TRI-ENV-11: The system collides with a seaweed farm unit.

## **Mechanical Risks**

- TRI-MEC-01: Corrosion due to North Sea water damages the vehicle.
- TRI-MEC-02: The structure cannot withstand the loads it is subjected to and fails.
- TRI-MEC-03: Drag is higher than expected which reduces the endurance of the vehicle.
- TRI-MEC-05: The propulsion system fails.
- TRI-MEC-08: The transition from normal to swept-back wing configuration fails
- TRI-MEC-09: The ejection maneuver fails
- TRI-MEC-10: Not all the water is expelled from the wings
- TRI-MEC-11: The water chamber does not contain enough pressure to elevate the system out of the water

## **TRI-PWR: Power Risks**

- TRI-PWR-01: Power delivered by the power system is lower than consumption.
- TRI-PWR-02: Charging time is longer than expected.
- TRI-PWR-03: Battery overheating.
- TRI-PWR-04: Power not being delivered to the subsystems.
- TRI-PWR-05: Failure due to component damage.
- TRI-PWR-06: The ejection manoeuvre to launch out of the water fails
- TRI-PWR-07: The servos connected to the control surfaces fail
- TRI-PWR-08: Water getting into the batteries
- TRI-PWR-09: The batteries explode
- TRI-PWR-10: The propellers on the tail control surfaces fail
- TRI-PWR-11: The propeller on the nose fails

## **Software and Control Risks**

- TRI-SFT-01: Software bug making the system inoperative.
- TRI-SFT-02: System responding badly to control inputs.
- TRI-SFT-04: Sensor malfunction.
- TRI-SFT-05: Flight computer malfunction.
- TRI-SFT-06: System drifts away from seaweed farm due to orientation loss
- TRI-SFT-07: The data from sonar and camera does not get stored and are irretrievable

## **Communication Risks**

- TRI-COM-01: Loss of signal from the base (if used).
- TRI-COM-02: Loss of GNSS signal (if used).
- TRI-COM-05: Contact loss due to long underwater operation times.

## **Instrumentation Risks**

- TRI-INS-01: Water sampling subsystem fails.
- TRI-INS-03: Instruments not saving the data.
- TRI-INS-04: Instruments overheating.
- TRI-INS-05: Instruments orientation fails.

## **TRI-SYS: System Integration Risks**

- TRI-SYS-01: Interfaces between subsystems do not physically fit.
- TRI-SYS-02: Software interfaces between subsystems do not fit.
- TRI-SYS-03: Malfunctioning subsystem cannot be accessed for repair.
- TRI-SYS-04: Material in the assembly is a catalyst for corrosion.
- TRI-SYS-05: Validation and verification do not uncover all issues.
- TRI-SYS-06: Adhesives used to connect the different parts of the vehicles gets loose
- TRI-SYS-07: Adhesive is not watertight



### 15.3.1. Risk Evaluation

Table 15.1 shows a risk map. It compares the likelihood of a risk with the consequence, both on a scale from 1 to 5.

**Table 15.1:** Risk Map: green area: low risk, blue area: moderate risk, yellow area: high risk, red area: unacceptable risk

		Consequence				
		1	2	3	4	5
Likelihood			TRI-ENV-01, TRI-ENV-02			5
			TRI-ENV-06	TRI-MEC-01	TRI-OPR-02, TRI-SFT-01	4
	TRI-OPR-09	TRI-ENV-04 TRI-INS-01	TRI-SYS-01, TRI-SYS-02, TRI-SYS-04 TRI-ENV-05, TRI-ENV-11, TRI-PWR-02 , TRI-OPR-03, TRI-OPR-07 TRI-OPR-08, TRI-OPR-09, TRI-COM-02 TRI-COM-05, TRI-OPR-10 TRI-MEC-03, TRI-PWR-04, TRI-MEC-09	TRI-SYS-05, TRI-OPR-06, TRI-OPR-14, TRI-PWR-06, TRI-OPR-19, TRI-MEC-10, TRI-PWR-07	TRI-PWR-08, TRI-PWR-09	3
			TRI-OPR-04, TRI-SFT-04 TRI-COM-01 TRI-INS-04, TRI-INS-05, TRI-OPR-16, TRI-OPR-17, TRI-PWR-10, TRI-PWR-11, TRI-SYS-06	TRI-SYS-03, TRI-ENV-08, TRI-PWR-01, TRI-PWR-03 TRI-PWR-05, TRI-OPR-05, TRI-SFT-02, TRI-SFT-05, TRI-MEC-05, TRI-ENV-11, TRI-PWR-05, TRI-SFT-06, TRI-OPR-15, TRI-SFT-07, TRI-SYS-07	TRI-MEC-02, TRI-MEC-08, TRI-MEC-11	2
			TRI-INS-03	TRI-COM-05, TRI-OPR-18	TRI-OPR-11	1

Table 15.2: Risk mitigation table

Risk	Consequence	Treatment Strategy	Control Measures Implemented
TRI-OPR-02	Team has to go to rescue the system. The system or target structure might be damaged.	Mitigate	The system shall be designed to minimise the risk of needing rescue It is though quite likely that the need to be rescued from the windfarm will occur.
TRI-OPR-03	The system could be lost or not able to perform its mission.	Mitigate	Design a robust system and validate
TRI-OPR-05	Sending a damaged system out to rough offshore environments might lead to failure.	Mitigate	Design the inspection system well
TRI-OPR-06	The system is not allowed to operate and by definition fails.	Accept	Not much can be done about regulation
TRI-OPR-08	The system cannot perform its mission and fails. Could be temporary or permanent.	Mitigate	Equip system with a capability to respond appropriately
TRI-OPR-09	More maintenance increases costs and disturbs the operations schedule.	Mitigate	Design robustly
TRI-OPR-10	Damage and possibly critical damage to the system	Mitigate	Design the control system so that collision is avoided
TRI-OPR-11	The system is lost, the system pollutes the environment	Avoid and accept	Test recovery system
TRI-OPR-14	The system crashes and has to be launched again	Mitigate and avoid	Before launch, check thoroughly that all subsystems are operational
TRI-OPR-15	The drone crashes to the ground and sustains damage	Mitigate and avoid	check the net before every mission and ensure it is fully operable
TRI-OPR-16	The drone entangles and sustains damage	Mitigate	Design the propellers such that the risk of them not stopping is minimal
TRI-OPR-17	The system needs longer to reach the set thrust	Accept	Make sure that enough thrust can be provided by the propulsion system such that the speed can be increased successfully
TRI-OPR-18	Mission has to be postponed which may negatively affect the schedule and not all units can be inspected in the available time	Mitigate	Check the catapult regularly for any defects and repair immediately
TRI-OPR-19	The nose propeller may break	Mitigate and avoid	Design the propeller such that the risk of it not folding is minimal
TRI-ENV-01	The system fails to reach the farm, the system is not controllable.	Mitigate and avoid	Plan missions, taking into account weather forecasts such that the system avoids unsuitable conditions
TRI-ENV-02	The system comes into contact with the existing structures, the system fails to get close enough to the farm structures for the measurements	Mitigate and avoid	Plan missions, taking into account weather forecast such that the system avoids unsuitable conditions
TRI-ENV-04	The corrosion will cause structure degradation, if undetected and untreated can lead to failure.	Mitigate	Adjust the design such that the impact of seawater is not problematic

Continued on next page

Table 15.2 – continued from previous page

Risk	Consequence	Treatment Strategy	Control Measures Implemented
TRI-ENV-05	The system pollutes the environment negatively impacting the local flora and fauna, as well as the seaweed.	Mitigate	Redesign the system such that it doesn't pollute the environment
TRI-ENV-06	The system fails to reach the required position, a possible collision with structural elements	Mitigate	Design the system such that it counteracts the current
TRI-ENV-07	Unexpected temperatures outside of the expected range can limit the performance of the system.	Accept and avoid	Implement margins when designing
TRI-ENV-08	The system generates a negative impact on the local environment	Accept	Such an event is unlikely and hard to account for
TRI-ENV-10	It is not possible to obtain the needed measurements and images.	Mitigate	Redesign the system to account for the lower visibility
TRI-ENV-11	System might get entangled in the nets and get damaged itself or damages the nets	Mitigate and avoid	Keep enough distance between the system and the nets.
TRI-MEC-01	The structure fails, the system becomes inoperative.	Avoid	Design so that corrosion is not detrimental, maintain often
TRI-MEC-02	The structure fails, system inoperative	Mitigate	Design for all possible acting loads
TRI-MEC-03	The system might not be able to reach the station, has to return to base.	Mitigate	Design for an endurance margin
TRI-MEC-05	System will fail to reach the farm/base, failure to complete the mission	Mitigate	Design for a reliable system, component failure not critical, testing
TRI-MEC-08	System is unable to perform air-to-water transitions	Mitigate	Include extensive testing when designing; frequently check the mechanism
TRI-MEC-09	The system is unable to get out of the sea	mitigate	Design such that the risk is minimised; the maneuver can be repeated multiple times
TRI-MEC-10	The wings will be too heavy to sweep forward again and might fall back into the sea	Mitigate and avoid	design the wing such that enough wholes exist for the water to escape the structure
TRI-MEC-11	The system is unable to get out of the sea	mitigate	Design such that the risk is minimised, check the pressures before launch
TRI-PWR-01	Subsystems will use more power than expected reducing the system's endurance and leading to failure due to a lack of power.	Mitigate	Ensure thorough communications and perform tests on power budget
TRI-PWR-02	The operational planning will be distorted due to the longer charging time.	Mitigate	Test battery in various environmental conditions
TRI-PWR-03	If the battery's temperature exceeds a threshold temperature, it will fail.	Mitigate	Make sure the battery is being air-cooled.
TRI-PWR-04	Subsystems will be inoperative due to a lack of power.	Mitigate	Careful design and manufacturing to avoid failure of hardware or add a backup connection
TRI-PWR-05	The power subsystem will fail as it does not meet its requirements anymore.	Mitigate	Add proper object detection and avoid obstacles near the operating area

Continued on next page

Table 15.2 – continued from previous page

Risk	Consequence	Treatment Strategy	Control Measures Implemented
TRI-PWR-06	The system is not able to fly back to base	Mitigate and avoid	Repeat the ejection manoeuvre
TRI-SFT-01	Mission is not carried out.	Avoid	Test the system, verify and validate the model
TRI-SFT-02	System is not as efficient as it should be or unable to carry out the mission.	Mitigate	Test the model, design for the most extreme expected inputs
TRI-SFT-04	The system becomes less efficient.	Avoid	Use reliable sensors, testing
TRI-SFT-05	Less efficient carrying out of the mission or putting it in jeopardy.	Avoid	Test the system, use a reliable established solution
TRI-SFT-06	The system cannot find its way back	Mitigate and avoid	design such that the system can return once it is oriented properly again
TRI-SFT-07	The seaweed growth nor water quality can be analysed	avoid	check before launch if all technology is operable
TRI-COM-01	Potential loss of data	Mitigate	Establish a reliable data retrieval system at the base
TRI-COM-02	Makes it harder to carry out the mission, risk of losing the system	Mitigate	The autonomous system is to be designed to continue on-path until the connection is back on
TRI-COM-05	Water depth poses a risk to communication	Mitigate	Take depth and communication range into account when designing Design the autonomous control system so that collision is avoided
TRI-INS-01	Water quality measurement is not performed	Mitigate	Test the sampling mechanism, take multiple samples
TRI-INS-03	No monitoring data is generated	Accept	Accept it can happen and use tested instrumentation
TRI-INS-04	The gathered monitoring data is incomplete	Mitigate	Design for cooling, choose instruments not prone to overheating for the mission needs
TRI-INS-05	The monitoring data cannot be used	Mitigate	Design, Verify and Validate instrument orientation subsystem, design for accurate body orientation control
TRI-SYS-01	At least one of the subsystems has to be redesigned increasing costs and threatening the time schedule.	Mitigate	Ensure proper communication between departments
TRI-SYS-02	At least one part of the software has to be rewritten increasing costs and threatening the time schedule.	Mitigate	Ensure proper communication between departments
TRI-SYS-03	If one of these inaccessible components fail, it cannot be replaced and a larger part of the entire system has to be replaced.	Mitigate	Ensure that components with low reliability are accessible
TRI-SYS-04	Corrosion will occur more rapidly than initially predicted.	Mitigate	Team should ensure that all used materials are compatible
TRI-SYS-05	The overlooked errors might lead to unexpected malfunctioning of a part of the system.	Accept	It is always possible that some aspects of V&V are overlooked
TRI-SYS-06	Water may leak into the nosecone	Mitigate and avoid	Design such that all parts fit each well and no gaps exist
TRI-SYS-07	Water may leak into the nosecone	Mitigate and avoid	Reassess the adhesive regularly

### 15.3.2. Risk Treatment

The steps taken to reduce risks can be observed in Table 15.2, which shows the post-risk map. Here, mitigation steps are outlined.

**Table 15.3:** Post-Treatment Risk Map: green area: low risk, blue area: moderate risk, yellow area: high risk, red area: unacceptable risk

Consequence				
	1	2	3	4
Likelihood				5
				4
	TRI-ENV-04, TRI-ENV-10, TRI-OPR-07, TRI-OPR-08, TRI-MEC-03		TRI-SYS-05, TRI-OPR-09, TRI-PWR-09	TRI-OPR-06
	TRI-INS-01, TRI-OPR-09, TRI-OPR-17, TRI-MEC-09	TRI-SYS-03, TRI-ENV-01, TRI-ENV-02, TRI-ENV-06, TRI-MEC-01, TRI-OPR-16, TRI-OPR-18, TRI-OPR-19, TRI-MEC-10, TRI-SYS-06	TRI-PWR-04, TRI-OPR-04, TRI-MEC-05, TRI-OPR-14, TRI-PWR-06, TRI-COM-05, TRI-MEC-11, TRI-PWR-07, TRI-PWR-08	TRI-ENV-08, TRI-OPR-02, TRI-SFT-01
		TRI-INS-05, TRI-SFT-06, TRI-OPR-15, TRI-SFT-07, TRI-SYS-07	TRI-SYS-01, TRI-SYS-02, TRI-ENV-05, TRI-ENV-07, TRI-PWR-02, TRI-OPR-03, TRI-SFT-04, TRI-COM-01, TRI-COM-02, TRI-COM-05, TRI-INS-04, TRI-INS-03, TRI-PWR-10, TRI-PWR-11	TRI-PWR-01, TRI-PWR-03, TRI-PWR-05, TRI-OPR-05, TRI-SFT-02, TRI-SFT-05, TRI-SYS-04, TRI-ENV-11, TRI-MEC-08
				1

### 15.4. Reliability, Availability, Maintainability, Safety

This outlines the design decisions contributing to the Reliability, Availability, Maintainability, Safety (RAMS) of the design. The consideration of these design aspects is of high impact on how the design performs in carrying its mission, over its lifetime and as a commercial product. Below, the most critical decisions related to these aspects are listed.

#### Reliability

Reliability is concerned with ensuring that the design experiences as few failures as possible. In the Puffin design, it was ensured that the complexity is kept at a level as low as possible. That shall in turn reduce the likelihood of failure. To decrease the complexity, in air and in water propulsion systems are separated rather than integrated in one. Also, instead of using one camera for air and water, two cameras are used. That also increases redundancy. A level of redundancy was also ensured in the water-to-air transition, as the pressure in the air tank allows for two launch attempts. For structures, a safety factor of 1.25 is mostly used, while for the folding wing mechanism, it is 1.5. This way, the vehicle shall endure loads significantly above the required ones. Due to the usage of multiple technologies with a low TRL, extensive testing is needed and planned as outlined in Figure 17.2.

#### Availability

The vehicle is designed such that it can operate in most conditions to be encountered at the Borselle windpark. For the worst case design scenario, the system shall be able to operate in winds of up to 10-11 m/s and a wave height of 1.8 [m] [1]. This means that the system can operate 84.5% of the time [74]. The main feature of the design allowing it to operate in the broad range of conditions is its ability to dive underwater and perform the inspection while underwater. Furthermore, the vehicle only needs to carry out the inspection of the 40 systems once a month. Given that that inspection takes only 2 days, a lot of redundancy is left when it comes to the time in which the inspection has to be carried out.

#### Maintainability

Maintainability refers to how easy it is to keep the vehicle operational. The main mean of ensuring that in case of Puffin is limiting the use of permanent fasteners as much as possible. Payload and most of the other parts are bolted to the structural frame to allow for easy replacement. In order to help with maintenance, access hatches are going to be implemented, such that replacement of parts can be carried out without the need to destroy the CFRP skin. To further improve maintainability, components off the shelf are used as much as possible, all the motors, flight computer, servos, cameras or sonar. Only parts that need to be custom developed for the purposes of the vehicle or are cheaper to obtain this way are not COTS. This allows for faster access to the components and lower downtime. Especially as a stock of the most commonly replaceable items will be kept.

#### Safety

Safety is a critical aspect of the design. In the context of SEAMOS, it is understood as avoiding causing damage to the vehicle, environment or the infrastructure. Most of these aspects are covered by the obstacle-avoidance capability of the vehicle. Both of the cameras will be recognizing any objects or animals that the vehicle might

come into contact with and the controller will adjust the path of the Puffin accordingly. Other precautions are also taken, such as the altitude of the vehicle while it passes through the seaweed system being 17m under the wind turbine blades. Regarding the safety for the environment, emitting no pollutants is a critical aspect of the design. That is why Puffin is a fully electric vehicle. In case of malfunction, the vehicle has to be retrieved, which is why positive buoyancy of the vehicle is ensured. In case of an emergency landing, it would float up to the surface and await rescue.

## 16 Lifecycle analysis

The Life Cycle analysis is a sustainability evaluation tool. The following chapter is an iteration on the Preliminary Inventory[1], defining the goal and scope of the LCA and presenting suggestions for the most beneficial applications. The actual quantification of emission is not performed due to software accessibility limitations. The Preliminary Inventory directly follows from the Life Cycle Assessment convention[75]. The LCA preparation presented in this report is heavily limited by the available resources and should be revised for the actual quantification procedure.

### 16.1. Goal definition

The goal definition, as specified in the Midterm Report[1], is to be iterated for the current design stage in order to ensure the relevance of the results. The intended application is the evaluation of the sustainability Puffin design, establishing the environmental impact of each of the design elements. The evaluation will be performed based on the existing databases, the convention model accuracy is limited to low and medium accuracy. The LCA is performed in order to determine unsustainable elements and processes allowing for possible beneficial iterations, classifying the system as 'Situation A'(Micro-level decision support). The target audience is the development team responsible for further steps in the project. The LCA is intended for internal use of the development team, it is not going to be available to the public. The system could be compared to other available monitoring methods in the offshore industry. The supervisors of the preliminary inventory stage of the LCA process are Salua Hamaza and Clemens Dransfeld, the supervision of further LCA steps is not yet defined. The user behaviour, following the needs of the Seaweed Company and possible clients defined in Chapter 14, is expected to be monthly deployment throughout the whole year. As the subsystems and manufacturing processes are defined, the system boundary is updated and presented in.

### 16.2. Scope Definition

The scope of the LCA has to be defined. The scope definition has remained unchanged throughout development. The expected outcomes of the complete LCA procedure are the Life Cycle Inventory, LCI model and Life Cycle Impact Assessment, as established in [1]. The outcomes follow the ISO 14044 standard. The Functional unit definition is revised and presented in Table 16.1. The system allows for underwater inspection of structures using sonar sensing with the aerial transition.

**Table 16.1:** Functional unit description for the Puffin design, as defined in [1]

Obligatory properties	Positioning properties
Monitoring of the seaweed farm structure	Good diving depth
Water sampling	Sensor and visual sensing
Monitoring seaweed growth	Good range and endurance
Autonomous	
Functional unit	
Water sample collection and underwater monitoring of 40 seaweed farm units structure located within the Borssele wind farm in the span of 10 years	
Reference flow	
Autonomous drone with aquatic ability (The Puffin)	

Due to the diving capability, underwater sensing and from-the-air visual inspection possible the range of appli-

cations covers the monitoring of offshore structures. The LCI modelling framework is established following the ILCD convention recommendations. The decision context is Micro-level decision support, classified as 'Situation type A'. The system is multi-functional, the evaluation has to be broken down using conventional techniques to ensure the outcome correctly represents the real-life impact. The LCA will be performed by applying subdivision, system expansion and the average process for the background modelling. The requirements are to be established for the goal. The used data shall be geographically, timely and technologically relevant for the assembly in Netherlands and operation in the Borssele wind farm in the span of 10 years. The LCA will be performed using the OpenLCA<sup>1</sup> software and the Ecoinvent<sup>2</sup>. The LCA should be reviewed by an external unbiased LCA expert to ensure quality control throughout the process, as well as of the final outcomes.

### 16.3. Preliminary Inventory

The physical value chain presents the flow of the resources and processes included. As the mechanisms are specifically designed for the needs of the Puffin, the exact in- and outputs of the systems are not possible to be defined. The data will come from the Ecoinvent database, providing low and medium-accuracy data. The data should be documented, its specificity, source, type and access method should be established and presented. The LCI model requires the definition and quantification of input and output flows into each of the individual processes. The quantification of the flows is dependent on the quantity of the reference flow. The LCI process will be performed using the OpenLCA software. Model parameters should be iterated, the sensitivity analysis will allow for high confidence in the LCA outcomes.

### 16.4. Recommendations

The LCA is a comparison tool. It should be used for the evaluation of different quantified emissions of possible scenarios. The Puffin design has been developed with a high focus on sustainability. The input and output flows should be established for each of the processes mentioned in Section 17.2, in order to evaluate the sustainability of the design and the complete design process. The OpenLCA should be used for analysing the processing methods, an example being nose cone CFRP manufacturing. The needed subsystem can be achieved using layup technology or compression moulding, the quantification of the flows for the scale of the reference flow would help determine the process with the least environmental impact. The initial manufacturing plan is presented in Section 17.1. The material choices could be impacted by the quantification, the used recycled CFRP and stainless steel might possibly be a design hot spot and different materials and design solutions should be researched. The LCA should be implemented in the development, as it is highly beneficial for finding improvements to the development process in terms of minimising emissions. Future steps should utilise the LCA method to accurately establish and define in detail the optimal manufacturing methods. Without the data, the LCA is just a convention, a potential evaluation method.

## 17 Future Phases

This chapter entails a description of the phases after research and development. This includes manufacturing and the steps to reach a marketable product as displayed in the product design and development logic. The project Gantt chart is also included.

### 17.1. Manufacturing, Assembly and Integration Plan

Figure 17.1 displays the manufacturing, assembly and integration plan (MAI plan). It includes all relevant material used and the processes to obtain the resultant system. The flowchart is colour-coded in the following manner:

- Green - Raw material
- Blue - Small parts
- Red - Off-the-shelf parts
- Purple - Large determining parts of the system

---

<sup>1</sup>OpenLCA

<sup>2</sup>Ecoinvent



- Yellow - Subsystems

Many parts have already been researched and decided to be off-the-shelf to save development costs. Furthermore, all skins are formed from CFRP, hence the inside frames, parts, and payload must be attached through an adhesive. To allow for replacement during maintenance, the payload and other parts are bolted to frames which then use the adhesive to be fixed against the fuselage.

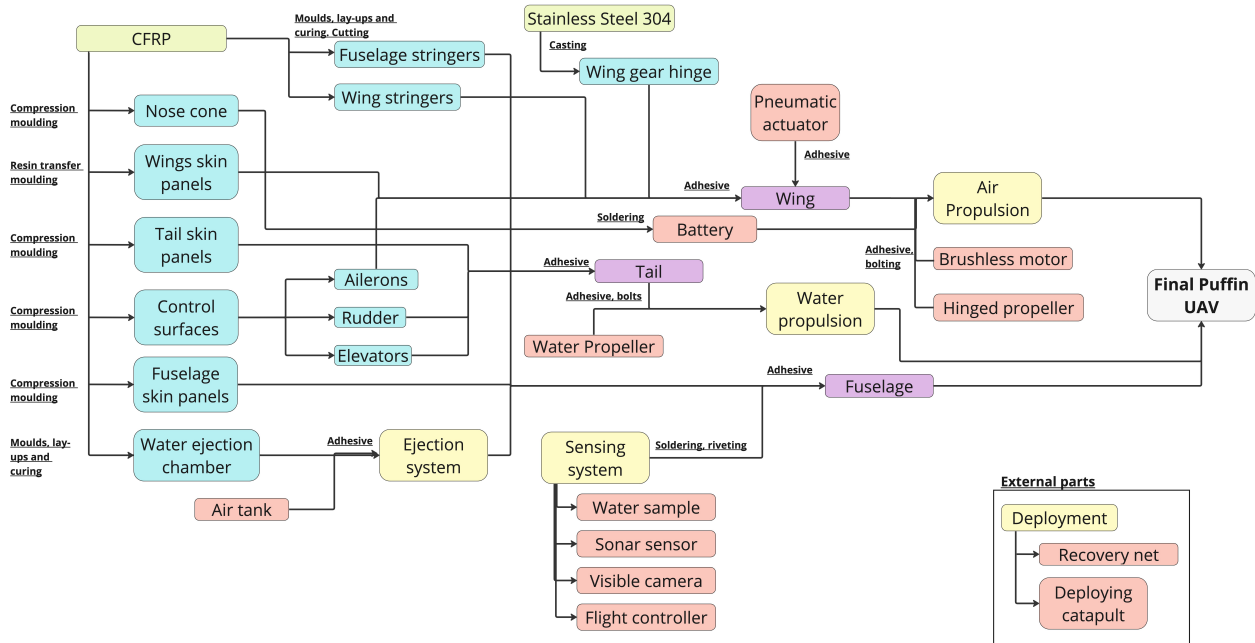


**Figure 17.1:** The manufacturing, assembly and integration flowchart plan (MAI)

The external parts for the system are all off-the-shelf. Only the catapult will have to be specially made however, this is done by a separate company.

**Water ejection chamber manufacturing** To manufacture the water ejection chamber a combination of methods will be used[76]; rotational moulding and lay-ups. Firstly, the chamber mould will be attached to a mandrel and spun. While spinning a polymer powder is deposited and distributed within the mould; this is heated and cured to form an inner lining. The mandrel and the mould are removed to provide a surface for CFRP lay-ups. These lay-ups are also cured.

**Material testing** As a form of verification and validation, the materials will undergo testing to ensure they fulfil their material properties. The tests thought to be most relevant are listed below[77].

**Tensile test** - A piece of material is placed between two clamps which gradually pull the piece in tension with increasing force. The material can be observed for yield and ultimate failure.

**Hardness testing** - Press a hard object into the material. The penetration depth is then measured.

**Corrosion testing** - Immerse the material in 5-20% of sodium chloride. After a period of time, the material is removed and analysed.

**Fatigue testing** - A fatigue test machine will use a rotating eccentric weight to provide random loads on the material. The fatigue is then observed.

## 17.2. Product Design and Development Logic

The product design and development logic, as displayed in Figure 17.2, shows the suggested sequence of activities necessary to deliver the puffin as a market-ready final product. The activities directly follow the outcomes of the Final Report. The main elements involve manufacturing and testing the prototypes of the subsystems and the integrated system, as well as establishing the logistics of a sustainable production and manufacturing stage. Focus is also on establishing and meeting the needs of the market, creating a competitive solution for the offshore monitoring market. The design, if not meeting the requirements, shall be iterated.

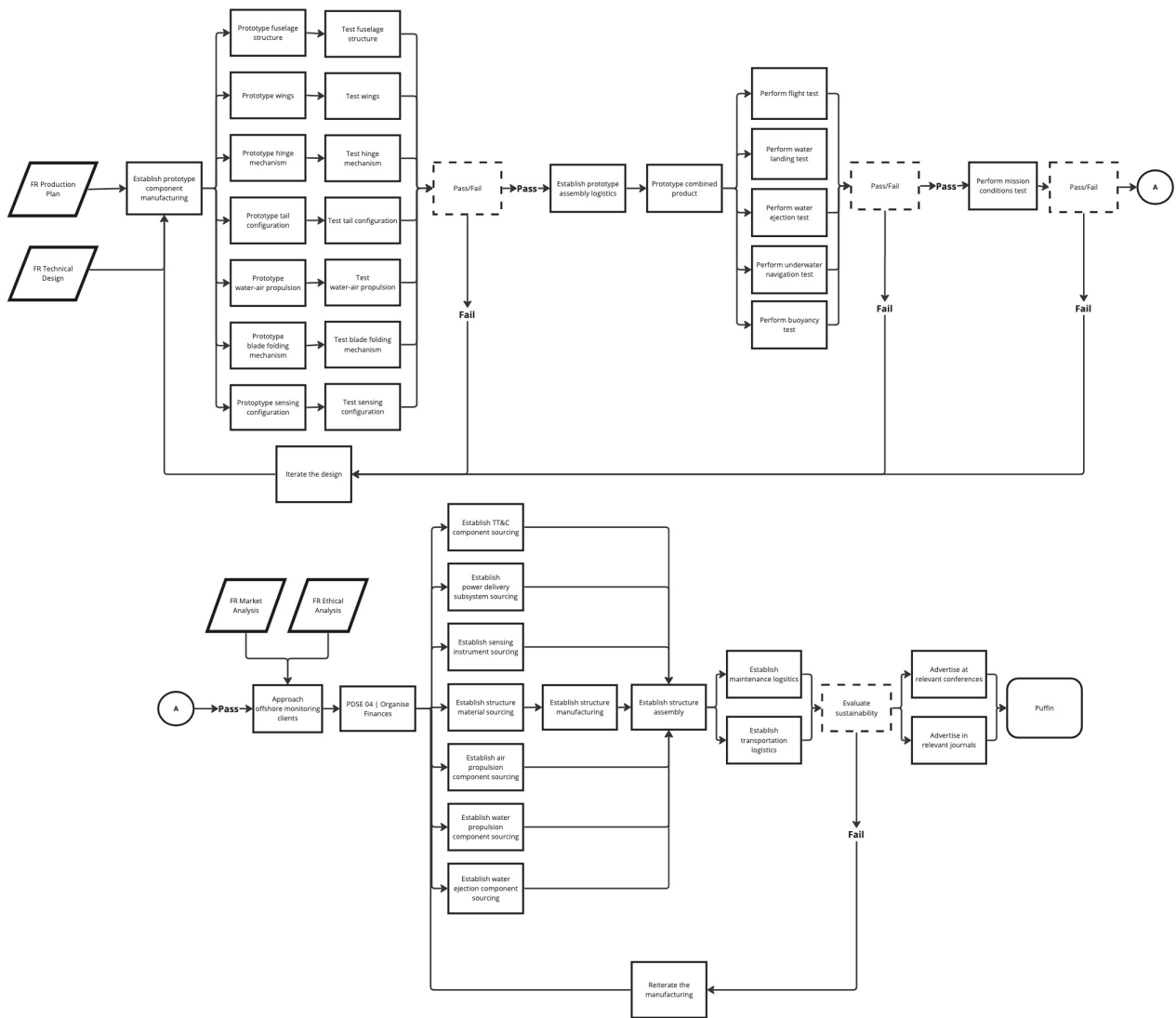


Figure 17.2: Project design and development logic

### 17.3. Project Gantt Chart

The project Gantt chart displays a timeline of all post-DSE activities.

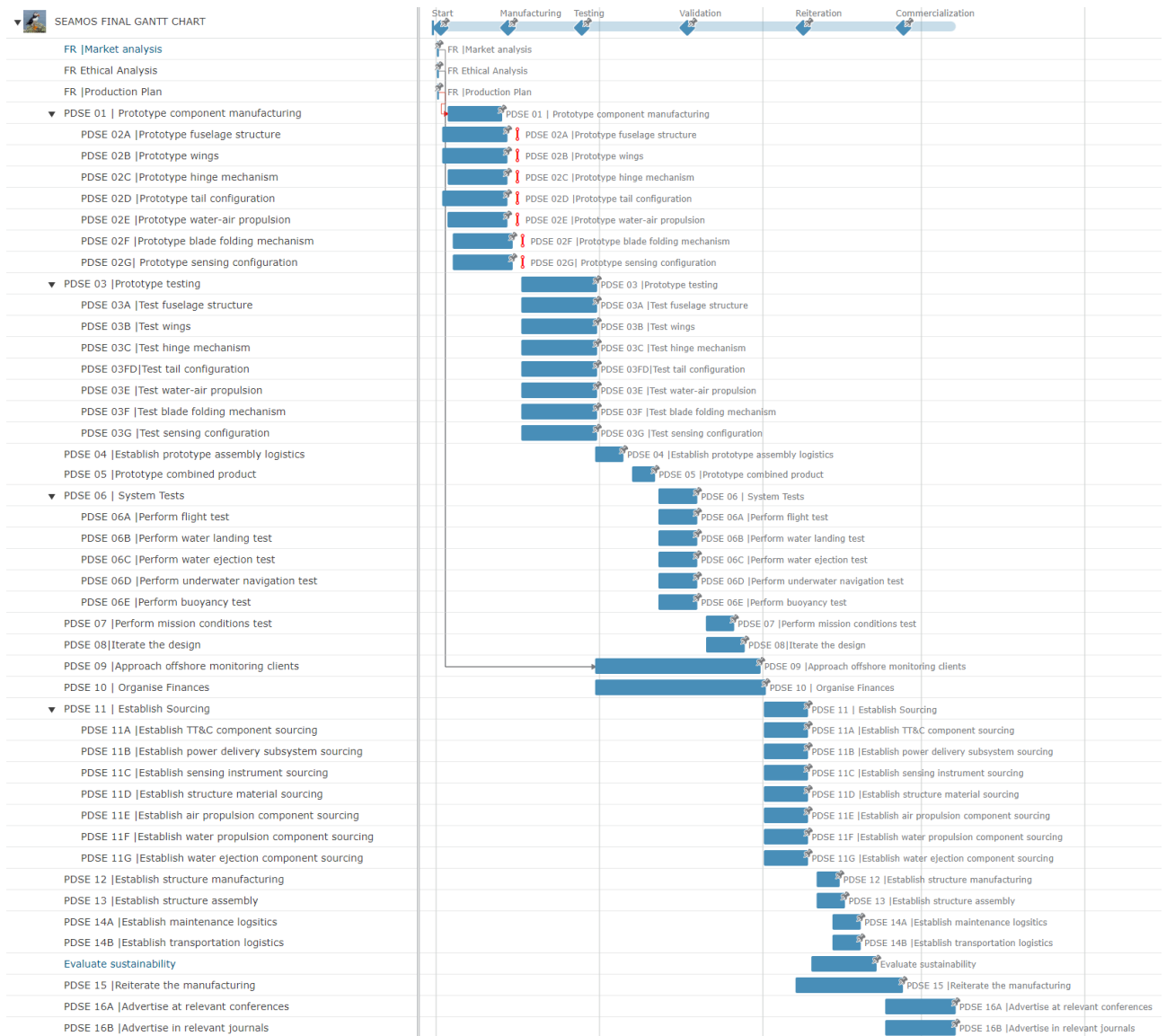


Figure 17.3: Project Gantt Chart - Post DSE timeline

# 18 Conclusion

**Table 18.1:** Summary of system budgets

Budget	Value
Production Cost	[€] 58,500
Maintenance per month	[€] 1100
MTOM	13.8 [kg]
Power required	300 [Wh]
Power supply	482.4 [Wh]

The Puffin was designed to monitor offshore aquaculture as commissioned by the Seaweed Company. In commissioning the Puffin, the Seaweed Company hopes to decrease the monitoring expenses arising from measurements of seaweed growth and farm structural integrity at the Borssele wind park. Points of interest are monitored monthly across an area of 160 [Ha], year-round, in offshore conditions. Driving requirements are the range from shore to the wind park, observation of underwater points of interest, sustainability, and total system cost. The present, manual approach, is to be replaced by an autonomous system, cutting costs and improving coverage.

The presented design, the Puffin, combines novel technologies allowing it to launch from shore, fly to the Borssele wind park, dive to a submerged state, conduct its underwater monitoring mission, escape from the water, and return to the launch site. The design features a 90-degree sweep mechanism, fully autonomous underwater control,

and an impulsive launch system.

A summary of Puffin budgets is indicated in Table 18.1. In terms of market and return on investment, the design has achieved the purpose of creating a cheaper solution, it is however over the originally stated budget. A return on investment investigation was undertaken to justify a cost increase: it was found that over its lifetime, the Puffin is [€] 90,000 cheaper than current marine vessel solutions and that in four months all investment will be recuperated (excluding R & D costs). Furthermore, the product could enable the validation of blue carbon credits due to the frequency and type of data that can be acquired. These credits may be sold or traded on carbon exchanges for additional revenue. In addition, not only are there multiple applications for the product, for example, offshore wind turbines, but the seaweed market is a large growing market with much potential. The only disadvantage is that it is quite new and unexplored - low maturity.

The sustainability of the product has been upheld by the use of recycled CRFP, and zero on-mission emissions. Outside of the product mission profile, the lean manufacturing method is used to ensure less waste. In addition, by allowing the seaweed market to be more accessible, a snowball effect of using less meat within the culinary industry will aid with sustainability in the long run. Quantification of emissions will be revised by a life cycle analysis (LCA) at a later time, with mitigation measures implemented in future design iterations.

Some aspects of the design are still in need of refinement. While the overall feasibility of the architecture is demonstrated, various elements should be developed in more detail:

1. In modelling vehicle behaviour, individual components (such as water impact loading) are accounted for, but an integrated simulation is missing. The transition from aerial to aquatic locomotion and vice versa is a novel behaviour, and investigation of dynamics during these phases may have interesting implications. A complete model would incorporate higher fidelity aero-hydrodynamic loading and analysis of (sloshing of) internal fluids.
2. Building on more complete dynamic models, design for and modelling of control and stability should be revisited. Modelling in particular, with constraints on communication and sensor data, should demonstrate that the degree of autonomy required can be executed technically.
3. Component layout and assembly is preliminary, joined by a similarly preliminary structural design. The collection of unique mechanisms (wing sweep, multiple propulsion systems, water impact) drives a complex structure. Efficient integration may achieve significant gains, but inefficient integration may incur heavy penalties.
4. Emission quantification using the Life Cycle Analysis conventions, design hot spot determination, and comparison of possible manufacturing scenarios should allow for design process iterations improving the sustainability of the system.
5. Airfoil optimisation will increase range without incurring extra cost. Currently, a NACA airfoil has been selected, however, NACA airfoils are not optimised for the specific application. Therefore airfoil optimisation has to be done using CFD tools to make the most efficient wing possible.

Pending further development, the Puffin is uniquely positioned to generate value in a market with a large potential for growth.

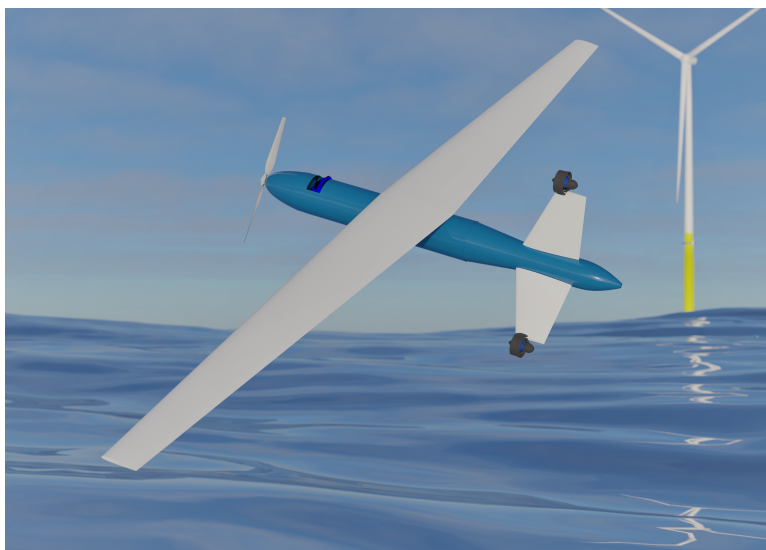


**Figure 18.1:** Final Puffin render

# Bibliography

- [1] Ronsse, L., Vusser, M. D., Seffer, B., Kumar, S., Oosthoek, E., Krzyżanowski, K., Grobusch, J., van Zutphen, E., Heliński, M., and Zwikker, R., “Preliminary Design of SEAMOS,” , 2023.
- [2] Prof. Dr. Eberhard Gill, “Verification and Validation for the Attitude and Orbit Control System,” , March 2023. URL <https://brightspace.tudelft.nl/d2l/1e/content/512955/viewContent/2888774/View>.
- [3] Ronsse, L., Vusser, M. D., Seffer, B., Kumar, S., Oosthoek, E., Krzyżanowski, K., Grobusch, J., van Zutphen, E., Heliński, M., and Zwikker, R., “Market Insights & Design Options,” , 2023.
- [4] Wilson, R., and Heath, M., “Increasing turbidity in the North Sea during the 20th century due to changing wave climate,” *Ocean Science*, 2019.
- [5] Caltech, “Bottle Reference Chart,” , n.d. [Accessed June 15th 2023].
- [6] Elight, “A complete guide to beyond the visual line of sight commercial drone operations,” , n.d. URL <https://www.elight.com/bvlos/>, [Accessed May 24th 2023].
- [7] Federal Aviation Association, “Automatic Dependent Surveillance-Broadcast (ADS-B),” , n.d.. URL [https://www.faa.gov/air\\_traffic/technology/adsb](https://www.faa.gov/air_traffic/technology/adsb), [Accessed May 24th 2023].
- [8] Federal Aviation Association, “UAS Remote Identification,” , n.d.. URL [https://www.faa.gov/uas/getting\\_started/remote\\_id](https://www.faa.gov/uas/getting_started/remote_id), [Accessed May 24th 2023].
- [9] Eli, “PNEUMATIC CATAPULT PL-40,” , 2016. URL <https://www.uav.ee/products/uav-pneumatic-catapult-pl-40/>.
- [10] Siddall, R., Ancel, A. O., and Kovac, M., “Wind and water tunnel testing of a morphing aquatic micro air vehicle,” *Royal Society of London*, 2017. doi:10.1098/rsfs.2016.0085.
- [11] Zufferey, R., Ancel, A. O., Farinha, A., Siddall, R., Armanini, S. F., Nasr, M., Brahmali, R. V., Kennedy, G., and Kovac, M., “Consecutive aquatic jump-gliding with water-reactive fuel,” *Science Robotics*, Vol. 4, No. 34, 2019, p. eaax7330. doi:10.1126/scirobotics.aax7330, URL <https://www.science.org/doi/abs/10.1126/scirobotics.aax7330>.
- [12] Zuffery, R., Siddal, R., Armanini, S. F., and Kovac, M., “Between Sea and Sky: Aerial Aquatic Locomotion in Miniature Robots,” *Biosystems and Biorobotics*, Vol. 29, 2023. doi:https://doi.org/10.1007/978-3-030-89575-4.
- [13] Siddall, R., Kennedy, G., and Kovac, M., *High-Power Propulsion Strategies for Aquatic Take-off in Robotics*, 2018, pp. 5–20. doi:10.1007/978-3-319-51532-8\_1.
- [14] Siddall, R., Kennedy, G., and Kovac, M., *High-Power Propulsion Strategies for Aquatic Take-off in Robotics*, 2018, pp. 5–20. doi:10.1007/978-3-319-51532-8\_1.
- [15] Borchsenius, J., and Pinder, S., “Underwater glider propulsion using chemical hydrides,” *OCEANS’10 IEEE SYDNEY*, IEEE, 2010, pp. 1–8.
- [16] University of Hertfordshire, 2023. URL <http://sitem.herts.ac.uk/aeru/ppdb/en/Reports/110.htm#:~:text=Calcium%20hydroxide%20is%20an%20inorganic,health%20issues%20have%20been%20identified>.
- [17] Sharma, S., Sharma, D., Soni, S. L., Singh, D., and Jhalani, A., “Performance, combustion and emission analysis of internal combustion engines fuelled with acetylene—a review,” *International Journal of Ambient Energy*, Vol. 43, No. 1, 2022, pp. 622–640.
- [18] Pozzoni, L., Paravan, C., and Galfetti, L., “ADN-based Formulations Analysis for Green Solid Propellants,” , 2022.
- [19] NASA, “Buckling of Thin-Walled Truncated Cones,” *NASA Space Vehicle Design Criteria*, , No. NASA SP-8019, 1968.

- [20] NASA, "Buckling of Thin-Walled Circular Cylinders," *NASA Space Vehicle Design Criteria*, , No. NASA SP-8007, 1965.
- [21] Zufferey, R., Siddall, R., Armanini, S. F., and Kovac, M., *Between Sea and Sky: Aerial Aquatic Locomotion in Miniature Robots*, Springer, 2022.
- [22] Michelhaugh, T. A., "WING-FOLDING MECHANISM OF THE GRUMMAN WILDCAT," AMSE, 2006. URL <https://www.asme.org/wwwasmeorg/media/resourcefiles/aboutasme/who%20we%20are/engineering%20history/landmarks/238-grumman-wildcat-sto-wing-wing-folding-mechanism.pdf>.
- [23] Kothia, D., Singh, J., and Dadhich, A., "DESIGN, ANALYSIS AND OPTIMIZATION OF FOLDING WING MECHANISM FOR EFFECTIVE UTILIZATION OF AIR SIDE AREA," *International Journal of Aerospace and Mechanical Engineering*, Vol. 3, 2016.
- [24] Pandey, A., Yuk, J., Chang, B., Fish, F. E., and Jung, S., "Slamming dynamics of diving and its implications for diving-related injuries," *ScienceAdvances*, 2022. doi:10.1126/sciadv.abo5888.
- [25] Jung, S., "Swimming, flying, and diving behaviors from a unified 2D potential model," *SciRep*, 2021. doi: <https://doi.org/10.1038/s41598-021-94829-7>.
- [26] droneblog, "Why Don't Drones Use Ducted Fans?" , 2023. URL <https://www.droneblog.com/why-dont-drones-use-ducted-fans/>, [Accessed June 9th 2023].
- [27] Nagel, L., "What is an Electronic Speed Controller & How Does an ESC Work," , 2022. URL <https://www.tytorobotics.com/blogs/articles/what-is-an-esc-how-does-an-esc-work>, [Accessed June 9th 2023].
- [28] Wood, A., "Fundamental Forces in Flight," , 2022. URL <https://aerotoolbox.com/forces-in-flight/>, [Accessed June 9th 2023].
- [29] O.M. Al-Hababbeh , M. Al-Saqqa, M. Safi, T. Abo Khater, "Review of magnetohydrodynamic pump applications," , 2016. URL <https://docs.rs-online.com/8d60/0900766b816faefd.pdf>.
- [30] MAN Energy Group, "Basic principles of ship propulsion," , 2022. URL <https://www.man-es.com/docs/default-source/document-sync/basic-principles-of-ship-propulsion-eng.pdf>.
- [31] Carlton, J., *Marine Propellers and Propulsion*, Elsevier Ltd, 2017.
- [32] Davies, A., "Pump up the pump jet?" *Australian Strategic Policy Institutes*, 2017. URL <https://www.aspistrategist.org.au/pump-up-the-pump-jet/>.
- [33] Griffiths, G., *Technology and Applications of Autonomous Underwater Vehicles*, Taylor & Francis, 2003.
- [34] OpenImpulse, "Batteries and Accumulators Demystified," , n.d. URL <https://www.openimpulse.com/blog/2013/08/batteries-and-accumulators-demystified/>.
- [35] Harsha Vardhan, D., Ramesh, A., and Chandra Mohan Reddy, B., "A Review On Materials Used For Marine Propellers," *Materials Today: Proceedings*, Vol. 18, 2019, pp. 4482–4490. doi:<https://doi.org/10.1016/j.matpr.2019.07.418>, URL <https://www.sciencedirect.com/science/article/pii/S2214785319325970>, 9th International Conference of Materials Processing and Characterization, ICMPC-2019.
- [36] Tiwari, B. K., and \*, R. S., "Design and Analysis of a Variable Buoyancy System for Efficient Hovering Control of Underwater Vehicles with State Feedback Controller," *Journal of Marine Science and Engineering*, 2020. doi:<https://doi.org/10.3390/jmse8040263>.
- [37] Brenden Epps, "OpenProp v2.3 theory document," , 2010.
- [38] A. Cervone, "Systems Engineering and Aerospace Design," , 2022.
- [39] Cook, M. V., "Chapter 12 - Aerodynamic Modelling," *Flight Dynamics Principles (Third Edition)*, edited by M. V. Cook, Butterworth-Heinemann, 2013, third edition ed., pp. 353–369. doi:<https://doi.org/10.1016/B978-0-08-098242-7.00012-2>, URL <https://www.sciencedirect.com/science/article/pii/B9780080982427000122>.
- [40] Raymer, D. P., *Aircraft Design: A Conceptual Approach*, American Institute of Aeronautics and Astronautics, 1992.



- [41] No Author, "Empennage General Design," , n.d. URL [https://www.fzt.haw-hamburg.de/pers/Scholz/H00U/AircraftDesign\\_9\\_EmpennageGeneralDesign.pdf](https://www.fzt.haw-hamburg.de/pers/Scholz/H00U/AircraftDesign_9_EmpennageGeneralDesign.pdf), [Accessed June 12th 2023].
- [42] Guo, D., "Modelling and Experimental Investigations of a Bi-modal Unmanned Underwater/Air System," , 2019. URL [researchrepository.rmit.edu.au/esploro/outputs/graduate/Modelling-and-experimental-investigations-of-a/9921864166401341?institution=61RMIT\\_INST](https://researchrepository.rmit.edu.au/esploro/outputs/graduate/Modelling-and-experimental-investigations-of-a/9921864166401341?institution=61RMIT_INST).
- [43] Sadreay, M. H., *Design of Unmanned Aerial Systems*, John Wiley & Sons Ltd, 2020.
- [44] airfoiltools, "NACA 0012 AIRFOILS (n0012-il)," , 2023. URL <http://airfoiltools.com/airfoil/details?airfoil=n0012-il>.
- [45] Sharpe, P., "Aerosandbox 4.0.9 Documentation," , ???? URL <https://aerosandbox.readthedocs.io/en/master/autoapi/index.html>, [Accessed May 22nd 2023].
- [46] Renilson, M., *Submarine Hydrodynamics*, Springer, 2015.
- [47] Mathis de Vusser, "Aircraft Tutorial: BAe Hawk T Mk1 Design," , 2021. [Accessed June 15th 2023].
- [48] Crowell Sr, G. A., "The descriptive geometry of nose cones," URL: <http://www.myweb.cableone.net/cjcrowell/NCEQN2.doc>, 1996.
- [49] SLAM, R. U. F. A. U. S.-B., "Relocating Underwater Features Autonomously Using Sonar-Based SLAM," *IEEE Journal of Oceanic Engineering*, Vol. 38, No. 3, 2013, pp. 500–513. doi:10.1109/JOE.2012.2235664.
- [50] Potokar, E., Ashford, S., Kaess, M., and Mangelson, J., "HoloOcean: An Underwater Robotics Simulator," *Proc. IEEE Intl. Conf. on Robotics and Automation, ICRA*, Philadelphia, PA, USA, 2022.
- [51] Prof. Dr. Eberhard Gill, March 2023. URL <https://brightspace.tudelft.nl/d21/le/content/512955/viewContent/2888774/View>.
- [52] van den Burg, S., Visscher, M., Sonneveld, A., Berges, B., Jansen, L., Sharp, F., Steinmann, J., Arora, G., and Bogers, M., "Uptake of new technology for ocean observation," *European Maritime and Fisheries Fund (EMFF)*, 2021. URL <https://edepot.wur.nl/548848>.
- [53] Johan, G., Linette, d. S., Ioannis, G., Eric, D., and Castro, A., "Marine sensors; the market, the trends and the value chain," *Sensor Systems for a Changing Ocean (SSCO), 2014 IEEE*, 2014. URL [https://www.researchgate.net/publication/273950460\\_Marine\\_sensors\\_the\\_market\\_the\\_trends\\_and\\_the\\_value\\_chain](https://www.researchgate.net/publication/273950460_Marine_sensors_the_market_the_trends_and_the_value_chain).
- [54] FAO, "The State of World Fisheries and Aquaculture," *Food and Agriculture Organization of the United Nations*, 2022. URL <https://www.fao.org/3/cc0461en/online/sofia/2022/fisheries-and-aquaculture-projections.html>.
- [55] North Sea Farmers, Februari 2023. URL <https://www.northseafarmers.org/>.
- [56] Ferdouse, F., Holdt, S. L., Smith, R., Murúa, P., and Yang, Z., "The global status of seaweed production, trade and utilization," *GLOBEFISH RESEARCH PROGRAMME*, Vol. 124, 2018. URL <https://www.fao.org/3/CA1121EN/ca1121en.pdf>.
- [57] Grand View Research, "Commercial Seaweed Market Size, Share & Trends Analysis Report By Product," 2022. URL <https://www.grandviewresearch.com/industry-analysis/commercial-seaweed-market>.
- [58] DNV, "Marine Aquaculture Forecast," 2021. URL <https://www.dnv.com/focus-areas/offshore-aquaculture/marine-aquaculture-forecast/index.html#:~:text=Marine%20aquaculture%20will%20more%20than,weight%20to%2074%20Mt%2Fyrl>.
- [59] European Union Aviation Safety Agency, "Concept of Operations for Drones: A risk based approach to regulation of unmanned aircraft," , 2023. URL [https://www.easa.europa.eu/sites/default/files/dfu/204696\\_EASA\\_concept\\_drone\\_brochure\\_web.pdf](https://www.easa.europa.eu/sites/default/files/dfu/204696_EASA_concept_drone_brochure_web.pdf).
- [60] European Union Aviation Safety Agency, "Open Category," , 2023. URL <https://www.easa.europa.eu/en/the-agency/faqs/open-category#category-understanding-the-%E2%80%98open%E2%80%99-category>.
- [61] UAV Coach, "Drone Laws in Netherlands," , 2014. URL <https://uavcoach.com/drone-laws-in-netherlands/>.

- [62] Ministerie van Infrastructuur en Waterstaat, "Code of conduct for safe passage through off-shore wind farms," , February 2018. URL <file:///Users/emmavanzutphen/Downloads/code-of-conduct-for-safe-passage-through-offshore-wind-farms.pdf>.
- [63] Ramírez, L., Fraile, D., and Brindley, G., Feb 2020. URL <https://windeurope.org/wp-content/uploads/files/about-wind/statistics/WindEurope-Annual-Offshore-Statistics-2019.pdf>.
- [64] Planit, "ROV Pilot Technician," , 2023. URL [planitplus.net/JobProfiles/View/730/53](http://planitplus.net/JobProfiles/View/730/53).
- [65] Essam Shehab, S. T., Arshyn Meiirbekov, "Cost Modelling for Recyling Fiber-Reinforced Composites: State-of-the-Art and Future Research," *Polymers*, 2022. doi:<https://doi.org/10.3390/polym15010150>.
- [66] Wang, D. J., "eVTOL Design Short Course," , 2023. URL <https://ocw.snu.ac.kr/sites/default/files/NOTE/1%20Preparations%20Before%20Designing%20Aircraft.pdf>, [Accessed May 22nd 2023].
- [67] Netherlands Enterprise Agency, R., "R&D tax credit (WBSO)," , 2022. URL <https://business.gov.nl/subsidy/wbso/>.
- [68] innovativetax, "The advantages of the Dutch R & D tax incentives," , 2022. URL <https://www.innovativetax.com/news/the-advantages-of-the-dutch-r-d-tax-incentives.html>.
- [69] Droprise, "Deep Trekker DTG3," , n.d. URL <https://www.droprise.be/en/shop/deep-trekker-revolution-kopie/>.
- [70] L, J., "How is a blue carbon credit generated?" , 2022. URL <https://carboncredits.com/what-are-blue-carbon-credits-everything-you-need-to-know/>.
- [71] S Mashoreng, Y. A. L. N., and Isyrini, R., "Cultivated seaweed carbon sequestration capacity," *The 2nd International Symposium on Marine Science and Fisheries*, 2019. doi:10.1088/1755-1315/370/1/012017.
- [72] Latheef, A., "Huge Momentum' is Underway for Blue Carbon," , 2022. URL <https://blog.opisnet.com/blue-carbon-momentum>.
- [73] Veraart, J., de Groot, A., Jacobs, C., Jans, W., Velthuis, M., and Klostermann, J., "Methods to assess Blue Carbon Potential of Seaweed Culture at the North Sea: feasibility study," , 2022. URL <https://edepot.wur.nl/537676>.
- [74] DNV, *Site Studies Wind Farm Zone Borssele*, Netherlands Enterprise Agency, 2015.
- [75] Michael Z. Hauschild, Ralph K. Rosenbaum, Stig Irving Olsen, *Life Cycle Assessment Theory and Practice*, Springer, 2018. doi:10.1007/978-3-319-56475-3.
- [76] British Plastics Federation, June 2023. URL [https://www.bpf.co.uk/plastipedia/processes/Rotational\\_Moulding.aspx](https://www.bpf.co.uk/plastipedia/processes/Rotational_Moulding.aspx).
- [77] Kenneth E. Hofer, June 2018. URL <https://www.britannica.com/technology/materials-testing>.